THE EFFECTS OF APOLIPOPROTEIN A-1 EXPRESSION ON EYE GROWTH OF CHICKS

XIAO HU

PhD

The Hong Kong Polytechnic University

2020

The Hong Kong Polytechnic University

School of Optometry

The Effects of Apolipoprotein A-1 Expression on Eye Growth of Chicks

XIAO Hu

A thesis submitted in partial fulfilment of the requirements for the degree of Doctor of Philosophy

March 2018

CERTIFICATE OF ORIGINALITY

I hereby declare that this thesis is my own work and that, to the best of my knowledge and belief, it reproduces no material previously published or written, nor material that has been accepted for the award of any other degree or diploma, except where due acknowledgement has been made in the text.

(Signed)

XIAO HU (Name of student)

Abstract

Aims

Myopia has become not only a public health issue, but also a socioeconomic problem affecting many youngsters worldwide (Zheng et al., 2013). Therefore, it is important to control the myopia epidemic so as to save people from sight-threatening diseases associated with myopia.

Previous studies have identified a number of key signaling molecules in myopia development, such as dopamine (Zhang and Wildsoet, 2015, Mao et al., 2010b), apolipoprotein A-1 (apoA1) (Bertrand et al., 2006), retinoic acid (McFadden et al., 2004a, Summers et al., 2016), early growth response 1 (Fischer et al., 1999, Ashby et al., 2007a, Mathis and Schaeffel, 2007) and TGF-β (Rohrer and Stell, 1994). However, a full picture of how these signaling molecules may work together in biochemical cascades that eventually modulate eye growth is still unclear (Bertrand et al., 2006). Unravelling the biology of myopia could help reveal key molecular targets and develop novel therapeutics for myopia control in the future.

The present study profiled the retinal differential protein expression in lens induced myopia (LIM) and hyperopia (LIH) in chicks. ApoA1was thought to be one of key stop signals in eye development. We attempted to examine if altering apoA1 may be effective in controlling myopia development in chicks, and the mechanisms behind its action.

Methods

White leghorn chicks (Gallus gallus) were used in our studies. There were four main experiments in this thesis. Experiment 1 was to explore the retinal apoA1 protein expression in LIH, LIM and control chick eyes. Experiment 2 studied the apoA1 mRNA differential expression in LIH, LIM and control chick eyes. Experiment 3 examined the direct effect of apoA1 on myopic eye growth when apoA1 protein is intravitreally injected. Experiment 4 studied the indirect effect of apoA1 on normal growth, myopic and hyperopic progression by oral administration of nicotinic acid. Proteomic analysis was applied to reveal the biological mechanism of eye growth in the presence of apoA1 and nicotinic acid.

The spherical equivalent refraction (spherical power + half of cylindrical power) was measured by steak retinoscopy. Ocular parameters were measured by high frequency A-scan ultrasound system (30MHz probe sampled at 100MHz). Sealing Foiland LightCycler® 480 system from Roche Company and LightCycler® 480 SYBR Green I Master kit were used to perform qPCR analysis. Western blot and liquid chromatography coupled tandem mass spectrometry (LC MS/MS) were used to identify and analyze differential protein expressions. SPSS software (version 23, SPSS, Chicago, Illinois, USA) was used for statistical analysis.

Results

ApoA1 protein differential expression in LIM, LIH and control chick eyes

Positive optical lenses of +10D could effectively induce hyperopic eye growth after 4 days of LIH (plano vs. LIH, mean±SD; VCD: 0.283±0.073mm vs. -0.121±0.044mm, P<0.001, n=5; AXL: 0.496±0.062mm vs. 0.120±0.058mm, P<0.001, n=5). Whereas, -10D lenses led to myopic eye growth after 4 days (Len Induced Myopia, LIM) (plano vs. LIM, mean±SD; VCD: 0.283±0.073mm vs. 0.713±0.084mm, P<0.001, n=6; AXL: 0.496±0.062mm vs. 0.983±0.093mm, P<0.001, n=6). Retinal apoA1 protein expression was found to increase in LIH (by MS analysis, LIH/plano=2.174, P=0.026, n=5). The results were consistent with previous studies (Bertrand et al., 2006, Chun et al., 2015, Summers et al., 2016). However, the retinal apoA1 expression did not show any down-regulation in LIM when compared to the control (by MS analysis, LIM/plano=0.935, P=1.000, n=6). According to pathway analysis by differential expression proteins, insulin signaling pathway, regulation of actin cytoskeleton, endocytosis and hippo signaling pathways were identified.

ApoA1 mRNA differential expression in LIM, LIH and control chick eyes

LIH induced significant changes in the mRNA expression of apoA1 as early as after one day of lens wear and the changes remained significant at 4 days (after 1 day LIH, LIH/plano=1.195, P=0.030, n=7; after 4 days LIH,

LIH/plano=1.430, P=0.049, n=8; recovery, + 10D/plano=1.198, P=0.200, n=7). Similarly, the LIM eyes demonstrated a significant differential mRNA expression of apoA1 after 1 day (LIM/plano=1.460, P=0.023, n=8), 4 days of lens wear (LIM/plano=1.549, P=0.033, n=8) and after the removal of lens (LIM/plano=1.303, P=0.062, n=8).

Direct effect of apoA1 on myopic progression by apoA1 protein intravitreal injection

Intravitreal injection of apoA1 protein could retard myopia in LIM eyes of different stages of myopia development. In this experiment, 10µl of total 2µg apoA1 protein was randomly injected into the treatment eye while 10µl of control mixture (1×PBS and 0.1% sodium lauroyl sarcosine, PH 7.4) was injected to the control eye. The results showed that apoA1 retarded the myopia development in LIM chicks if injected daily from PN4 to PN6 (changes between PN4 to PN7 were compared; Treatment vs. control, mean±SD; VCD: 0.008±0.101mm vs. 0.154±0.144mm, P=0.013; AXL: 0.115±0.090mm vs. 0. 321±0.128mm, P=0.002, n=8). It was also affected in LIM chicks (lens wear from PN4 to PN12) if injected daily from PN9 to PN11 (changes between PN9 to PN12; Treatment vs. control, mean±SD; VCD: 0.079±0.130mm vs. 0.224±0.099mm, P=0.001; AXL: 0.196±0.145mm vs. 0. 363±0.111mm, P=0.016, n=7). ApoA1 could even reverse the myopia development in LIM chicks (lens wear from PN4 to

PN22) if injected daily from PN19 to PN21 (changes between PN19 to PN22; Treatment vs. control, mean±SD; VCD: -0.057±0.024mm vs. 0.070±0.076mm, P=0.049; AXL: 0.064±0.045mm vs. 0. 253±0.056mm, P=0.003, n=4).

Effect of nicotinic acid on normal growth, myopic and hyperopic progression

Nicotinic acid is known to increase apoA1 expression in the blood plasma. The effects of oral administration of nicotinic acid on LIM, LIH and normal eye growth were examined in this study. Nicotinic acid significantly retarded eyes growth in both the LIH (NA LIH vs. LIH, mean±SD; VCD: -0.223±0.046mm vs. -0.121±0.044mm, P=0.012; AXL: -0.021±0.097mm vs. 0. 120±0.058mm, P=0.030, n=4) and LIM eyes (NA LIM vs. LIM, mean±SD; VCD: 0.548±0.146mm vs. 0.713±0.084mm, P=0.015; AXL: 0.801±0.172mm vs. 0. 983±0.093mm, P=0.046, n=8). However, nicotinic acid did not affect normal eye growth. In terms of pathway analysis based on differential expression proteins, insulin signaling pathway, regulation of actin cytoskeleton and endocytosis pathways were identified in this experiment.

Conclusion

The present study profiled the retinal differential expression proteins in LIM and LIH in chicks. ApoA1 was found to be highly expressed in hyperopic eye. Increasing the retinal apoA1 by direct intravitreal injection of apoA1 or by oral intake of nicotinic acid led to retardation in eye growth in chicks. Therefore, the results strongly suggested that apoA1 is a "stop" signal to eye growth. Modulating the retinal apoA1 expression with new therapeutics could be a novel way to control human myopia in the future.

List of presentations

Poster and paper presentation:

Hu XIAO, King-kit Li, Rachel Chun, Bing Zuo, Bingjie Chen, Chi-ho To. "Effect of Nicotinic Acid on Eye Growth in Chicks" Presented at 9TH INTERNATIONAL SYMPOSIUM OF OPHTHALMOLOGY (ISO), 2012, China.

Hu XIAO, Panfeng Wang, King-kit Li, Rachel Ka-man Chun, Bing Zuo, Bingjie Chen, Sze-wan Shan, Chi-Wai Do, Thomas C. Lam, Chi Ho To. "Effect of oral administration of nicotinic acid on ocular growth of lens-induced myopic chicks." Presented at The Association for Research in Vision and Ophthalmology, 2015, USA.

Hu XIAO, Thomas C. Lam, Sze-wan Shan1, King-kit Li, Rachel Ka-man Chun, Bing Zuo, JingFang BIAN, Chi-Wai Do, Chi Ho To. "Changes in retinal proteome in lens induced myopic chicks by novel SWATH analysis. "Presented at15th International Myopia Conference (IMC), 2015, China.

Hu XIAO, Thomas C. Lam, Sze-wan Shan, King-kit Li, Chi Ho To. "Building a comprehensive chick retinal proteome dataset by liquid chromatography (LC) fractionation for tandem MS and SWATH analysis." Presented at 15th Human Proteome Organization World Congress, 2016 China.

Hu XIAO, Sze-wan Shan, Thomas C. Lam, Rachel Ka-man Chun, Chi Ho To. "Quantitative proteomics analysis of chick retina in response to nicotinic acid (NA) oral intake and lens-induced myopia (LIM)." Presented at The Association for Research in Vision and Ophthalmology, 2017, USA.

Hu XIAO, Sze-wan SHAN, Thomas C. Lam, Rachel Ka-man CHUN, Chi Ho TO. "Quantitative proteomics analysis of chick retina in response to nicotinic acid (NA) oral intake and lens-induced myopia (LIM)." Presented at International Conference of Vision & Eye Research, 2017, Hong Kong, China.

Acknowledgements

I would like to express my deepest gratitude to my supervisor Professor Chi-ho TO, for his guidance, support and encouragement. He always gave me professional suggestions and steer the direction of my scientific research.

I would like to thank Dr. Chuen Lam for his help and direction on proteomic experiment. I would also like to thank my labmates and friends Mr. King Kit LI, Dr. Sze-wan Shan, Dr. Ka-man Chun, Dr. Chi-wai DO, Ms. BIAN JingFang, Dr. Wang Panfeng, Dr. BING Zuo, Dr. WANG JianChao, Dr. WANG DanYang, Dr. CHEN BingJie, Ms. Fengjuan YU, Mr. Ka Lok LI, Mr. Ka Wai CHEUNG, Ms. Hoi Lam LI and Dr. Dennis TSE for their continuous help and friendship.

Finally, I would like to give sincere and heartfelt thanks to my parents and XIN Wen for their patience, support and understandings.

Table of contents

Chapter 1: Introduction

1.1 Myopia

1.1.1 Background

A normal or emmetropic eye is capable of receiving sharply focused image of a distant object onto the retina. At near, when the image falls behind the retina, accommodation is triggered so that the image is re-focused onto the retina by the crystalline lens (Morgan et al., 2012). In a hyperopic eye, the image of a distant object is formed behind retina, and it can be re-focused by exerting accommodation (Morgan et al., 2012). Whereas in the case of myopic eye, the image of a distant object is formed in front of the retina and cannot be re-focused by accommodation (Morgan et al., 2012).

Refractive status of an eye can be defined by the axial length of the eye and optical power of cornea and lens (Morgan et al., 2012). Axial length includes of anterior chamber depth, lens thickness and vitreous chamber depth (Morgan et al., 2012).

Most animals, including human, are born with hyperopia and the axial length of eyeball is too short for its optical power (Morgan, 2003). With time, the eye continues to grow in a regulated manner so that the retinal focal plane can eventually match with the optical power of the eye (Morgan, 2003). This vision-dependent process of eye growth is called

“emmetropization” (Morgan, 2003). When the retinal focal plane successfully matches with the optical power, the emmetropization process is said to be completed and the eye becomes emmetropic or free of any refractive error (Siegwart and Norton, 2011, Morgan, 2003). In human, most children are born with hyperopia (Cook and Glasscock, 1951). The refractive errors of these children are normal distribution (Mayer et al., 2001). After one or two years old, this distribution narrows and the mean is about +1 to +2 dioptres (D) (Mayer et al., 2001). At this moment, the corneal optical power becomes stable (Gordon and Donzis, 1985). The optical power of lens decreases rapidly until 12 years old and slowly decreases in adult (Gordon and Donzis, 1985, Jones et al., 2005). The eyeball continues to grow with the body until 14 to 17 years old (Morgan, 2003). It suggests that axial elongation acts to match with the optical power until body growth ceases, even if the eye has reached emmetropia (Morgan, 2003). Axial length is the most important factor in considering myopia development (Morgan, 2003, Morgan et al., 2012). In fact, the elongation of vitreous chamber depth which is a major component of axial length has the strongest correlation to refractive and myopic development (Morgan et al., 2012).

Due to unknown reasons, eye growth may fail to match with the focal plane and ends up either before or behind the focal plane, hyperopia or myopia will be resulted respectively (Siegwart and Norton, 2011, Morgan, 2003). In

many animal models, these phenomena can be reproduced by imposing different optical inputs to the eye (Meng et al., 2011). It is known that positive optical lenses produce myopic defocus and form its image formed in front of the retina; whereas negative optical lenses impose hyperopic defocus which focuses image behind the retina. By applying these defocus signals, different animal models were produced: imposing myopic defocus (with positive lens) to developing animal eyes can retard eye growth and it is called lens induced hyperopia (LIH); while projecting hyperopic defocus (with negative lens) can accelerate eye growth and is called lens induced myopia (LIM) (Morgan, 2003). In addition, translucent lens can induce myopia development that is called form deprivation myopia (FDM) (Morgan, 2003).

1.1.2 Epidemiology

Recent studies reported that there is a myopia "boom" in the developed countries in East and Southeast Asia (Dolgin, 2015, Morgan et al., 2018) which have a high prevalence of high myopia (Morgan et al., 2018, Dolgin, 2015). The estimated number of myopia and high myopia is 5 billion and 1 billion respectively by 2050 (Holden et al., 2016). It predicted that almost half of the world population will be myopic, with 10% of highly myopic population by 2050 (Morgan et al., 2018, Holden et al., 2016). Morgan et al have reported that 80-90% young persons (17-18 years old) were myopic in

developed countries of East and Southeast Asia (Morgan et al., 2012, Morgan et al., 2018). This is in stark contrast to the western world where the prevalence of myopia was around 20%-40% (Morgan et al., 2012, Cumberland et al., 2015). The prevalence of myopia was even lower at 5-10% in under-developed countries in the world (Soler et al., 2015, Anera et al., 2009, Morgan et al., 2018).

High myopia is usually defined as more than -6D, moderate myopia as from -3D to -6D and mild myopia as less than -3D. Morgan et al (Morgan et al., 2017) have further shown that the prevalence of high myopia increased even faster than the total myopia population. In East and Southeast Asia, the prevalence of high myopia in young adults (17-18 years old) is about 10-20% (Morgan et al., 2018). Indeed, it was evident that there were more high myopes in the young population than the old population (Asakuma et al., 2012, Liu et al., 2010). It was reasoned to be due to both an increase in the prevalence of high myopia in young children as well as an early onset of myopia (Morgan et al., 2018). Pathological myopia develops frequently in high myopia with characteristic ocular degeneration and vision impairments (Morgan et al., 2012). Pathological myopia typical results in degenerative changes in the retina, choroid and sclera (Morgan et al., 2012, Jones and Luensmann, 2012). These progressive pathological changes could lead to significant eye diseases and blindness, such as glaucoma (Nitta et al., 2017, Chen et al., 2012), cataract (Leske et al., 1991) and retinal detachment and

degeneration (Saw, 2006, Jones and Luensmann, 2012). Therefore, it is important to control myopia so as to save sights in these myopic populations and beyond. In addition, it has been proposed that myopia is more than a public health issue, but also is a socioeconomic problem affecting the community as well as the individually profoundly (Zheng et al., 2013, Dolgin, 2015, Morgan et al., 2012).

1.1.3 The etiology of myopia

Hereditary factors of myopia

Hereditary factors have been considered important in myopia development (Parssinen et al., 2019, Sorsby and Fraser, 1964). Children whose parents are myopic are of high risk to become myopia, especially high myopia (Mutti et al., 2002, Ip et al., 2007). Researchers have suggested that myopic parents share not only the "myopic genes" with their children, but also the living environments (Morgan et al., 2018, Morgan et al., 2012). Unexpectedly, clustering analysis of these family data has shown that hereditary factor did not appear to be an important factor in myopia development (Morgan et al., 2012). While myopia has become very prevalent in East and Southeast Asia in recent years, its prevalence could not have been due to the presence of many myopic parents in the region in the first place. Therefore it argues against genetic factor as being the more

important factor than environmental ones in explaining the recent myopia boom (Morgan et al., 2012). In addition, the hereditary factors also failed to explain the speed of the increasing in the prevalence of myopia (Morgan et al., 2018). However, other studies have argued that both the hereditary and environmental factors could influence the myopia development together (Morgan, 2003, Young, 2009, Baird et al., 2010, Wojciechowski, 2011).

Environmental factors of myopia

Environmental factors of myopia are widely believed to be important in myopia development (Goss, 2000, Hepsen et al., 2001, Saw et al., 2002). They include outdoor time, near work and education level (Morgan et al., 2012, Ip et al., 2008a, Morgan et al., 2018, Greene and Medina, 2016, Goss, 2000). Zylbermann et al have reported the students who spent a lot of time on reading had more and higher myopia than those who read less (Zylbermann et al., 1993). Others have reported the prevalence of myopia is higher in urban areas, suggesting that city-like environment may be more myopigenic (Ip et al., 2008a, Paritsis et al., 1983). Ting et al have shown that microscopists have a higher risk of developing myopia and sustained accommodation may have been the culprit (Ting et al., 2004). When focusing at near objects, the eye exerts accommodation to bring the focal plane onto the retina from behind (Gwiazda et al., 1993, Seidemann and Schaeffel, 2003) and clear the blur image brought by near objects (Abbott et

al., 1998). The sustained accommodative effort in extensive near work has been thought to lead to myopia development (Charman, 1999). In addition to excessive near work and reading, overcrowded environment might also promote myopic eye growth (Ip et al., 2008b).

Rose et al have reported that more outdoor time can lead to less myopia in children (Rose et al., 2008). Jones et al have also reported that increasing outdoor time may decrease the risk of myopia in the children with myopic parents (Jones et al., 2007). In addition to having more open space, daytime outdoor environment also provides brighter light which may be another essential factor in modulating eye growth (Rose et al., 2008). In fact, strong light could help retard myopic eye growth as evident in a number of animal experiments (Maimone, 2008, Backhouse et al., 2013).

1.1.4 Treatment of myopia

There are two key goals in myopia control: to delay the onset of myopia and to retard myopia progression for existing myopes (Morgan et al., 2018). Before myopia developed in children, more outdoor time can effectively delay the onset of myopia (Morgan et al., 2018, Morgan et al., 2012). After myopia has developed, the focus of control should be on the retardation of axial elongation of the eyeball (Morgan et al., 2012, Morgan et al., 2018).

Outdoor interventions for myopia control

Increasing time of outdoor can inhibit both the onset of myopia and axial elongation (Rose et al., 2008, Jones et al., 2007, Wu et al., 2013). The bright outdoor light has been showed to slow the onset as well as the progression of myopia development (Wu et al., 2013). In addition, outdoor light can increase the production of vitamin D which may also inhibit myopia development (Mutti, 2014). Retinal dopamine was known to increase with bright light and it acts to slow eye growth (Zhou et al., 2017, Chen et al., 2017). A number of studies have shown that increase in brightness of artificial lighting illumination can retard LIM and FDM in animals (Ashby et al., 2009, Smith et al., 2012, Ashby and Schaeffel, 2010, Smith et al., 2013). Indeed, bright indoor lighting has been shown to protect eye from myopia development in human (Hua et al., 2015). In addition to bright light, outdoor environment generally has less myopigenic hyperopic defocus in the entire visual field as compared to indoor environment (Cooper and Tkatchenko, 2018).

The wavelength of light is different between outdoor and indoor conditions (Torii et al., 2017a, Torii et al., 2017b). Different indoor light sources can generate different spectra of wavelength (Torii et al., 2017a, Torii et al., 2017b). Moreover, the glass windows may filtrate out short wavelength light, such as violet light (Torii et al., 2017a, Torii et al., 2017b). It was found that blue light can slow myopic and normal eye growth in guinea

pigs, while green light can promote eye growth (Liu et al., 2011, Jiang et al., 2014). Whereas, red light may promote myopic development and prevent the LIH effect in guinea pigs (Liu et al., 2011, Jiang et al., 2014). In chicks, blue light can also slow eye growth while red light promotes myopia development (Rucker and Wallman, 2009, Seidemann and Schaeffel, 2002). The exact mechanism of wavelength control eye growth is still unclear at present.

Optical strategies for myopia control

To prevent excessive accommodation and myopia development, a number of clinical studies have been conducted using progressive addition lenses (PAL) (Gwiazda et al., 2004, Gwiazda et al., 2005, Leung and Brown, 1999, Edwards et al., 2002). Using addition powers of +1.5 or +2.0 D, PAL was shown to be effective in slowing myopia development by 0.25D per year (Li et al., 2011).

A number of studies have indicated that the peripheral retina was the most important part in myopia or hyperopia induction (Smith et al., 2009, Smith et al., 2005). Sankaridurg et al (2010) has indicated that the peripheral hyperopic defocus was the main cause of myopia progression. They designed a lens which corrected the peripheral hyperopic defocus, but it has no significant effect on the retardation of myopic development (Sankaridurg et al., 2010). Tse et al (2011) has explored the effect of the novel dual plane

lens con system on chicks' eye growth (Tse and To, 2011). It showed that the myopic or hyperopic development was closely related to spatial ratio of defocus (Tse and To, 2011). Higher proportion of myopic defocus led to hyperopia development, while higher proportion of hyperopic defocus promoted myopia progression (Tse and To, 2011). A similar study has shown that dual power lens could inhibit myopic progression (Liu and Wildsoet, 2011). Carly et al (2013) has designed a novel defocus incorporated soft contact (DISC) to explored the inhibition effect on myopic eye growth in Hong Kong (Lam et al., 2014). This clinical trial showed that DISC can significantly control myopic development compared to single vision lens after 2 years (SER was less -0.20D and AXL shorter 0.11mm)(Lam et al., 2014). Most recently, Lam et al (2017) have designed a novel spectacle called defocus incorporated multiple segments (DIMS)(Lam and To, 2017). This lens, with center correction SER zone and periphery separated and multiple myopic defocus segments, can significantly inhibit myopic progression by about 60% after 3 years in 160 Chinese myopic children (Lam and To, 2017).

Orthokeratology (OK) has been used widely in the clinic for myopia control with significant effect (Villa-Collar et al., 2019, Lipson et al., 2018). Cho et al (2005) has explored the OK lens effect on children myopic development comparison to single vision lens in Hong Kong for 2 years (Cho et al., 2005). The study showed that the OK lens can significantly slow eye

growth, the changes of axial length (AXL) and vitreous chamber depth (VCD), early as 6 months after treatment, and continued to the end of experiment (2 years) (Cho et al., 2005). But the spherical equivalent refractive error (SER) did not significantly change from 6 to 24 months (Cho et al., 2005). The Corneal Reshaping and Yearly Observation of Nearsightedness study (CRAYON) has been reported by Walline et al in 2009(Walline et al., 2009). This CRAYON study compared the effect of OK lens to soft contact lens (data from the Contact Lens and Myopia Progression study, CLAMP) (Walline et al., 2004, Walline et al., 2009). It showed that OK lens can inhibit myopic development more than soft contact lens (VCD less 0.10mm and AXL less 0.16mm annually) (Walline et al., 2009). However, cessation of OK lens wear may accelerate eye growth (Cho and Tan, 2018). The underlying mechanism of controlling myopic development by OK is still unclear now (Cho and Cheung, 2012, Kakita et al., 2011, Chen et al., 2013, Cho et al., 2005, Cho and Tan, 2018). Some studies have hypothesized that OK lead to the peripheral myopic defocus (Queiros et al., 2010, Kang and Swarbrick, 2011, Ticak and Walline, 2013). Seven months after discontinuation OK lens treatment, in 8-14 years old children, the myopia development was rebounded but could be well controlled when OK lens was resumed (Cho and Cheung, 2017).

Pharmacological approach

In recent year, the use of low dose atropine has gained popularity as a mean to control myopia. Atropine is a competitive antagonist of muscarinic acetylcholine receptor (Matesic and Luthin, 1991). Atropine can paralyze the ciliary muscles and produces cycloplegia – a loss of accommodation (Tran et al., 2018). Early in 1874s, Derby et al firstly suggested the use atropine to control acquired and progressive myopic development (Derby, 1874). Later studies have found that atropine can inhibit myopia development in animals without affecting the accommodative mechanism (McBrien et al., 1993). In addition, atropine was still effective in slowing eye growth even after the optic nerve was cut (Schaeffel et al., 1990) where accommodative system was abolished (Troilo et al., 1987a). These studies indicated that atropine's effect on slowing eye growth may not be through the accommodative pathway (McBrien et al., 1993). However, the exact mechanism of how atropine works is still unclear.

There are a number of known side effects of prolonged usage of atropine in myopia control. Since atropine leads to mydriasis and loss of accommodation, people may experience photophobia and require optical correction for near vision. Moreover, eyes are exposed to more UV light with mydriasis which could be conducive to developing cataract and retinal damages (Chia et al., 2012, North and Kelly, 1987). Clinically, Chiang et al have reported 1% atropine can significantly inhibit human myopia

development when applied once a week (Chiang et al., 2001). The myopia progression in the treatment group was slowed by 0.08D per year, while the control group developed myopia at a rate of 0.23D per year (Chiang et al., 2001). Similarly, Chua et al have found that 1% atropine strongly inhibited myopic growth to 0.14D per year comparing to the control group of 0.6D per year.

The dose-response characteristic of atropine on myopia control has been comprehensively studied. Shih et al have studied the dosing effect of atropine at 0.5%, 0.25% and 0.1% nightly on eye growth (Shih et al., 1999). The increase in myopia was 0.04D per year in 0.5% group, 0.45D per year in 0.25% group and 0.47D per year in 0.1% group (Shih et al., 1999). During 2 years of atropine treatment, patients did not experience myopic development 61% in 0.5% group, 49% in 0.25% group and 42% in 0.1% group (Shih et al., 1999). In other studies, 0.01% atropine has been proposed to be effective and clinically acceptable for myopia control (Chia et al., 2012, Chia et al., 2014, Tong et al., 2009). It was found that 0.01% atropine can effectively control myopia development and it has minimal side effect to the eye (Chia et al., 2012, Chia et al., 2014). They have also reported that long term use of 0.01% atropine was successful in controlling myopia for five years (Chia et al., 2014, Chia et al., 2012, Yam et al., 2019). Yam et al (2019) has explored the effect of gradient low concentrations of atropine on myopic progression (Yam et al., 2019). The 0.05%, 0.025% and

0.01% atropine were used to 438 myopic children by eye drop for 1 year (Yam et al., 2019). All of these three concentrations of atropine eye drop could significantly slow myopic progression (Yam et al., 2019). The most effective concentration was 0.05% (Yam et al., 2019).

To optimize the myopia control effect, studies have advocated combination of OK and low dosage atropine (Kinoshita et al., 2018). With OK and low dosage atropine (0.01%) together, a recent study has shown that the axial length of the treatment group increased by only 0.09mm after one year; whereas in OK only group, the change of axial length was 0.19mm (Kinoshita et al., 2018). A similar study has indicated that combination of 0.01% atropine and OK significantly inhibited axial elongation after one month treatment than OK only (Tan et al., 2019). The Change of axial length after one month was 0.05mm in combination of 0.01% atropine and OK group, while 0.02mm in OK only group (Tan et al., 2019).

1.2 Animal study

1.2.1 Animal model

The provision of suitable animal models allow a variety of factors be manipulated in experiments and studies related to myopia and eye growth (Schaeffel and Feldkaemper, 2015). These animal models have greatly contributed to the advance of myopia research in recent years. (Schaeffel

and Feldkaemper, 2015).

Chick

Chick was first used as animal myopia model as early as 1978 (Wallman et al., 1978) and it remains the most commonly used animal models for myopia research. The advantages of chick as myopia animal model include (i) good optics of the eye, (ii) its visual acuity is fully developed within 48 hours of hatching (Over and Moore, 1981), (iii) its ability of identifying colours (Osorio et al., 1999), (iv) fast growth and turn around rate, (v) low rearing cost, (vi) its ability to detect and compensate for small optical defocus as low as 1D, (vii) its eyes being displaced laterally with independent accommodation - this is beneficial in myopia research as it minimizes the interaction between two eyes (Schmid and Wildsoet, 1997). In chick, the process of emmetropization starts from hatching and lasts for about two months (Wallman et al., 1981). During this period, the growing eye can be induced to become myopic or hyperopic by negative (LIM) or positive lenses (LIH) respectively (Norton, 1999). The range of optical powers being able to compensate by chick eye ranges between +25D to -30D (Irving et al., 1992). However the time window of plasticity or sensitivity to LIH or LIM declines with age (Irving et al., 1992).

Tree shrew

In 1977, Sherman et al proposed that tree shrew can be used as a myopic animal model (Sherman et al., 1977). There are many advantages of tree shrew for myopia experiment (McBrien and Norton, 1992). Tree shrew is a mammalian species and it possesses similar emmetropization mechanism and refractive development as in the human (Schaeffel and Feldkaemper, 2015). Moreover, tree shrew can be readily induced to myopia and hyperopia by optical lenses and induced myopia by form deprivation (Schaeffel and Feldkaemper, 2015). In addition, being a mammalian species similar to human, tree shrew can be subjected to genetic and proteomic studies by relating to databases of the human (Schaeffel and Feldkaemper, 2015).

Guinea pig

In 1995, McFadden et al reported guinea pig can be a myopia animal model for the first time (McFadden and Wallman, 1995b). Being a tame animal, guinea pig is easy to handle, treated and manipulated for experimentation (Schaeffel and Feldkaemper, 2015). since guinea pig is also a mammalian species, it likely shares similar underlying mechanism on myopia development with human (Schaeffel and Feldkaemper, 2015). Guinea pig have big eyes which are easy to measure and provides abundant materials for laboratory analysis (Schaeffel and Feldkaemper, 2015). Guinea pig can

be subjected to LIM, LIH and FDM and produces refractive changes very similar to chick and tree shrew (Schaeffel and Feldkaemper, 2015, Howlett and McFadden, 2006). The visual acuity of guinea pig is good and sits between that of the chick and tree shrew (Schaeffel and Feldkaemper, 2015).

Monkey

In 1978, Raviola et al studied the eye growth of rhesus monkey (Raviola and Wiesel, 1978). In all myopia animal models, rhesus monkey is perhaps the closest to human in terms of its physiology. It has a fovea and other similar ocular structures as human (Raviola and Wiesel, 1978). Rhesus monkey has better visual acuity than chick (Schaeffel and Feldkaemper, 2015). However, they are expensive as experimental model and its growth rate is slow. Usually, they are employed for confirmation purposes of findings from other animal models before human study is considered (Schaeffel and Feldkaemper, 2015).

Mouse

Mouse is the most widely used animal model in nearly all biological research (Schaeffel and Feldkaemper, 2015). Mouse models are frequently engineered genetically or physiologically to express human diseases for research study (Szczerkowska et al., 2019, Tkatchenko et al., 2010b). The

anatomical structures, biochemical and genetic processes of mouse are well studied and characterised (Tkatchenko et al., 2010b). Mouse is easy to handle in the laboratory and is cheap with fast turn-over rate (Schaeffel and Feldkaemper, 2015). However, there are a number of disadvantages for mouse as a myopia animal model. The small eyeball in mouse renders treatment and measurement very difficult and inaccurate (Schmucker and Schaeffel, 2004, Schaeffel and Feldkaemper, 2015). It has poor visual ability and lacks of colour vision. In terms of the ocular anatomy, the mouse eye has no fovea and accommodation (Tkatchenko et al., 2010a, Schaeffel and Feldkaemper, 2015). Although it can be subjected to LIM and FDM, the growth responses from mouse were typically slow and the rate of developing significant refractive changes is slower than that in the chick, tree shrew and guinea pig (Schaeffel et al., 2004, Schaeffel and Feldkaemper, 2015).

Other animal models

The tilapia fish (Shen et al., 2005), zebra fish (Shen et al., 2005, Yeh et al., 2010), kestrel (Andison et al., 1992) and rabbit (Tokoro, 1970, Menezo et al., 1999) have all been described and used as myopia animal model for exploring myopia development and its underlying biochemical mechanism.

1.2.2 Lens induced myopia (LIM), lens induced hyperopia (LIH) and form deprivation myopia (FDM)

Lens induced myopia (LIM) and Lens induced hyperopia (LIH)

When negative lens is worn by animal, the eyeball elongates to match the retina with the focal plane of the lens. The imposed hyperopic defocus produces myopia in animal and this process is called lens induced myopia (LIM)(Morgan et al., 2013). On the other hand, positive lens projects myopic defocus to the animal eye and can slow down eye growth. This process is called lens induced hyperopia (LIH)(Morgan et al., 2013).

LIM and LIH can be established in many animal models as described above. They have contributed very significantly to our understanding of the biological and biochemical mechanism of ametropic development of the eye. Common animal models include chick (Schaeffel et al., 1988), tree shrew (Shaikh et al., 1999), guinea pig (Howlett and McFadden, 2009), mouse (Barathi et al., 2008), marmoset (Graham and Judge, 1999a), rhesus monkey (Hung et al., 1995) and fish (Shen and Sivak, 2007).

There are a number of anatomical changes occurred in LIM and LIH chick eyes (Wallman et al., 1995, Winawer and Wallman, 2002, Zhu et al., 2005). The thickness of choroid (CT) was significantly decreased with negative lens and increased with positive lens (Beresford et al., 2001, X et al., 2004, Zhu et al., 2005). Moreover, in the recovery from lens wear, the choroidal

thickness increased when the negative lens was removed in LIM or decreased when the positive lens was removed in LIH. The vitreous chamber depth (VCD) and axial length (AXL) typically increased significantly in the LIM; where with LIH, the VCD and AXL decreased significantly (Zhu et al., 2005, Winawer and Wallman, 2002).

Form-deprivation myopia （FDM）

In 1977, Wiesel et al reported that a translucent lens can induce significantly myopia in monkey (Wiesel and Raviola, 1977), but complete occlusion did not affect eye growth (Raviola and Wiesel, 1978). Translucent lens induced myopia is called form-deprivation myopia (FDM). Later studies found that the FDM process is reversible after the removal of the translucent lens (Zhou et al., 2007). Even after the cutting of optical nerve, the translucent lens could still induce myopia development (Troilo et al., 1987a) which suggested that the development of FDM may not require accommodation or any direct feedback from and brain (Cooper and Tkatchenko, 2018).

Many animal species could respond to FDM treatment and produce myopia; they include chick (Wallman et al., 1978, Troilo et al., 1987b), tree shrew (Sherman et al., 1977), guinea pig (Mcfadden and Wallman, 1995a), mouse (Schaeffel et al., 2004, Barathi et al., 2008), marmoset (Graham and Judge, 1999b), rhesus monkey (Smith et al., 1999), fish (Shen et al., 2005), rabbit (Verolino et al., 1999) and kestrel (Andison et al., 1992).

1.2.3 Retina is key to emmetropization, hyperopia and myopia development

Optical signals received by retina are usually transduced as electrical messages and biological signals. In this biological process, accommodation, retina, optic nerves were all thought to be important and working together to effect emmetropization and refractive development.

However, later studies has suggested that accommodation may not play an important role in LIM (Troilo, 1990) and FDM (Wildsoet, 2003). In addition, FDM could not be stopped by cutting the ciliary or optic nerves (Troilo et al., 1987b). In animals with damaged Edinger-Westphal nucleus, the eyes were still capable of being induced towards myopia by negative lens (Troilo, 1990). In addition, sectors of translucent occluders can induce myopia development in the corresponding part of the eye (Wallman et al., 1987, Wang et al., 2015). It has been shown that the size of the form deprived area on the retina correlated well with the amount of myopia developed in the chick eyes (Wang et al., 2015). Smith et al has explored which was the most essential part of retina to respond to myopic induction. After fovea ablated by laser, the infant monkeys could continuous emmetropization process (Smith et al., 2007). Moreover, the macular damaged eye could be induced myopia by diffuser lens (Smith et al., 2007).

After FDM, the macular ablation monkeys' eyes could recovery (Smith et al., 2005). The lens with center plus and periphery mines could lead to myopia development; on the contrary, the lens with center minus and periphery plus could contribute to hyperopia development in monkeys (Smith et al., 2009, Smith, 2011).

So, the retina is considered the most fundamental site in the emmetropization process, as well as in the development of hyperopia and myopia.

1.2.4 Retinal anatomy

Retina is an essential and innermost tissue of the eye. In the fourth week of embryogenic process, a pair of optic vesicles are developed from forebrain which is derived from neuroepithelium (Hosseini et al., 2014, Ali and Sowden, 2011). The optic vesicle grows and grooves as a cup which is called optic cup (Hosseini et al., 2014, Ali and Sowden, 2011). The optic cup consists of two layers, inner layer developing neurosensory retina and outer layer forming retinal pigment epithelium (RPE) (Hosseini et al., 2014, Ali and Sowden, 2011). The inner layer thickens and differentiates as rod cell, cone cell, bipolar cell and ganglion cell (Hosseini and Taber, 2018, Ali and Sowden, 2011). The gap of inner and outer layers decreases until disappearance in eye development process (Hosseini and Taber, 2018, Ali

and Sowden, 2011) (Figure 1.1). The photoreceptor cells (rod cell and cone cell) and RPE cells connect through RPE microvilli (Hosseini and Taber, 2018).

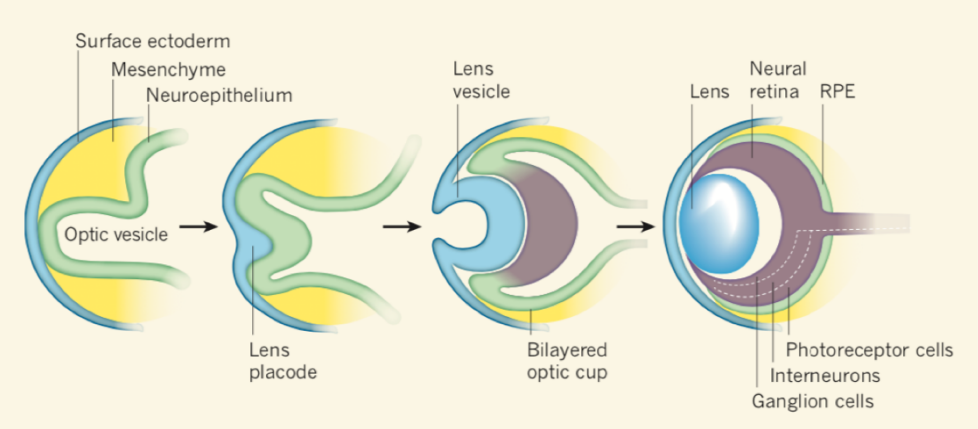

Figure 1.1 Schematic representation of retinal embryogenic process in embryonic stem cell. Modified from research article by Ali et al (Ali and Sowden, 2011).

The characters of neurosensory retina are transparent, thin, complex and light sensitive (Goldberg et al., 2016, Babel and Houber, 1970). The structure of retina is the same in all vertebrates, such as human and chick (Morris et al., 1976). There are ten layers of retina, including of inner limiting membrane layer, nerve fiber layer, ganglion cell layer, inner plexiform layer, inner nuclear layer, outer plexiform layer, outer nuclear layer, outer limiting membrane layer, photoreceptor layer and retinal

pigment epithelium layer (Babel and Houber, 1970, Goldberg et al., 2016, Hosseini et al., 2014).

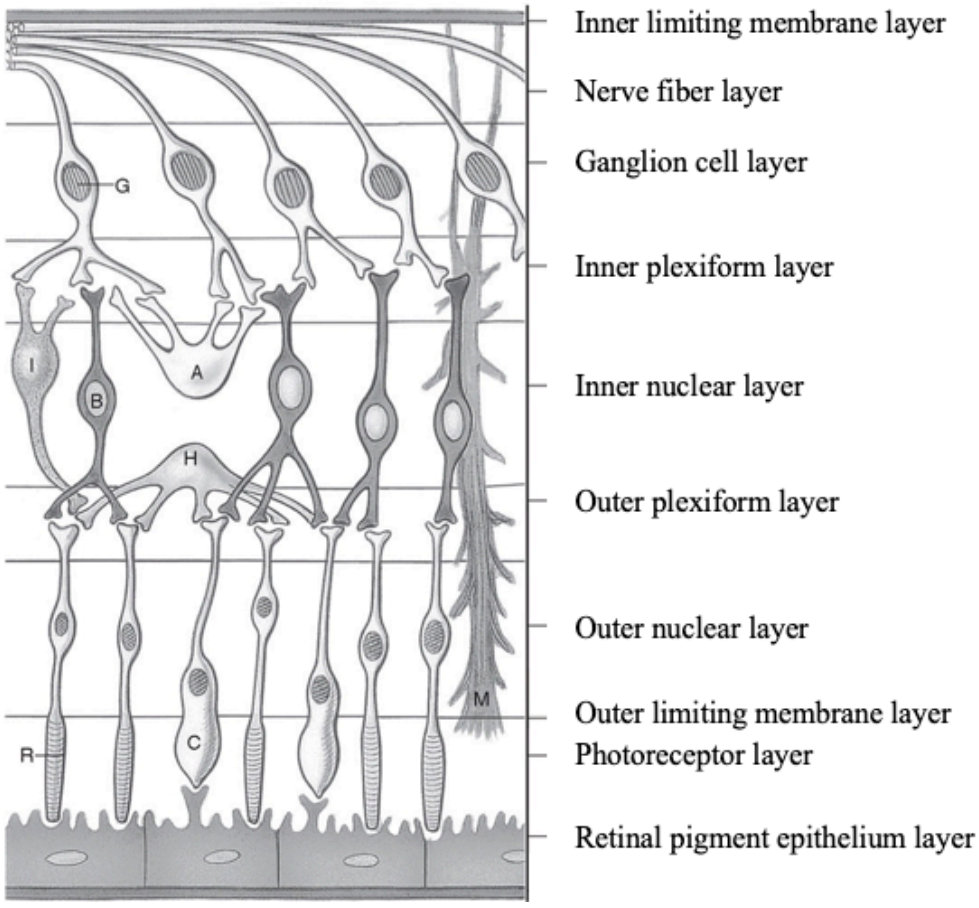

Figure 1.2 Schematic representation of retinal ten layers. Modified from page 131, Fundamentals and Principles of Ophthalmology, American Academy of Ophthalmology (AAO) (2016-2017) (Ophthalmology, 2016-2017).

Inner limiting membrane layer

The inner limiting membrane is composed of astrocytes and Müller cells. It is a membrane between vitreous body and retina (Ophthalmology, 2016-2017).

Nerve fiber layer

The nerve fiber is the axon of ganglion cell. It is from ganglion cell nuclei to lateral geniculate body which is the visual center in brain. The layer of nerve fiber between inner limiting membrane and ganglion cell is important to transmit visual signal from ganglion cell to lateral geniculate body (Ophthalmology, 2016-2017).

Ganglion cell layer

The ganglion cell layer consists of ganglion cell nucleus. Ganglion cell receives visual signal from bipolar cell and amacrine cell. Then, it transmits signal to lateral geniculate body by nerve fiber (Ophthalmology, 2016-2017).

Inner plexiform layer

The inner plexiform layer is a close reticulum neuronal synapse structure in histology image. It is connection of ganglion cell and amacrine and bipolar cells (Ophthalmology, 2016-2017).

Inner nuclear layer

The inner nuclear layer is composed by three kinds of cell nucleuses, including bipolar cell, horizontal cell and amacrine cell. These cells receive visual signal from photoreceptor cell and transmit to ganglion cell after integration (Ophthalmology, 2016-2017).

Outer plexiform layer

The outer plexiform layer is a reticulum neuronal synapse structure. It is the connection of horizontal and bipolar cell and photoreceptor cell (Ophthalmology, 2016-2017).

Outer nuclear layer

The outer nuclear layer consists of two kinds of cell nucleuses, including rod and cone cell. The rod and cone cell belong to photoreceptor cells. Rod cell is light sensitive but cone cell is color sensitive (Ophthalmology, 2016-2017).

Outer limiting membrane layer

The outer limiting membrane layer is a kind of network membrane to separate the nucleuses and inner segment of rod and cone cells (Ophthalmology, 2016-2017).

Photoreceptor layer

The photoreceptor layer is composed of the inner and out segments of rod and cone cells. It is the most important layer to receive light signal and transform to bioelectrical signals (Ophthalmology, 2016-2017).

Retinal pigment epithelium (RPE) layer

The RPE layer is a single layer from outer layer of neuroepithelium. This layer is between neurosensory retina and choroid. RPE can provide nourishment to neurosensory retina and light absorption (Ophthalmology, 2016-2017).

1.2.5 Biochemical factors

In eye growth, it can be conceptualised that there are two major group of factors that regulate eye growth - the "GO" factors that promote eye growth, and the "STOP" factors that slow down eye growth (Morgan, 2003). Previous studies have suggested that dopamine (Zhang and Wildsoet, 2015, Mao et al., 2010b), early growth response 1 (Fischer et al., 1999, Ashby et al., 2007a, Mathis and Schaeffel, 2007) and apolipoprotein A-1 (Bertrand et al., 2006) are "STOP" factors in myopia development. On the other hand, the "GO" factor include retinoic acid (McFadden et al., 2004a, Summers et al., 2016) and hypoxia factor (Wu et al., 2018a). Transforming growth

factor beta (TGF-β) (Rohrer and Stell, 1994) is unclear since the effect on eye growth is not consistent. The list of factors is ever increasing with time, but the full picture of the biochemical cascades is yet to be emerged. It probably awaits novel high throughput technology such as proteomics and the like to provide a more comprehensive picture (Bertrand et al., 2006).

Dopamine (DA) – Stop signal

DA is a well-known neurotransmitter and hormone (Berridge et al., 2009). It is essential to nerve system, including brain and eye (Witkovsky, 2004). DA can increase cone cell activity but decrease rod cell (Witkovsky, 2004). This may lead to enhance colour sensitivity at bright environment (Witkovsky, 2004). Stone et al (1989) has firstly reported that DA was close related to eye growth (Stone et al., 1989). Besharse et al (2016) has indicated that dopamine and melatonin were light and dark circadian regulator in animals (Besharse and McMahon, 2016). Megaw et al (2006) have reported that the up-regulation of DA and 3,4-dihydroxyphenylacetic acid (DOPAC) linearly response to light (Megaw et al., 2006). Feldkaemper et al (2013) has found that retinal DA may contribute to inhibition of myopic eye growth in children outdoor activity (Feldkaemper and Schaeffel, 2013). In FDM chicks' retina, the DA and DOPAC which is the metabolite of DA (Cohen et al., 1983) were significantly decreasing, as well as down-regulation in LIH (Papastergiou et al., 1998, Guo et al., 1995). Without deprivation, DA

increased to normal level (Pendrak et al., 1997). Gao et al (2006) has explored if DA can inhibit FDM in rabbits by intravitreal injection. The activation of DA, apomorphine was injected to chicks' vitreous chamber to slow eye growth (Iuvone et al., 1991). The precursor of DA, levodopa inhibit FDM development by intravitreal injection in guinea pigs (Mao et al., 2010a). Interestingly, the 6-hydroxydopamine can decrease dopamine, while it has been found to inhibit FDM (Li et al., 1992). Another similar study showed reserpine can inhibit dopamine but slow eye growth (Schaeffel et al., 1995). The reason of paradoxial effect of dopamine in myopic development is still unclear (Zhou et al., 2017).

Retinoic acid (RA) – Go signal

RA (all-trans-retinoic acid) is a vitamin A (all-trans-retinol) derivative (Duester, 2008). The main function is to promote cellular growth (Duester, 2008). RA can be produced by choroid and it affected the sclera extracellular matrix to promote eye growth (Mertz and Wallman, 2000, Troilo et al., 2006). McFadden et al (2004) has been shown that RA increased in myopic guinea pigs' eye and deceased in hyperopic eye (McFadden et al., 2004b). Moreover, oral administration of RA could promote eye growth (McFadden et al., 2004b). Huo et al (2013) has indicated that RA could activate retinoic acid receptor beta (RARβ) and then increase extracellular signal-regulated kinase (ERK 1/2) and c-Jun N-

terminal kinase (JNK)(Huo et al., 2013). The activation of ERK 1/2 and JNK could promote scleral fibroblasts proliferation (Huo et al., 2013). Summers et al (2016) has reported that apolipoprotein A-1 could bind with RA in choroid and then inhibited the effect of RA on scleral fibroblasts to slow eye growth (Summers et al., 2016).

Early growth response 1 (Egr-1) – Stop signal

Egr-1 also called as ZENK which is a well-known transcription factor (Knapska and Kaczmarek, 2004). It expresses swiftly to respond to different growth stimuli (Sukhatme et al., 1987). Commonly, egr-1 is known to influence cell proliferation (Calogero et al., 2004), differentiation (Shafarenko et al., 2005) and synaptic plasticity (Cole et al., 1989). Fischer et al (1999) has reported that egr-1 down-regulated in LIM and FDM, but up-regulated in LIH and recovery after FDM (Fischer et al., 1999). It suggested that egr-1 might be a stop signal in eye growth. Studies have also shown that the egr-1 expression decreased rapidly in LIM and FDM, while increased quickly in recovery from FDM (Ashby et al., 2010b, Ashby et al., 2007b). Schippert et al studied egr-1 null mice and found that these mice had longer eyeball than normal (Schippert et al., 2007).

Transforming growth factor beta (TGF-β)

TGF-β is an important multifunctional cytokine (Huang and Chen, 2012).

Its main function is about cell proliferation, differentiation and migration (Huang and Chen, 2012, Guo and Chen, 2012). Honda et al (1996) has reported that TGF-β could protect eye elongation and decrease in FDM (Honda et al., 1996). Jobling et al (2009) has found that TGF-β was down-regulated in myopic tree shrew and suggested it controlled the eye growth by the retinoscleral cascade (Jobling et al., 2009). Zhang et al (2016) have shown that TGF-β2 increased in LIH but TGF-β3 also increased in LIM (Zhang et al., 2016). Recently, the underlying mechanism and cascade of TGF-β in eye growth is unclear and awaits further study in the future.

Hypoxia factor – Go signal

Wu et al (2018) has profiled the signaling pathways in mice's sclera cell(Wu et al., 2018a). They have identified that hypoxia signaling pathway, eIF2 signaling pathway and mTOR signaling pathway were significantly up-regulated during myopia development (Wu et al., 2018a). Especially, hypoxia inducible factor 1 α (HIF-1α) was identified both in single cell RNA sequencing (scRNA-seq) in mice and genome wide association study (GWAS) analysis in human (Wu et al., 2018a). HIF-1α was found to be increased in myopic mice and guinea pig sclera (Wu et al., 2018a). On the other hand, the anti-hypoxia agent can inhibit myopic progression by inhibition of HIF-1α (Wu et al., 2018a). In addition, hypoxia environment induced type I collagen down regulation in human sclera (Wu et al., 2018a).

The down-regulation of type I collagen can lead to scleral extracellular matrix (ECM) remodel structure to thinner and then promote ocular axial elongation (Wu et al., 2018a, Wallman and Winawer, 2004, Siegwart and Norton, 2002, Gentle et al., 2003).

Apolipoprotein A-1 (ApoA1) – Stop signal

ApoA1 is a major protein of high-density lipoprotein in most animals (Mangaraj et al., 2016, Gorshkova et al., 2002, Gordon et al., 2016). In human, apoA1 gene encodes a protein of 28kDa (Shackelford and Lebherz, 1983) and it plays a key function in lipid metabolism by promoting liver excretion of cholesterol (Gorshkova et al., 2002, Rogers et al., 1998). Bertrand et al (2006) has reported that apoA1 has an inhibitory function in the development of myopia (Bertrand et al., 2006). Summers et al (2016) has studied that the apoA1 may bind with retinoic acid, and then played an important role in eye growth after birth (Summers et al., 2016). A recent study by Lam et al (2006) showed that the protein apoA1 was down-regulated in LIM and FDM chick retina after 3 days of treatment (Lam et al., 2006). From the above evidence, apoA1 has been considered as a key and early stop signal in the development of myopia (Lam et al., 2006, Bertrand et al., 2006, Summers et al., 2016). Interestingly, Sham et al (2010) have reported a correlation between breast feeding and more hyperopic refractive error in the young Singaporean population (Sham et al.,

2010). It was intriguing to postulate that since breast milk is rich in HDL (and hence apoA1), those breast-fed population may have received sufficiently high dose of apoA1 to remain as hyperopic (Rudnicka et al., 2008, Sham et al., 2010).

ApoA1 expression in the blood plasma could be increased clinically by nicotinic acid (Parsons and Flinn, 1959, Nagai et al., 2000, Sharma et al., 2006). A previous study has showed that there was 20%-30% increase in the HDL level in hyperlipidaemic patients after nicotinic acid treatment for 70 weeks (1-3g/day, mean dosage is 1.5g/day) (Birjmohun et al., 2004). The function of nicotinic acid is to decrease hepatic removal of apoA1while it has no effect on the synthesis of apoA1.The increase in HDL level is achieved by decreasing hepatic removal of apoA1(Parsons and Flinn, 1959) while the synthesis of apoA1 remained unchanged (Jin et al., 1997). The hepatic toxic dose of nicotinic acid is more than 3 g/day for adults (Knip et al., 2000) which can lead to a reversible acute toxic reaction called niacin maculopathy. It causes thickening of the macula, impairs vision and even leads to blindness (Gass, 1973). The solubility of nicotinic acid in water is 18g/L at normal room temperature and the routes of administration are intramuscular and oral administration in human.

Since apoA1 plays an important role in slowing myopia development in chicks (Lam et al., 2006) and nicotinic acid can raise the apoA1 in blood serum (Parsons and Flinn, 1959, Nagai et al., 2000, Sharma et al., 2006,

Lam et al., 2006), we hypothesized in the present study that nicotinic acid intake may have an inhibitory effect on myopic eye growth in chicks.

1.3 Methodology in this study

1.3.1 Western blot

Western blot is a classical and common analytical technique in relative quantification of protein expression (Kim, 2017, Hirano, 2012, Hnasko and Hnasko, 2015, Mahmood and Yang, 2012). It can separate proteins from samples by molecular weight by gel electrophoresis (Hnasko and Hnasko, 2015). Then, the separated proteins are transfer to a membrane (nitrocellulose or polyvinylidene difluoride, NC or PVDF) by electroblotting (Mahmood and Yang, 2012). In membrane, different molecular weight protein present as a specific band. Non-fat dry milk is used to block the area of no protein band in membrane (Kim, 2017). Specific primary antibody is used to identify and bind target protein. And secondary antibody is used to link the primary antibody and some enzyme or biotin to produce light signal to develop the protein band visible (Mahmood and Yang, 2012). The thickness or luminance of target band present the amount of specific protein (Mahmood and Yang, 2012).

Sample preparation

Sample preparation is the beginning of protein measurement process (Mahmood and Yang, 2012). Tissue are stored in -80 ºC fridge and lysed in liquid nitrogen to protect protein from denaturing (Hnasko and Hnasko, 2015). The protease inhibitors are usually included in lysis buffer (Mahmood and Yang, 2012). The homogenization and sonication are common method to break cell structure to extract proteins (Mahmood and Yang, 2012). In this study, our samples were chicks' retinas. Homogenization method was used to break chicks' retinal cell.

After proteins extraction, the same and appropriate amount of total proteins samples are mixed with loading buffer and boiled for proteins denaturation (Mahmood and Yang, 2012, Hirano, 2012). The main components of loading buffer are glycerol, dye and β-mercaptoethanol (Mahmood and Yang, 2012, Kim, 2017). Glycerol is used to add the density of samples to gather to the button of well (Mahmood and Yang, 2012). Dye is used to visualize sample, so that researcher to know the location of the front of proteins in each sample (Mahmood and Yang, 2012). β-mercaptoethanol is used to reduce disulfide bonds of proteins (Mahmood and Yang, 2012, Hnasko and Hnasko, 2015). β-mercaptoethanol and boiling can promote protein denaturation, so that the negative charge of amino acids is not neutralized. After denaturation, all proteins with negative charge can run in electric field.

Gel electrophoresis

Sodium dodecyl sulfate-polyacrylamide gel electrophoresis (SDS-PAGE) is commonly used in biochemistry for separating proteins (Hnasko and Hnasko, 2015, Mahmood and Yang, 2012). Polyacrylamide gel (PAGE) is a network structure which has molecular sieving effect. Sodium dodecyl sulfate (SDS) is an anionic surfactant which can sever the protein structure via breaking hydrogen and disulfide bonds (Mahmood and Yang, 2012, Liu et al., 2014). The SDS can cover the depolymerized proteins. The negative charge in SDS is significantly large than corresponding proteins. The SDS provides similar negative charge to each denatured protein before moving in electric field. So, the movement speed of each protein is only determined by molecular weight (Mahmood and Yang, 2012, Liu et al., 2014).

In SDS-PAGE gel, there are two sections with different PH value and acrylamide concentration, stacking (PH=6.8) and separating (PH=8.8) gels (Mahmood and Yang, 2012, Kim, 2017). The stacking gel is the up section with lower polyacrylamide concentration (Mahmood and Yang, 2012). It can allow proteins to go through easily but become sharp and thin bands at the boundary between stacking and separating gels (Mahmood and Yang, 2012). With higher polyacrylamide concentration, the separating gel can appropriately limit proteins running speed due to molecular size (Mahmood and Yang, 2012, Liu et al., 2014). The smaller proteins run faster than bigger proteins in electric field and separating gel (Mahmood and Yang,

2012). All the denatured proteins with SDS is negative charge. They can run from negative electrode to positive electrode in electric field (Mahmood and Yang, 2012, Hnasko and Hnasko, 2015). The higher voltage leads to faster movement, while the lower voltage leads to slower running. But the high voltage may result in distorted bands and overheat environment (Mahmood and Yang, 2012).

Blotting

When the smallest proteins arrive in the appropriate location, all the proteins will be transferred from SDS-PAGE gel to membrane (NC or PVDF membrane) by the other electric field which is vertical to gel electrophoresis process (Mahmood and Yang, 2012, Liu et al., 2014, Kim, 2017). The electric field can promote proteins migrating from SDS-PAGE gel to membrane surface (Mahmood and Yang, 2012). In blotting process, it is important to keep a cold environment since voltage may also lead to overheat environment as gel electrophoresis process (Mahmood and Yang, 2012, Liu et al., 2014).

Antibody incubation

Before antibody incubation, the blocking is an essential process to protect antibodies from attaching to membrane (Mahmood and Yang, 2012). There may be nonspecific development if antibodies bind to residual area of

membrane without corresponding proteins (Mahmood and Yang, 2012, Liu et al., 2014). The dried non-fat milk is diluted in Tris-Buffered Saline and Tween (TBST) buffer. This solution incubate membrane to block residual area of membrane (Kim, 2017, Mahmood and Yang, 2012).

After sufficient blocking, the membrane will be moved to primary antibody solution for incubation (Mahmood and Yang, 2012). And then, the membrane will be moved to secondary antibody for incubation (Kim, 2017, Hnasko and Hnasko, 2015). The antibodies (primary and secondary antibodies) are also diluted by TBST buffer. The primary antibody corresponds to target protein and the secondary primary antibody corresponds to primary antibody (Mahmood and Yang, 2012, Liu et al., 2014). The secondary antibody is a kind of label antibody with special radioisotopes, fluorophores or enzyme (Mahmood and Yang, 2012, Liu et al., 2014). The horseradish peroxidase (HRP) is widely used in western blot experiment (Liu et al., 2014, Mahmood and Yang, 2012). HRP is a stable, safety and inexpensive label enzyme. HRP can catalyzes the luminol oxidation to produce light signal (Mahmood and Yang, 2012).

Development and quantification

The beginning of development is luminol oxidation by HRP (Mahmood and Yang, 2012). The light signal is captured in a dark room (Mahmood and Yang, 2012, Liu et al., 2014, Hnasko and Hnasko, 2015). The luminance of

each band presents the amount of target proteins in each sample (Hnasko and Hnasko, 2015, Mahmood and Yang, 2012). The quantification is semi-quantitative but not absolute quantitative (Mahmood and Yang, 2012, Liu et al., 2014). The reasons are that the variations in loading and transfer rate (Liu et al., 2014, Mahmood and Yang, 2012).

1.3.2 Liquid chromatography tandem mass spectrometry (LC-MS)

Liquid chromatography tandem mass spectrometry (LC-MS) is a widely used analytical technique in chemistry, biochemistry, biotechnology and detection of environment, food and medicine (Pitt, 2009, Cappiello et al., 2002, Niessen, 2006). Liquid chromatography (LC) can separate components in mixture solution by physical theory (Pitt, 2009, Cappiello et al., 2002, Niessen, 2006). Mass spectrometry (MS) can measure the mass to charge (m/z) of charged ions by magnetic fields (Pitt, 2009, Cappiello et al., 2002, Niessen, 2006). The mass to charge ratio is unique and characteristic to component, such as fragments of peptides (Pitt, 2009, Niessen, 2006). After bioinformatic analysis, the corresponding of peptides and proteins can be identified specifically and sensitively (Pitt, 2009, Niessen, 2006). The tandem of LC physical separation and MS mass to charge ratio functions is LC-MS theory (Pitt, 2009, Cappiello et al., 2002, Niessen, 2006).

Sample preparation

The samples are lysed or homogenized in liquid nitrogen (described 1.3.1). Dithiothreitol is used to break disulfide bonds in proteins (Cleland, 1964). After breaking disulfide bonds, iodoacetamide was used to alkylate free sulfhydryl groups on the cysteine residues (Anson, 1940). The denatured proteins can be sufficiently digested into peptides by proteinase, such as trypsin which can cleave the proteins at the carboxyl side of the amino acids of lysine and arginine (Rodriguez et al., 2008). It is important to remove salts, detergent and other constituents which can lead to precipitate. Because they may clog or damage chromatography column and raise excessive pressure with LC system. This can significantly reduce chromatographic performance efficiency and also lead to final results unreliable. Moreover, the residual component may reduce the accuracy and efficiency of bioinformatic analysis.

Liquid chromatography

There are a lot of kinds of liquid chromatography, such as adsorption, partition, ion exchange, size exclusion and affinity chromatography (Niessen, 2006, Snyder et al., 2011). In this study, the ion exchange chromatography was used to separate component from mixture sample solutions.

Ion exchange chromatography can separate charged component by changing buffer PH (Niessen, 2006, Snyder et al., 2011). The amino acid is zwitterion based on carboxylic acid group and amino group (Niessen, 2006, Snyder et al., 2011). The carboxylic acid group can be deprotonated and carried negative charge in greater PH solution (Niessen, 2006, Snyder et al., 2011). On the contrary, the amino group can be protonated and carried positive charge in lower PH solution (Niessen, 2006, Snyder et al., 2011). The anion exchanger column is designed to catch the negative charge peptides and cation exchanger column is designed to catch the positive charge peptides in LC system (Niessen, 2006, Snyder et al., 2011).

In liquid chromatography, there are two phases which are stationary phase and mobile phase. In stationary phase, the peptides can attach to column and other contaminants are removed out. In mobile phase, the peptides can be wash out by charge and molecular size(Snyder et al., 2011, Niessen, 2006).

Mass spectrometry

Mass spectrometry is an analytical technique to measure the mass to charge ratio for each charged ion by electric or magnetic fields (Pitt, 2009, Niessen, 2006). There are three main components formed MS system, including ion source, mass analyzer and detector (Niessen, 2006, Pitt, 2009).

The ion source is an interface between liquid chromatography system and mass spectrometry system (Pitt, 2009). It is important to change the liquid

phase samples to gas phase and produce ions. The gas phase with charge ions can fly in vacuum and magnetic fields in mass spectrometry. There are two classical interfaces, electrospray ionization (ESI) and matrix-assisted laser desorption/ionization (MALDI) (Pitt, 2009, Lam et al., 2002, Cappiello et al., 2002). The ESI interface is used high voltage to change the liquid to aerosol with ions (Cappiello et al., 2002, Niessen, 2006). The ESI interface can generate multiply charged ions and extend the identification and measurement range of macromolecules. The MALDI interface is depends on laser energy absorbing matrix to change the solution to aerosol with ions. Both ESI and MALDI interface can separate and ionize macromolecules safety and completely.

The mass analyzer is vacuum space with electric or magnetic fields. In mass analyzer, the gas phase ions can fly under the electric or magnetic fields. There are different kinds of mass analyzer, including quadrupole, time of flight (TOF), ion traps and quadrupole time of flight (QTOF) (Heller et al., 2003, Bateman et al., 2002). QTOF analyzer was used in this study. The QTOF combine time of flight and quadrupole (four parallel rods arranged in a square formation) instruments together (Heller et al., 2003, Bateman et al., 2002). It is high sensitivity and accuracy in both identification and quantification analysis (Heller et al., 2003, Bateman et al., 2002).

The detector can detect ions and amplifies the signals to calculate the mass to charge ratio. All the signal will be transfer to display as data in computer to further bioinformatic analysis.

1.4 Research gaps and objectives

Myopia has become a hot research topic recently (Wu et al., 2016, Wong and Saw, 2016, Walline, 2016). A growing number of biochemical factors have been proposed that could promote or inhibit myopic development (Bertrand et al., 2006). However, the entirety of myopia mechanism and its related biochemical factors are yet to be fully revealed (Bertrand et al., 2006). In the current study, the major focus was to explore the underlying biochemical mechanism in myopic development firstly using high throughput experimental approach. The LC-MS approach was employed to identify and quantify the differential expression of proteins among LIH, LIM and normal growing chick retinas.

Among the large numbers of differentially expressed proteins and their related regulatory pathways, we have selected one of the most important and potential candidate proteins for further study. This candidate protein was apolipoprotein A-1 which has been implicated as an important eye growth signal in studies by Bertrand (Bertrand et al., 2006) and Summers (Summers et al., 2016).

In chapter 3, we asked if the chick retina can express apoA1 protein locally. The result showed that chicks' retina indeed expressed apoA1 mRNA. It follows that chick retina would also be able to produce apoA1 protein locally.

In chapter 4, the experiment studied if exogenous apoA1 protein could directly inhibit myopic development by intravitreal injection. Similarly, in chapter 5, the study was focused on nicotinic acid which can increase plasma apoA1 concentration. Nicotinic acid was administered to examine its effect on hyperopic, myopic and normal eye growth in chicks.

Chapter 2: Differential protein expressions in lens induced hyperopic (LIH) and myopic (LIM) chick retinas

2.1 Introduction

For myopia study, the most commonly used animal model is chick (detail description in chapter 1). The approaches where negative or positive lenses are attached to the animal eyes is called lens induced myopia (LIM) or lens induced hyperopia (LIH) (Morgan et al., 2013). In myopia development, the retina is considered as the first site of action in the emmetropization process. There are a host of biochemical factors that drive myopia development, such as dopamine (Zhang and Wildsoet, 2015, Mao et al., 2010b), apolipoprotein A-1 (apoA1) (Bertrand et al., 2006), retinoic acid (McFadden et al., 2004a, Summers et al., 2016), early growth response 1 (Egr-1) (Fischer et al., 1999, Ashby et al., 2007a, Mathis and Schaeffel, 2007) and TGF-β (Rohrer and Stell, 1994). The full picture of these biochemical factors and processes is still unclear (Bertrand et al., 2006). Understanding the underlying biochemical mechanism is important in devising effective control myopic in the future.

Bertrand et al (2006) has reported that apoA1 has an inhibitory function in the development of myopia (Bertrand et al., 2006). Summers et al (2016) suggested that apoA1 may act by binding with retinoic acid to effect downstream control in eye growth after birth (Summers et al., 2016). A recent study by Lam et al (2006) showed that the protein apoA1 in myopic

retina was down regulated in LIM and FDM chick retina after 3 days of treatment. However, the apoA1 expressions were not significantly different between the treatment and the control in LIM and FDM at day 7 (Lam et al., 2006). It is proposed that apoA1 may be considered as a key and early signal in the development of myopia (Lam et al., 2006, Bertrand et al., 2006, Summers et al., 2016).

Novel protein analysis strategies based on liquid chromatography tandem mass spectrometry (LC-MS) has become available and gained popularity (Domon, 2012, Collins et al., 2013). The sequential window acquisition of all theoretical fragment ion spectra (SWATH) is an advanced and widely used label-free strategy (Collins et al., 2013). With information dependent acquisition (IDA) method, a spectral ion library can be generated which is important to extract target fragment ions mass spectra from data independent acquisition (DIA) for quantification of proteomic dataset (Vowinckel et al., 2013). Shan et al (2018) has studied the differential expression proteins in normal guinea pigs retinas by SWATH strategy (Shan et al., 2018a). In that study, 3138 proteins were found at 1% FDR (Shan et al., 2018a, Shan et al., 2018b). Comparison of 3 days and 12 days old guinea pigs' retinas, 48 differential expression proteins were identified (Shan et al., 2018b, Shan et al., 2018a). With pathway analysis, these differential expression proteins were found to mainly belong to proliferation, glycogen energy and visual phototransduction pathways (Shan

et al., 2018a, Shan et al., 2018b). This study comprehensively profiled proteins differential expression in normal guinea pig retinas and revealed the related growth pathways in normal eyes (Shan et al., 2018b, Shan et al., 2018a). However, there are few studies exploring the proteomic pathways among LIH, LIM and normal chick retina by SWATH analysis. In this study, we firstly comprehensively profiled the protein expression and analyzed the underlying biological pathways in LIH, LIM and control chick retina.

2.2 Objective

The aim was to comprehensively profile differential protein expressions in LIH and LIM chick retinas using LC-MS (SWATH) method and to characterize the related biochemical cascades by pathway analysis. In addition, the study zoomed into the apoA1 protein expressions in LIH and LIM.

2.3 Materials and methods

2.3.1 Animal

White leghorn chicks (Gallus gallus) were hatched from specific pathogen free (SPF) eggs from Jinan, China at 37.5°C and 75% humidity for one month (Wang et al., 2015). After hatching, chicks were settled in the circumstance at 25℃ and 12/12 hours of light/dark cycle (Chun et al.,

2015). Water and food were refilled daily by staff from Centralized Animal Facilities (CAF), the Hong Kong Polytechnic University. All operations to animals in experiments strictly followed the ARVO regulation on the Use of Animals in Research and the Animal Subjects Research Ethic Subcommittee (ASEC)(Wang et al., 2015, Wu et al., 2018b).

2.3.2 Experimental design

For LIH experiment

Sixteen white leghorn chicks at 4 days after hatching (PN4) were randomly distributed into two groups (LIH group =8; plano group =8). All chicks were orally fed 1ml saline daily for 10 days (PN4 to PN14). The aim of saline oral administration was to keep the same experimental condition with the nicotinic acid treatment experiment in chapter 5. At PN10, +10D lens was attached to both eyes of LIH group chicks while plano lens to both eyes of plano group chicks. All chicks wore lenses for 4 days (PN10 to PN14). The measurements (refractive error and ocular parameters) were performed at PN4, PN10 and PN14 for all chicks.

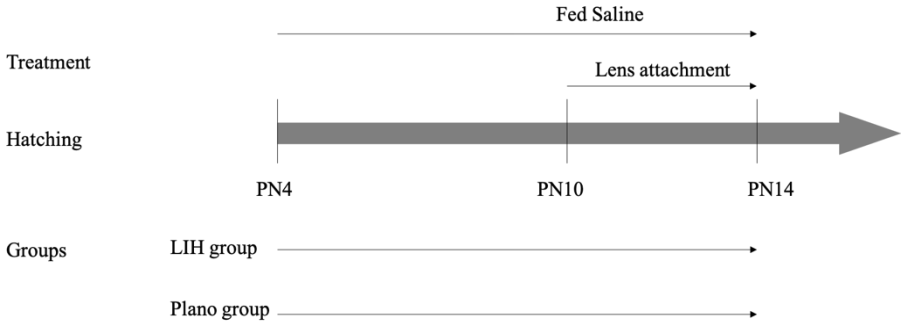

For LIM experiment

Sixteen white leghorn chicks at 4 days after hatching (PN4) were randomly distributed into two groups (LIM group =8; plano group =8). All chicks were orally fed 1ml saline daily for 10 days (PN4 to PN14). At PN10, -10D lens was attached to both eyes of LIM group chicks while plano lens to both eyes of plano group chicks. All chicks wore lenses for 4 days (PN10 to PN14). The measurements (refractive error and ocular parameters) were performed at PN4, PN10 and PN14 for all chicks.

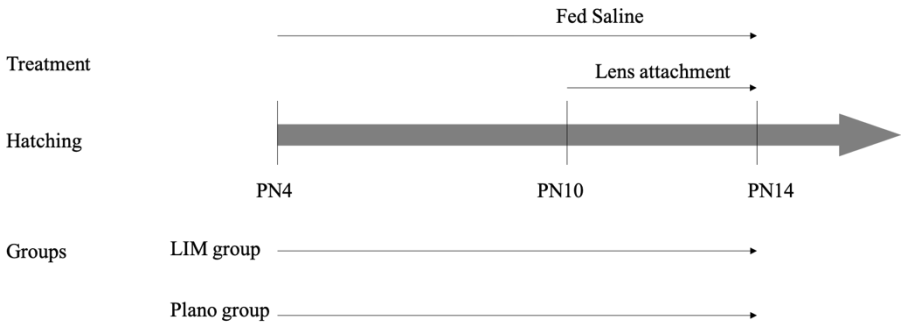

A cocktail of ketamine and xylazine (90mg: 10mg) was used to anesthetize chicks by 100mg/kg dose intramuscular injection. After anesthetization, transcardial perfusion was performed by phosphate-buffered saline (PBS) buffer 50ml per chick at a rate of 25ml/min. After transcardial perfusion, chicks were sacrificed by carbon dioxide overdose. The eyes were extracted without connective tissue and muscle and carefully washed by PBS buffer. The eyes were dissected on an iced package and retina sample collected

without vitreous body and retinal pigment epithelium (RPE) layer. Liquid nitrogen was used to quickly freeze the retinal samples which were stored at -80°C for later use.

For each chick, only the left eye was used for both statistical comparison (refractive error and ocular parameters) and protein differential expression analysis in this experiment.

2.3.3 Extraction of protein from retinal tissue

The frozen retina was homogenized with 300μl protein extraction buffer (table 2.3.1) at 1600×g for 7 minutes. The lysate was incubated in room temperature for 10 minutes and moved to 1.5ml Eppendorf tube with autoclaved. Spun at 16000×g for 20 minutes at 4°C, the supernatant was transferred into a new 1.5ml Eppendorf tube with autoclaved.

Table 2.3.1 Protein extraction buffer (PH = 8.0 - 9.0) for 10ml

Urea	7M
Tris	40mM
Thiourea	2M
Biolytes	0.2%
CHAPS	2%
ASB (Calbiochem, San Diego, CA, USA)	1%

Mini Protease inhibitor cocktail (Roche Applied Science, Switzerland)	1 tablet

2.3.4 Protein quantification

A protein quantification kit (Bio-Rad Protein Assay from Bio-Rad Laboratories Company) was used for measuring protein concentration in this experiment. The total protein concentration was determined by the change in absorbance of the solution as measured by Spectrophotometer SP-300 Plus (Optima, Japan) with 595nm. A standard curve was made with five concentrations (0, 0.2, 0.4, 0.6, 0.8μg/μl) by bovine serum albumin (BSA; 2μg/μl) and five corresponding absorbance. The total protein concentration was calculated by their absorbance as compared to a standard curve.

2.3.5 Western blotting

Each retinal sample (15μl volume and 25μg protein) was mixed with loading buffer (4×) and was incubated at 95°C for 5 minutes. Then, these denatured mixtures were loaded into a 10% sodium dodecyl sulfate–polyacrylamide gel (SDS-PAGE). The PageRuler^{TM} pre-stained protein ladder Plus (SM1811, Fermentas) was loaded as molecular weight markers. A constant voltage was applied at 60mV for 150 minutes for the electrophoresis. After electrophoresis, the proteins were separated by different molecular size and ready to be transfer to the polyvinylidene

difluoride (PVDF) membrane (Immuno-blot PVDF membrane, BioRed). The transfer apparatus was made of sponge, whatman paper, filter paper, gel, PVDF membrane, whatman paper, sponge from negative pole to positive pole. The Mini Trans-Blot Electrophoretic Transfer Cell system (Bio-Rad Protein Assay from Bio-Rad Laboratories Company) with transfer buffer and ice pack was used for transferring protein from gel to PVDF membrane. A constant voltage was set at 57V for 90 minutes. After transfer completed, the PVDF membrane was blocked into 5% non-fat dry milk (Nestle, Switzerland) in 1×TBSTbufferfor 1 hour at room temperature. The TBST buffer was made of 0.1M Tris-HCL, 0.5M NaCl and 0.05% Tween-20 (PH = 8.0). The primary antibody (Table 2.3.4) which was diluted by 0.3% non-fat dry milk in 1×TBST buffer was used to incubate PVDF membrane after blocking at 4°C over-night. The 1×TBST buffer was used to wash membrane thrice (20 minutes once) at room temperature. The secondary antibody (Table 2.3.2) which was diluted by 0.3% non-fat dry milk in 1×TBST buffer was used to incubate membrane at room temperature for 1 hour. After 1×TBST buffer thrice (20 minutes once) washing, the membrane was incubated into an enhanced chemiluminescent substrate mixture (Stable Peroxide Solution: Luminol/Enhancer solution= 1:1, SuperSignal® West Pico, Thermo Scientific) for 5 minutes at room temperature. The chemiluminescent signals were detected and captured as a

picture (TIFF format) and quantified by the Image Studio™ Software version 5.0 (LI-COR Corporate, US).

Table 2.3.2 List of antibodies

	Protein	Antibody	Dilution
Primary antibody	ApoA1	Rabbit anti-Chick ApoA1 polyclonal antibody	1:1000
	GapDH	Mouse anti-Chick GapDH polyclonal antibody	1:10000
Secondary antibody	ApoA1	HRP-Goat anti-Rabbit IgG (H+L) conjugate	1:2000
	GapDH	HRP-Goat anti-Mouse IgG (H+L) conjugate	1:40000

2.3.6 Library building for LC-MS (SWATH)

2.3.6.1 Sample preparation

Each retinal sample (75μg protein) was reduced by 8mM dithiothreitol (DTT) at 37°C for 1 hour. Iodoacetamide (20mM) was used to alkylate free sulfhydryl groups on the cysteine residues in the dark at 25°C for 30 minutes. 100% acetone was used for protein precipitation at -20°C for 12 hours. The sample was spun it at 16000×g for 20 minutes in 4°C and then the supernatant was removed and discarded. The protein pellet was washed

with 500µl 80% acetone, and spun at 16000×g for 20 minutes in 4°C. Subsequently, the sample was air-dried in room temperature after removing supernatant. A mixture (1M urea and 25mM ammonium bicarbonate) was used to dissolve the dry protein pellet at room temperature. After that, 20µg protein of the sample mixture was digested by 0.8µg trypsin (sample: trypsin= 25:1, w/w) at 37°C for 12 hours. After digestion, 0.5% formic acid was used to acidify the sample to stop digestion.

2.3.6.2 Liquid chromatography

For peptides fractionation, a pooled retinal protein sample (520µg total protein amount) from 37 chicks' retinas (10µg from each retina sample) was used to build a library. All these chicks were 14 days old and from six groups (plano group = 6; s group = 5; SA Minus10 group = 8; NA plano group = 6; NA LIH group = 4 and NA LIM group = 8). The Eksigentekspert^{tm} ultraLC 100 system (Sciex) integrated with a PolySULFOETHYL ATM Column that is 100×4.6mm column and 5µm porous (200 A°) from PolyLC INC was used to fractionate the peptides. Mobile buffer A contained 10mM ammonium formate (PH=3.0) and 25% CAN. On the other hand, Mobile buffer B contained 500mM ammonium formate (PH=6.8) and 25% ACN. The flow rate of is 0.2 ml/min with linear gradient: 0-10 minutes, 100% A; 10-50 minutes, 100-50% A; 50-55 minutes, 50% A; 55-65 minutes, 50-0% A; 65-80 minutes, 0% A.

For separation by liquid chromatography, 6µl each sample (3 µg) was separated in 120 minutes with Ekisgent 415 nano liquid chromatography system (Ion-exchange Chromatography). Peptides were loaded on a trap column (200 µm× 0.5 mm, ChromXP C18, 3 µm, 120 A) for desalting. The loading buffer was made of 5% v/v acetonitrile and 0.1% v/v formic acid. The flow rate was 3µl/min and loading time was 15 minutes. The samples were then injected into analytical column (Nano-LC column, 75µm×15cm, ChromXP C18, 3 µm, 120 A) for separation (table 2.3.3).

Table 2.3.3 Separation Parameter

Time (minutes)	Buffer A	Buffer B
1	95%	5%
120	95-65%	5-35%
4	65%	35%
6	65-20%	35-80%
10	20%	80%
2	20-95%	80-5%
17	95%	5%

Buffer A: 5% v/v acetonitrile and 0.1% v/v formic acid

Buffer B: 98% v/v acetonitrile and 0.1% v/v formic acid

2.3.6.3 Mass spectrometry

A TripleTOF 6600 mass spectrometer (QTOF, SCIEX) was used in this experiment. The electro spray ionization (ESI) parameter set as below (Table 2.3.4).

Table 2.3.4 ESI Parameter

Item	Setting
ISVF	2300 V
CUR	30 psi
GS1	15 psi
IHT	120 ℃

ISVF: ion spray voltage floating

CUR: curtain gas

GS1: ion source gas

IHT: inter face heater temperature

The IDA method was conducted at a range between 350 and 1500 m/z (250 ms accumulation time). Then, the MS/MS range was selected as between 100 and 1800 m/z (80 ms accumulation time). The high sensitivity mode was chosen as 40 intense ions (2-4V). The rolling collision energy (CE) was set as below (table 2.3.5).

Table 2.3.5 IDA Collision Energy Parameter

Charge	Slope	Intercept
Unknown	0.0575	9
1	0.0575	9
2	0.0625	-3
3	0.0625	-5
4	0.0625	-6
5	0.0625	-6

CE= (slope) × (m/z) + (intercept)

The DIA method was also conducted at a range between 350 and 1500 m/z (25 m/z fixed loop). The MS/MS setting was the same as the IDA method.

2.3.6.4 Protein identification and relative quantification

For building ion libraries, twenty fractions and one single injection pool sample were individually performed as the DDA acquisitions (3μg each). Protein identifications were searched against Uniprot gallus gallus database (version, 28849 entries) with ProteinPilot 5.0 software. The parameters were set to iodoacetamide as cysteine alkylation, trypsin as digestion enzyme, thorough as search effort and biological modifications as ID focus. The false discovery rate (FDR) was set as 1%. A fractionated library was grouped by combination of 20 fractionated DDAs, while a single injected library was

generated by the single injected pool DDA. The ion library was used to extract corresponding peptide fragment peak in further relative quantification analysis.

For relative quantification (SWATH) analysis, the PeakView 2.0 software (SCIEX) was used to extract corresponding peptide fragment peak via the ion library. The parameters were set to 6 fragments per peptide and 6 peptides per protein. At least 99% confidence and 1% FDR peptides were included to relative quantification without shared peptides and modifications. The ion library mass tolerance was 75 ppm, XIC Extraction Window was set at 20 minutes and XIC width was 75 ppm. Eleven high abundant peptides from different proteins covered 18 and 118 minutes were chosen for retention time (RT) alignment (Table 2.3.6). After RT alignment, the extracted peaks data were analyzed via MarkerView 1.2.1 software (SCIEX). The iPathwayGuide (Advaita Corporation, https://www.advaitabio.com) was used to pathway analyze from differential expression proteins.

Table 2.3.6 Peptides for retention time (RT) alignment

Peptides	RT (min)
IRDEMVATEQER	18.59
EPITVSSEQMC[CAM]K	27.14
GN[Dea]PTVEVDLYTHK	36.23

SVLQGGALDGVYR	42.73
DNLADDIMR	50.17
ADDGTPFVQMIK	54.62
YISPDQLADLYK	62.49
AVFVDLEPTVIDEVR	71.75
MEDTEPFSPELLSAMMR	87.17
GGILGDLTSSDVGVELPIILMHPK	97.19
SANLVASTLGAILNQLR	117.76

2.3.7 Statistical analysis

Statistical analysis was performed by SPSS software (version 23, SPSS, Chicago, Illinois, USA). The normality was tested by Shapiro-Wilk test. The levene's test was used to test for homogeneity. The refractive errors, ocular parameters, proteins differential expression in western blot and LC-MS SWATH were compared with a one-way ANOVA (parameter) or Kruskal-Wallis test (non-parameter). The data was reported as the mean ± SD and the P value less than 0.05 was considered statistically significant.

2.4 Results

2.4.1 LIH vs. Plano for 4 days

Comparison between LIH and plano for 4 day, the LIH eyes became significantly more hyperopic than the controls. The changes in VCD and

AXL in LIH eyes were significantly less than that of the plano lenses induced eyes. The changes in CT and SER in LIH eyes were significant when compared to that of the control eyes (with plano lenses). There was no significant difference in ACD, LT, RT and ST between LIH and control eyes (Table 2.4.1, Fig 2.4.1).

Table 2.4.1 The comparisons of ocular parameters and refractive error change after 4 days LIH

Treatment		N	Mean	Std. Deviation	Sig. (2-tailed)	
ACD (mm)	Plano	6	0.092	0.048	0.166	ǂ
	LIH	5	0.131	0.099		
LT (mm)	Plano	6	0.121	0.067	1.000	Ł
	LIH	5	0.109	0.066		
VCD (mm)	Plano	6	0.283	0.073	0.000	Ł
	LIH	5	-0.121	0.044		
AXL (mm)	Plano	6	0.496	0.062	0.000	Ł
	LIH	5	0.120	0.058		
RT (mm)	Plano	6	-0.011	0.028	0.079	Ł
	LIH	5	0.019	0.018		
CT (mm)	Plano	6	-0.010	0.047	0.000	Ł
	LIH	5	0.287	0.118		

ST (mm)	Plano	6	0.009	0.018	1.000	Ⱨ
	LIH	5	0.003	0.009		
SER (D)	Plano	6	-1.333	0.258	0.000	Ⱨ
	LIH	5	7.150	0.548		

ⱧP value for one-way ANOVA (Bofferroni)

ǂP value for Kruskal-Wallis test

After 4 days of LIH, the relative expression of apoA1 protein was detected by western blotting. The relative expression of apoA1 protein was normalized against GapDH which showed no significant difference between these two groups (Table 2.4.2, Figure 2.4.1).

Table 2.4.2 Relative expression of apoA1 protein normalized to GapDH after 4 days LIH

Treatment		N	Mean	Std. Deviation	Sig. (2-tailed)	
ApoA1/GapDH	Plano	5	0.259	0.092	0.067	ǂ
	LIH	5	1.283	0.929		

ⱧP value for one-way ANOVA (Bofferroni)

ǂP value for Kruskal-Wallis test

After 4 day of LIH, the quantification of apoA1 protein was performed by LC-MS (SWATH). The expression of apoA1 protein was significantly higher in LIH group than that of the plano group (Table 2.4.3, Figure 2.4.1).

Table 2.4.3 Quantification of apoA1 protein after 4 days LIH by LC-MS (SWATH)

Treatment	N	Mean	Std. Deviation	Sig. (2-tailed)	
Plano	6	4.6E+05	9.0E+04	0.026	ǂ
LIH	5	1.0E+06	5.7E+05		

ǂP value for oneway ANOVA (Bofferroni)

ǂP value for Kruskal-Wallis test

After SWATH analysis, there were 1227 proteins identified with at least 2 peptides per protein. 63 proteins were found to be changed by $|\log_2 (\text{fold change})| \geq 0.379$ and P-value < 0.05 (Figure 2.4.2).

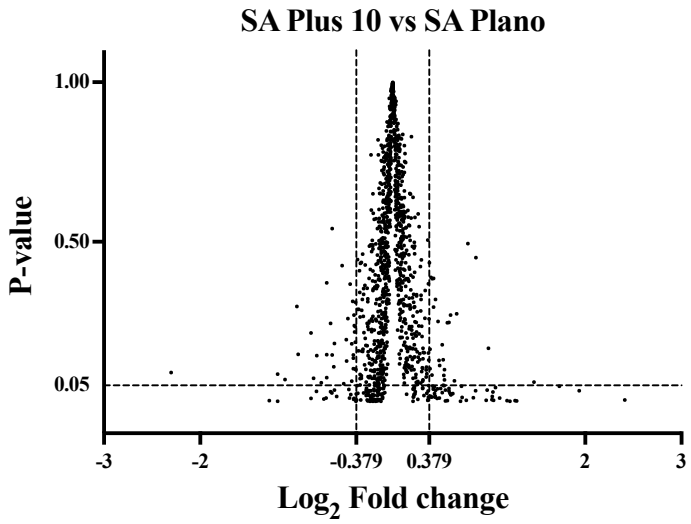

Figure 2.4.2 Volcano plot: All 1227 identified proteins (with at least 2 peptides per protein) are represented in terms of their Log2 fold changes (X-axis) and p-values of their change (Y-axis).

Among these 63 proteins, 17 proteins were found to be down-regulated while 46 proteins were up-regulated with LIH (appendix 2). These 63 proteins were categorized by Gene Ontology database (PANTHER classification system) classifications based on their molecular function, biological process, cellular component and protein class (below pie charts).

LIH vs. Plano

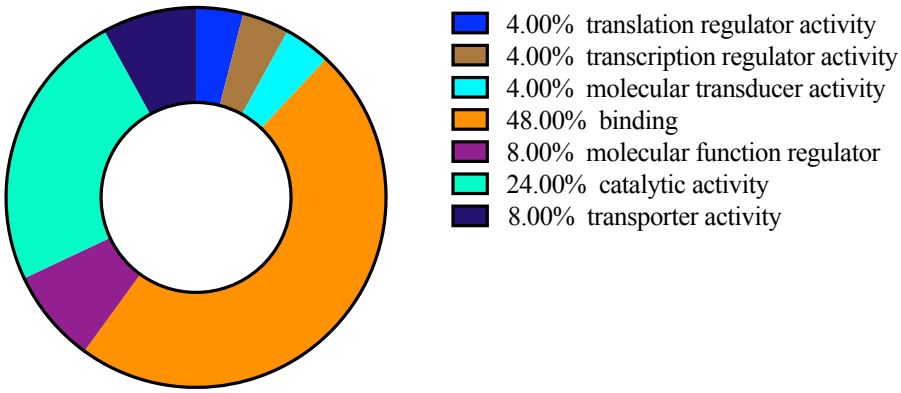

Molecular function

LIH vs. Plano

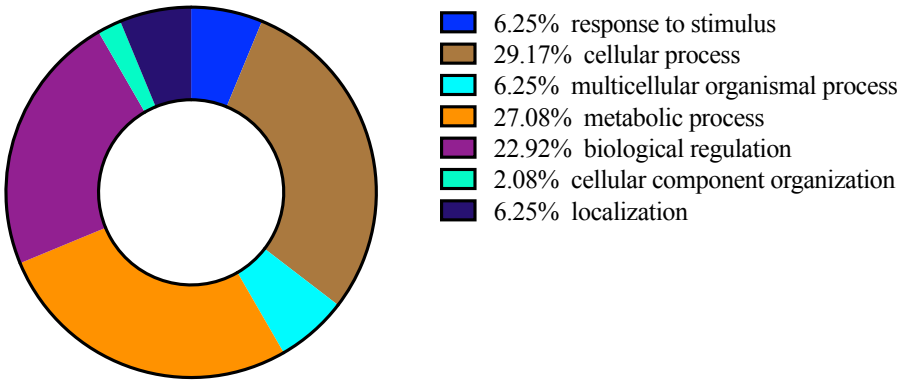

Biological process

LIH vs. Plano

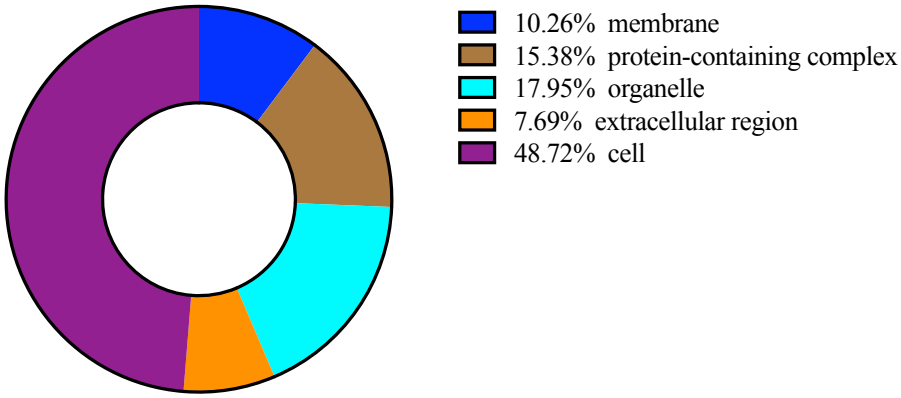

Cellular component

LIH vs. Plano

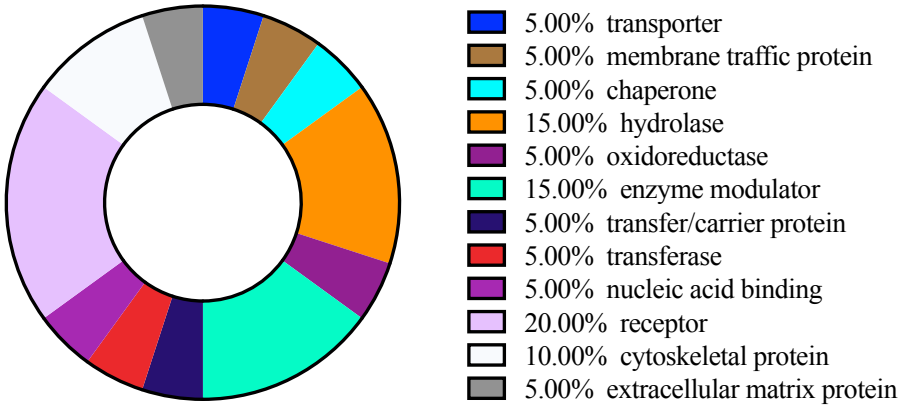

Protein class

Pathway analysis was performed via iPathwayGuide database (Advaita Corporation) (Table 2.4.4).

Table 2.4.4 List of the top identified pathways and up/down regulation genes

Pathway	Protein	
	Up regulation	Down regulation
Insulin signaling pathway	GYS	
Regulation of actin cytoskeleton	PIR121	ARP2/3
Endocytosis		ARP2/3, DNM3
PPAR signaling pathway	APOA1	

2.4.2 LIM vs. Plano for 4 days

Comparison between LIM and plano control eyes for 4 day, the LIM eyes became significantly more myopic than the controls. The changes in VCD and AXL in LIM eyes were significantly more than that of the plano control eyes. The changes in SER in LIM eyes were significantly less than that of the plano control eyes. There was no significant difference in ACD, LT, RT, CT and ST between LIM and plano control eyes (Table 2.4.5, Fig 2.4.1).

Table 2.4.5 The comparisons of ocular parameters and refractive error change after 4 days LIM

Treatment		N	Mean	Std. Deviation	Sig. (2-tailed)	
ACD (mm)	Plano	6	0.092	0.048	0.166	ǂ
	LIM	8	0.156	0.062		
LT (mm)	Plano	6	0.121	0.067	1.000	Ɨ
	LIM	8	0.113	0.061		
VCD (mm)	Plano	6	0.283	0.073	0.000	Ɨ
	LIM	8	0.713	0.084		
AXL (mm)	Plano	6	0.496	0.062	0.000	Ɨ
	LIM	8	0.983	0.093		
RT (mm)	Plano	6	-0.011	0.028	0.734	Ɨ
	LIM	8	-0.024	0.014		
CT (mm)	Plano	6	-0.010	0.047	1.000	Ɨ
	LIM	8	-0.002	0.037		
ST (mm)	Plano	6	0.009	0.018	0.363	Ɨ
	LIM	8	-0.003	0.012		
SER (D)	Plano	6	-1.333	0.258	0.000	Ɨ
	LIM	8	-8.875	0.463		

ƗP value for oneway ANOVA (Bofferroni)

ǂP value for Kruskal-Wallis test

After 4 days of LIM, the relative expression of apoA1 protein was detected by western blot. The relative expression of apoA1 protein normalized to GapDH was not significantly different between these two groups (Table 2.4.6, Figure 2.4.1).

Table 2.4.6 Relative expression of apoA1 protein normalized to GapDH after 4 days LIM

Treatment		N	Mean	Std. Deviation	Sig. (2-tailed)	
ApoA1/GapDH	Plano	6	0.553	0.404	0.598	ǂ
	LIM	8	0.257	0.165		

ǂP value for oneway ANOVA (Bofferroni)

ǂP value for Kruskal-Wallis test

After 4 days of LIM, apoA1 protein was quantified by LC-MS (SWATH). The expression of apoA1 protein was not significant different between these two groups (Table 2.4.7, Figure 2.4.1).

Table 2.4.7 Quantification of apoA1 protein after 4 days LIM by LC-MS (SWATH)

Treatment	N	Mean	Std. Deviation	Sig. (2-tailed)	
Plano	6	4.6E+05	9.0E+04	1.000	ǂ
LIM	8	4.3E+05	8.1E+04		

ǂP value for oneway ANOVA (Bofferroni)

ǂP value for Kruskal-Wallis test

In the SWATH analysis, there were 1291 proteins identified with at least 2 peptides per protein. 13 proteins were found to be changed by $|\log_2$ (fold change)$| \geq 0.379$ and P-value < 0.05 (Figure 2.4.3).

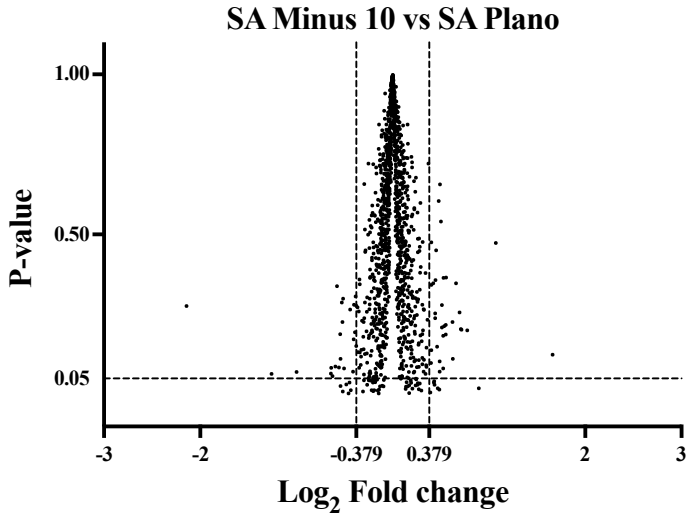

Figure 2.4.3 Volcano plot: All 1291 identified proteins (with at least 2 peptides per protein) are represented in terms of their Log2 fold changes (X-axis) and p-values of their change (Y-axis).

Among these 13 proteins, 6 proteins were found down-regulated while 7 proteins were up-regulated in LIM (appendix 2). These 13 proteins were categorized by Gene Ontology database (PANTHER classification system) classifications based on their molecular function, biological process, cellular component and protein class (below pie charts).

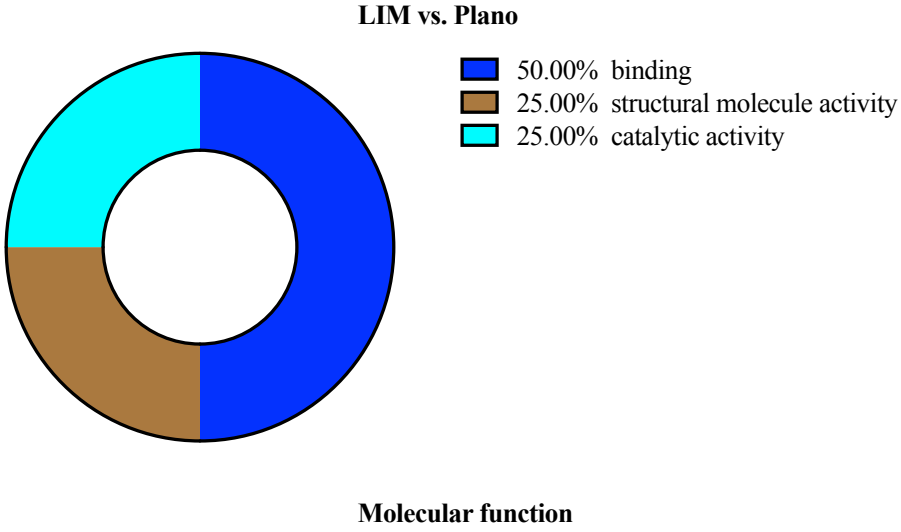

LIM vs. Plano

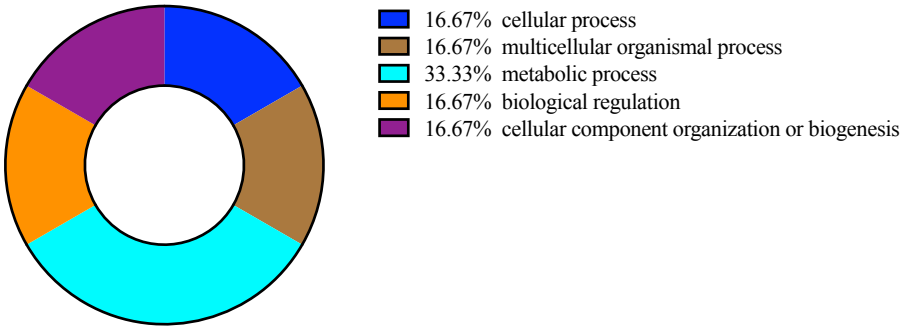

Biological process

LIM vs. Plano

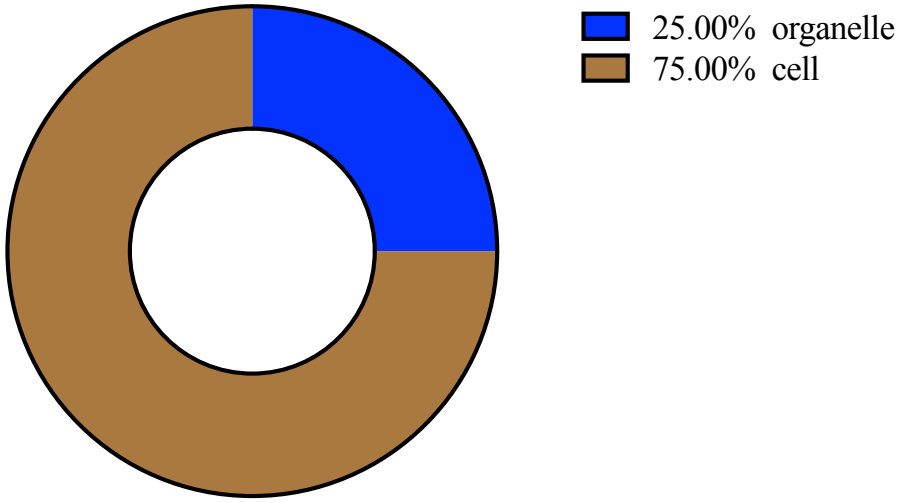

Cellular component

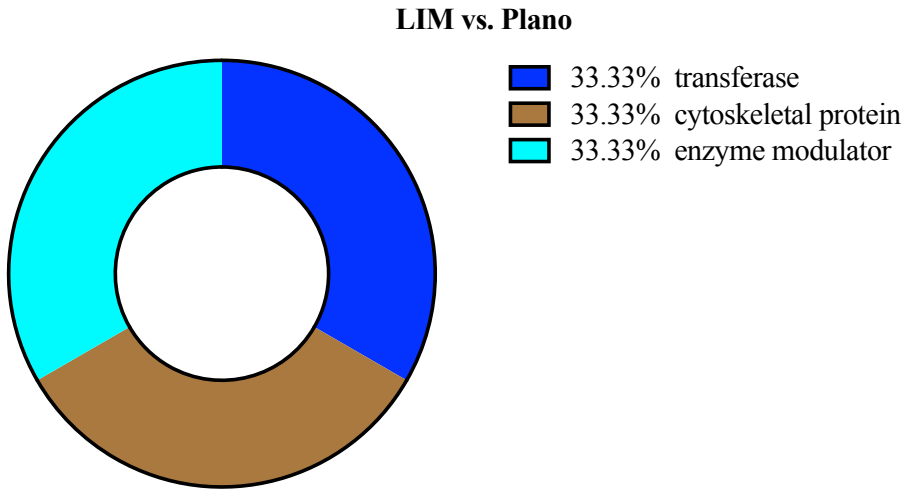

Pathway analysis was performed via iPathwayGuide database (Advaita Corporation) (Table 2.4.8).

Table 2.4.8 The list of identified pathway and up/down regulation genes

Pathway	Protein Up regulation
Insulin signaling pathway	PYG
Hippo signaling pathway	CRB
Endocytosis	RAB11

2.4.3 LIH vs LIM for 4 days

Comparison between LIH and LIM for 4 day, the LIH eyes became significantly more hyperopic than the LIM eyes. The changes in VCD and AXL in LIH eyes were significantly less than that of the LIM eyes. The changes in RT, CT and SER in LIH eyes was significantly more than that of the LIM eyes. There was no significant difference in ACD, LT and ST between LIH and plano lenses induced eyes (Table 2.4.9, Fig 2.4.1).

Table 2.4.9 The comparisons of ocular parameters and refractive error change after 4 days LIH or LIM

Treatment		N	Mean	Std. Deviation	Sig. (2-tailed)	
ACD (mm)	LIH	5	0.131	0.099	0.166	ǂ
	LIM	8	0.156	0.062		
LT (mm)	LIH	5	0.109	0.066	1.000	Ɨ
	LIM	8	0.113	0.061		
VCD (mm)	LIH	5	-0.121	0.044	0.000	Ɨ
	LIM	8	0.713	0.084		
AXL (mm)	LIH	5	0.120	0.058	0.000	Ɨ
	LIM	8	0.983	0.093		
RT (mm)	LIH	5	0.019	0.018	0.005	Ɨ
	LIM	8	-0.024	0.014		

CT (mm)	LIH	5	0.287	0.118	0.000	Ⱨ
	LIM	8	-0.002	0.037		
ST (mm)	LIH	5	0.003	0.009	1.000	Ⱨ
	LIM	8	-0.003	0.012		
SER (D)	LIH	5	7.150	0.548	0.000	Ⱨ
	LIM	8	-8.875	0.463		

ⱧP value for one-way ANOVA (Bofferroni)

ǂP value for Kruskal-Wallis test

After 4 days of LIH and LIM, the relative expression of apoA1 protein was detected by western blot. The relative expression of apoA1 protein normalized to GapDH in LIH group was significantly more than LIM groups (Table 2.4.10, Figure 2.4.1).

Table 2.4.10 Relative expression of apoA1 protein normalized to GapDH after 4 days LIH or LIM

Treatment		N	Mean	Std. Deviation	Sig. (2-tailed)	
ApoA1/GapDH	LIH	5	1.283	0.929	0.001	ǂ
	LIM	8	0.257	0.165		

ⱧP value for one-way ANOVA (Bofferroni)

ǂP value for Kruskal-Wallis test

After 4 days of LIH and LIM, the quantification of apoA1 protein was performed by LC-MS (SWATH). The expression of apoA1 protein was significantly higher in LIH group than that of the LIM group (Table 2.4.11, Figure 2.4.1).

Table 2.4.11 Quantification of apoA1 protein after 4 days LIH or LIM by LC-MS (SWATH)

Treatment	N	Mean	Std. Deviation	Sig. (2-tailed)	
LIM	8	4.3E+05	8.1E+04	0.010	ǂ
LIH	5	1.0E+06	5.7E+05		

ǂP value for one-way ANOVA (Bofferroni)

ǂP value for Kruskal-Wallis test

After SWATH analysis, there were 1272 proteins identified with at least 2 peptides per protein. 79 proteins were found to be changed by $|\log_2$ (fold change)$| \geq 0.379$ and P-value < 0.05 (Figure 2.4.4).

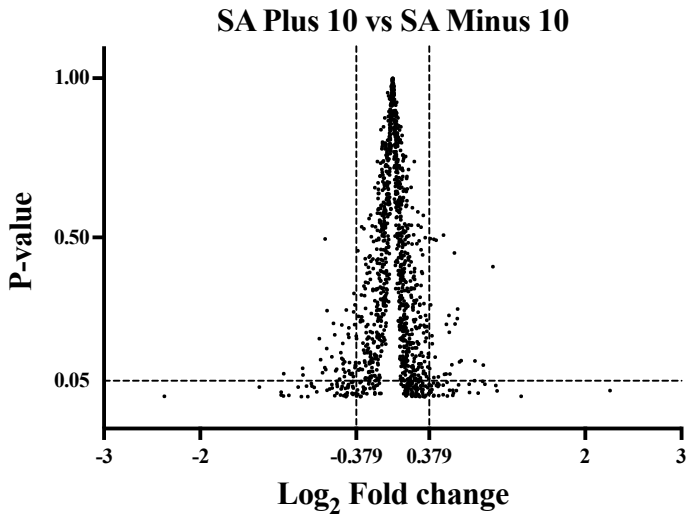

Figure 2.4.4 Volcano plot: All 1272 identified proteins (with at least 2 peptides per protein) are represented in terms of their Log2 fold changes (X-axis) and p-values of their change (Y-axis).

Among these 79 proteins, 46 proteins were found to be down-regulated while 33 proteins were up-regulated after LIM compare to LIH (appendix 2). These 79 proteins were categorized by Gene Ontology database (PANTHER classification system) classifications based on their molecular function, biological process, cellular component and protein class (below pie charts).

LIM vs. LIH

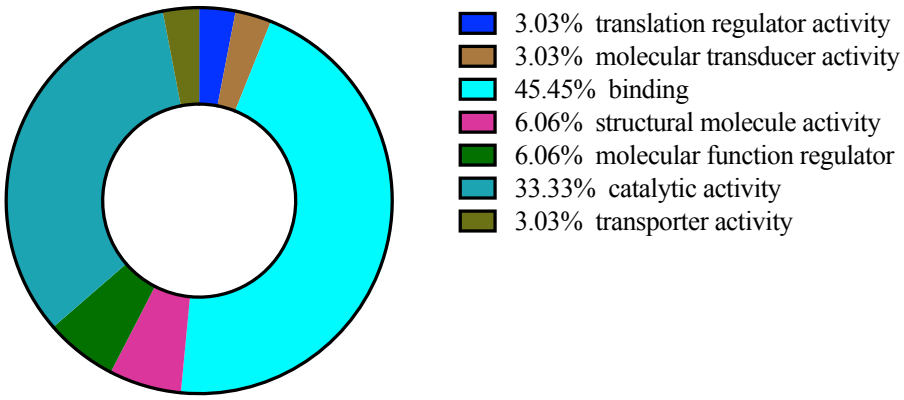

Molecular function

LIM vs. LIH

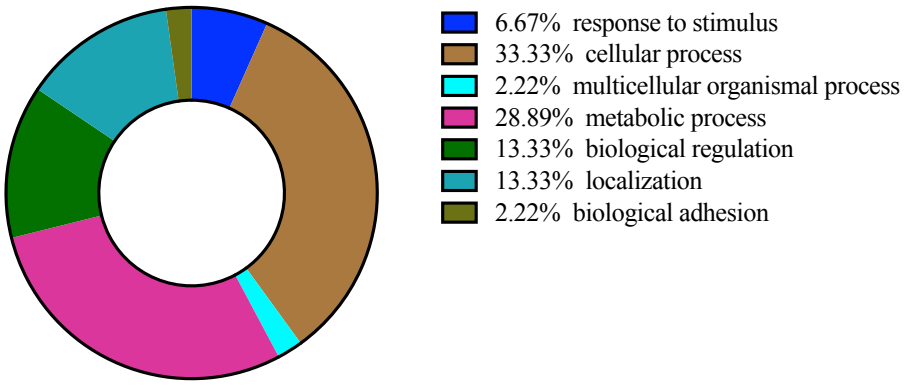

Biological process

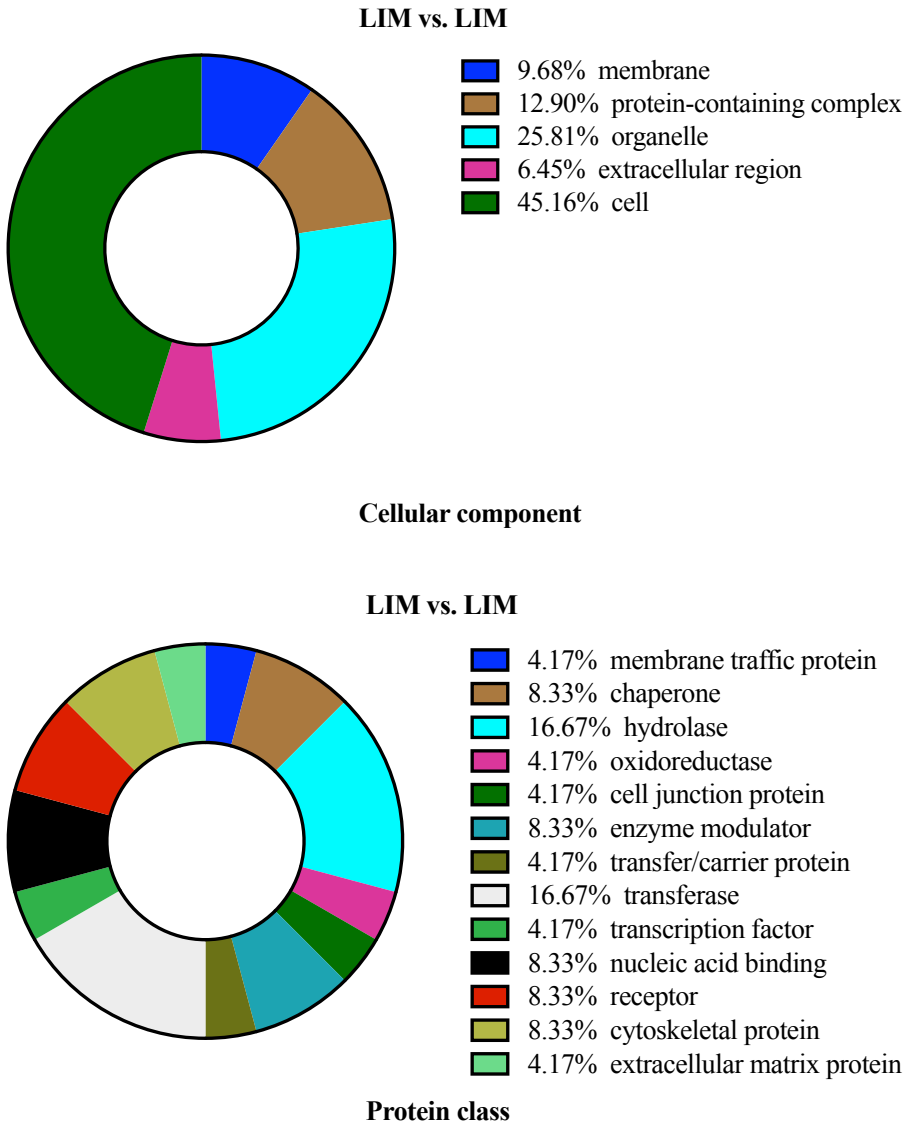

Pathway analysis was performed via iPathwayGuide database (Advaita Corporation) (Table 2.4.12).

Table 2.4.12 List of the top identified pathways and up/down regulation genes (LIH vs LIM)

Pathway	Protein	
	Up regulation	Down regulation
Insulin signaling pathway	GYS	PYG
Regulation of actin cytoskeleton	PIR121	ARP2/3
Endocytosis		ARP2/3, RAB11, DNM3
Hippo signaling pathway		CRB

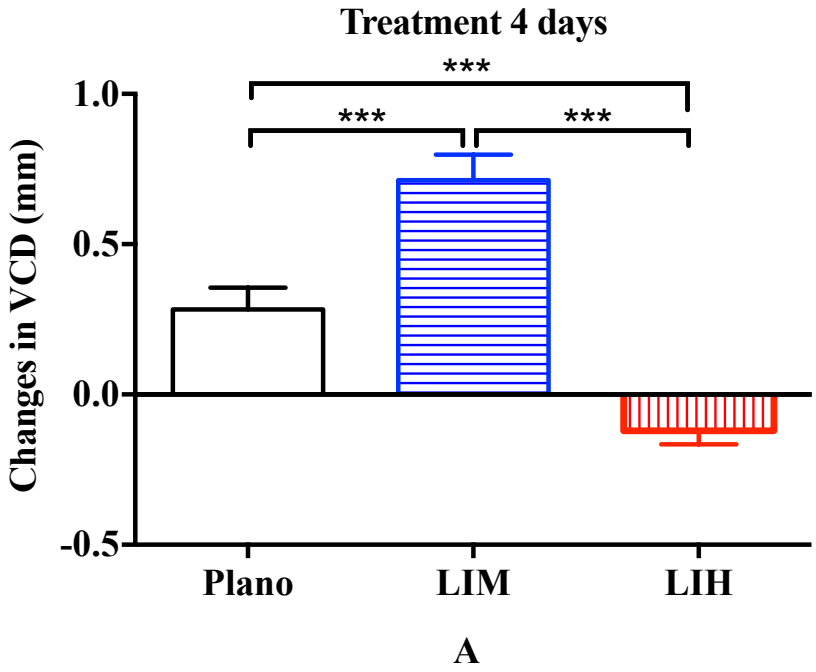

A

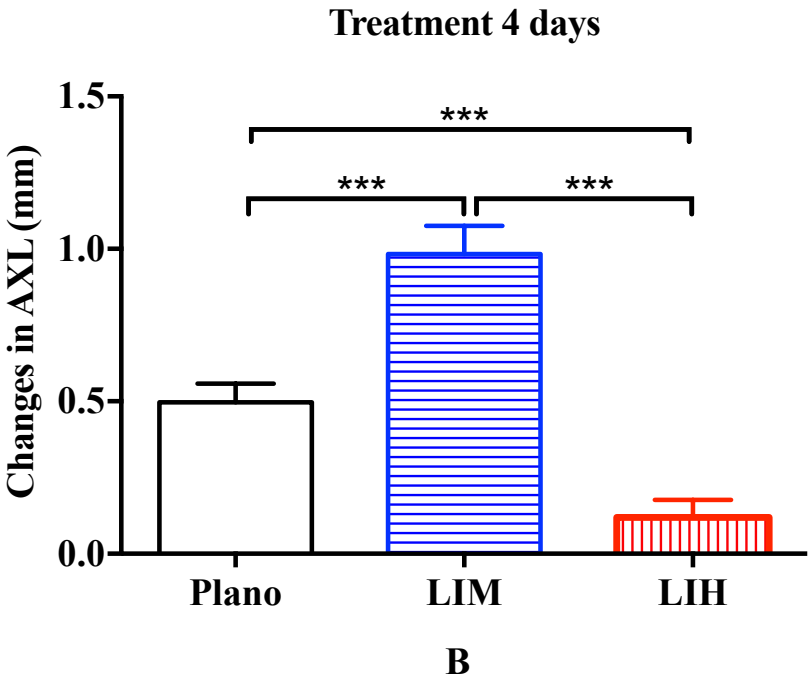
Treatment 4 days
Changes in AXL (mm)
1.5
1.0
0.5
0.0
***
***
***
Plano
LIM
LIH

B

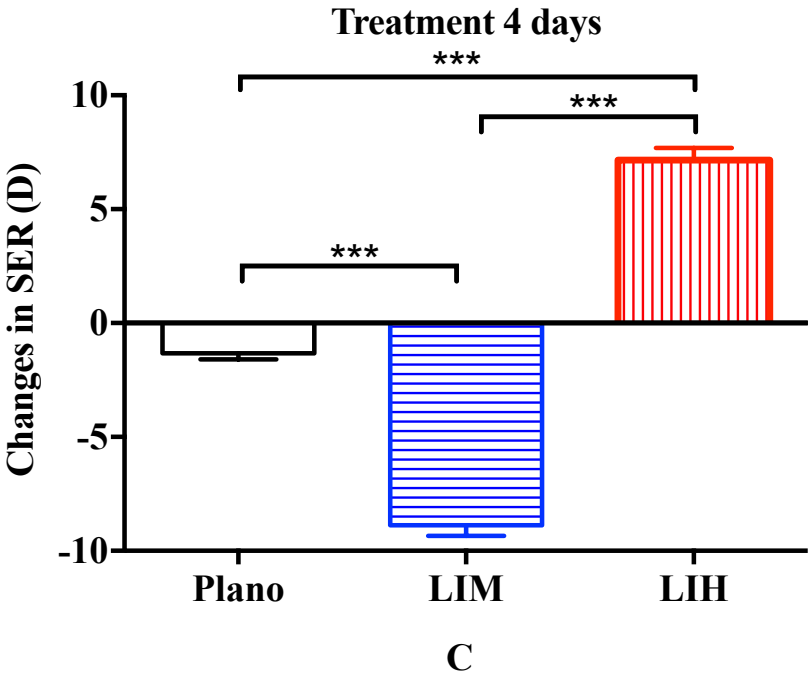
Treatment 4 days
Changes in SER (D)
10
5
0
-5
-10
***
***
***
Plano
LIM
LIH

C

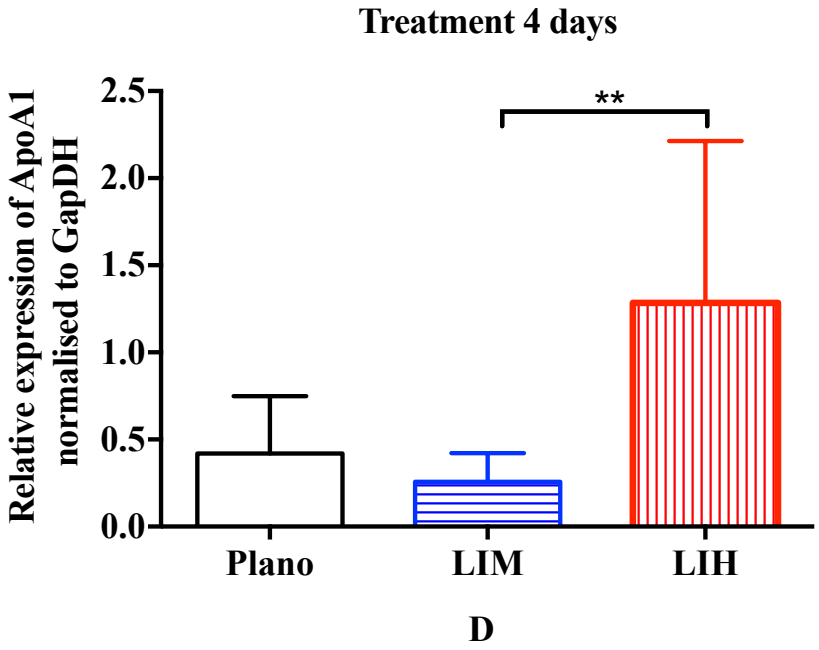

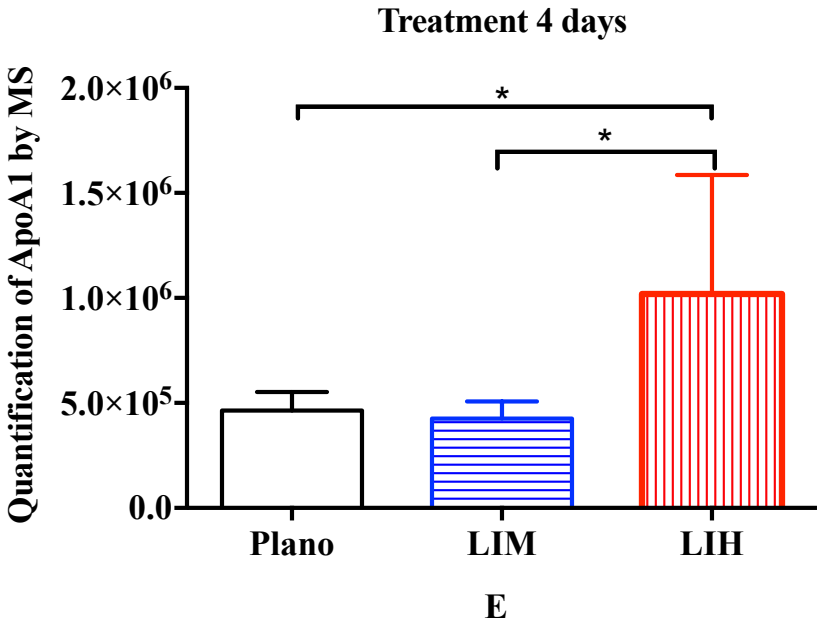

Figure 2.4.1 The comparisons of ocular parameters and apoA1 protein expression after treatment 4 days.

The effects of LIH, LIM and plano on change in (A) VCD (mm), (B) AXL (mm), (C) SER (D), (D) relative expression of apoA1 protein normalized to GapDH by western blot and (E) quantification of apoA1 protein by LC-MS after treatment 4 days. Mean ±SD, *p<0.05, **p<0.01, ***p<0.001.

2.4.4 Summary results

Protein

LIH vs. Plano	4 days lens induced	Significantly more hyperopic (Ocular parameters & Refractive error)
	Protein (ApoA1) by western blot at day 14	Not significantly different
	Protein (ApoA1) by LC-MS (SWATH) at day 14	Up regulation in LIH group
LIM vs. Plano	4 days lens induced	Significantly more myopic (Ocular parameters & Refractive error)
	Protein by western blot at day 14	Not significantly different
	Protein by LC-MS (SWATH) at day 14	Not significantly different

LIH vs. LIM	4 days lens induced	Significantly more hyperopic in LIH group (Ocular parameters & Refractive error)
	Protein (ApoA1) by western blot at day 14	Up regulation in LIH group
	Protein (ApoA1) by LC-MS (SWATH) at day 14	Up regulation in LIH group

2.5 Discussion

In term of the changes in ocular parameters and reflective errors after 4 days of treatment, LIH induced hyperopic eye growth, while LIM induced myopic eye growth expectedly. The LIH eyes were significantly more hyperopic than the LIM eyes. These were consistent with previous studies (Lam et al., 2006, Zhu et al., 2005, Winawer and Wallman, 2002).

The relative apoA1 protein expression of the LIH group was not significantly different from the control group according to the western blot results (up-regulation 4.954-fold in LIH, P=0.067), but it was significantly increased in LIH group by LC-MS (SWATH) (up-regulation 2.174-fold in LIH, P=0.026). The reason probably because the Western blot is not as sensitive and accurate as LC-MS (SWATH). In LIM experiment, the apoA1 protein relative expression was not significantly differentially expressed (down-regulation 0.465-fold by western bolt detection, P=0.598; down-

regulation 0.935-fold by LC-MS detection, P=1.000). This result was consistent with a previous study on apoA1 expression in LIM (Bertrand et al., 2006). However, when comparing the LIH and LIM results, apoA1 expressions were significantly higher in LIH group than LIM group by both western blot (up-regulation 4.992-fold in LIH than LIM, P=0.001) and LC-MS (SWATH) (up-regulation 2.326-fold in LIH than LIM, P=0.010) methods. In a previous study, Lam et al (2006) showed that apoA1 in myopic retina was down-regulated in LIM and FDM chicks' retina after 3 days of manipulation (down regulation of 1.47-folds in LIM, $p<0.05$; 1.98-folds in FDM, $p<0.05$; 1.91-folds in induced by occluders, $p=0.071$).

With the SWATH analysis, four pathways were implicated: insulin signaling pathway, regulation of actin cytoskeleton, endocytosis and hippo signaling pathway (figure 2.5.1, figure 2.5.2, figure 2.5.3 and figure 2.5.4).

Insulin signaling pathway

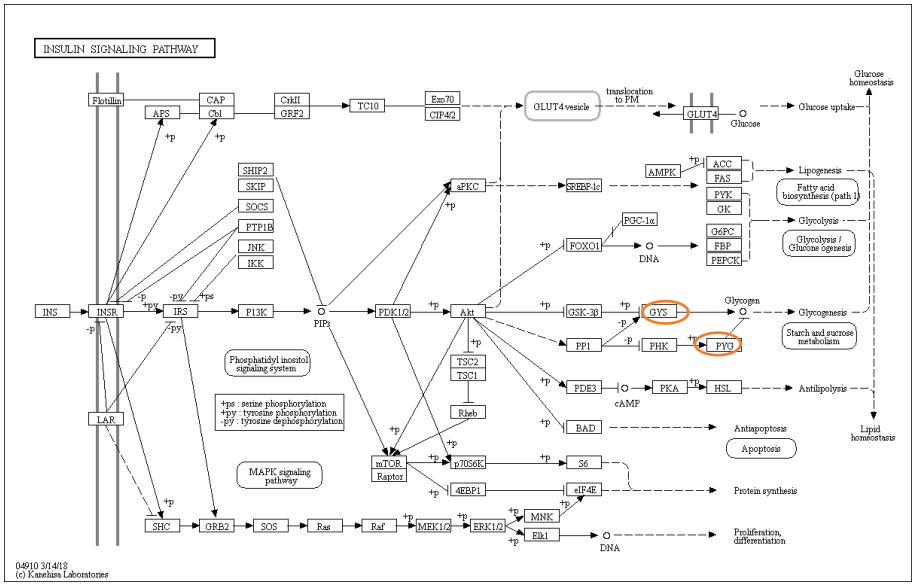

Figure 2.5.1 Insulin signaling pathway map from KEGG website (https://www.kegg.jp/kegg-bin/show_pathway?map04910)

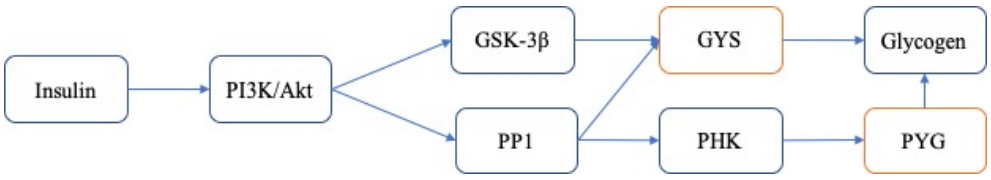

In this experiment, GYS (Glycogen synthase) was up-regulated in LIH and the PYG (glycogen phosphorylase) was down-regulated in LIM. Comparing to LIM, LIH up-regulated GYS but down-regulated PYG. GYS is a key enzyme in glycogenesis, converting glucose into glycogen (Seldin et al., 1994, Buschiazzo et al., 2004, Palm et al., 2013). PYG is an important

factor in tricarboxylic cycle (TCA)(Livanova et al., 2002, Alemany et al., 1986). GYS can promote the glycogen synthesis from glucose (Seldin et al., 1994, Buschiazzo et al., 2004, Palm et al., 2013); on the contrary, PYG can catabolize glycogen into glucose subunits (Alemany et al., 1986, Livanova et al., 2002). Intuitively, less energy may be needed in slow eye growth as in the LIH group. Therefore, more GYS is expressed so as to convert glucose into glycogen in the LIH group. Conversely, up-regulation of PYG expression can increase both acetyl-CoA and adenosine triphosphate (ATP) which can provide more energy for accelerated eye growth in myopia development.

Insulin signaling pathway has been reported that it can promote myopia development (Penha et al., 2012). The insulin signaling pathway includes two sub-pathways: the PI3K-Akt signaling pathway and MEK/MRK pathway (Sun et al., 1991). PI3k/Akt pathway can be activated in normal, LIH and LIM, but MEK/MRK pathway can be activated in normal and LIH only (Penha et al., 2012). The PI3K-Akt signaling pathway regulates glucose metabolism process (Burgering and Coffer, 1995). Huang et al (2019) has reported that the PIK3CG-PRKAR2B in PI3K/Akt pathway is highly related to myopic development in the chick retina (Huang et al., 2019). On the other hand, The MEK/MRK pathway is related to cell growth, such as cycle, migration, proliferation and differentiation (Puro and Agardh, 1984, Mill et al., 1985, Heidenreich and Toledo, 1989). Although

the current study did not find any significant changes in the MEK/MRK pathway, its relevance to eye growth awaits further study in the future.

Regulation of actin cytoskeleton

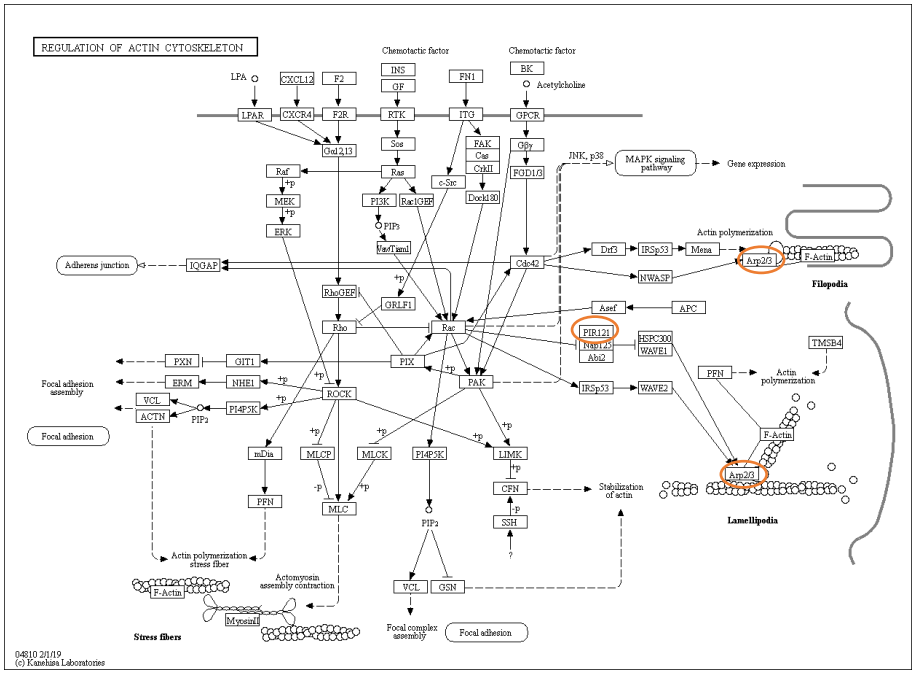

Figure 2.5.2 Regulation of actin cytoskeleton pathway map from KEGG website (https://www.kegg.jp/kegg-bin/show_pathway?map04810)

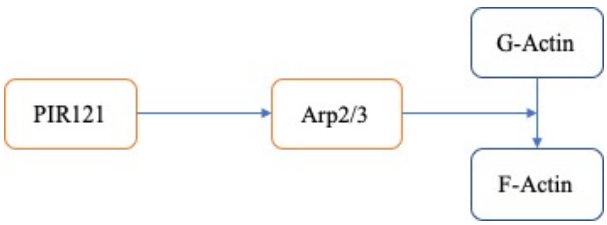

In this pathway, PIR121 (cytoplasmic FMR1 interacting protein) was up-regulated and Arp2/3 (actin related protein 2/3 complex) was down regulated in LIH eyes. However, there was not significantly change in this pathway in LIM. Comparing to LIM, PIR121 was up-regulated and Arp2/3 was down-regulated in LIH.

Actin is a kind of microfilaments, which is a major component of the cytoskeleton (Otterbein et al., 2001, Goley and Welch, 2006, Doherty and McMahon, 2008). G-actin is the monomer of actin, whereas F-actin is the polymer of actin (Doherty and McMahon, 2008, Otterbein et al., 2001). Actin is important in a lot of cellular processes, such as cell cycle, growth, division, vesicle and motility (Doherty and McMahon, 2008). Arp2/3 complex is essential in the regulation of actin cytoskeleton pathway (Goley and Welch, 2006). Arp2/3 can promote G-actin polymerization to F-actin which can in turn promote cell proliferation (Tran et al., 2015, Hoffman et al., 2018). Previous studies has reported that PIR121 can inhibit Arp2/3 expression (Lee et al., 2017). In the current study, we hypothesized that LIH increases PIR121 expression which inhibits Arp2/3 and in turn leads to the down regulation of F-actin polymerization. The result is the inhibition of cell and tissue growth. In other words, the retardation of eye growth in the LIH may be mediated through the down-regulation of the actin cytoskeleton pathway. However, this pathway was not significantly changed in the LIM.

Endocytosis pathway

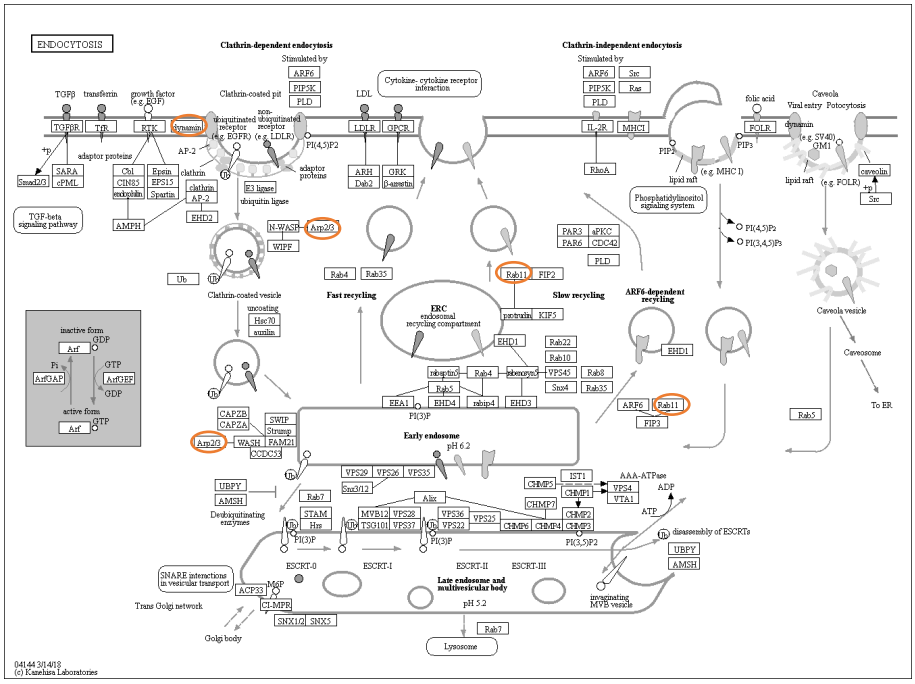

Figure 2.5.3 Endocytosis pathway map from KEGG website

(https://www.kegg.jp/kegg-bin/show_pathway?map04144)

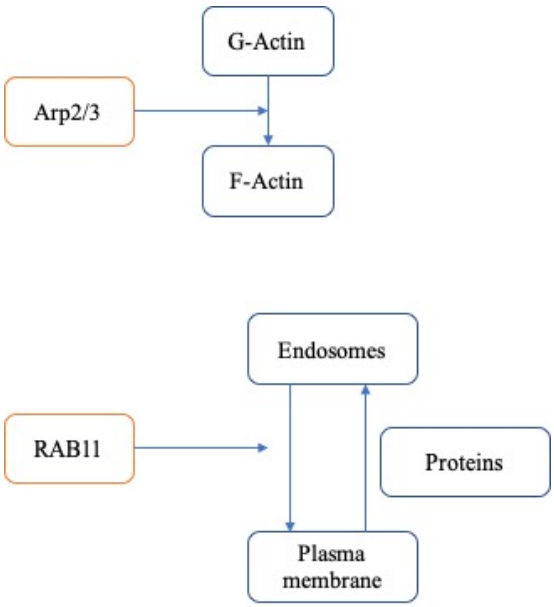

In this pathway, Arp2/3 (actin related protein 2/3 complex) and DNM3 (dynamin GTPase 3) were down regulated in LIH. RAB11 (Ras-related protein Rab-11A) was up regulated in LIM eyes. Compared to LIM, LIH showed Arp2/3, DNM3 and RAB11 down-regulation.

As described above, Arp2/3 plays an important role in the regulation of actin cytoskeleton pathway (Goley and Welch, 2006). It can enhance G-actin polymerization to F-actin and can promote cell proliferation (Tran et al., 2015, Hoffman et al., 2018). However, in addition to actin cytoskeleton pathway, Galletta et al (2008) has shown that Arp2/3 regulators is also key to endocytosis in yeast (Galletta et al., 2008). Arp2/3 can promote cell endocytic vesicle generation and movement into cytoplasm (Galletta et al., 2008). Decrease in DNM3 expression could also down regulate the endocytosis pathway (Ferguson and De Camilli, 2012).Therefore, since both the Arp2/3 and DNM3 were down-regulated, it is postulated that the endocytosis pathway may also be slowed down in LIH. RAB11 can recycle proteins from endosomes to the plasma membrane as observed in the transport of molecules from the trans-Golgi network to the plasma membrane and in phagocytosis (Chen et al., 1998, Schlierf et al., 2000, Cox et al., 2000, Ullrich et al., 1996). Since RAB11 was up-regulated in the LIM, it suggested that endocytosis pathway may be up-regulated accordingly. The results in this study showed that LIH may inhibit

endocytosis activity while LIM may promote endocytosis activity. Considering the effect of eye growth with LIM and LIH, it is hypothesized that the down-regulation of endocytosis pathway may inhibit tissue growth in the eye. It may be plausible that the slowing of endocytosis pathway leads to an accumulation of "STOP" signals, such as apoA1 protein, and thereby retards eye growth. Conversely, up regulating endocytosis may promote the removal of "STOP" signals and facilitates accelerated eye growth as seen in the case of LIM.

Hippo signaling pathway

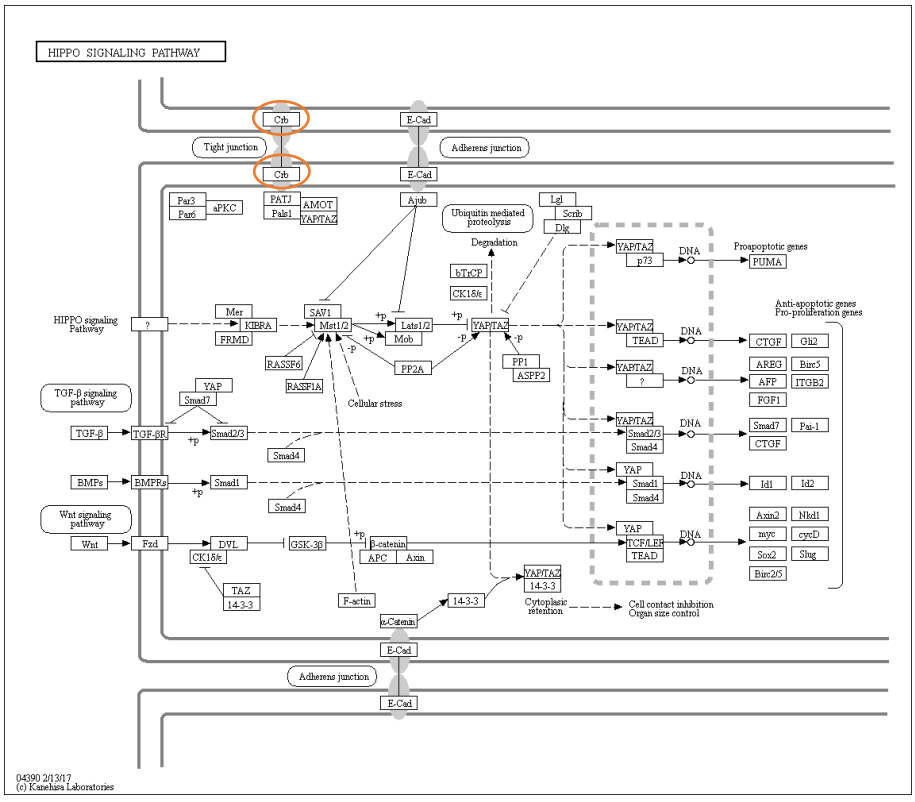

Figure 2.5.4 Hippo signaling pathway map from KEGG website (https://www.kegg.jp/kegg-bin/show_pathway?map04144)

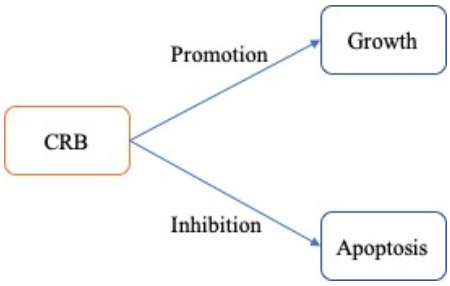

In this pathway, CRB (Crumbs) was up-regulated in LIM when compared to the plano control eye; however, it was not significantly changed in LIH (compared to plano control). Compared to LIH, CRB was also up-regulated in LIM.

CRB is a transmembrane protein (Robinson et al., 2010, Grzeschik et al., 2010) and it has been shown that the overexpression of CRB contributed to the overgrowth of tissues (Humbert et al., 2008). In addition, overexpression of CRB promoted the imaginal discs growth (Lu and Bilder, 2005) and inhibited its apoptosis in the eye (Grzeschik and Knust, 2005), Therefore, the increase in CRB expression could promote eye growth.

System biology according proteomic data

Penha et al (2012) have reported that insulin promoted eye growth. There are two sub-pathways included in insulin pathway, the PI3k/Akt and

MEK/MRK pathways (Penha et al., 2012). It has been shown that PIK3CG gene is strongly correlated to myopia in a genome-wide association study (GWAS) (Huang et al., 2019). This gene is a key to PI3k/Akt pathway and insulin signaling pathway. Incidentally, dopamine is upstream of PI3k/Akt pathway and can inhibit Akt expression (Beaulieu et al., 2007) and dopamine can also increase cAMP (Beaulieu et al., 2007). Previous work from this lab has reported that cAMP can increase apoA1 and retard myopia (Chun et al., 2015). In our current experiment, LIH up regulated GYS and PYG was down-regulated by LIM and both GYS and PYG play significant roles in the insulin signaling pathway. ApoA1 has also been suggested to interact with a number of known myopia signals such as EGR-1 (ZENK) and ascorbic acid. Hasan et al have indicated that EGR-1 (ZENK) expression is regulated by insulin and glucose levels (Hasan et al., 2003), and EGR-1 (ZENK) expression is correlated well to different refractive development induced by optical lens wear (Fischer et al., 1999, Bitzer and Schaeffel, 2002, Ashby et al., 2007a, Ashby et al., 2010a). EGR-1 (ZENK) has been reported to be an upstream modulator of apoA1 and can promote apoA1 expression (Kilbourne et al., 1995). Summers et al (2016) proposed that apoA1 may bind with retinoic acid and modulates post-natal eye growth (Summers et al., 2016). The plasminogen (Honda et al., 1996) and Wnt (Tamai et al., 2000) pathways are thought to be downstream of apoA1 signalling. TGF-β is a GO factor in ocular axial growth (Rada and Brenza,

1995) and it has been reported as a downstream regulator of plasminogen (Honda et al., 1996). It is plausible that apoA1 may down-regulate plasminogen pathway, and then inhibit TGF-β to effect slow growth. Wnt pathway has been proposed to promote ocular axial growth and it is inhibited by apoA1 (Carre et al., 2010, Li et al., 2016, Ma et al., 2014). Hippo pathway is downstream of Wnt pathway and it functions to effect growth of mammalian liver (Dong et al., 2007). The Hippo pathway is also related to TGF-β but the underlying interconnection between Hippo pathway and myopia development awaits further research.

Bertrand et al (2006) has reported that apoA1 can slow myopia development. They employed a ppar-α agonist (GW7647) and showed that it increased apoA1 and inhibited eye growth (Bertrand et al., 2006). Lam et al (2006) also shown that the protein apoA1 in myopic retina was down regulated in LIM and FDM chick retina after 3 days of LIM or FDM. However, there was no significant difference between the treatment and the control groups in LIM and FDM after 7 days (Lam et al., 2006). Therefore, there is a substantial body of literature supports the notion that ApoA1 is a key and early stop signal to the development of myopia (Lam et al., 2006, Bertrand et al., 2006, Summers et al., 2016).

Overall, from pathway analysis and literature review, it is apparent that apoA1 and its related system biology may play an important role in ocular growth and myopia development. Elucidation of the function of apoA1 may

path the way for therapeutic control of myopia and hyperopia development in the future.

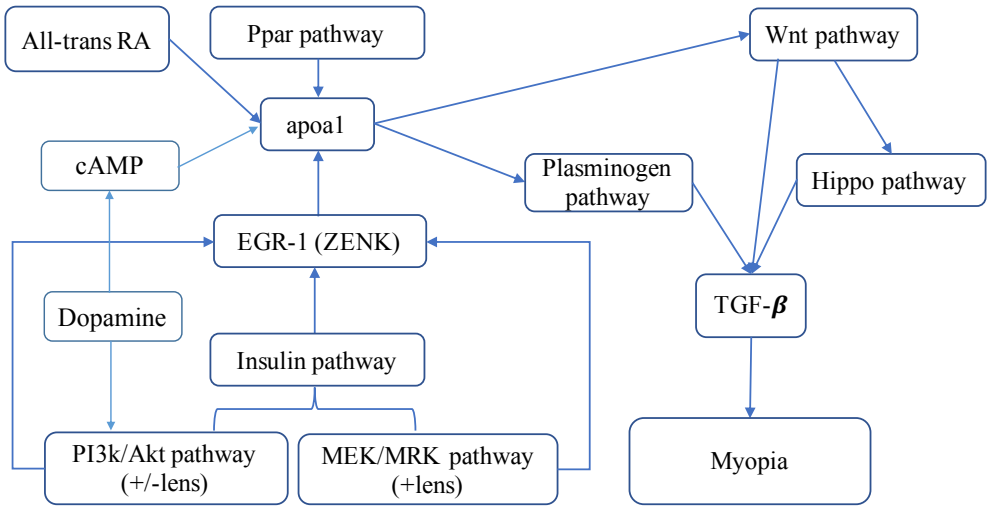

2.6 Conclusions

In the current study, the effect of apoA1 protein expression on LIH and its eye growth is early and significant, but not in the LIM.

In terms of the insulin signaling pathway, LIH increased GYS to convert glucose into glycogen assuming less energy is needed; on the contrary, LIM increased PYG to release glucose from glycogen indicating that more energy is needed in accelerated eye growth. In the pathway regulating actin cytoskeleton, LIH up-regulated PIR121 and then down-regulated Arp2/3 at downstream of PIR121 to decreasing F-actin down regulation and then inhibit cell growth. However, LIM may not regulate this pathway. In endocytosis pathway, LIH decreased ARP2/3 and DNM3 to down-regulated this pathway which can inhibit to tissue growth, and maybe it can inhibit the

removal of apoA1 protein in LIH. On the contrary, LIM increased RAB11 so as to up-regulate endocytosis and facilitate tissue growth, and may also promote the removal of retinal apoA1 protein. In hippo signaling pathway, LIM leads to CRB up-regulation to promote eye growth.

Chapter 3: Differential apoA1 mRNA expressions in lens induced hyperopic (LIH) and myopic (LIM) chick retinas

3.1 Introduction

In chapter 2, apoA1 protein was found to be differentially expressed in LIM and LIH. However, it was unclear if the retinal apoA1 protein was synthesized by the retina/choroid complex or it was recruited from the blood plasma.

Previously, Simo et al (2009) have reported that there was apoA1 mRNA expression in the human retina, suggesting that apoA1 may be produced locally at the retina (Simo et al., 2009). Summers et al (2006) have also found that apoA1 mRNA expression in the chick choroid and it indicated choroidal tissue can produce apao1 locally (Summers et al., 2016). However, it is unclear if the chick retina can also produce apoA1 or express apoA1 mRNA locally.

Therefore, we attempted to examine if apoA1 mRNA expression could be detected in the chick retinas. In addition, we asked if the level of apoA1 mRNA expressions may correlate with the protein expressions in LIM and LIH as found in the current study (Chapter 2).

3.2 Objective

The aim was to investigate whether chick retinas could express apoA1 mRNA.

3.3 Materials and methods

3.3.1 Animal

White leghorn chicks (Gallus gallus) were hatched from specific pathogen free (SPF) eggs from Jinan, China at 37.5°C and 75% humidity for one month (Wang et al., 2015). After hatching, chicks were settled in the circumstance at 25℃ and 12/12 hours of light/dark cycle (Chun et al., 2015). Water and food were refilled daily by staff from Centralized Animal Facilities (CAF), the Hong Kong Polytechnic University. All operations to animals in experiments strictly followed the ARVO regulation on the Use of Animals in Research and the Animal Subjects Research Ethic Subcommittee (ASEC)(Wang et al., 2015, Wu et al., 2018b).

3.3.2 Experimental design

For LIH experiment

Twenty-four white leghorn chicks at 4 days after hatching (PN4) were randomly distributed into three groups (group A=8; group B=8; group C=8). All chicks were orally fed 1ml saline daily (group A: PN4 to PN11; group B: PN4 to PN14; group C: PN4 to PN16). At PN10, +10D lens was randomly attached to treatment eye while plano lens was mounted to the follow eye as control for each chick. Random numbers were generated by Microsoft Excel software for randomization purposes. In group A, chicks

wore lenses for 1 day (PN10 to PN11). In group B and C, chicks wore lenses for 4 days (PN10 to PN14). After lenses removed, group C chicks were recovered for 2 days (PN14 to PN16). The measurements (refractive error and ocular parameters) were performed before and after lens induced treatment (PN10 and PN14) for group A and B, while before and after recovery (PN14 and PN16) for group C. The spherical equivalent power (spherical power + half of cylindrical power) was measured by steak retinoscopy. Ocular parameters were measured by high frequency A-scan ultrasound system (30MHz probe sampled at 100MHz).

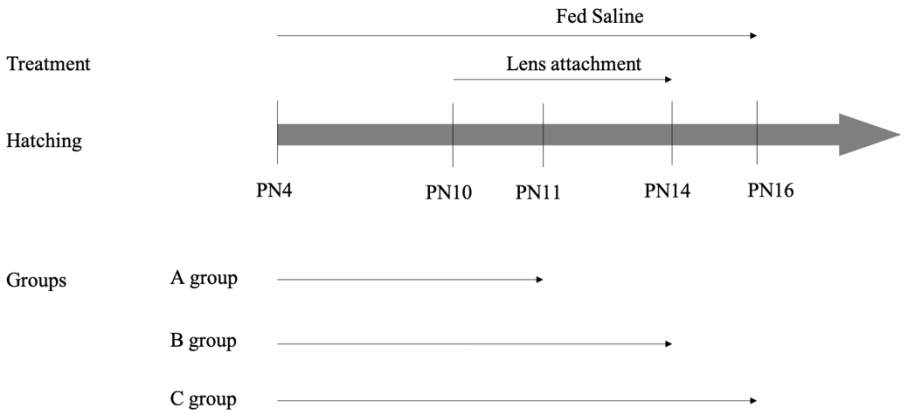

For LIM experiment

Twenty-four white leghorn chicks at 4 days after hatching (PN4) were randomly distributed into three groups (group D=8; group E=8; group F=8). All chicks were orally fed 1ml saline daily (group D: PN4 to PN11; group E: PN4 to PN14; group F: PN4 to PN16). At PN10, -10D lens was randomly attached to treatment eye while plano lens was given to the follow eye of

each chick. The random numbers were generated by Microsoft Excel software. In group D, chicks wore lenses for 1 day (PN10 to PN11). In group E and F, chicks wore lenses for 4 days (PN10 to PN14). After lenses removal, group F chicks were recovered for 2 days (PN14 to PN16). The measurements (refractive error and ocular parameters) were performed before and after lens induced treatment (PN10 and PN14) for group D and E, while before and after recovery (PN14 and PN16) for group F. The spherical equivalent power (spherical power + half of cylindrical power) was measured by steak retinoscopy. Ocular parameters were measured by high frequency A-scan ultrasound system (30MHz probe sampled at 100MHz).

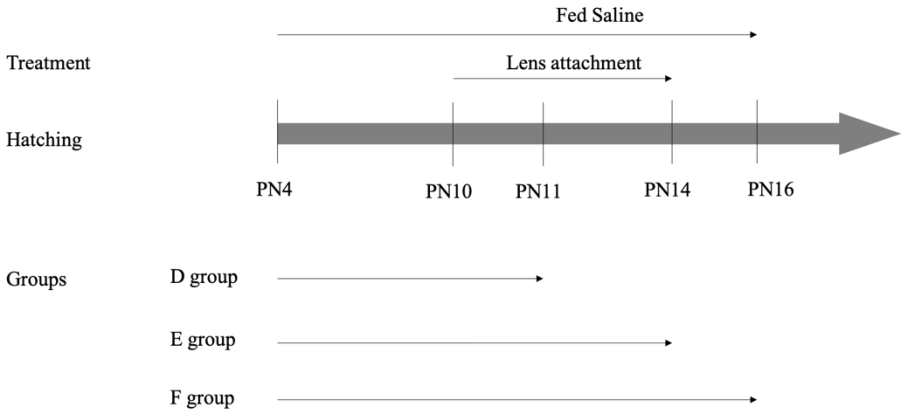

A cocktail of ketamine and xylazine (90mg: 10mg) was used to anesthetize chicks by 100mg/kg dose intramuscular injection. After anesthetization, transcardial perfusion was performed by Phosphate-buffered saline (PBS) buffer 50ml per chick at a rate of 25ml/min. After transcardial perfusion,

chicks were sacrificed by carbon dioxide overdose. The eyes were removed without connective tissues and muscle and then it was carefully washed with PBS. The eyes were dissected at low temperature (iced cooled) and the retina was collected without vitreous body and retinal pigment epithelium (RPE). Liquid nitrogen was used to quickly freeze the retinal samples which were stored at -80°C for later use.

3.3.3 Extraction of mRNA from retinal tissue

A commercialized available kit (RNeasy Fibrous Tissue Mini Kit from QIAGEN Company) was used to extract mRNA from retinal tissues. The frozen retina was homogenized with 300µl lysis buffer (β-mercaptoethanol: RLT buffer = 1:100) at 1600×g for 7 minutes. The lysate was incubated in room temperature for 10 minutes and moved to 1.5ml Eppendorf tube with autoclaved. Then10µl proteinase K solution and 590µl RNase-free water was added to the homogenate to incubate at 55°C for 10 minutes. After incubation, the mixture was centrifuged at 10000×g for 3 minutes at 20°C. Then, the supernatant was pipetted into a new 1.5ml autoclaved Eppendorf tube and then mixed with 450µl ethanol (100%). The mixture was transferred to the RNeasy Mini spin column with a 2ml collection tube and centrifuged at 10000×g for 30 seconds at 20°C. After 350µl buffer RW1 washing, in principle, DNA and mRNA could be retained in this column. DNase buffer (80µl, DNase I: buffer RDD = 1:7) was pipetted into this

column and incubated at 20°C for 15 minutes. The column was washed once by 350μl buffer RW1 and twice by 500μl RPE. After digestion and washing, only mRNA would be retained in column. RNase-free water (30μl) was used to collect mRNA via incubation 1 minute and centrifugation at 10000×g for 1 minute at 20°C. The quantity of mRNA was estimated by A260 (A260 = sample A260 – blank A260; 1 A260 = 0.04μg/μl single-stranded RNA). The quality of mRNA was assessed by A260/A280 ratio (approximately 1.9-2.0; pure DNA = 1.8; pure RNA = 2.0).

3.3.4 Complementary DNA (cDNA)

A commercially available kit (High Capacity cDNA Reverse Transcription Kits by Applied Biosystems Company) was used to convert mRNA to cDNA in this experiment. Each 0.3162μg mRNA sample was mixed with 2μl RT buffer (10×), 0.8μl dNTP Mix (100mM, 25×), 2μl RT Random Primers (10×) and 1μl MultiScribe™ Reverse Transcriptase to 20μl. The optimization thermal cycler conditions were 25°C for 10 minutes, 37°C for 120 minutes, 85°C for 5 minutes and finally 4°C to stop reaction. These cDNA samples were stored at -80°C.

3.3.5 Quantitative real-time polymerase chain reaction (qPCR)

For qPCR analysis, 2μl cDNA each sample was amplified using a LightCycler® 480 SYBR Green I Master kit, Multiwell Plate (96 well), Sealing Foiland LightCycler® 480systemfrom Roche company. The primers used in these experiments were shown as table 3.3.1 and the qPCR programs as table 3.3.2. The LightCycler® 480 software 1.5.1 was used to perform qPCR and analyze results. The cross-point cycle (Cp) which is also called threshold cycle (Ct) was recorded during exponential amplification phase. For relative quantification, E-method was used in these qPCR experiments. E-method calibrated the special efficiency by standard curve for target or reference gene. It is more accurate, especially small difference in gene expression, than traditional $\Delta\Delta C_T$ method which defines efficiency as 2 directly. The normalized ratio = $E^{Cp_{apoA1}-Cp_{GapDH}}$. All measurements were performed in triplicate.

Table 3.3.1 Primers used for these experiments

		Sequence (5'->3')
ApoA1	Forward primer	TCAGCACGAAGATGAGAGGC
	Reverse primer	TCAGCCAGCTTCAGGTCAAG
GapDH	Forward primer	GGGTGGTGCTAAGCGTGTTA
	Reverse primer	ACGCTGGGATGATGTTCTGG

Table 3.3.2 qPCR programs for these experiments

Program Name	Target (°C)	Hold (hh:mm:ss)	Ramp Rate (°C/s)	Cycles
Pre-incubation	95	00:05:00	4.40	1
Amplification	95	00:00:30	4.40	40
	63	00:00:30	2.20	
	72	00:01:00	4.40	
Melting curve	95	00:00:05	4.40	1
	65	00:01:00	2.20	
	97	00:00:00	0.11	
Cooling	40	00:00:30	2.20	1

3.3.6 Statistical analysis

Statistical analysis was performed by SPSS software (version 23, SPSS, Chicago, Illinois, USA). The normality was tested by Shapiro-Wilk test. The refractive errors, ocular parameters and mRNA relative expression were compared with paired student's t-test (parameter test) or signed rank test (non-parameter test). The data was reported as the mean ± SD and the P value less than 0.05 was considered statistically significant.

3.4 Results

3.4.1 LIH vs Plano

3.4.1.1 Treatment 1 day

The LIH eyes became significantly more hyperopic than the control. Both the vitreous chamber depth (VCD) and axial length (AXL) were significantly less than that of the control. The choroidal thickness (CT) was significantly larger than that of the control as well. The spherical equivalent refractive error (SER) was significantly more hyperopic than plano group. There was no significant difference in anterior chamber depth (ACD), lens thickness (LT), retina thickness (RT) and sclera thickness (ST) between LIH and plano lenses induced eyes (Table 3.4.1, Figure 3.4.1).

Table 3.4.1 The comparisons of ocular parameters change after 1 day LIH

Group		N	Mean	Std. Deviation	Sig. (2-tailed)	
ACD (mm)	Plano	7	0.041	0.023	0.311	§
	LIH	7	0.023	0.028		
LT (mm)	Plano	7	-0.022	0.045	0.063	§
	LIH	7	0.051	0.061		
VCD (mm)	Plano	7	0.119	0.053	0.000	§
	LIH	7	-0.131	0.067		

AXL (mm)	Plano	7	0.137	0.037	0.000	§
	LIH	7	-0.057	0.047		
RT (mm)	Plano	7	-0.009	0.017	0.198	§
	LIH	7	0.003	0.016		
CT (mm)	Plano	7	-0.005	0.024	0.000	§
	LIH	7	0.191	0.032		
ST (mm)	Plano	7	0.002	0.012	0.588	§
	LIH	7	-0.001	0.008		
SER (D)	Plano	7	0.214	0.267	0.000	§
	LIH	7	4.286	0.567		

§P value for paired student's t-test

||P value for signed rank test

After 1 day of LIH, the relative expression of apoA1 mRNA was detected by qPCR. The mRNA relative expression was significantly higher in LIH retinas than that of the control (Table 3.4.2, Figure 3.4.1).

Table 3.4.2 Relative expression of apoA1 mRNA after treatment 1 day

Group	N	Mean	Std. Deviation	Sig. (2-tailed)	
LIH	7	1.138	0.531	0.030	§
Plano	7	0.952	0.460		

§P value for paired student's t-test

||P value for signed rank test

3.4.1.2 Treatment for 4 days

Comparison between LIH and plano for 4 day, the LIH eyes became significantly more hyperopic than the controls. The changes in VCD and AXL in LIH eyes were significantly less than that of the plano lenses induced eyes. The changes in RT, CT and SER in LIH eyes was significantly more than that of the plano lenses induced eyes. There was no significant difference in ACD, LT and ST between LIH and plano lenses induced eyes (Table 3.4.3, Fig 3.4.1).

Table 3.4.3 The comparisons of ocular parameters change after treatment 4 days

Group		N	Mean	Std. Deviation	Sig. (2-tailed)	
ACD (mm)	Plano	8	0.083	0.034	0.214	§
	LIH	8	0.115	0.052		
LT (mm)	Plano	8	0.149	0.058	1.000	||
	LIH	8	0.162	0.054		
VCD (mm)	Plano	8	0.373	0.069	0.008	||
	LIH	8	-0.164	0.162		
AXL (mm)	Plano	8	0.605	0.108	0.000	§
	LIH	8	0.113	0.135		
RT (mm)	Plano	8	-0.017	0.016	0.026	§
	LIH	8	0.008	0.031		
CT (mm)	Plano	8	0.006	0.033	0.000	§
	LIH	8	0.316	0.117		
ST (mm)	Plano	8	-0.007	0.018	0.465	§
	LIH	8	0.000	0.014		
SER (D)	Plano	8	-0.313	0.458	0.000	§
	LIH	8	8.688	0.799		

§P value for paired student's t-test

||P value for signed rank test

After 4 days of LIH, the relative expression of apoA1 mRNA was detected by qPCR. The mRNA relative expression was significantly higher in LIH retinas than those induced by plano lens (Table 3.4.4, Figure 3.4.1).

Table 3.4.4 Relative expression of apoA1 mRNA after treatment 4 days

Group	N	Mean	Std. Deviation	Sig. (2-tailed)	
LIH	8	1.281	0.571	.049	§
Plano	8	0.896	0.475		

§P value for paired student's t-test

||P value for signed rank test

2.4.1.3 Recovery of 2 days

Comparison the recovery for 2 days after LIH and plano, the LIH group eyes became significantly more myopic than the controls. The changes in VCD and AXL in LIH group eyes were significantly more than that of the plano group eyes. The changes in RT, CT and SER in LIH group eyes were significantly less than that of the plano group eyes. There was no significant difference in ACD, LT and ST between these two groups (Table 3.4.5, Figure 3.4.1).

Table 3.4.5 The comparisons of ocular parameters change after recovery 2 days

Group		N	Mean	Std. Deviation	Sig. (2-tailed)	
ACD (mm)	Plano	7	0.013	0.034	0.372	§
	LIH	7	0.029	0.026		
LT (mm)	Plano	7	0.081	0.045	0.703	§
	LIH	7	0.074	0.027		
VCD (mm)	Plano	7	0.036	0.048	0.000	§
	LIH	7	0.357	0.136		
AXL (mm)	Plano	7	0.130	0.060	0.001	§
	LIH	7	0.460	0.166		
RT (mm)	Plano	7	0.003	0.012	0.028	§
	LIH	7	-0.008	0.012		
CT (mm)	Plano	7	-0.005	0.026	0.000	§
	LIH	7	-0.252	0.112		
ST (mm)	Plano	7	0.006	0.010	0.544	§
	LIH	7	0.010	0.017		
SER (D)	Plano	7	-0.286	0.488	0.000	§
	LIH	7	-4.643	0.988		

§P value for paired student's t-test

||P value for signed rank test

After 2 days of recovery, the relative expression of apoA1 mRNA was detected by qPCR. The mRNA relative expression was no significant difference between these two groups (Table 3.4.6, Figure 3.4.1).

Table 3.4.6 Relative expression of apoA1 mRNA after recovery 2 days

Group	N	Mean	Std. Deviation	Sig. (2-tailed)	
LIH	7	1.154	0.340	0.200	§
Plano	7	0.963	0.232		

§P value for paired student's t-test

||P value for signed rank test

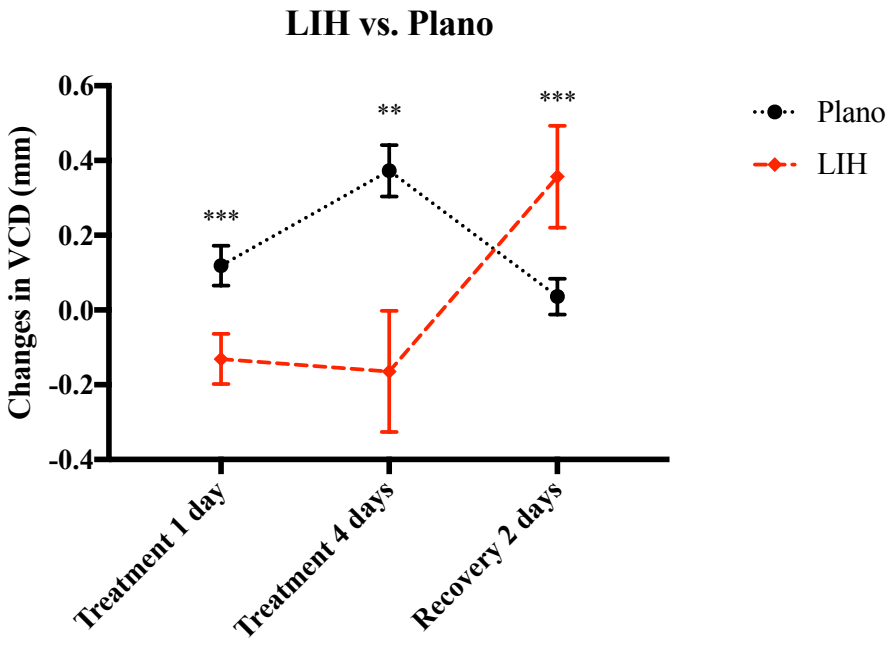

A

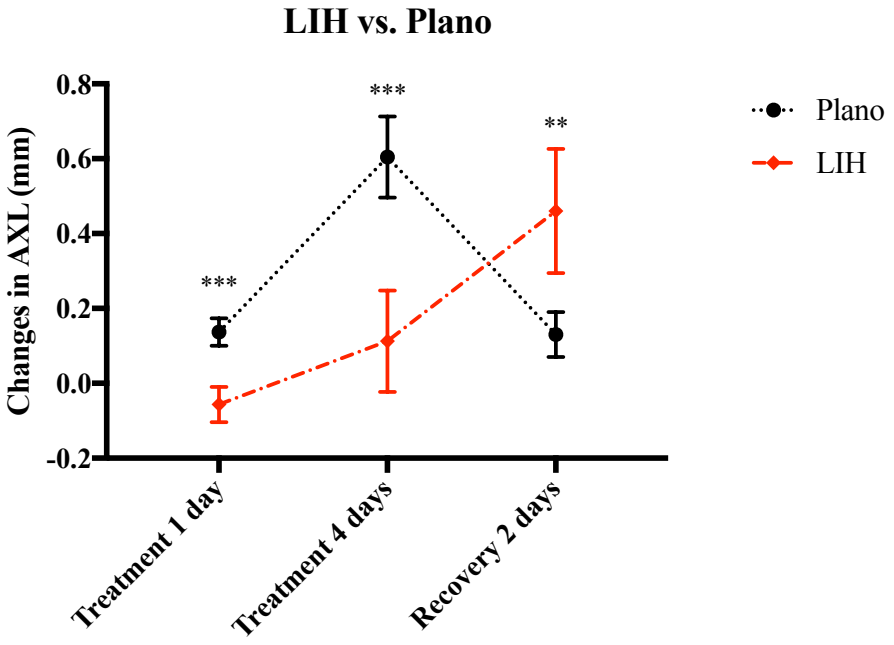
LIH vs. Plano
Changes in AXL (mm)
0.8
0.6
0.4
0.2
0.0
-0.2
***
***
**
Treatment 1 day
Treatment 4 days
Recovery 2 days
Plano
LIH

B

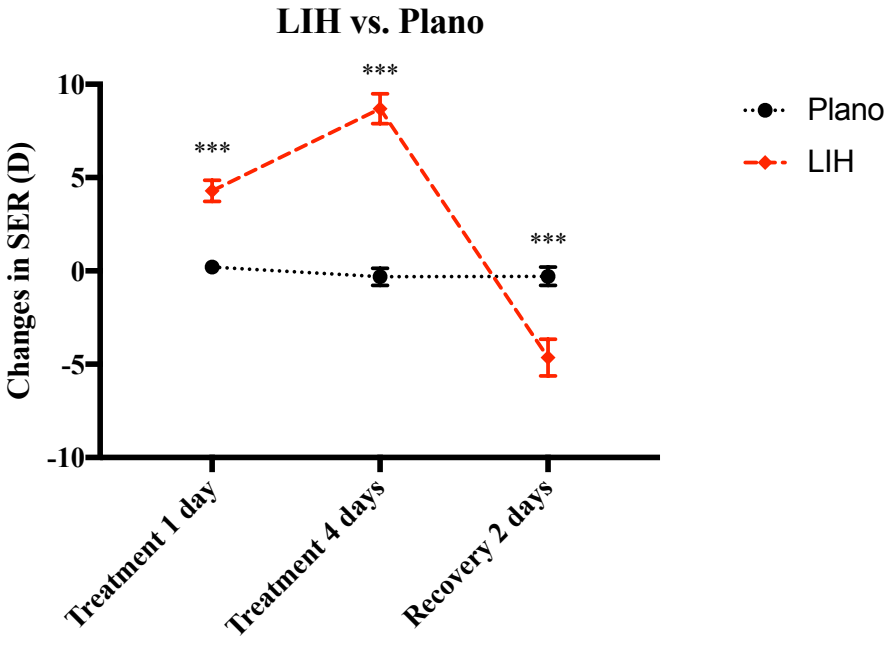
LIH vs. Plano
Changes in SER (D)
10
5
0
-5
-10
***
***
***
Treatment 1 day
Treatment 4 days
Recovery 2 days
Plano
LIH

C

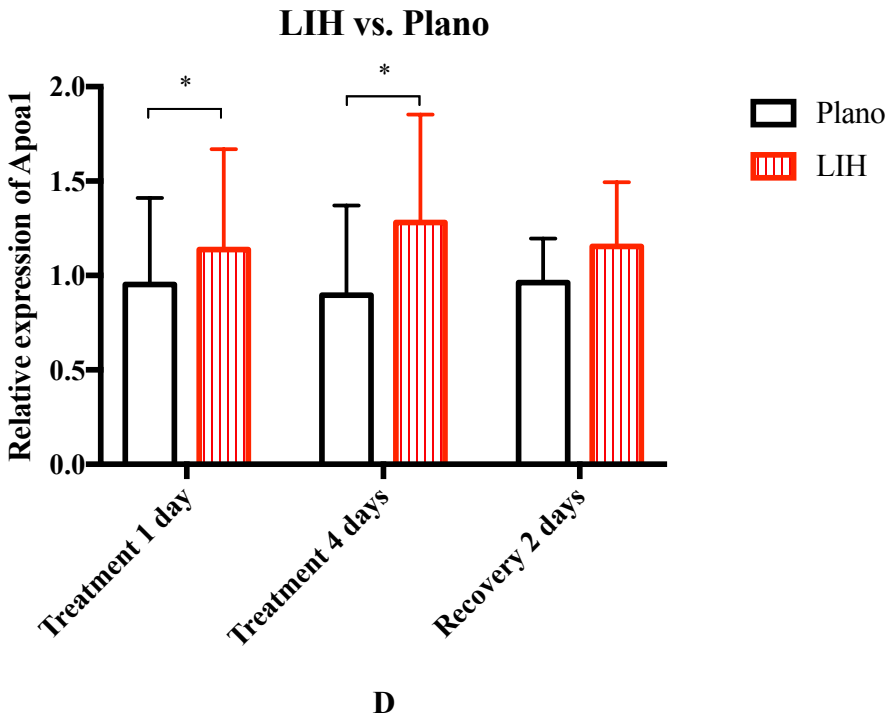

Figure 3.4.1 The comparisons of ocular parameters change and relative expression of apoA1 mRNA after treatment 1 day and 4 days and recovery 2 days.

The effects of LIH on change in (A) VCD (mm), (B) AXL (mm), (C) SER (D) and relative expression of apoA1 mRNA after treatment 1 day and 4 days and recovery 2 days. Mean ±SD, *p<0.05, **p<0.01, ***p<0.001.

3.4.2 LIM vs Plano

3.4.2.1 Treatment for 1 day

Comparison between LIM and plano for 1 day, there was no significant difference in change of ocular parameters and refractive error between these two groups (Table 3.4.6, Figure 3.4.2).

Table 3.4.6 The comparisons of ocular parameters and refractive error change after treatment 1 day

Group		N	Mean	Std. Deviation	Sig. (2-tailed)	
ACD (mm)	Plano	8	-0.031	0.081	0.727	||
	LIM	8	0.008	0.032		
LT (mm)	Plano	8	0.003	0.211	0.727	||
	LIM	8	0.059	0.063		
VCD (mm)	Plano	8	0.040	0.077	0.064	§
	LIM	8	0.085	0.071		
AXL (mm)	Plano	8	0.012	0.232	0.070	||
	LIM	8	0.152	0.056		
RT (mm)	Plano	8	-0.008	0.010	0.854	§
	LIM	8	-0.007	0.017		
CT (mm)	Plano	8	-0.022	0.016	0.993	§
	LIM	8	-0.022	0.022		
ST (mm)	Plano	8	0.006	0.009	0.095	§
	LIM	8	-0.004	0.015		
SER (D)	Plano	8	-0.063	0.563	0.812	§
	LIM	8	-0.188	1.280		

§P value for paired student's t-test

||P value for signed rank test

After 1 day of LIM, the relative expression of apoA1 mRNA was detected by qPCR. The mRNA relative expression was significantly higher in LIM retinas than in the control (Table 3.4.7, Figure 3.4.2).

Table 3.4.7 Relative expression of apoA1 mRNA after treatment 1 day

Group	N	Mean	Std. Deviation	Sig. (2-tailed)	
LIM	8	1.450	0.523	0.023	§
Plano	8	0.993	0.280		

§P value for paired student's t-test

||P value for signed rank test

3.4.2.2 Treatment for 4 days

Comparison between LIM and plano for 4 days, the LIM eyes became significantly more myopic than the controls. The changes in VCD and AXL in LIM eyes were significantly more than that of the plano lenses induced eyes. The changes in RT, CT and SER in LIM eyes were significantly less than that of the plano lenses induced eyes. There was no significant difference in ACD, LT and ST between LIM and plano eyes (Table 3.4.8, Fig 3.4.2).

Table 3.4.8 The comparisons of ocular parameters and refractive error change after treatment 4 days

Group		N	Mean	Std. Deviation	Sig. (2-tailed)	
ACD (mm)	Plano	8	0.101	0.034	0.328	§
	LIM	8	0.122	0.054		
LT (mm)	Plano	8	0.152	0.036	0.804	§
	LIM	8	0.161	0.090		
VCD (mm)	Plano	8	0.276	0.111	0.000	§
	LIM	8	0.725	0.166		
AXL (mm)	Plano	8	0.529	0.115	0.000	§
	LIM	8	1.009	0.163		
RT (mm)	Plano	8	-0.004	0.011	0.016	§
	LIM	8	-0.021	0.014		
CT (mm)	Plano	8	0.025	0.031	0.027	§
	LIM	8	-0.006	0.024		
ST (mm)	Plano	8	0.013	0.011	0.501	§
	LIM	8	0.008	0.023		
SER (D)	Plano	8	-0.688	0.651	0.008	||
	LIM	8	-7.438	0.320		

§P value for paired student's t-test

||P value for signed rank test

After 4 days LIM, the relative expression of apoA1 mRNA was detected by qPCR. The mRNA relative expression was significantly higher in LIM retinas than those induced by plano lens (Table 3.4.9, Figure 3.4.2).

Table 3.4.9 Relative expression of apoA1 mRNA after treatment 4 days

Group	N	Mean	Std. Deviation	Sig. (2-tailed)	
LIM	8	1.369	0.649	0.033	§
Plano	8	0.884	0.213		

§P value for paired student's t-test

||P value for signed rank test

3.4.2.3 Recovery of 2 days

Comparison the recovery for 2 days after LIM and plano, the LIM group eyes became significantly more hyperopic than the controls. The changes in VCD and AXL in LIM group eyes were significantly less than that of the plano group eyes. The changes in RT, CT and SER in LIM group eyes were significantly more than that of the plano group eyes. There was no significant difference in ACD, LT and ST between these two groups (Table 3.4.10, Figure 3.4.2).

Table 3.4.10 The comparisons of ocular parameters and refractive error after recovery of 2 days

Group		N	Mean	Std. Deviation	Sig. (2-tailed)	
ACD (mm)	Plano	8	0.039	0.018	0.727	||
	LIM	8	0.033	0.046		
LT (mm)	Plano	8	0.034	0.048	0.937	§
	LIM	8	0.035	0.040		
VCD (mm)	Plano	8	0.156	0.060	0.005	§
	LIM	8	-0.066	0.173		
AXL (mm)	Plano	8	0.228	0.098	0.002	§
	LIM	8	0.002	0.170		
RT (mm)	Plano	8	-0.011	0.011	0.015	§
	LIM	8	0.010	0.019		
CT (mm)	Plano	8	0.009	0.089	0.001	§
	LIM	8	0.277	0.130		
ST (mm)	Plano	8	0.006	0.016	0.390	§
	LIM	8	0.016	0.022		
SER (D)	Plano	8	-0.500	0.802	0.000	§
	LIM	8	6.813	0.704		

§P value for paired student's t-test

||P value for signed rank test

After 2 days of recovery, the relative expression of apoA1 mRNA was detected by qPCR. The mRNA relative expression was no significant difference between these two groups (Table 3.4.11, Figure 3.4.2).

Table 3.4.11 Relative expression of apoA1 mRNA after recovery 2 days

Group	N	Mean	Std. Deviation	Sig. (2-tailed)	
LIM	8	0.899	0.422	0.062	§
Plano	8	0.690	0.215		

§P value for paired student's t-test

||P value for signed rank test

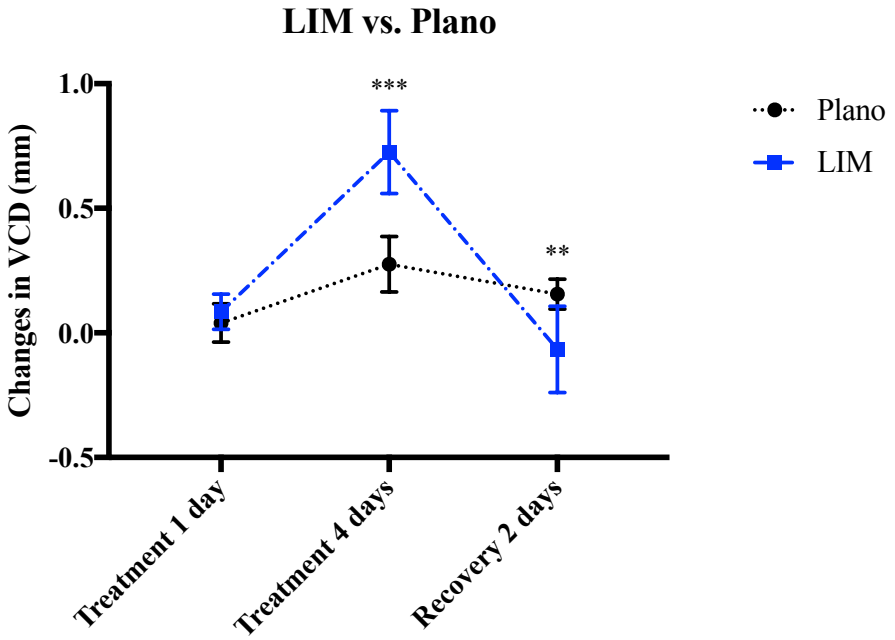
LIM vs. Plano
Changes in VCD (mm)
1.0
0.5
0.0
-0.5
***
**
Treatment 1 day
Treatment 4 days
Recovery 2 days
Plano
LIM

A

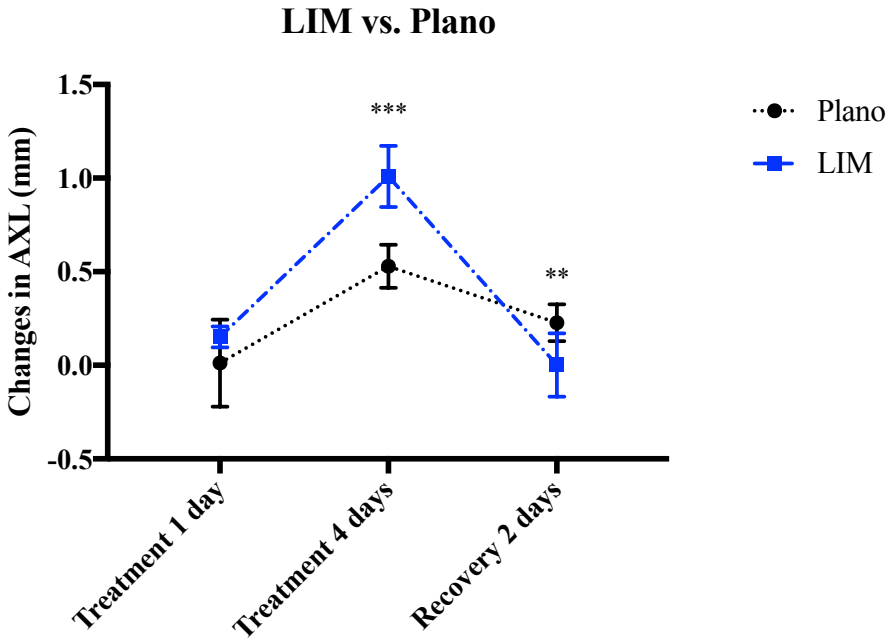
LIM vs. Plano
Changes in AXL (mm)
1.5
1.0
0.5
0.0
-0.5
***
**
Treatment 1 day
Treatment 4 days
Recovery 2 days
Plano
LIM

B

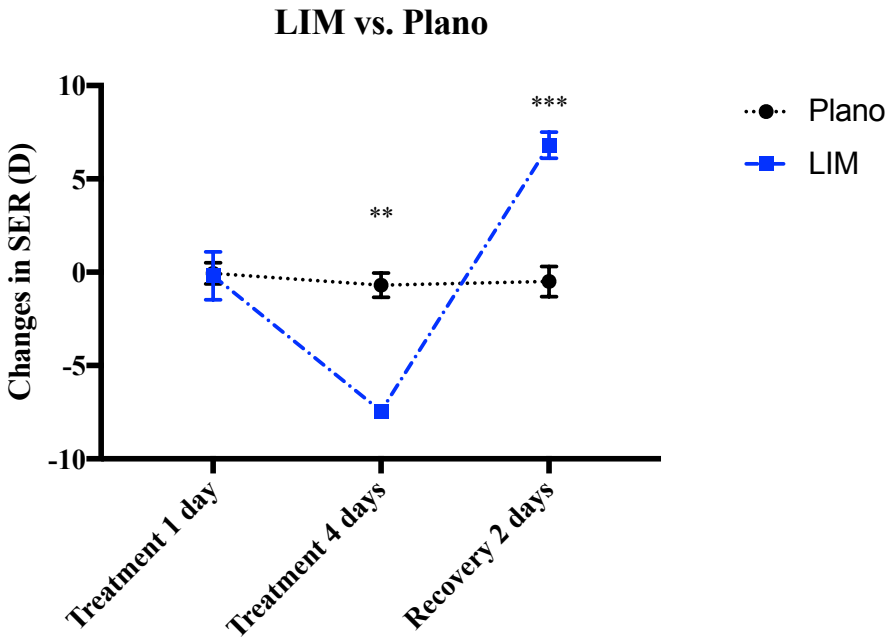
LIM vs. Plano
Changes in SER (D)
10
5
0
-5
-10
**
***
Plano
LIM
Treatment 1 day
Treatment 4 days
Recovery 2 days

C

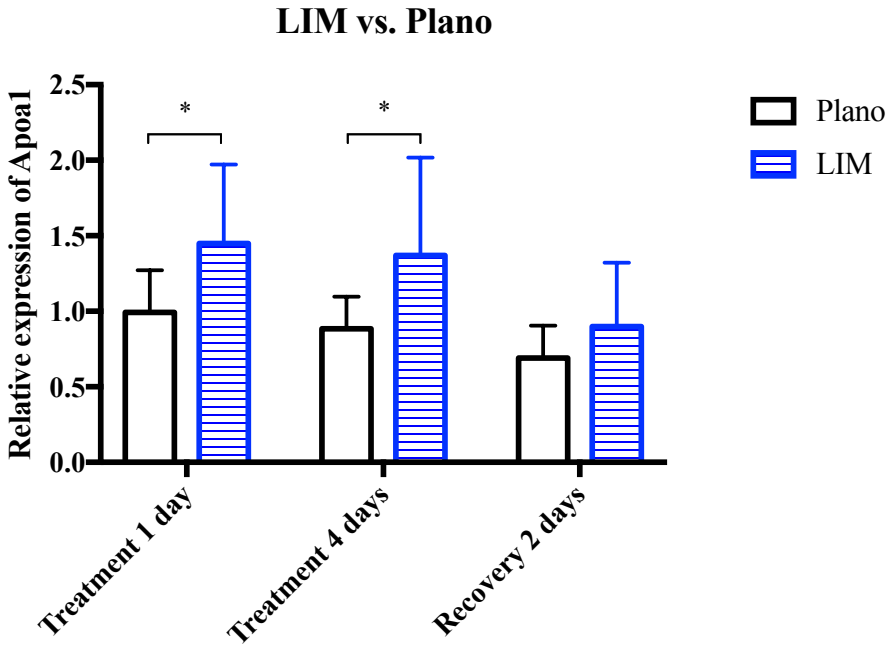
LIM vs. Plano
Relative expression of Apoa1
2.5
2.0
1.5
1.0
0.5
0.0
*
*
Plano
LIM
Treatment 1 day
Treatment 4 days
Recovery 2 days

D

Figure 3.4.2 The comparisons of ocular parameters change and relative expression of apoA1 mRNA after treatment 1 day and 4 days and recovery 2 days.

The effects of LIM on change in (A) VCD (mm), (B) AXL (mm), (C) SER (D) and relative expression of apoA1 mRNA after treatment 1 day and 4 days and recovery 2 days. Mean ±SD, *p<0.05, **p<0.01, ***p<0.001.

3.4.3 LIH vs. LIM

3.4.3.1 Treatment 1 day

Comparison between LIH lenses and LIM for 1 day, the eyes with LIH became significantly more hyperopic than LIM eyes. The changes in vitreous chamber depth (VCD) and axial length (AXL) in LIH eyes were significantly less than that of the LIM eyes. The changes in spherical equivalent refractive error (SER) and choroid thickness (CT) in LIH eyes was significantly more than that of the LIM eyes. There was no significant difference in anterior chamber depth (ACD), lens thickness (LT), retina thickness (RT) and sclera thickness (ST) between LIH and LIM eyes (Table 3.4.12, Figure 3.4.3).

Table 3.4.12 The comparisons of ocular parameters after 1 day treatment

Group		N	Mean	Std. Deviation	Sig. (2-tailed)	
ACD (mm)	LIM	8	0.008	0.032	0.345	*
	LIH	7	0.023	0.028		
LT (mm)	LIM	8	0.059	0.063	0.810	*
	LIH	7	0.051	0.061		
VCD (mm)	LIM	8	0.085	0.071	0.000	*
	LIH	7	-0.131	0.067		
AXL (mm)	LIM	8	0.152	0.056	0.000	*
	LIH	7	-0.057	0.047		
RT (mm)	LIM	8	-0.007	0.017	0.232	#
	LIH	7	0.003	0.016		
CT (mm)	LIM	8	-0.022	0.022	0.000	*
	LIH	7	0.191	0.032		
ST (mm)	LIM	8	-0.004	0.015	1.000	#
	LIH	7	-0.001	0.008		
SER (D)	LIM	8	-0.188	1.280	0.000	*
	LIH	7	4.286	0.567		

*P value for Independent T-test

#P value for Mann-Whitney test

After 1 day of LIH and LIM, the relative expression of apoA1 mRNA was detected by qPCR. The mRNA relative expression was not significantly different between LIH and LIM retinas (Table 3.4.13, Figure 3.4.3).

Table 3.4.13 Relative expression of apoA1 mRNA after treatment 1 day

Group	N	Mean	Std. Deviation	Sig. (2-tailed)	
LIM	8	1.450	0.523	0.274	*
LIH	7	1.138	0.531		

*P value for Independent T-test

#P value for Mann-Whitney test

3.4.3.2 Treatment for 4 days

Comparison between LIH and LIM for 4 day, the eyes with LIH became significantly more hyperopic than the LIM eyes. The changes in VCD and AXL in LIH eyes were significantly less than that of the LIM eyes. The changes in RT, CT and SER in LIH eyes was significantly more than that of the LIM eyes. There was no significant difference in ACD, LT and ST between LIH and LIM eyes (Table 3.4.14, Fig 3.4.3).

Table 3.4.14 The comparisons of ocular parameters change after treatment 4 days

Group		N	Mean	Std. Deviation	Sig. (2-tailed)	
ACD (mm)	LIM	8	0.122	0.054	0.773	*
	LIH	8	0.115	0.052		
LT (mm)	LIM	8	0.161	0.090	0.960	*
	LIH	8	0.162	0.054		
VCD (mm)	LIM	8	0.725	0.166	0.000	#
	LIH	8	-0.164	0.162		
AXL (mm)	LIM	8	1.009	0.163	0.000	*
	LIH	8	0.113	0.135		
RT (mm)	LIM	8	-0.021	0.014	0.028	*
	LIH	8	0.008	0.031		
CT (mm)	LIM	8	-0.006	0.024	0.000	*
	LIH	8	0.316	0.117		
ST (mm)	LIM	8	0.008	0.023	0.419	*
	LIH	8	0.000	0.014		
SER (D)	LIM	8	-7.438	0.320	0.000	#
	LIH	8	8.688	0.799		

*P value for Independent T-test

#P value for Mann-Whitney test

After 4 days LIH, the relative expression of apoA1 mRNA was detected by qPCR. The mRNA relative expression was not significantly different between LIH and LIM retinas (Table 3.4.15, Figure 3.4.3).

Table 3.4.15 Relative expression of apoA1 mRNA after treatment 4 days

Group	N	Mean	Std. Deviation	Sig. (2-tailed)	
LIM	8	1.369	0.649	0.779	*
LIH	8	1.281	0.571		

*P value for Independent T-test

#P value for Mann-Whitney test

3.4.3.3 Recovery 2 days

Comparison the recovery for 2 days after LIH and LIM, the LIH group eyes became significantly more myopic than the LIM. The changes in LT, VCD and AXL in LIH group eyes were significantly more than that of the LIM group eyes. The changes in CT and SER in LIH group eyes were significantly less than that of the LIM group eyes. There was no significant difference in ACD and ST between these two groups (Table 3.4.16, Figure 3.4.3).

Table 3.4.16 The comparisons of ocular parameters after recovery of 2 days

Group		N	Mean	Std. Deviation	Sig. (2-tailed)	
ACD (mm)	LIM	8	0.033	0.046	0.851	*
	LIH	7	0.029	0.026		
LT (mm)	LIM	8	0.035	0.040	0.047	*
	LIH	7	0.074	0.027		
VCD (mm)	LIM	8	-0.066	0.173	0.000	*
	LIH	7	0.357	0.136		
AXL (mm)	LIM	8	0.002	0.170	0.000	*
	LIH	7	0.460	0.166		
RT (mm)	LIM	8	0.010	0.019	0.094	#
	LIH	7	-0.008	0.012		
CT (mm)	LIM	8	0.277	0.130	0.000	*
	LIH	7	-0.252	0.112		
ST (mm)	LIM	8	0.016	0.022	0.694	#
	LIH	7	0.010	0.017		
SER (D)	LIM	8	6.813	0.704	0.000	*
	LIH	7	-4.643	0.988		

*P value for Independent T-test

#P value for Mann-Whitney test

After 2 days of recovery, the relative expression of apoA1 mRNA was detected by qPCR. The mRNA relative expression was no significant difference between these two groups (Table 3.4.17, Figure 3.4.3).

Table 3.4.17 Relative expression of apoA1 mRNA after recovery 2 days

Group	N	Mean	Std. Deviation	Sig. (2-tailed)	
LIM	8	0.899	0.422	0.225	*
LIH	7	1.154	0.340		

*P value for Independent T-test

#P value for Mann-Whitney test

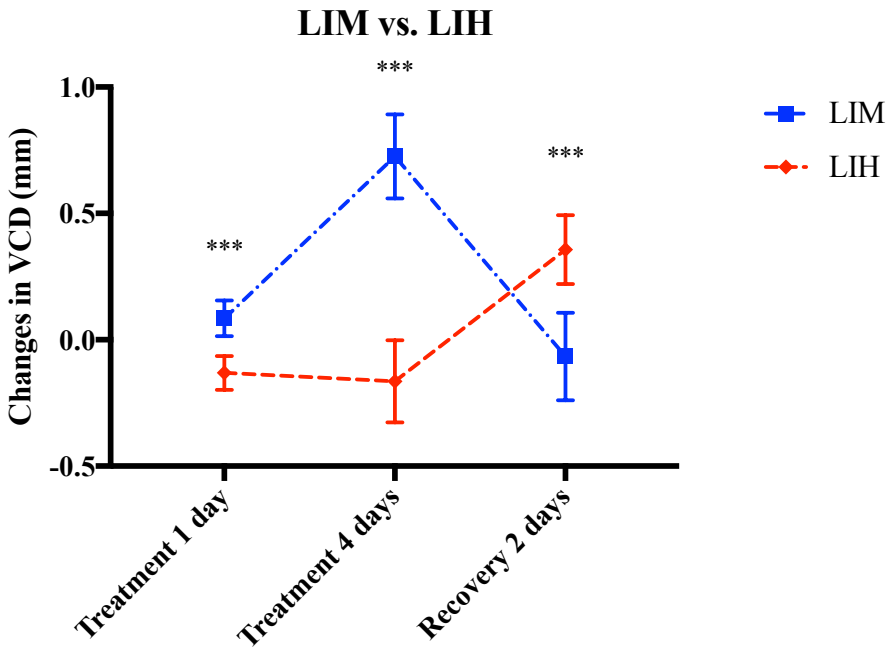
LIM vs. LIH
Changes in VCD (mm)
1.0
0.5
0.0
-0.5
***
***
***
Treatment 1 day
Treatment 4 days
Recovery 2 days
LIM
LIH

A

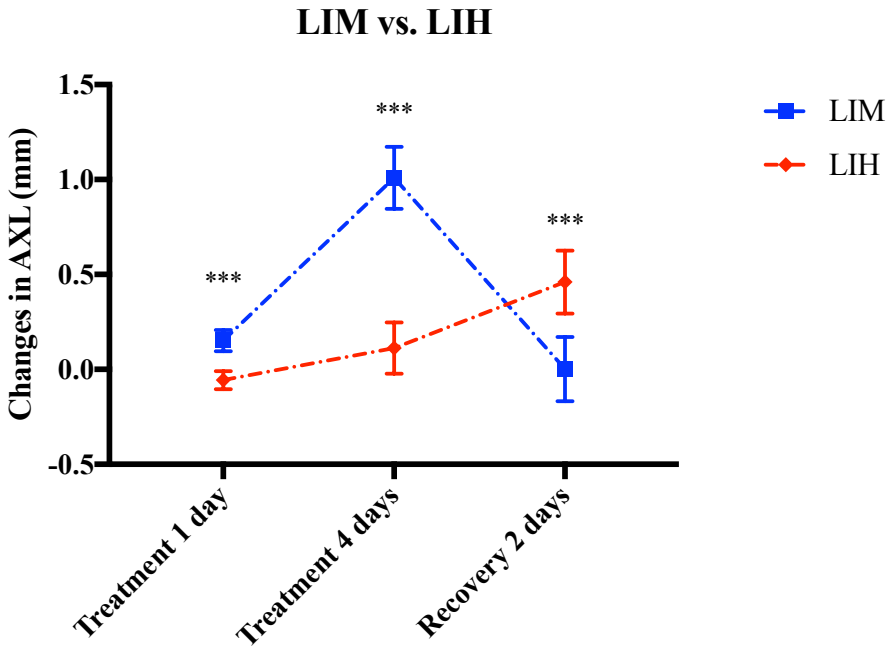
LIM vs. LIH
Changes in AXL (mm)
1.5
1.0
0.5
0.0
-0.5
***
***
***
Treatment 1 day
Treatment 4 days
Recovery 2 days
LIM
LIH

B

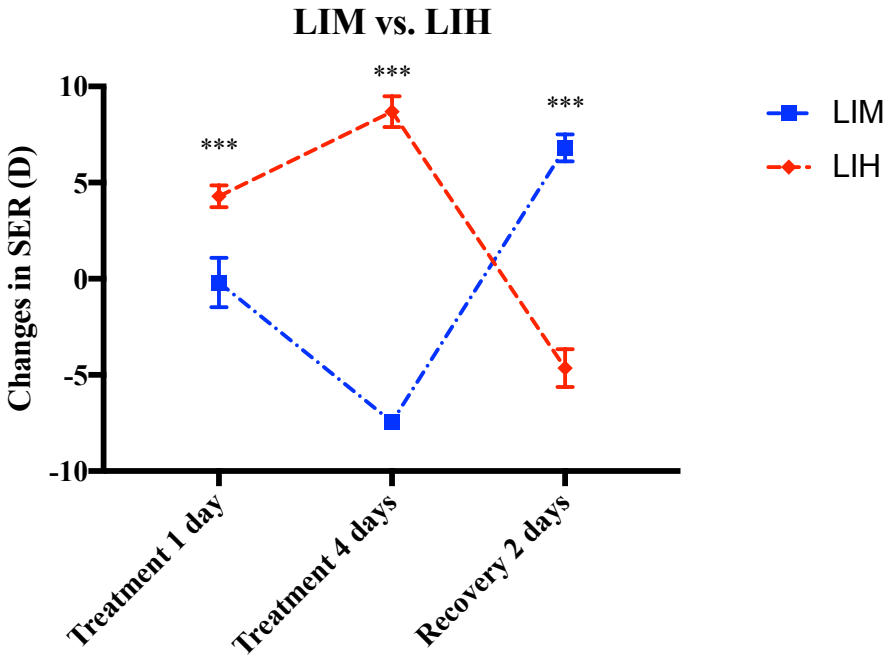
LIM vs. LIH
Changes in SER (D)
10
5
0
-5
-10
***
***
***
Treatment 1 day
Treatment 4 days
Recovery 2 days
LIM
LIH

C

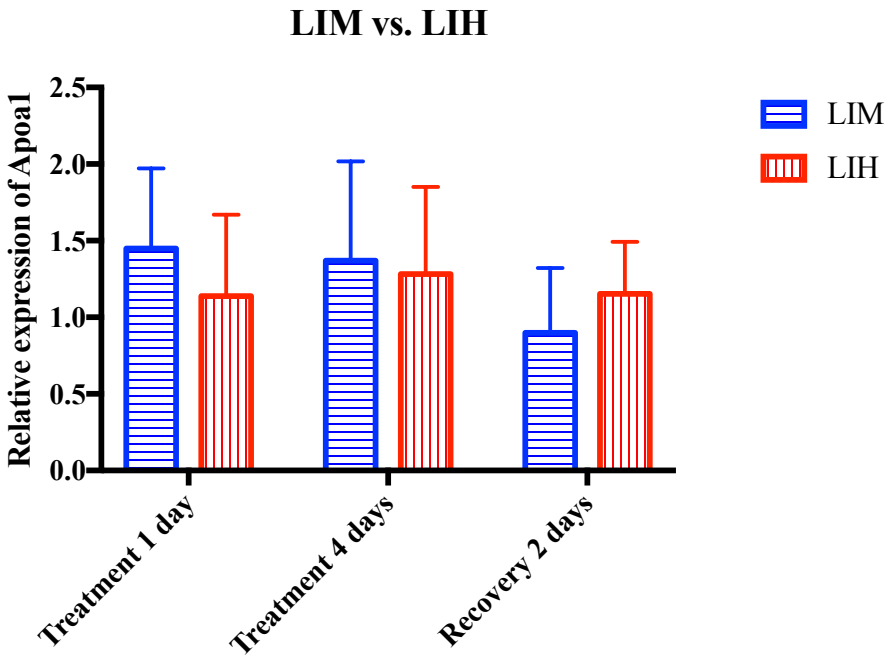
LIM vs. LIH
Relative expression of Apoa1
2.5
2.0
1.5
1.0
0.5
0.0
Treatment 1 day
Treatment 4 days
Recovery 2 days
LIM
LIH

D

Figure 3.4.3 The comparisons of ocular parameters and relative expression of apoA1 mRNA after LIM and LIH treatment for 1 day and 4 days and recovery of 2 days.

(A) VCD (mm), (B) AXL (mm), (C) SER (D) and relative expression of apoA1 mRNA after treatment for 1 day and 4 days and recovery 2 for days. Mean ±SD, *p<0.05, **p<0.01, ***p<0.001.

3.4.4 Summary of results

		mRNA
LIH vs. Plano	1 day LIH	Significantly more hyperopic (Ocular parameters & Refractive error)
	4 days LIH	Significantly more hyperopic (Ocular parameters &Refractive error)
	Recovery 2 days	Significantly more myopic (Ocular parameters & Refractive error)
	mRNA at day 11	Up regulation in LIH group
	mRNA at day 14	Up regulation in LIH group
	mRNA at day 16	Not significantly different
LIM vs. Plano	1 day induced	Not significantly different (Ocular parameters & Refractive error)
	4 days induced	Significantly more myopic (Ocular parameters & Refractive error)

	Recovery 2 days	Significantly more hyperopic (Ocular parameters & Refractive error)
	mRNA at day 11	Up regulation in LIM group
	mRNA at day 14	Up regulation in LIM group
	mRNA at day 16	Not significantly different
LIH vs. LIM	1 day induced	Significantly more hyperopic in LIH group (Ocular parameters & Refractive error)
	4 days induced	Significantly more hyperopic in LIH group (Ocular parameters & Refractive error)
	Recovery 2 days	Significantly more myopic in LIH group (Ocular parameters & Refractive error)
	mRNA at day 11	Not significantly different
	mRNA at day 14	Not significantly different
	mRNA at day 16	Not significantly different

3.5 Discussion

In the current mRNA study, they included three treatment periods with LIH and LIM (1 day, 4 days treatment and 2 days recovery). In each group, the chicks wore +10D or -10D lens randomly on one eye and plano lens on the

follow eye. For further comparison of LIH and LIM, the data from the LIH and LIM eyes were selected and analyzed.

In term of the changes in ocular parameters and refractive errors, the LIH eyes became more hyperopic than the plano and LIM eyes after 1 day treatment. The LIM eyes however did not become significantly more myopic when compared to the plano eyes. After 4 days of treatment, the LIH eyes became more hyperopic than the plano and LIM eyes, whereas the LIM eyes became more myopic than the plano eyes. After 2 days of recovery, the LIH eyes became more myopic than the plano and LIM eyes, and LIM eyes became more hyperopic than the plano eyes. These were consistent with previous studies (Lam et al., 2006, Zhu et al., 2005, Winawer and Wallman, 2002) and our earlier results (Chapter 2).

According to the qPCR results, apoA1 mRNA expression could be identified in the retinas of all three groups - LIH, LIM or normal eyes. Therefore, it strongly suggested that the chick can produce apoA1 protein locally in the retina. However, whether the observed apoA1 protein expressions in chick retina in response to LIH and LIM (Chapter 2) were solely or partly coming from the retina itself or from the choroid and the blood plasma is still unclear.

Moreover, the relative apoA1 mRNA expression was significantly increased after 1 day and 4 days of LIH, but no significant difference was found after 2 days of recovery. The fact that the apao1 mRNA expression in the retina

was increased at the early stage of LIH was not unexpected, since the apoA1 protein was found to be up-regulated in LIH (Chapter 2). However, it is unclear why the apoA1 mRNA expression was not significant different or lower after 2 days of recovery where apoA1 protein level was expected to be lower on recovery from LIH. Even more unexpectedly, the apoA1 mRNA expression in LIM was significantly increased after 1 day and 4 days of LIM. There was no significant difference of mRNA expression after 2 days of recovery when compared to the control (similar results were also observed during recovery from the LIH as described above). The discrepancy in protein and mRNA expression was unexpected and the reason is unclear. When comparing between the LIH and LIM, the relative apoA1 mRNA expression was not significant different between them after 1 day, 4 days and also after 2 days of recovery. Both LIM and LIH induced up-regulation of apoA1 mRNA expressions in the retinas when compared to the control. Apparently, there was inconsistence between the levels of protein and mRNA expressions of apoA1 in these conditions. It could be due to unknown regulation in transcription and translation of apoA1 at work (Maier et al., 2009). Furthermore, protein degeneration may contribute significantly to the regulation of both protein and gene expression processes (de Sousa Abreu et al., 2009). Protein degradation includes lysosomal degradation and ubiquitin mediated proteolysis (de Sousa Abreu et al., 2009). Studies have reported the correlation between mRNA and protein

expression was poor. It has only around 40% explanatory power in predicting protein expression from mRNA expression (Koussounadis et al., 2015, Maier et al., 2009, Ostlund and Sonnhammer, 2012). The fact that the source of retinal apoA1 could come from the choroid or/and the blood plasma may aid the interpretation of the incongruence between protein and mRNA expressions. Nevertheless, the reason for the discrepancy in apoA1 protein and mRNA expression in the current study remains unknown and may require further investigation.

3.6 Conclusions

In the current study, chick retinas can locally express apoA1 mRNA in LIH, LIM and normal growth groups. It follows that chick retinas can also synthesize apoA1 protein locally. The exactly source of apoA1 protein in chick retinas is still unclear, whether it was coming from the retina or both the retina and blood and other sources remains to be investigated.

The retinal apoA1 mRNA expressions were increased in LIH and LIM after 1 day and 4 days of treatment. However, after 2 days of recovery, the mRNA expression did not change significantly in both LIH and LIM. The underlying reason for the discrepancy between the apoA1 protein and mRNA expressions in these paradigms is still unclear.

Chapter 4: The effect of apoA1 protein on lens induced myopic chicks

4.1 Introduction

In chapter 2, apoA1 protein was found to be differentially expressed in LIM and LIH. In particular, retinal apoA1 was increased during hyperopic eye growth and presented itself as a "Stop" signal. In chapter 3, the results indicated that apoA1 could be synthesized locally at the retina. It suggested that the retina may regulate apoA1 protein expression in response to optical defocus signals, and in turn modulate eye growth.

Previous study by Bertrand et al (2006) has reported that apolipoprotein A-1 (apoA1) had an inhibitory effect on the development of myopia whereas the ppar-α agonist (GW7647) could increase apoA1 and inhibit eye growth (Bertrand et al., 2006). Summers et al (2016) suggested that the apoA1 may bind with retinoic acid, and then play an important role in eye growth after birth (Summers et al., 2016). A recent study by Lam et al (2006) showed that the retinal apoA1 was down-regulated in LIM and FDM chicks after 3 days of googles or lens wear, however the difference was no longer significant after 7 days (Lam et al., 2006). Therefore, apoA1 was considered as a key and early signal in the development of myopia (Lam et al., 2006, Bertrand et al., 2006, Summers et al., 2016).

The study by Bertrand et al (2006) explored GW7647 intravitreal injection

to increase apoA1 and slowed eye growth indirectly. However, it is unclear if apoA1 can modulate eye growth directly, such as by direct injection into vitreous chamber. Therefore, we asked in this chapter if directly increasing the retinal apoA1would have a retardation effect on eye growth using LIM as model.

4.2 Objective

To investigate the effect of intravitreal injection of apoA1 protein on myopic eye growth with LIM.

4.3 Materials and methods

4.3.1 Animal

White leghorn chicks (Gallus gallus) were hatched from specific pathogen free (SPF) eggs from Jinan, China at 37.5°C and 75% humidity for one month (Wang et al., 2015). After hatching, chicks were settled in the circumstance at 25℃ and 12/12 hours of light/dark cycle (Chun et al., 2015). Water and food were refilled daily by staff from Centralized Animal Facilities (CAF), the Hong Kong Polytechnic University. All operations to animals in experiments strictly followed the ARVO regulation on the Use of Animals in Research and the Animal Subjects Research Ethic Subcommittee (ASEC) (Wang et al., 2015, Wu et al., 2018b).

4.3.2 Experimental design

For plano apoA1 vs. plano experiment

Nine white leghorn chicks at 4 days after hatching (PN4) were orally fed with daily saline (1ml) and wore plano lenses on both eyes beginning at PN4. ApoA1 protein (10µl of total 2µg) was injected into the treatment eye while the sham solution (10µl, 1×PBS and 0.1% sodium lauroyl sarcosine, PH 7.4) was injected to the control eye. The assignment of control and experimental eyes of the chicks was randomized using the random numbers generated by Microsoft Excel. The intravitreal injection was performed daily for 3 days at the beginning of LIM. This experiment was used to explore the effect of apoA1 intravitreal injection at normal eye growth.

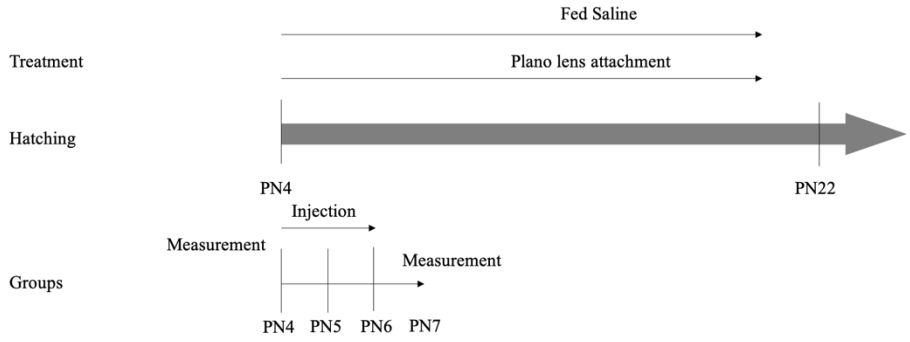

For LIM apoA1 vs. LIM experiment

Twenty-four white leghorn chicks at 4 days after hatching (PN4) were randomly distributed into three groups (Group A, B, and C, each group has 8 chicks). All chicks were orally fed with daily saline (1ml) and wore -10D lenses on both eyes beginning at PN4. ApoA1 protein (10µl of total 2µg)

was injected into the treatment eye while the sham solution (10μl, 1×PBS and 0.1% sodium lauroyl sarcosine, PH 7.4) was injected to the control eye. The assignment of control and experimental eyes of the chicks was randomised using the random numbers generated by Microsoft Excel. The intravitreal injection was performed daily for 3 days (group A: injected at the beginning of LIM; group B: injected after LIM for 5 days; group C: injected after LIM for 15 days). Group A was used to explore the effect of apoA1 intravitreal injection at the beginning of myopic development, as well as the group B at the developing stage of the myopic development and group C at the full developed stage of the myopic development.

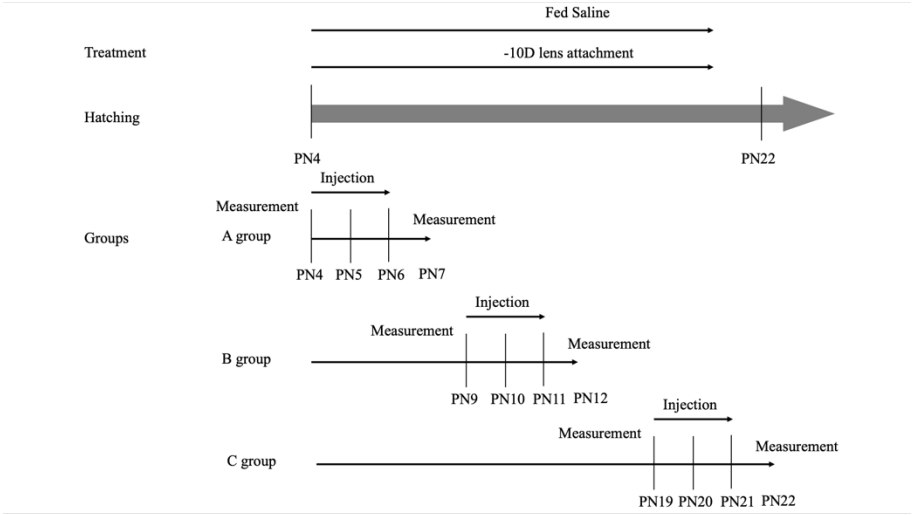

The chicks were anesthetized with 2% isoflurane at a 100% oxygen flow rate of 1L/min. Before and after intravitreal injection and lens wear, the spherical equivalent power (spherical power + half of cylindrical power) was measured by steak retinoscopy and ocular parameters were measured

by high frequency A-scan ultrasound system (30MHz probe sampled at 100MHz). All chicks were sacrificed by carbon dioxide overdose at the end of experiment.

4.3.3 Statistics

Statistical analysis was performed by SPSS software (version 23, SPSS, Chicago, Illinois, USA). The normality was tested by Shapiro-Wilk test. The refractive errors and ocular parameters were compared by paired student's t-test (parameter test) or signed rank test (non-parameter test). The data was reported as the mean ± SD and the P value less than 0.05 was considered statistically significant.

4.4 Results

4.4.1 Intravitreal injection from day 4 to 6 daily in normal eye growth

Comparison between apoA1 and sham treated 3 days and plano lens wear, the changes of ocular parameters and refractive error were not significant between these two groups (Table 4.4.1, Figure 4.4.1).

Table 4.4.1 The comparisons of ocular parameters and refractive error change between day 4 and 7 in normal eye growth

	N	Mean	Std. Deviation	Sig. (2-tailed)	
ACD (mm)_Control	9	0.033	0.033	0.129	§
ACD (mm)_Treatment	9	0.006	0.044		
LT (mm)_Control	9	0.104	0.045	0.325	§
LT (mm)_Treatment	9	0.087	0.046		
VCD (mm)_Control	9	-0.073	0.063	0.490	§
VCD (mm)_Treatment	9	-0.056	0.082		
AXL (mm)_Control	9	0.064	0.052	0.313	§
AXL (mm)_Treatment	9	0.037	0.081		
RT (mm)_Control	9	-0.016	0.024	1.000	||
RT (mm)_Treatment	9	-0.014	0.017		
CT (mm)_Control	9	0.004	0.051	0.156	§
CT (mm)_Treatment	9	-0.022	0.038		
ST (mm)_Control	9	0.010	0.010	0.090	§
ST (mm)_Treatment	9	-0.001	0.009		
SER (D)_Control	9	-0.833	0.250	0.860	§
SER (D)_Treatment	9	-0.806	0.391		

§P value for paired student's t-test

||P value for signed rank test

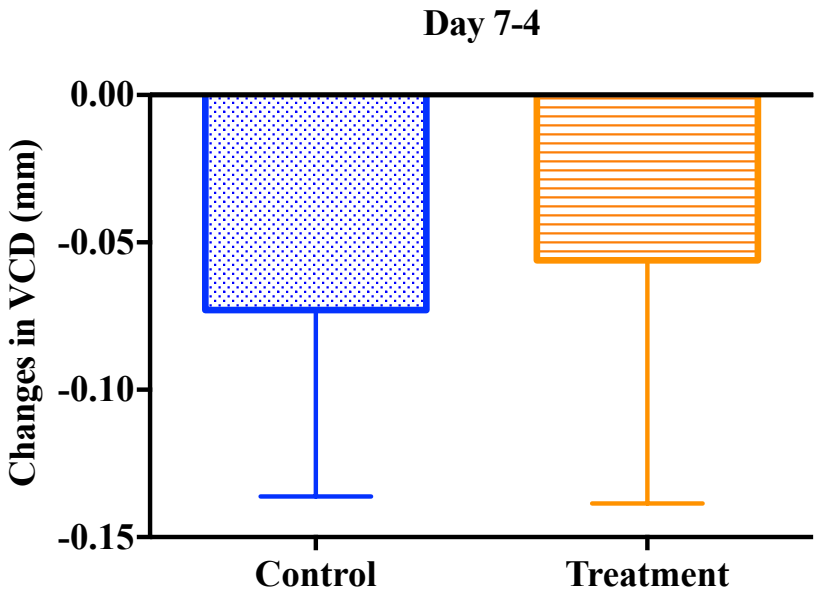
Day 7-4
0.00
-0.05
-0.10
-0.15
Changes in VCD (mm)
Control
Treatment

A

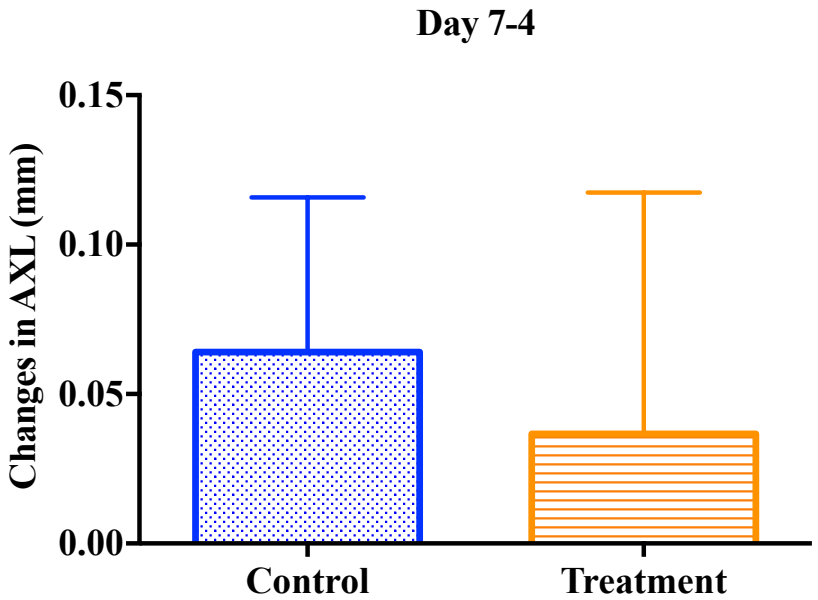
Day 7-4
0.15
0.10
0.05
0.00
Changes in AXL (mm)
Control
Treatment

B

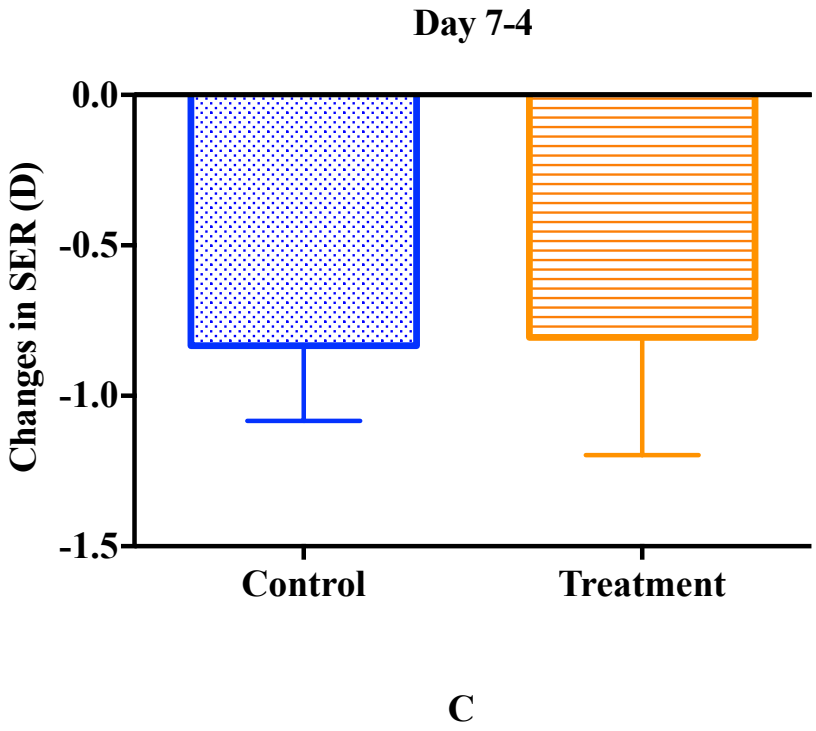

C

Figure 4.4.1 Changes of ocular parameters and refractive error between day 4 and 7 in normal eye growth.

The effects of intravitreal injection of apoA1 on (A) VCD (mm), (B) AXL (mm), (C) SER (D) between day 4 and 7 in normal eye growth. Mean ±SD, *p<0.05, **p<0.01, ***p<0.001

4.4.2 Intravitreal daily injection from day 4 to 6 in LIM

After 3 days, the LIM eyes treated with apoA1 became significantly less myopic than the control eyes (LIM with sham injection only). The changes in ACD, VCD and AXL in apoA1 treated eyes were significantly less than that of the control eyes. The changes in SER in apoA1 treated eyes were

significantly more than control eyes. There was no significant difference in LT, RT, CT and ST between apoA1 treatment and the control eyes (Table 4.4.2, Figure 4.4.2).

Table 4.4.2 The comparisons of ocular parameters and refractive error change between day 4 and 7

	N	Mean	Std. Deviation	Sig. (2-tailed)	
ACD (mm)_Control	8	0.045	0.040	0.024	§
ACD (mm)_Treatment	8	-0.008	0.036		
LT (mm)_Control	8	0.122	0.072	0.837	§
LT (mm)_Treatment	8	0.115	0.055		
VCD (mm)_Control	8	0.154	0.144	0.013	§
VCD (mm)_Treatment	8	0.008	0.101		
AXL (mm)_Control	8	0.321	0.128	0.002	§
AXL (mm)_Treatment	8	0.115	0.090		
RT (mm)_Control	8	-0.024	0.029	0.963	§
RT (mm)_Treatment	8	-0.023	0.011		
CT (mm)_Control	8	-0.062	0.050	0.483	§
CT (mm)_Treatment	8	-0.056	0.041		
ST (mm)_Control	8	0.000	0.012	0.277	§
ST (mm)_Treatment	8	0.009	0.018		
SER (D)_Control	8	-2.438	1.116	0.004	§

SER (D)_Treatment	8	-1.281	0.795

§P value for paired student's t-test

||P value for signed rank test

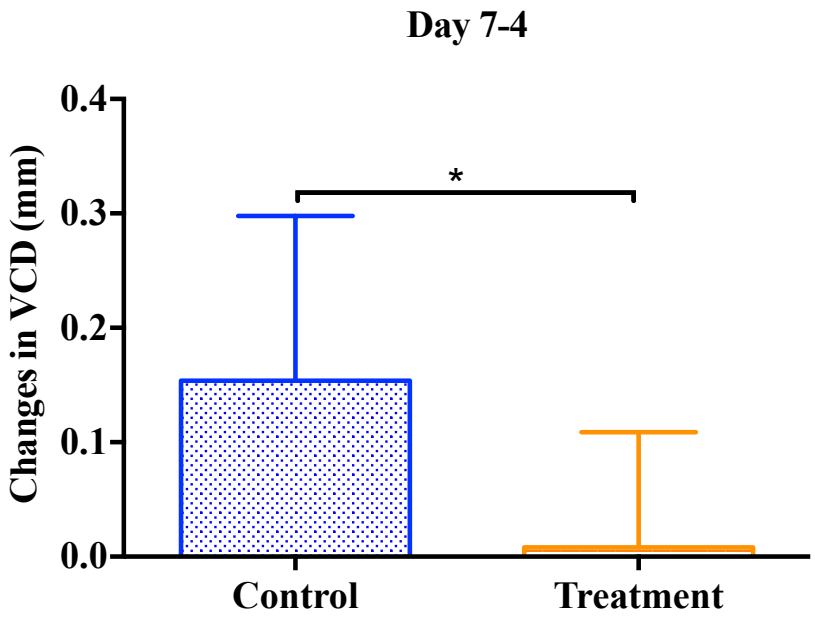

A

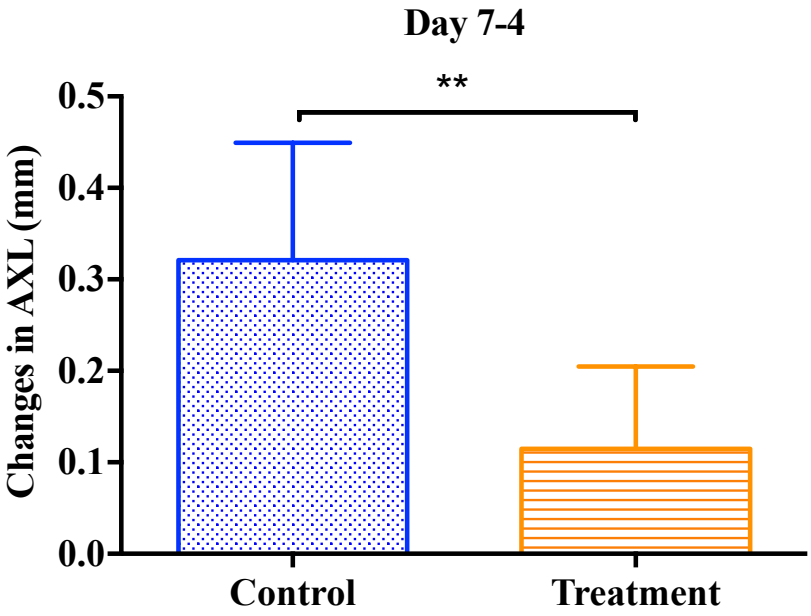
Day 7-4
**
0.5
0.4
0.3
0.2
0.1
0.0
Changes in AXL (mm)
Control
Treatment

B

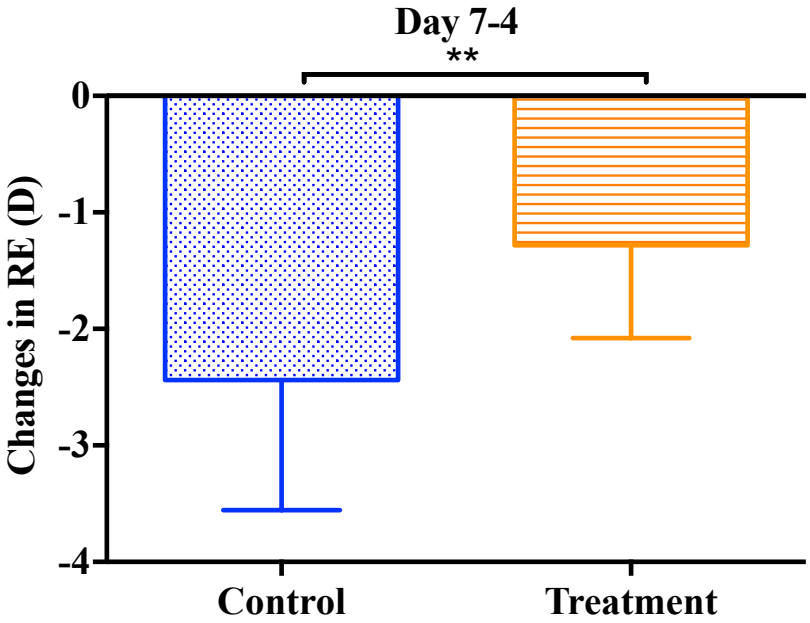
Day 7-4
**
0
-1
-2
-3
-4
Changes in RE (D)
Control
Treatment

C

Figure 4.4.2 Changes of ocular parameters and refractive error between day 4 and 7.

The effects of intravitreal injection of apoA1 on (A) VCD (mm), (B) AXL (mm), (C) SER (D) between day 4 and 7. Mean ±SD, *p<0.05, **p<0.01, ***p<0.001

4.4.3 Intravitreal daily injection of apoA1 from day 9 to 11 in LIM

Comparison between apoA1 protein and control mixture intravitreal injection for 3 days in lens induced myopic eyes, the eyes treated by apoA1 protein became significantly less myopic than the controls. The changes in ACD, VCD and AXL in apoA1 treated eyes were significantly less than control eyes. The changes in LT in apoA1 treated eyes were significantly more than control eyes. Especially, the change of SER was reverse to positive in apoA1 injection eyes but negative in control eyes. There was no significant difference in RT, CT and ST between apoA1 treatment and the control eyes (Table 4.4.3, Figure 4.4.3).

Table 4.4.3 The comparisons of ocular parameters and refractive error change between day 9 and 12

	N	Mean	Std. Deviation	Sig. (2-tailed)	
ACD (mm)_Control	7	0.148	0.053	0.003	§
ACD (mm)_Treatment	7	0.041	0.041		
LT (mm)_Control	7	-0.009	0.024	0.003	§
LT (mm)_Treatment	7	0.075	0.046		
VCD (mm)_Control	7	0.224	0.099	0.001	§
VCD (mm)_Treatment	7	0.079	0.130		
AXL (mm)_Control	7	0.363	0.111	0.016	||
AXL (mm)_Treatment	7	0.196	0.145		
RT (mm)_Control	7	-0.017	0.018	0.108	§
RT (mm)_Treatment	7	-0.009	0.016		
CT (mm)_Control	7	0.035	0.035	0.071	§
CT (mm)_Treatment	7	0.005	0.047		
ST (mm)_Control	7	0.009	0.020	0.796	§
ST (mm)_Treatment	7	0.011	0.006		
SER (D)_Control	7	-0.857	0.675	0.031	||
SER (D)_Treatment	7	2.071	1.730		

§P value for paired student's t-test

||P value for signed rank test

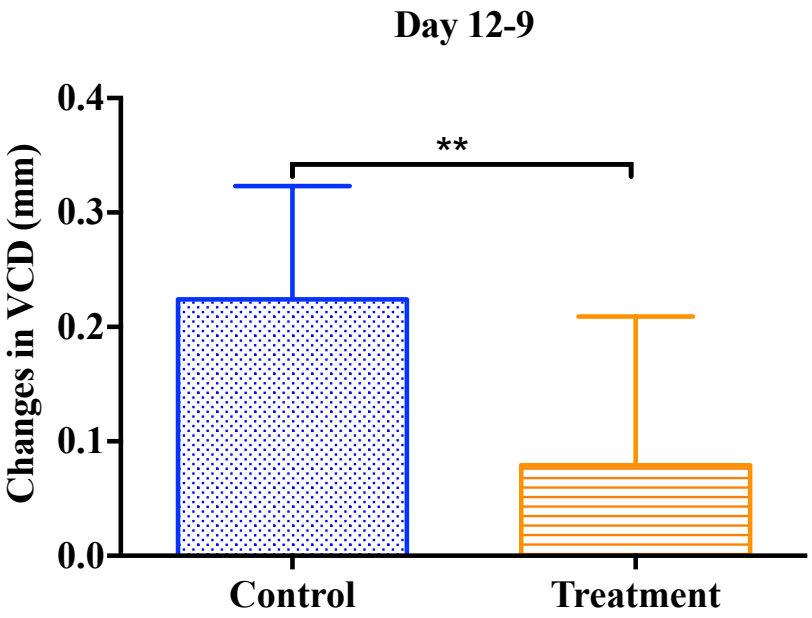
Day 12-9
Changes in VCD (mm)
0.4
0.3
0.2
0.1
0.0
**
Control
Treatment

A

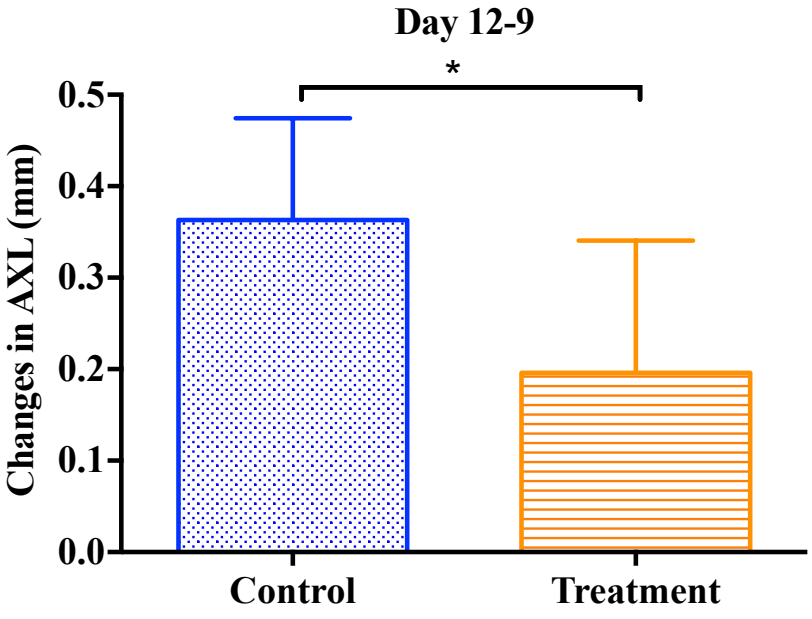
Day 12-9
Changes in AXL (mm)
0.5
0.4
0.3
0.2
0.1
0.0
*
Control
Treatment

B

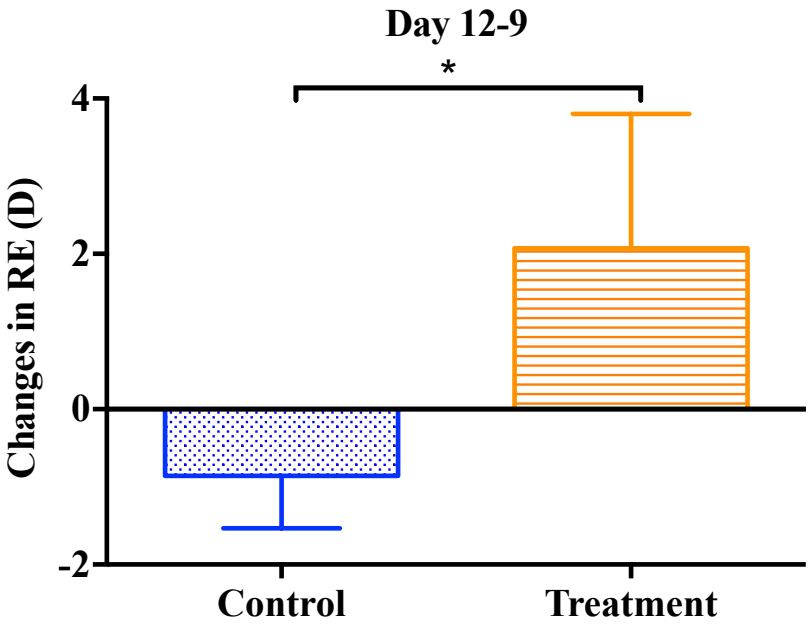

C

Figure 4.4.3 The comparisons of ocular parameters and refractive error change between day 9 and 12.

The effects of intravitreal injection of apoA1 on (A) VCD (mm), (B) AXL (mm), (C) SER (D) between day 9 and 12. Mean ±SD, *p<0.05, **p<0.01, ***p<0.001

4.4.4 Intravitreal injection from day 19 to 21 daily in LIM

Comparison between apoA1 protein injected eye and the control eye injected with control mixture for 3 days in LIM eyes, the experimental eye became significantly less myopic than the controls. The changes in ACD, VCD and AXL in apoA1 treated eyes were significantly less than that of the

control eyes. Interestingly, the change of VCD was negative which meant that the VCD was shorter and hence the change of SER was reversed in direction and became positive. There was no significant difference in LT, RT, CT and ST between apoA1 treatment and the control eyes (Table 4.4.4, Figure 4.4.4).

Table 4.4.4 The comparisons of ocular parameters and refractive error change between day 19 and 22

	N	Mean	Std. Deviation	Sig. (2-tailed)	
ACD (mm)_Control	4	0.115	0.064	0.005	§
ACD (mm)_Treatment	4	0.018	0.078		
LT (mm)_Control	4	0.067	0.043	0.461	§
LT (mm)_Treatment	4	0.103	0.064		
VCD (mm)_Control	4	0.070	0.076	0.049	§
VCD (mm)_Treatment	4	-0.057	0.024		
AXL (mm)_Control	4	0.253	0.056	0.003	§
AXL (mm)_Treatment	4	0.064	0.045		
RT (mm)_Control	4	0.013	0.021	0.295	§
RT (mm)_Treatment	4	-0.004	0.007		
CT (mm)_Control	4	0.006	0.022	0.748	§
CT (mm)_Treatment	4	0.001	0.040		
ST (mm)_Control	4	0.008	0.017	0.782	§

ST (mm)_Treatment	4	0.004	0.018		
SER (D)_Control	4	-0.188	0.239	0.002	§
SER (D)_Treatment	4	1.750	0.204		

§P value for paired student's t-test

||P value for signed rank test

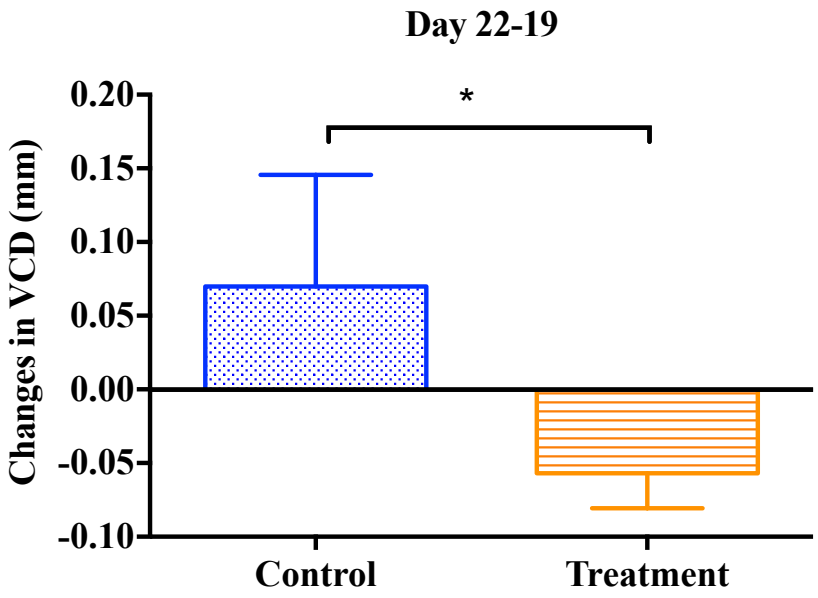

A

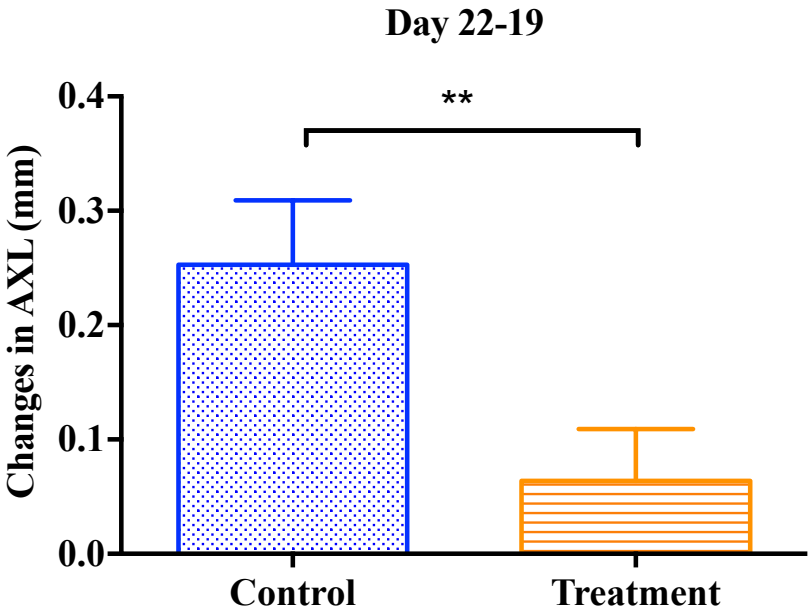
Day 22-19
**
Changes in AXL (mm)
0.4
0.3
0.2
0.1
0.0
Control
Treatment

B

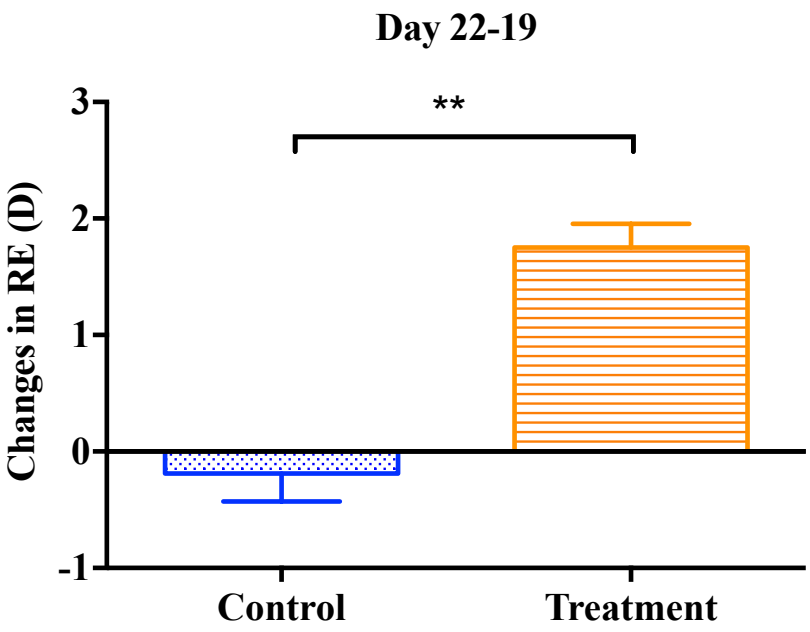
Day 22-19
**
Changes in RE (D)
3
2
1
0
-1
Control
Treatment

C

Figure 4.4.4 The comparisons of ocular parameters and refractive error change between day 19 and 22.

The effects of intravitreal injection of apoA1 on (A) VCD (mm), (B) AXL (mm), (C) SER (D) between day 19 and 22. Mean ±SD, *p<0.05, **p<0.01, ***p<0.001

4.4.5 Summary of results

The effects of apoA1 protein intravitreal injection on ocular parameters, refractive error, and apao1 protein expression were summarized as below.

Summary the effects of apoA1 protein intravitreal injection	
For plano apoA1 vs. plano experiment	
Day 7-4	Not significantly different in ocular parameters and refractive error was found.
For LIM apoA1 vs. LIM experiment	
Day 7-4	Significantly less myopia in LIM apoA1 than LIM group (Ocular parameters and refractive error).
Day 12-9	Significantly less myopia in LIM apoA1 than LIM group (Ocular parameters and refractive error) Reversal in SER changes in LIM apoA1 treated eyes
Day 22-19	Significantly less myopia in LIM apoa1 than LIM group (Ocular parameters and refractive error)

4.5 Discussion

In term of the changes in ocular parameters and reflective error between apoA1 group and sham treated group for 3 days (with no lens wear), there was no significant difference between these two groups. Apparently, apoA1 did not slow down or alter normal eye growth in chicks. However, in LIM and after 3 days of apoA1 intravitreal injection, the eyes became significantly less myopic in apoA1-injected group than the LIM alone group. The difference was evident both at the beginning of LIM treatment, LIM for 5 days or LIM for 15 days. The results indicated that intravitreal injection of apoA1 protein could significantly slow down eye growth. In addition, it could even reverse the changes in SER (at 5 days and 15 days) and shortened the VCD (at 15 days group).

Bertrand et al (2006) has reported that apolipoprotein A-1 (apoA1) is an "Stop" signal in the development of myopia and the ppar-α agonist (GW7647) could increase apoA1 and inhibit eye growth (Bertrand et al., 2006). Summers et al (2016) suggested that the apoA1 may bind with retinoic acid, and then play an important role in eye growth after born (Summers et al., 2016). Lam et al (2006) showed that the retinal apoA1 was

down-regulated in LIM and FDM chicks after 3 days of manipulation, however the difference was no longer significant after 7 days (Lam et al., 2006). In chapter 2, the apoA1 protein was found to be differentially expressed in LIM and LIH. In particular, retinal apoA1 was increased during hyperopic eye growth and presented itself as a "Stop" signal. However, there is no previous study directly investigating the effect of apoA1 on eye growth. The present results showed that apoA1 when directly injected into the vitreous can retard myopic development but did not affect normal eye growth.

Previous studies have reported that increase outdoor time (He et al., 2004, Smith et al., 2014), optical approaches (Goss, 1990, Cheng et al., 2010, Sankaridurg et al., 2010, Hiraoka et al., 2012, Sun et al., 2015), atropine (Gimbel, 1973, Galvis et al., 2016) and 7-methylxanthine (Hung et al., 2018, Trier et al., 2008) were useful strategies to control eye growth. However, the effect depends on factors such as the age of the subject, plasticity and affordability (Cooper and Tkatchenko, 2018, Sankaridurg et al., 2018). In this study, three groups were design to explore the effect of apoA1 intravitreal injection in different stages of animal development, which represented different ages and different amounts of pre-existing myopia. Group A (injection of apoA1 at the beginning of LIM) represented treatment at the onset of myopia development. Group B (LIM for 5 days) represented the stage when myopia was developing rapidly. Lastly, group C

(LIM for 15 days) represented the stage where myopia has fully developed (as in young adulthood). The results in all these groups showed significant retardation of eye growth when injected with apoA1. It was evident that apoA1 could retard myopia development or even reverse myopia irrespective of the stages of myopia development.

4.6 Conclusions

The apoA1 protein intravitreal injection can retard eye growth towards myopia in the LIM paradigm, but not in normal eye growth. It can retard myopia development at different stages: the onset, rapidly developing and fully developed stages. It could even reverse the refractive changes at the developing and fully developed stages. As an analogy to the development of human myopia, it may suggest that apoA1 as a potential myopia control method, may be effective in various stages of myopia development in human.

Chapter 5: The effect of nicotinic acid on eye growth in chicks

5.1 Introduction

It has been suggested that apoA1 is a stop signal to eye growth (Bertrand et al 2006). We have found that apoA1 can slow eye growth in chicks (In chapter 3) and that intravitreal injection of apoA1 can significantly retard LIM eyes growth at various developmental stages. It could even reverse eye growth at the fully developed stage. While the intravitreal injection of apoA1was a proof of concept study, there may be other less invasive and more clinically acceptable way to increase apoA1 expression in the retina. ApoA1 expression is known to be increased by nicotinic acid in human (Parsons and Flinn, 1959, Nagai et al., 2000, Sharma et al., 2006). Previous study showed that there was 20%-30% increase in HDL level in hyperlipidaemic patients after nicotinic acid treatment (1-3g/day, mean dosage is 1.5g/day) for 70 weeks (Birjmohun et al., 2004). The function of nicotinic acid is to inhibit hepatic removal of apoA1 (Parsons and Flinn, 1959) while the synthesis of apoA1 remained unchanged (Jin et al., 1997). The hepatic toxic dose of nicotinic acid is more than 3 g/day for adults (Knip et al., 2000).

ApoA1 is a “STOP” signal protein in eye growth as well as in the development of myopia (Lam et al., 2006). Based on the two observations:

(1) oral administration of nicotinic acid can increase apoA1 level in the blood serum of human (Parsons and Flinn, 1959, Nagai et al., 2000, Sharma et al., 2006), and (2) apoA1 could reduce myopia development in chicks (Lam et al., 2006), we hypothesized that oral administration of nicotinic acid, may increase the retinal apoA1 expression and retard myopic eye growth in chicks.

5.2 Objective

The aim was to explore the effect of nicotinic acid on normal, LIH and LIM eye growth in chicks.

5.3 Materials and methods

5.3.1 Animal

White leghorn chicks (Gallus gallus) were hatched from specific pathogen free (SPF) eggs from Jinan, China at 37.5°C and 75% humidity for one month (Wang et al., 2015). After hatching, chicks were settled in the circumstance at 25℃ and 12/12 hours of light/dark cycle (Chun et al., 2015). Water and food were refilled daily by staff from Centralized Animal Facilities (CAF), the Hong Kong Polytechnic University. All operations to animals in experiments strictly followed the ARVO regulation on the Use of Animals in Research and the Animal Subjects Research Ethic Subcommittee (ASEC) (Wang et al., 2015, Wu et al., 2018b).

5.3.2 Experimental design

For NA vs SA experiment

Sixteen white leghorn chicks at 4 days after hatching (PN4) were randomly distributed into two groups (plano group and NA plano group). Chicks were orally fed 1ml saline daily in plano group while 1ml nicotinic acid solution (Sigma-Alrich company, USA; 150mg/ml nicotinic acid and 50mg/ml sodium hydroxide in PBS; PH = 7) for NA plano group (PN4 to PN14). At PN10, plano lenses were attached to both eyes of all chicks for 4 days (PN10 to PN14). The measurements (refractive error and ocular parameters) were performed at PN4, PN10 and PN14 for all chicks.

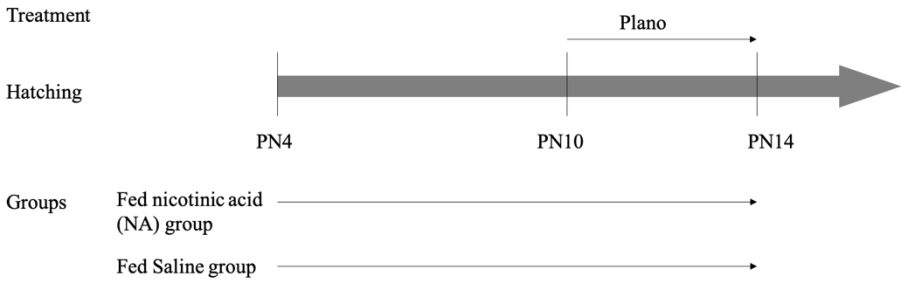

For NA LIH vs SA LIH experiment

Sixteen white leghorn chicks at 4 days after hatching (PN4) were randomly distributed into two groups (LIH group and NA LIH group). Chicks were orally fed 1ml saline daily in LIH group while 1ml nicotinic acid solution (Sigma-Alrich company, USA; 150mg/ml nicotinic acid and 50mg/ml sodium hydroxide in PBS; PH = 7) for NA LIH group (PN4 to PN14). At

PN10, +10D lenses were attached to both eyes of all chicks for 4 days (PN10 to PN14). The measurements (refractive error and ocular parameters) were performed at PN4, PN10 and PN14for all chicks.

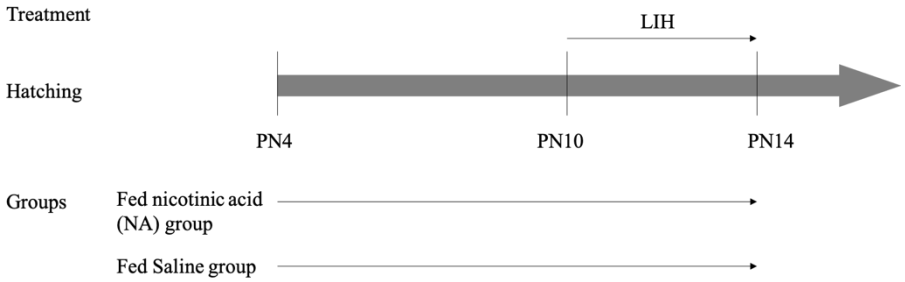

For NA LIM vs SA LIM experiment

Sixteen white leghorn chicks at 4 days after hatching (PN4) were randomly distributed into two groups (LIM group and NA LIM group). Chicks were orally fed 1ml saline daily in LIM group while 1ml nicotinic acid solution (Sigma-Alrich company, USA; 150mg/ml nicotinic acid and 50mg/ml sodium hydroxide in PBS; PH = 7) for NA LIM group (PN4 to PN14). At PN10, -10D lenses were attached to both eyes of all chicks for 4 days (PN10 to PN14). The measurements (refractive error and ocular parameters) were performed at PN4, PN10 and PN14for all chicks.

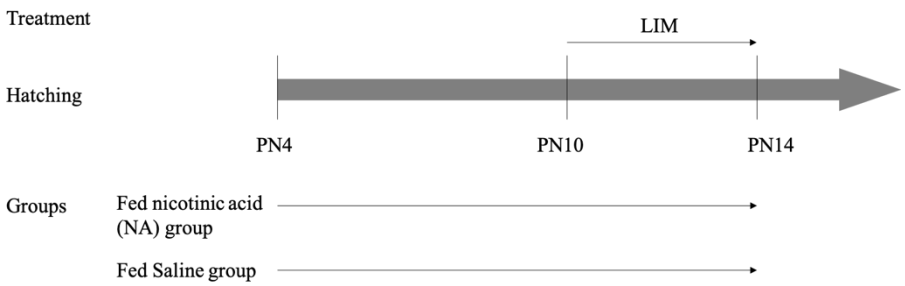

At PN14, after measurements, the transcardial perfusion (described in 2.3.1.2) was performed before chicks sacrificed by carbon dioxide overdose. The eyes were extracted without connective tissue and muscle and carefully washed by PBS buffer. The eyes were dissected on an iced package and retina sample collected without vitreous body and retinal pigment epithelium (RPE) layer. The liquid nitrogen was used to quickly frozen retina samples temporarily. The -80°C fridge was used to stored retina samples. For each chick, only left eye was used to both statistical comparison (refractive error and ocular parameters) and protein differential expression analysis in this experiment.

5.3.3 Extraction of protein from retinal tissue

The frozen retina was homogenized with 300μl protein extraction buffer (table 5.3.1) at 1600×g for 7 minutes. The lysate was incubated in room temperature for 10 minutes and was transferred to 1.5ml Eppendorf tube. Spun at 16000×g for 20 minutes at 4°C, the supernatant was transferred into a new 1.5ml Eppendorf tube. The retinal samples were stored at -80°C before further analysis.

Table 5.3.1 Protein extraction buffer (PH = 8.0 - 9.0) for 10ml

Urea	7M
Tris	40mM
Thiourea	2M
Biolytes	0.2%
CHAPS	2%
ASB (Calbiochem, San Diego, CA, USA)	1%
Mini Protease inhibitor cocktail (Roche Applied Science, Switzerland)	1 tablet

5.3.4 Protein quantification

A kit was used to measure protein concentration in this experiment (Bio-Rad Protein Assay from Bio-Rad Laboratories Company). The different total protein concentrations result in different colors which record different absorbance by Spectrophotometer SP-300 Plus (Optima, Japan) with 595nm. A standard curve was made of five concentrations (0, 0.2, 0.4, 0.6, 0.8μg/μl) by bovine serum albumin (BSA; 2μg/μl) and five corresponding absorbance. The total protein concentration was calculated by their absorbance from a standard curve.

5.3.5 Western blotting

A mixture of 25μg total protein of each sample and loading buffer (4×) was incubated at 95°C for 5 minutes. These denatured mixtures were loaded into a 10% sodium dodecyl sulfate–polyacrylamide gel (SDS-PAGE). The PageRuler^{TM} pre-stained protein ladder Plus (SM1811, Fermentas) was loaded as a reference or markers of protein molecular size. The voltage was set at 60mV constantly for 150 minutes. After electrophoresis, proteins were separated by their molecular weights and ready to be transferred to the polyvinylidene difluoride (PVDF) membrane (Immuno-blot PVDF membrane, BioRed). The transfer apparatus was made of sponge, whatman paper, filter paper, gel, PVDF membrane, whatman paper, sponge from negative pole to positive pole. The Mini Trans-Blot Electrophoretic Transfer Cell system (Bio-Rad Protein Assay from Bio-Rad Laboratories Company) with transfer buffer and ice pack was used to transfer protein from a PAGE gel to PVDF membrane. The voltage was constant at 57V for 90 minutes. After transfer was completed, the PVDF membrane was blocked with 5% non-fat dry milk (Nestle, Switzerland) in 1×TBST buffer for 1 hour at room temperature. The TBST buffer was made of 0.1M Tris-HCL, 0.5M NaCl and 0.05% Tween-20 (PH = 8.0). The primary antibody (Table 2.3.4) which was diluted by 0.3% non-fat dry milk in 1×TBST buffer was used to incubate PVDF membrane after blocking at 4°C over-night. The 1×TBST buffer was used to wash membrane thrice (20 minutes once) at room

temperature. The secondary antibody (Table 5.3.2) which was diluted by 0.3% non-fat dry milk in 1×TBST buffer was used to incubate membrane at room temperature for 1 hour. After 1×TBST buffer thrice (20 minutes once) washing, the membrane was incubated into an enhanced chemiluminescent substrate mixture (Stable Peroxide Solution: Luminol/Enhancer solution= 1:1, SuperSignal® West Pico, Thermo Scientific) for 5 minutes at room temperature. The chemiluminescent signals were detected and captured as a picture (TIFF format) and quantified by the Image Studio™ Software version 5.0 (LI-COR Corporate, US).

Table 5.3.2 List of antibodies

	Protein	Antibody	Dilution
Primary antibody	ApoA1	Rabbit anti-Chick ApoA1 polyclonal antibody	1:1000
	GapDH	Mouse anti-Chick GapDH polyclonal antibody	1:10000
Secondary antibody	ApoA1	HRP-Goat anti-Rabbit IgG (H+L) conjugate	1:2000
	GapDH	HRP-Goat anti-Mouse IgG (H+L) conjugate	1:40000

5.3.6 LC-MS (SWATH)

5.3.6.1 Sample preparation

The 75μg total protein each sample was reduced by 8mM dithiothreitol (DTT) at 37°C for 1 hour. 20mM iodoacetamide was used to alkylate free sulfhydryl groups on the cysteine residues in the dark at 25°C for 30 minutes. 100% acetone was used for protein precipitation at -20°C for 12 hours. Spun it at 16000×g for 20 minutes in 4°C and then removed supernatant. Then, protein pellet was washed by using 500μl 80% acetone, and spinning at 16000×g for 20 minutes in 4°C. Subsequently, the sample was air-dried in room temperature after removing supernatant. A mixture (1M urea and 25mM ammonium bicarbonate) was used to dissolve the dry protein pellet at room temperature. Total 20μg protein was digested by 0.8μg trypsin (sample: trypsin= 25:1, w/w) at 37°C for 12 hours. After digestion, 0.5% formic acid was used to acidify the sample to stop digestion.

5.3.6.2 Liquid chromatography

For peptides fractionation, a pooled retinal protein sample (520μg total protein amount) from 37 chicks' retinas (10μg from each retina sample) was used to build a library. All these chicks were 14 days old and from six groups (plano group = 6; LIH group = 5; SA Minus10 group = 8; NA plano group = 6; NA LIH group = 4 and NA LIM group = 8). The

Eksigentekspert^{tm} ultraLC 100 system (Sciex) integrated with a PolySULFOETHYL ATM Column that is 100×4.6mm column and 5µm porous (200 A°) from PolyLC INC was used to fractionate the peptides. Mobile buffer A contained 10mM ammonium formate (PH=3.0) and 25% CAN. On the other hand, Mobile buffer B contained 500mM ammonium formate (PH=6.8) and 25% ACN. The flow rate of is 0.2 ml/min with linear gradient: 0-10 minutes, 100% A; 10-50 minutes, 100-50% A; 50-55 minutes, 50% A; 55-65 minutes, 50-0% A; 65-80 minutes, 0% A.

For separation by liquid chromatography, 6µl each sample (3 µg) was gradient separated in 120 minutes with Ekisgent 415 nano liquid chromatography (Ion-exchange Chromatography) system. Peptides were loaded on a trap column (200 µm× 0.5 mm, ChromXP C18, 3 µm, 120 A) for desalting. The loading buffer was made of 5% v/v acetonitrile and 0.1% v/v formic acid. The flow rate was 3µl/min and loading time was 15 minutes. Then samples were injected into analytical column (Nano-LC column, 75µm×15cm, ChromXP C18, 3 µm, 120 A) for separation (table 5.3.3).

Table 5.3.3 Separation Parameter

Time (minutes)	Buffer A	Buffer B
1	95%	5%
120	95-65%	5-35%
4	65%	35%
6	65-20%	35-80%
10	20%	80%
2	20-95%	80-5%
17	95%	5%

Buffer A: 5% v/v acetonitrile and 0.1% v/v formic acid

Buffer B: 98% v/v acetonitrile and 0.1% v/v formic acid

5.3.6.3 Mass spectrometry

The TripleTOF 6600 mass spectrometer (QTOF, SCIEX) was used in this experiment. The electro spray ionization (ESI) parameter set as below (Table 5.3.4).

Table 5.3.4ESI Parameter

Item	Setting
ISVF	2300 V
CUR	30 psi
GS1	15 psi
IHT	120 ℃

ISVF: ion spray voltage floating

CUR: curtain gas

GS1: ion source gas

IHT: inter face heater temperature

The IDA method was between 350 and 1500 m/z (250 ms accumulation time) as MS range. Then, the MS/MS range was between 100 and 1800 m/z (80 ms accumulation time). The high sensitivity mode was chosen as 40 intense ions (2-4V). The rolling collision energy (CE) was set as below (table 5.3.5).

Table 5.3.5 IDA Collision Energy Parameter

Charge	Slope	Intercept
Unknown	0.0575	9
1	0.0575	9
2	0.0625	-3
3	0.0625	-5
4	0.0625	-6
5	0.0625	-6

CE= (slope) × (m/z) + (intercept)

The DIA method was between 350 and 1500 m/z (25 m/z fixed loop). The MS/MS setting was the same as IDA method.

5.3.6.4 Protein identification and relative quantification

For building ion libraries, twenty fractions and one single injection pool sample were individually performed DDA acquisitions (3μg each). Protein identifications were searched against Uniprot gallus gallus database (version, 28849 entries) with ProteinPilot 5.0 software. The parameters were set to iodoacetamide as cysteine alkylation, trypsin as digestion enzyme, thorough as search effort and biological modifications as ID focus. The false discovery rate (FDR) was set as 1%. A fractionated library was grouped by combination of 20 fractionated DDAs, while a single injected library was

generated by the single injected pool DDA. The ion library was used to extract corresponding peptide fragment peak in further relative quantification analysis.

For relative quantification (SWATH) analysis, the PeakView 2.0 software (SCIEX) was used to extract corresponding peptide fragment peak via the ion library. The parameters were set to 6 fragments per peptide and 6 peptides per protein. At least 99% confidence and 1% FDR peptides were included to relative quantification without shared peptides and modifications. The ion library mass tolerance was 75 ppm, XIC Extraction Window was 20 minutes and XIC width was 75 ppm. Eleven high abundant peptides from different proteins covered 18 and 118 minutes was chosen for retention time (RT) alignment (Table 5.3.6). After RT alignment, the extracted peaks data were analyzed via MarkerView 1.2.1 software (SCIEX). The iPathwayGuide (Advaita Corporation, https://www.advaitabio.com) was used to pathway analyze from differential expression proteins.

Table 5.3.6 Peptides for retention time (RT) alignment

Peptides	RT (min)
IRDEMVATEQER	18.59
EPITVSSEQMC[CAM]K	27.14
GN[Dea]PTVEVDLYTHK	36.23
SVLQGGALDGVYR	42.73
DNLADDIMR	50.17
ADDGTPFVQMIK	54.62
YISPDQLADLYK	62.49
AVFVDLEPTVIDEVR	71.75
MEDTEPFSPELLSAMMR	87.17
GGILGDLTSSDVGVELPIILMHPK	97.19
SANLVASTLGAILNQLR	117.76

5.3.7 Statistics

Statistical analysis was performed by SPSS software (version 23, SPSS, Chicago, Illinois, USA). The normality was tested by Shapiro-Wilk test. The levene's test was used to homogeneity test. The refractive errors, ocular parameters, proteins differential expression in western blot and LC-MS SWATH were compared with an independent sample student's t-test (parameter) or Mann-Whitney rank sum test (non-parameter). The data was

reported as the mean ± SD and the P value less than 0.05 was considered statistically significant.

.

5.4 Results

5.4.1 The effect of NA on normal eye growth before lens wear

Comparison between nicotinic acid and saline treated 6 days and before lens wear, the changes of ocular parameters and refractive error were not significant between these two groups (Table 5.4.1, Figure 5.4.1).

Table 5.4.1 The comparisons of ocular parameters and refractive error change after 6 days nicotinic acid treated and before lens wear

Treatment		N	Mean	Std. Deviation	Sig. (2-tailed)	
ACD (mm)	NA plano	18	0.084	0.042	0.695	*
	Plano	19	0.090	0.049		
LT (mm)	NA plano	18	0.256	0.071	0.578	#
	Plano	19	0.244	0.082		
VCD (mm)	NA plano	18	0.118	0.117	0.247	*
	Plano	19	0.168	0.138		
AXL (mm)	NA plano	18	0.458	0.125	0.367	*
	Plano	19	0.501	0.163		
RT (mm)	NA plano	18	-0.003	0.020	0.855	*

	Plano	19	-0.005	0.016		
CT (mm)	NA plano	18	-0.025	0.048	0.212	*
	Plano	19	-0.004	0.054		
ST (mm)	NA plano	18	0.009	0.014	0.407	*
	Plano	19	0.013	0.017		
SER (D)	NA plano	18	-1.097	0.625	0.075	#
	Plano	19	-1.290	0.548		

*P value for Independent T-test

#P value for Mann-Whitney test

NA means nicotinic acid treatment group

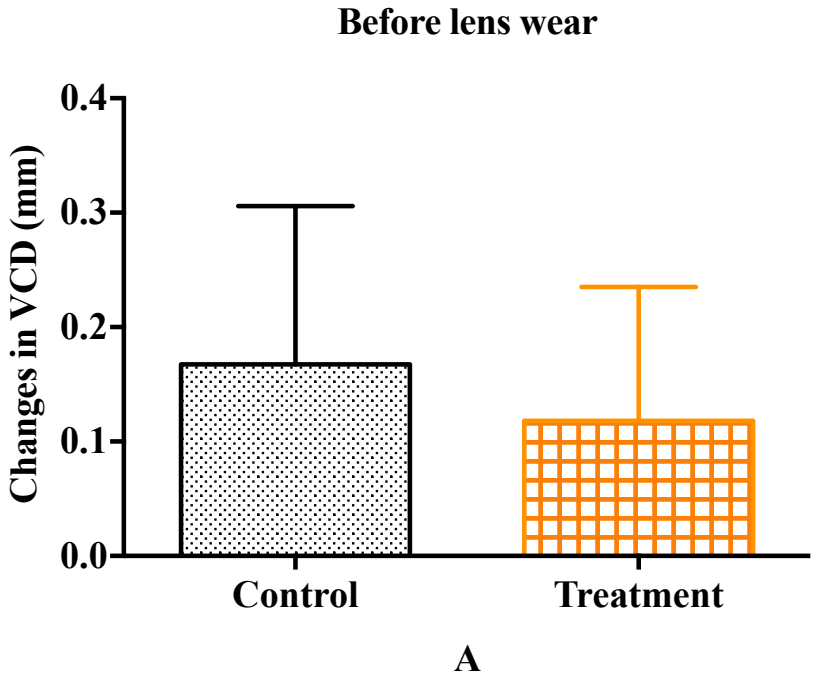

A

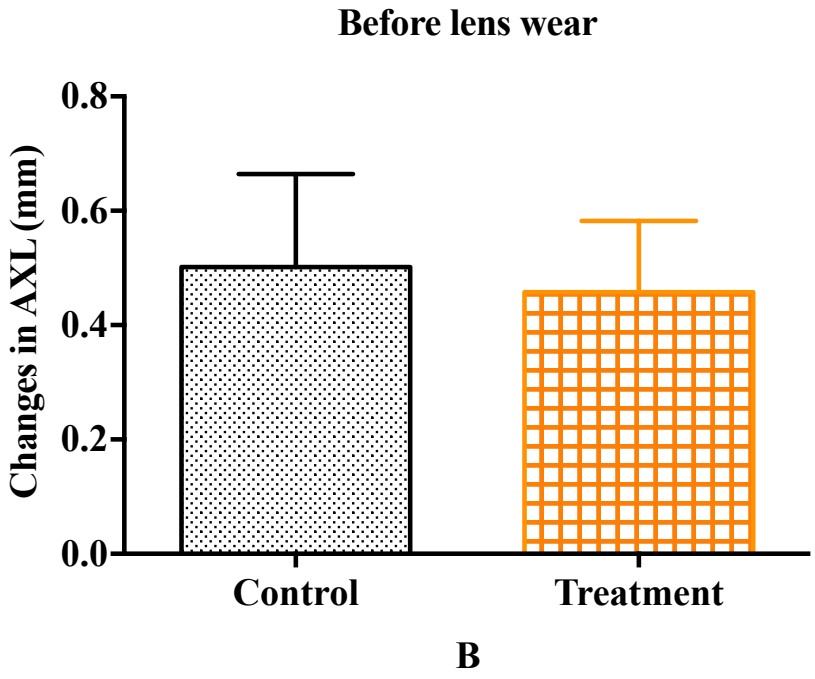

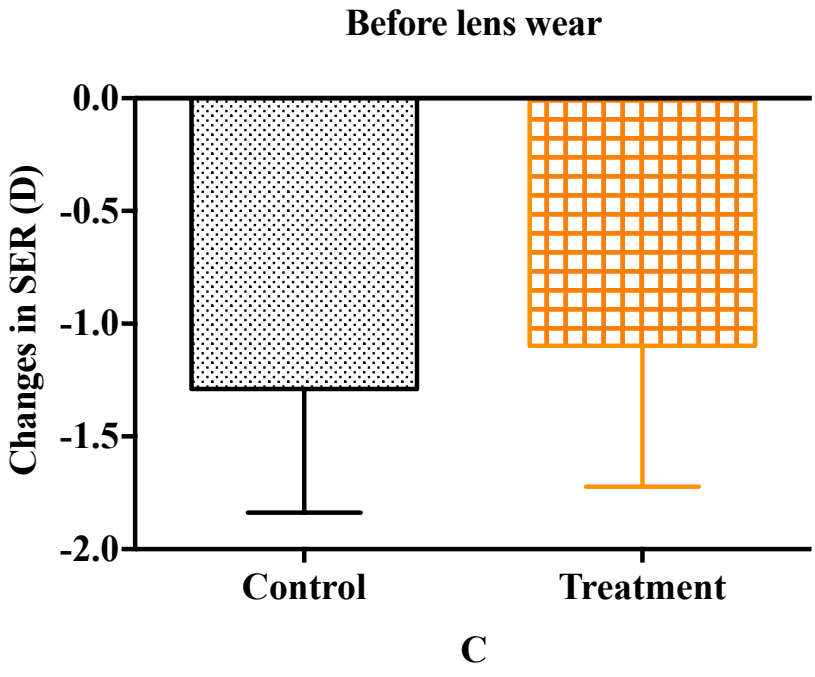

Figure 5.4.1 The comparisons of ocular parameters and refractive error change after 6 days nicotinic acid treated and before lens wear.

The change in (A) VCD (mm), (B) AXL (mm) and (C) SER (D) before lens wear. Mean ±SD, *p<0.05, **p<0.01, ***p<0.001.

5.4.2 The effect of NA on plano lens wear 4 days

Comparing nicotinic acid and saline treated eyes 10 days with plano lenses induced for 4 day, there was no significantly difference between these two groups (Table 5.4.2, Fig 5.4.2).

Table 5.4.2 Comparisons of ocular parameters and refractive error changes after 10 days of nicotinic acid treatment and plano lens wear of 4 days

Treatment		N	Mean	Std. Deviation	Sig. (2-tailed)	
ACD (mm)	NA	6	0.082	0.023		
	plano				0.657	*
	Plano	6	0.092	0.048		
LT (mm)	NA	6	0.126	0.065		
	plano				0.905	*
	Plano	6	0.121	0.067		
VCD (mm)	NA	6	0.272	0.068		
	plano				0.631	#
	Plano	6	0.283	0.073		

AXL (mm)	NA plano	6	0.481	0.112	0.768	*
	Plano	6	0.496	0.062		
RT (mm)	NA plano	6	-0.020	0.009	0.460	*
	Plano	6	-0.011	0.028		
CT (mm)	NA plano	6	0.033	0.030	0.090	*
	Plano	6	-0.010	0.047		
ST (mm)	NA plano	6	0.005	0.011	0.647	*
	Plano	6	0.009	0.018		
SER (D)	NA plano	6	-0.833	0.540	0.066	#
	Plano	6	-1.333	0.258		

*P value for Independent T-test

#P value for Mann-Whitney test

NA means nicotinic acid treatment group

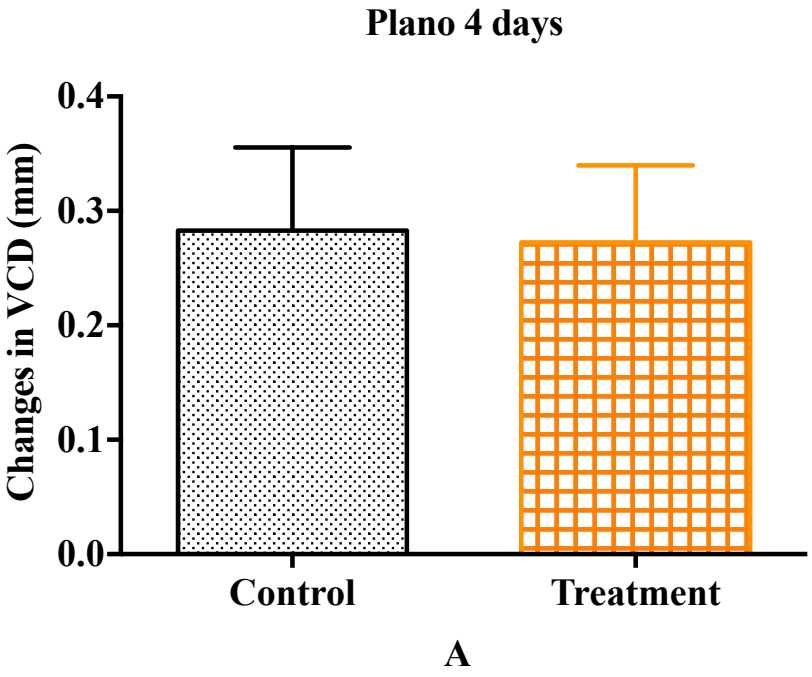
Plano 4 days
Changes in VCD (mm)
0.4
0.3
0.2
0.1
0.0
Control
Treatment

A

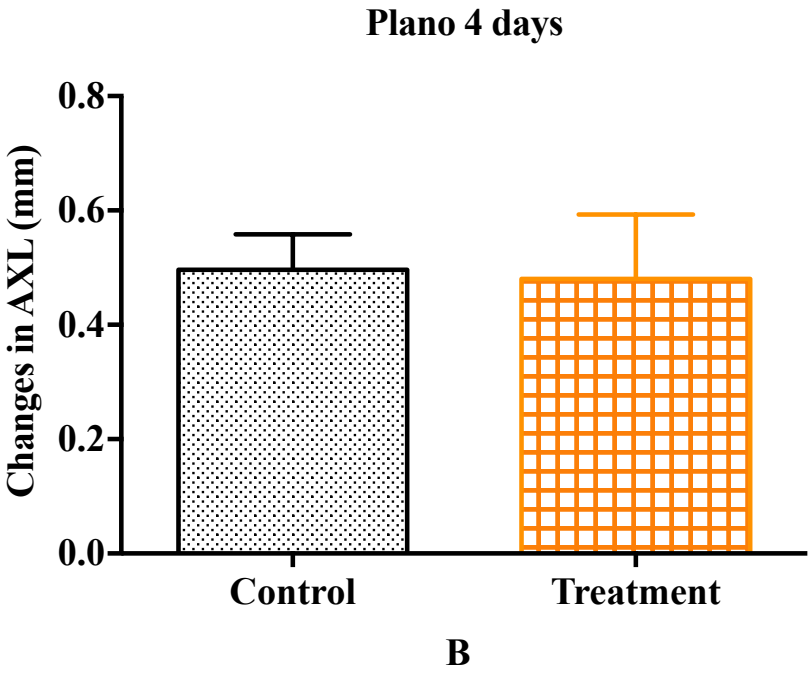
Plano 4 days
Changes in AXL (mm)
0.8
0.6
0.4
0.2
0.0
Control
Treatment

B

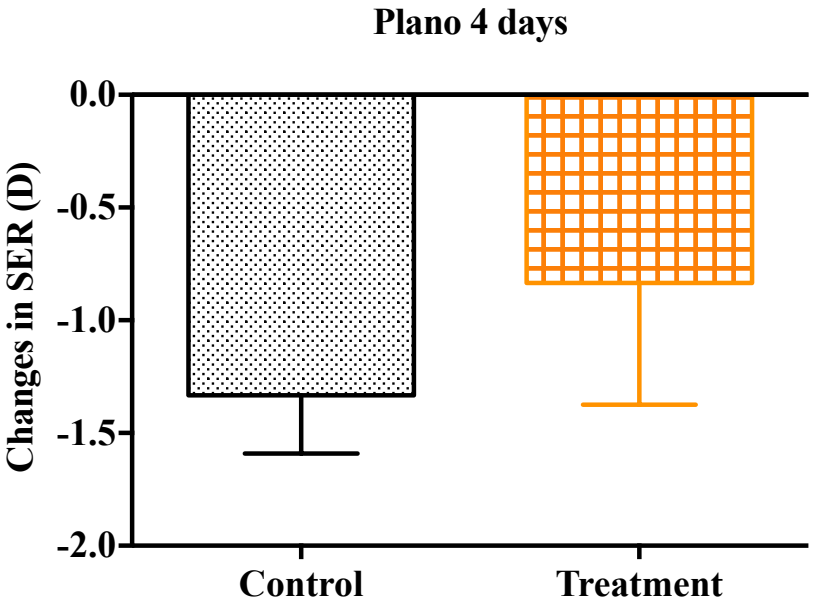
Plano 4 days
Changes in SER (D)
0.0
-0.5
-1.0
-1.5
-2.0
Control
Treatment

C

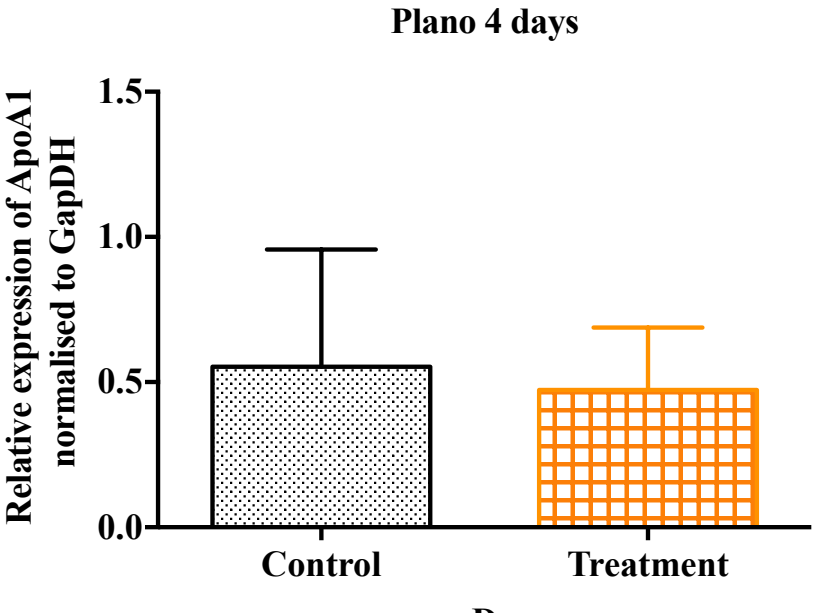
Plano 4 days
Relative expression of ApoA1 normalised to GapDH
1.5
1.0
0.5
0.0
Control
Treatment

D

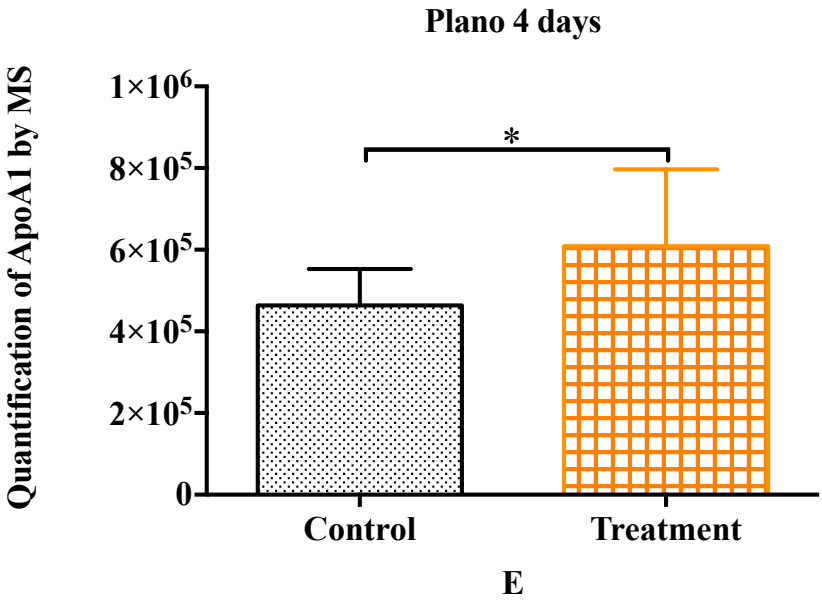

Figure 5.4.2 The comparisons of ocular parameters and refractive error change after 10 days of nicotinic acid treatment and plano lens wear for 4 days.

The change in (A) VCD (mm), (B) AXL (mm), (C) SER (D), (D) relative expression of apoA1 protein normalized to GapDH by western blot and (E) quantification of apoA1 protein by LC-MS after 10 days nicotinic acid treated and plano 4 days. Mean ±SD, *p<0.05, **p<0.01, ***p<0.001.

After 10 days of nicotinic acid treatment and plano lens wear for 4 days, the relative expression of apoA1 protein was detected by western blot. The relative expression of apoA1 protein normalized to GapDH was not significantly different between these two groups (Table 5.4.3, Figure 5.4.2)

Table 5.4.3 Relative expression of apoA1 protein normalized to GapDH after 10 days of nicotinic acid treatment and plano lens wear for 4 days

Treatment		N	Mean	Std. Deviation	Sig. (2-tailed)	
ApoA1/GapDH	NA plano	6	0.474	0.214	0.680	*
	Plano	6	0.553	0.404		

*P value for Independent T-test

#P value for Mann-Whitney test

After the treatment, the quantification of apoA1 protein was performed by LC-MS (SWATH). The expression of apoA1 protein was significantly higher in NA plano group than that of the plano group (Table 5.4.4, Figure 5.4.2).

Table 5.4.4 Quantification of apoA1 protein after 10 days of nicotinic acid treatment and plano lens wear for 4 days by LC-MS (SWATH)

Treatment	N	Mean	Std. Deviation	Sig. (2-tailed)	
NA plano	6	6.1E+05	1.9E+05	0.037	#
Plano	6	4.6E+05	9.0E+04		

*P value for Independent T-test

#P value for Mann-Whitney test

After SWATH analysis, there were 1256 proteins identified with at least 2 peptides per protein. Thirty-two proteins were found to be changed by $|\log_2 (\text{fold change})| \geq 0.379$ and P-value < 0.05 (Figure 5.4.3).

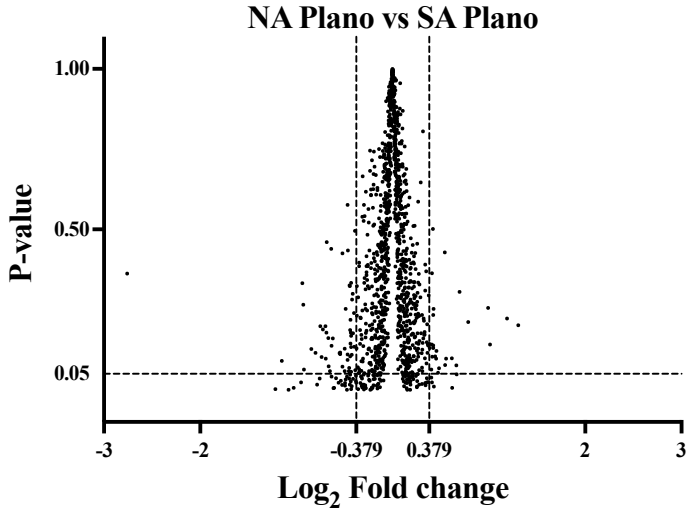

Figure 5.4.3 Volcano plot: All 1256 identified proteins (with at least 2 peptides per protein) are represented in terms of their Log2 fold changes (X-axis) and p-values of their change (Y-axis).

Among these 32 proteins, 27 proteins were found to be down-regulated while 5 proteins were up-regulated after 10 days of nicotinic acid treatment and wearing plano lens for 4 days (appendix 2). These 32 proteins were categorized by Gene Ontology database (PANTHER classification system)

classifications based on their molecular function, biological process, cellular component and protein class (below pie charts).

NA plano vs. Plano

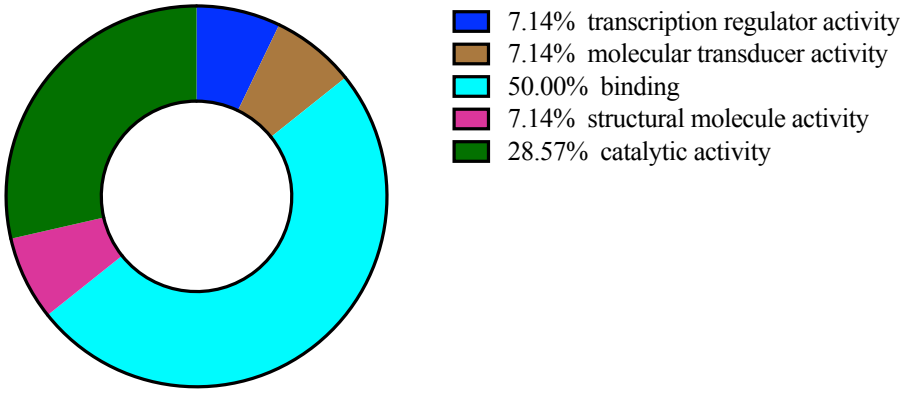

Molecular function

NA plano vs. Plano

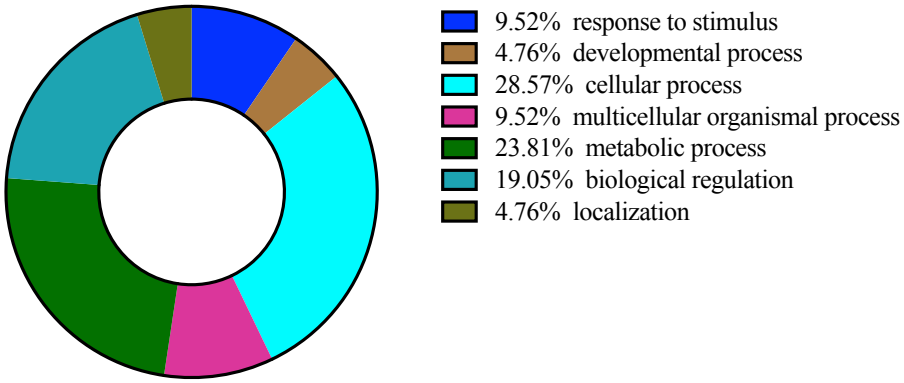

Biological process

NA plano vs. Plano

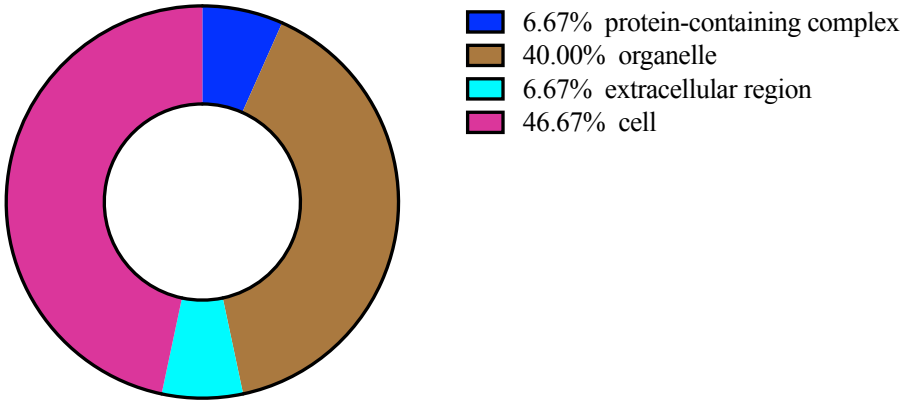

Cellular component

NA plano vs. Plano

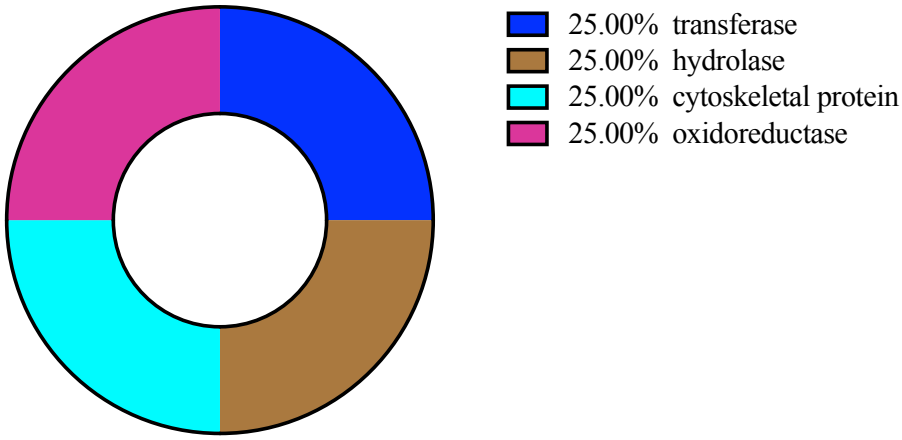

Protein class

Pathway analysis was performed via iPathwayGuide database (Advaita Corporation).

Table 5.4.5 The list of identified pathway and up/down regulation genes

Pathway	Protein
	Down regulation
Insulin signaling pathway	FASN

5.4.3 The effect of NA on LIH 4 days

Comparison between nicotinic acid and saline treated 10 days with LIH 4 day, the eyes treated by nicotinic acid became significantly more hyperopic than the control. The changes in VCD and AXL in nicotinic acid treated eyes were significantly less than that of the saline treated eyes. The absolute change in SER in nicotinic acid treated eyes was significantly more than that of the saline treated eyes. However, there was no significant difference in ACD, LT, RT, CT and ST between the two groups (Table 5.4.6, Fig 5.4.4).

Table 5.4.6 Comparisons of ocular parameters and refractive error change after 10 days of nicotinic acid treatment and LIH 4 days

Treatment		N	Mean	Std. Deviation	Sig. (2-tailed)	
ACD (mm)	NA LIH	4	0.065	0.048	0.261	*
	LIH	5	0.131	0.099		

LT (mm)	NA LIH	4	0.137	0.025	0.445	*
	LIH	5	0.109	0.066		
VCD (mm)	NA LIH	4	-0.223	0.046	0.012	*
	LIH	5	-0.121	0.044		
AXL (mm)	NA LIH	4	-0.021	0.097	0.030	*
	LIH	5	0.120	0.058		
RT (mm)	NA LIH	4	0.035	0.015	0.198	*
	LIH	5	0.019	0.018		
CT (mm)	NA LIH	4	0.355	0.063	0.337	*
	LIH	5	0.287	0.118		
ST (mm)	NA LIH	4	0.009	0.008	0.328	*
	LIH	5	0.003	0.009		
SER (D)	NA LIH	4	8.313	0.747	0.030	*
	LIH	5	7.150	0.548		

*P value for Independent T-test

#P value for Mann-Whitney test

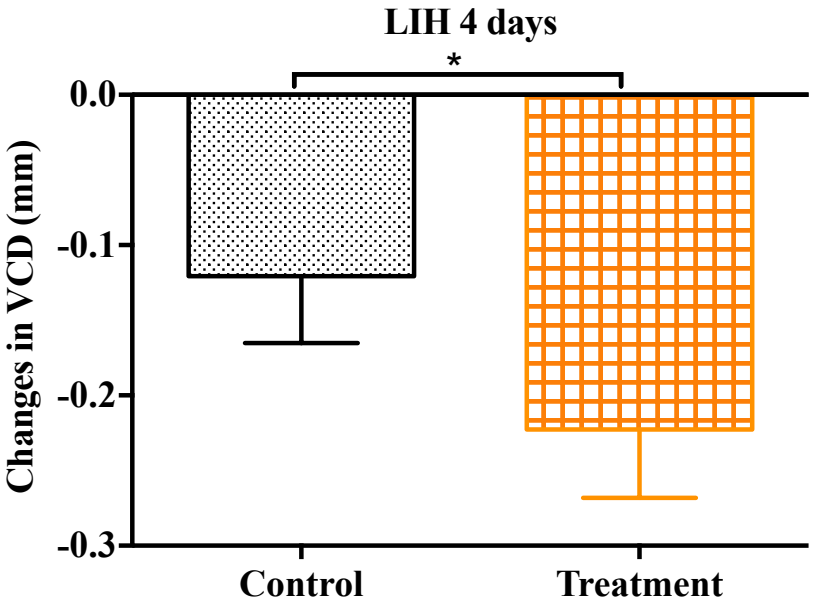
LIH 4 days
*
0.0
-0.1
-0.2
-0.3
Changes in VCD (mm)
Control
Treatment

A

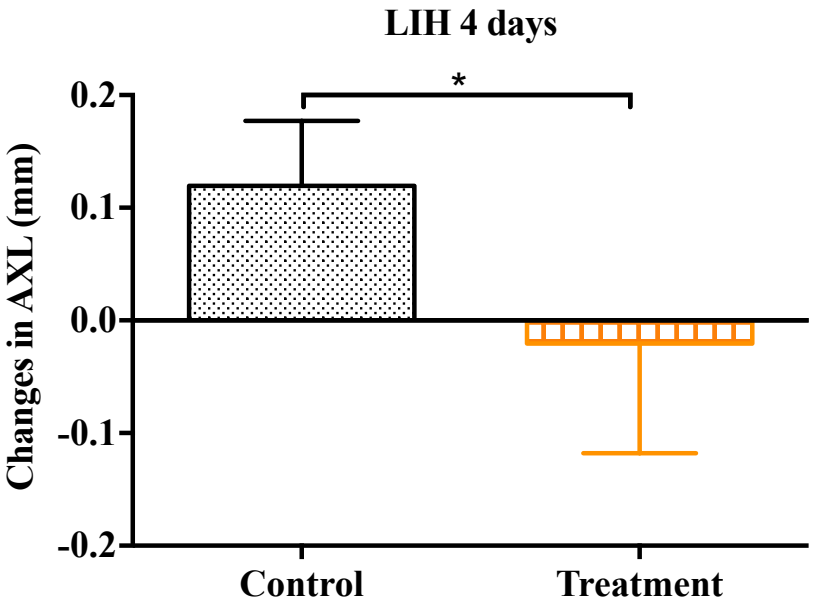
LIH 4 days
*
0.2
0.1
0.0
-0.1
-0.2
Changes in AXL (mm)
Control
Treatment

B

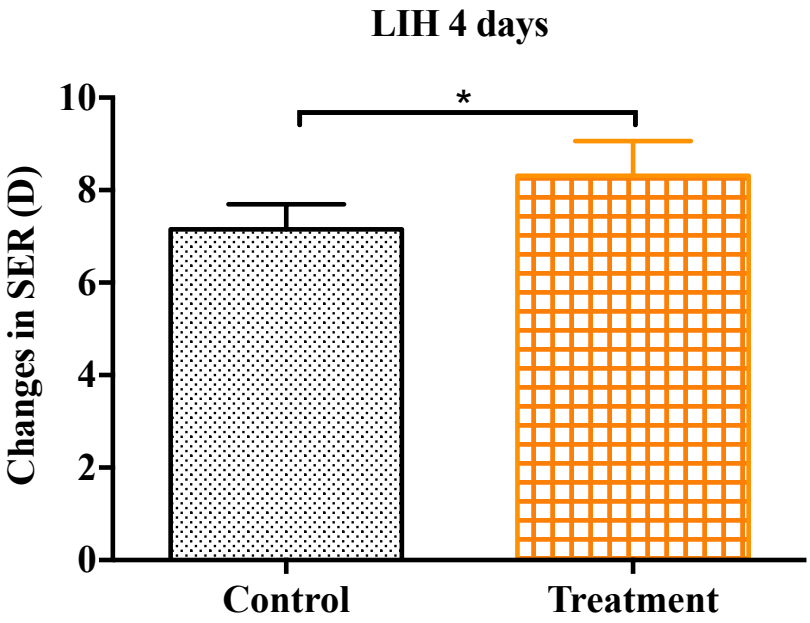
LIH 4 days
*
10
8
6
4
2
0
Changes in SER (D)
Control
Treatment

C

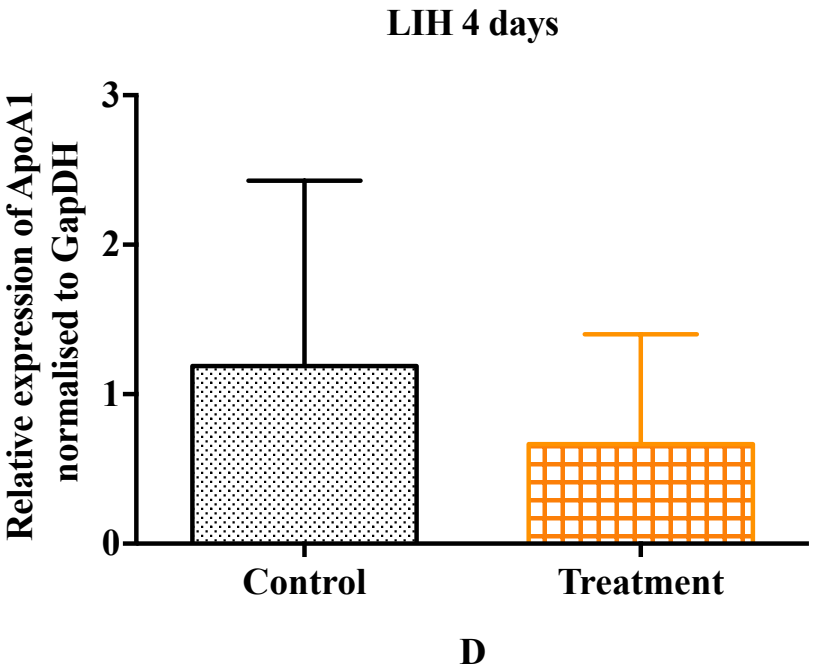
LIH 4 days
3
2
1
0
Relative expression of ApoA1 normalised to GapDH
Control
Treatment

D

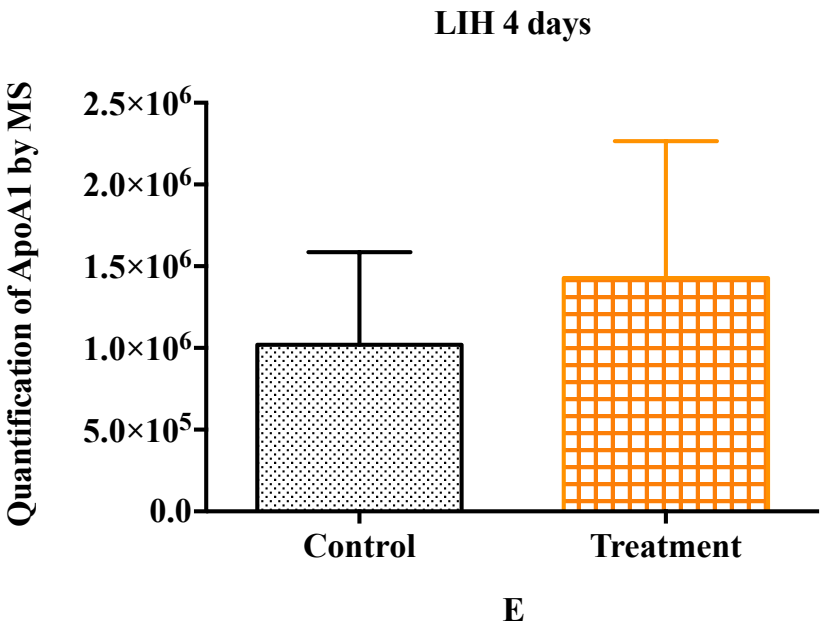

Figure 5.4.4 The change in (A) VCD (mm), (B) AXL (mm), (C) SER (D), (D) relative expression of apoA1 protein normalized to GapDH by western blot and (E) quantification of apoA1 protein by LC-MS after 10 days nicotinic acid treatment and LIH 4 days. Mean ±SD, *p<0.05, **p<0.01, ***p<0.001.

After the treatment, the relative expression of apoA1 protein in these retinas was detected by western blot. The relative expression of apoA1 protein normalized to GapDH was not significantly different between these two groups (Table 5.4.7, Figure 5.4.4)

Table 5.4.7 Relative expression of apoA1 protein normalized to GapDH after 10 days of nicotinic acid treatment and LIH 4 days

Treatment		N	Mean	Std. Deviation	Sig. (2-tailed)	
ApoA1/GapDH	NA LIH	4	0.666	0.735	0.624	#
	LIH	5	1.189	1.240		

*P value for Independent T-test

#P value for Mann-Whitney test

The apoA1 protein expressions of the NA treated and control eyes were further quantified by LC-MS (SWATH). The expression of apoA1 protein was not significant different between these two groups (Table 5.4.8, Figure 5.4.4).

Table 5.4.8 Quantification of apoA1 protein after 10 days of nicotinic acid treatment and LIH 4 days by LC-MS (SWATH)

Treatment	N	Mean	Std. Deviation	Sig. (2-tailed)	
NA LIH	4	1.4E+06	8.4E+05	0.221	#
LIH	5	1.0E+06	5.7E+05		

*P value for Independent T-test

#P value for Mann-Whitney test

According to the SWATH analysis, there were 1152 proteins identified with at least 2 peptides per protein being sequenced; 10 proteins were found to be changed by $|\log_2 (\text{fold change})| \geq 0.379$ and P-value < 0.05 (Figure 5.4.5).

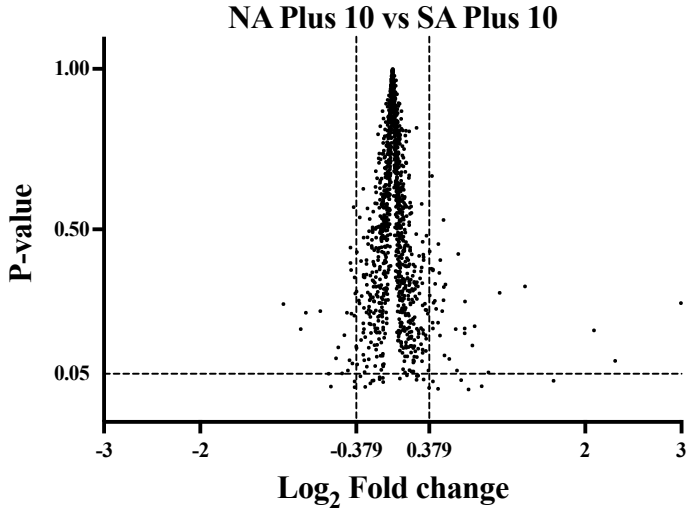

Figure 5.4.5 Volcano plot: All 1152 identified proteins (with at least 2 peptides per protein) are represented in terms of their Log2 fold changes (X-axis) and p-values of their change (Y-axis).

Among these 10 proteins, 3 proteins were found to be down-regulated while 7 proteins were up-regulated after 10 days of nicotinic acid treatment (appendix 2). These 10 proteins were categorized by Gene Ontology database (PANTHER classification system) classifications based on their

molecular function, biological process, cellular component and protein class (below pie charts).

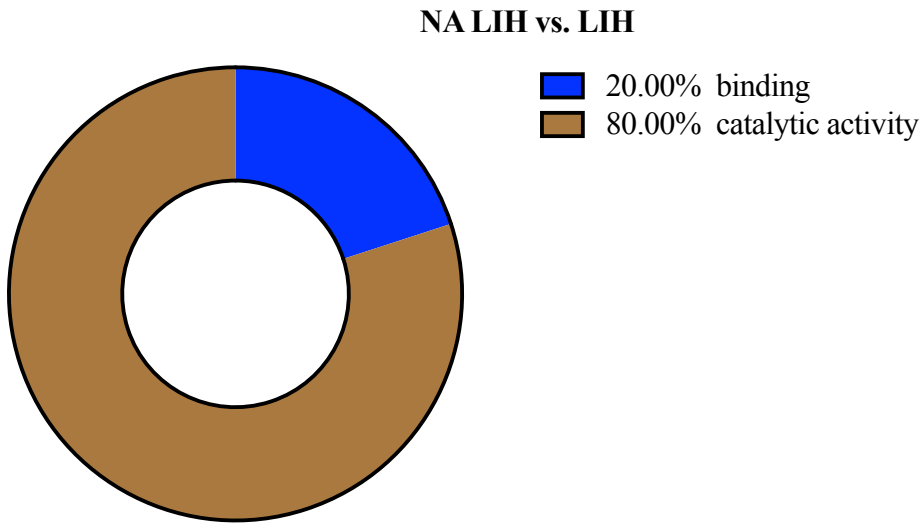

Molecular function

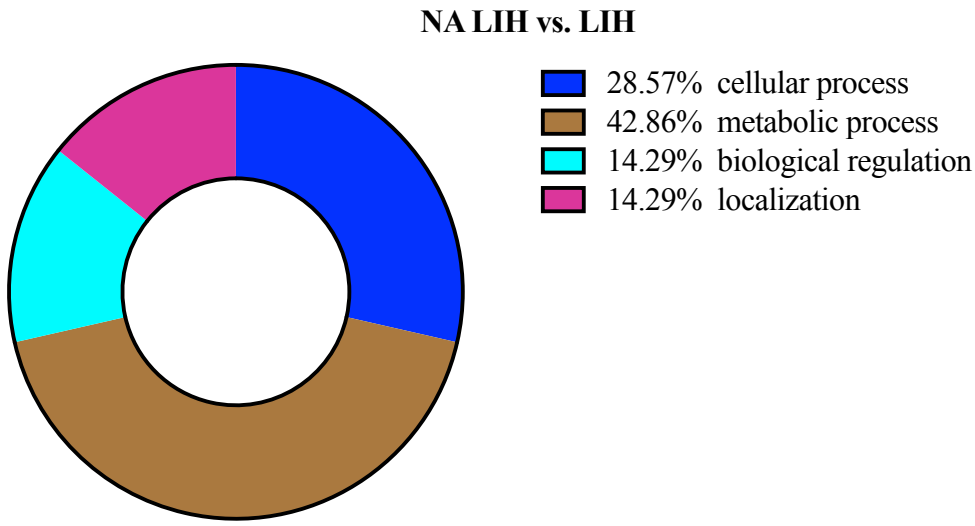

Biological process

NA LIH vs. LIH

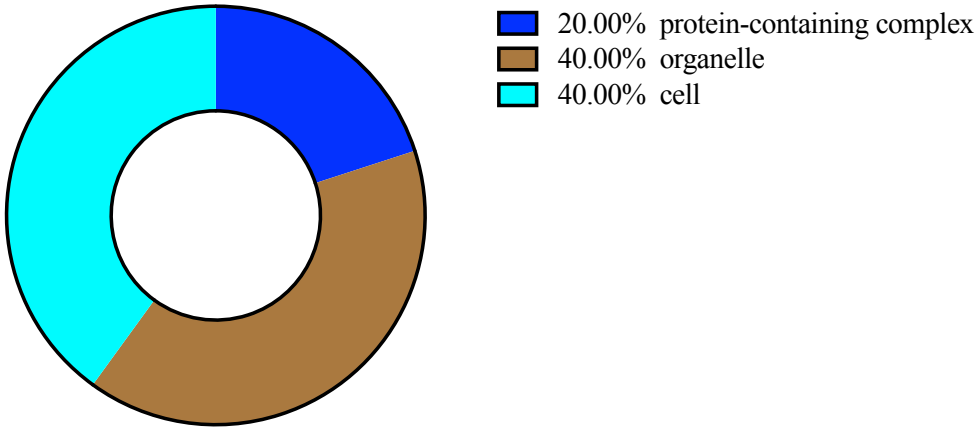

Cellular component

NA LIH vs. LIH

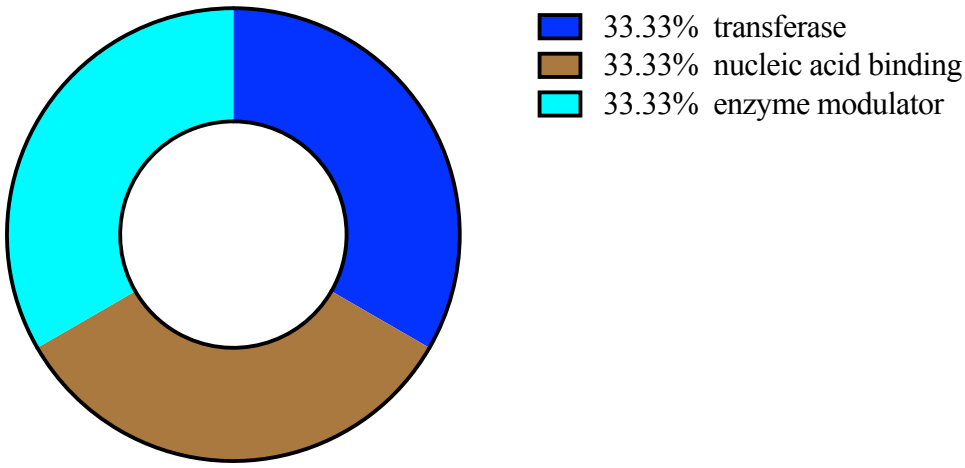

Protein class

Pathway analysis was performed via iPathwayGuide database (Advaita Corporation).

Table 5.4.9 The list of identified pathway and up/down regulation genes

Pathway	Protein	
	Up regulation	Down regulation
Endocytosis	CAPZA	VPS45

5.4.4 The effect of NA on LIM 4 days

Comparing between nicotinic acid and saline treated eyes for 10 days with LIM 4 day, the eyes treated with nicotinic acid became significantly less myopic than the controls. The changes in VCD and AXL in nicotinic acid treated eyes were significantly less than that of the saline treated eyes. The change in SER in nicotinic acid treated eyes was significantly more than that of the saline treated eyes. There was no significant difference in ACD, LT, RT, CT and ST between nicotinic acid and saline treated eyes (Table 5.4.10, Fig 5.4.6).

Table 5.4.10 The comparisons of ocular parameters and refractive error change after 10 days of nicotinic acid treatment and LIM for 4 days

Treatment		N	Mean	Std. Deviation	Sig. (2-tailed)	
ACD (mm)	NA LIM	8	0.170	0.074	0.958	#
	LIM	8	0.156	0.062		
LT (mm)	NA LIM	8	0.083	0.051	0.298	*
	LIM	8	0.113	0.061		
VCD (mm)	NA LIM	8	0.548	0.146	0.015	*
	LIM	8	0.713	0.084		
AXL (mm)	NA LIM	8	0.801	0.172	0.046	#
	LIM	8	0.983	0.093		
RT (mm)	NA LIM	8	-0.022	0.029	0.248	#
	LIM	8	-0.024	0.014		
CT (mm)	NA LIM	8	-0.023	0.030	0.240	*
	LIM	8	-0.002	0.037		
ST (mm)	NA LIM	8	0.001	0.013	0.545	*
	LIM	8	-0.003	0.012		
SER (D)	NA LIM	8	-5.563	0.513	0.000	*
	LIM	8	-8.875	0.463		

*P value for Independent T-test

#P value for Mann-Whitney test

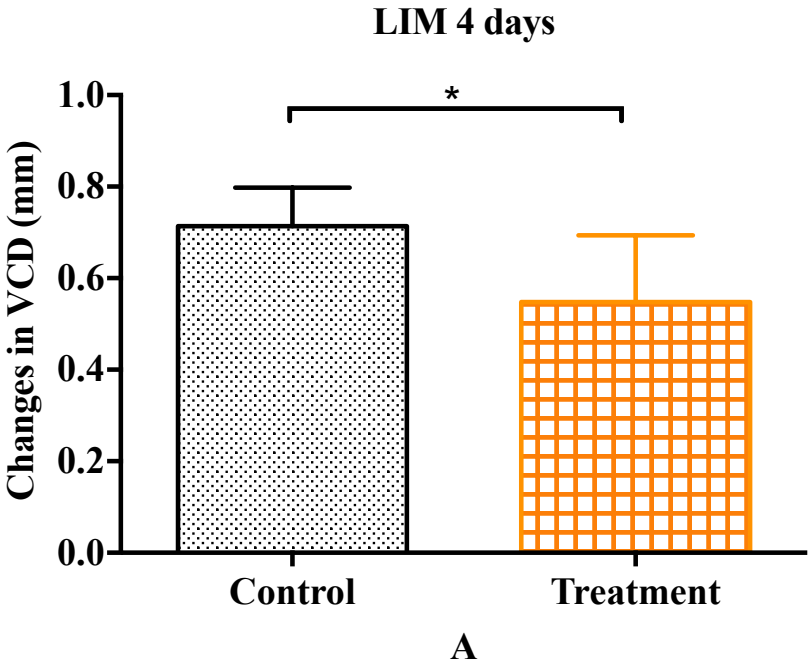
LIM 4 days
*
1.0
0.8
0.6
0.4
0.2
0.0
Changes in VCD (mm)
Control
Treatment

A

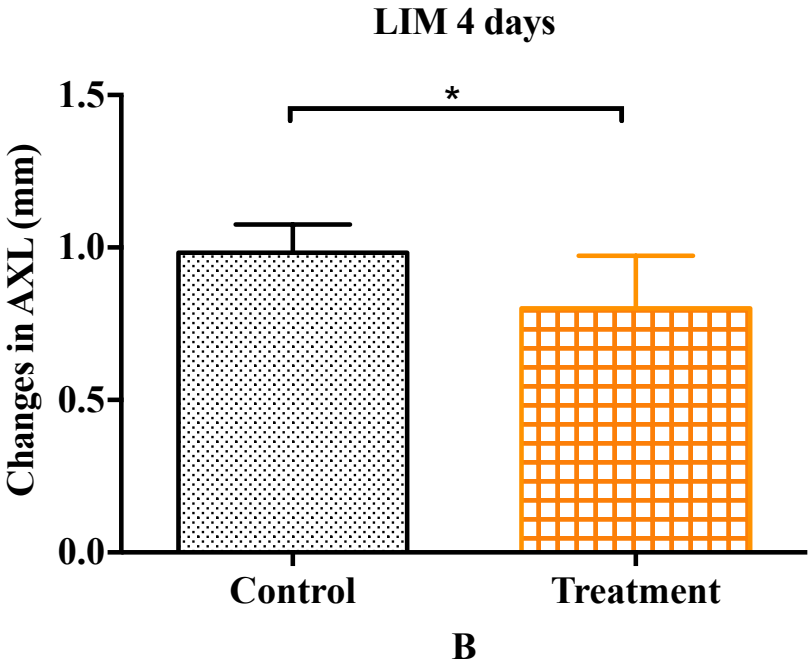
LIM 4 days
*
1.5
1.0
0.5
0.0
Changes in AXL (mm)
Control
Treatment

B

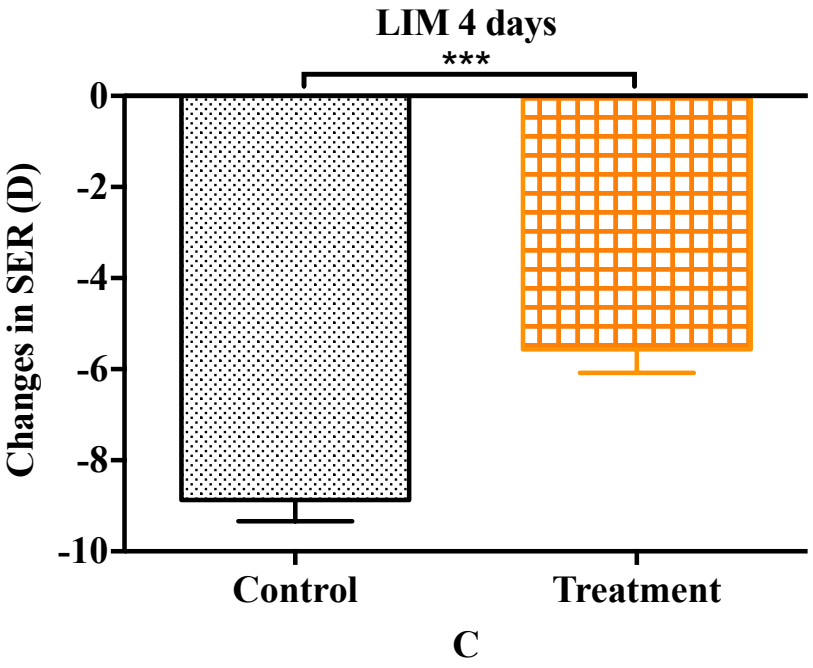
LIM 4 days
***
0
-2
-4
-6
-8
-10
Changes in SER (D)
Control
Treatment

C

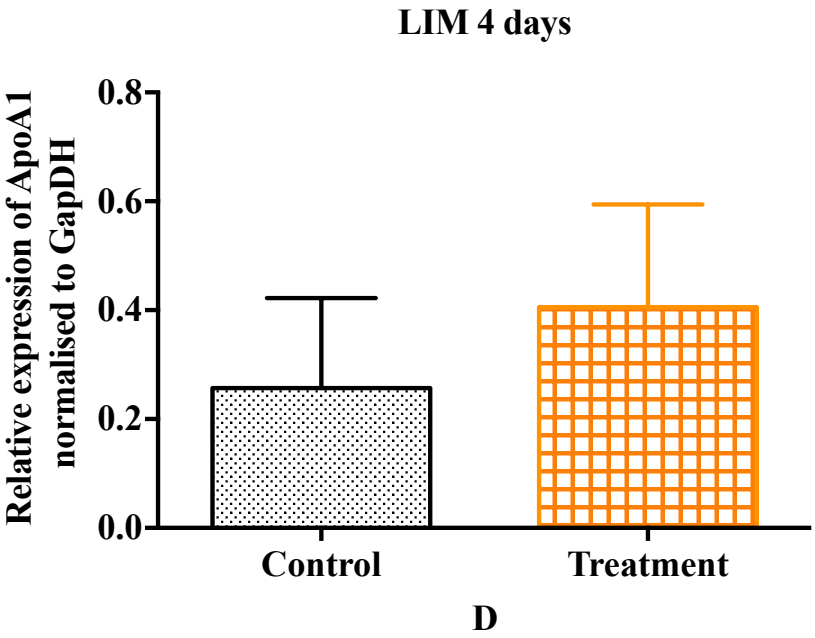
LIM 4 days
0.8
0.6
0.4
0.2
0.0
Relative expression of ApoA1 normalised to GapDH
Control
Treatment

D

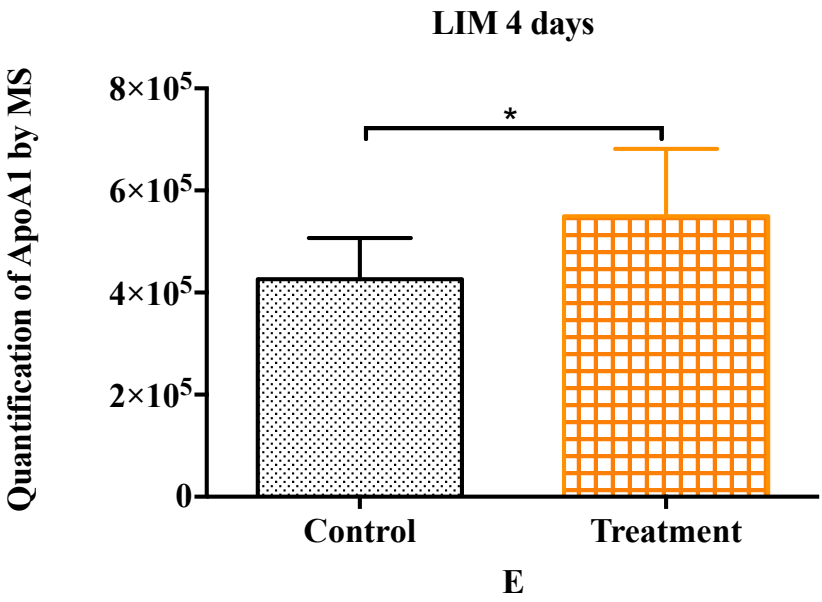

Figure 5.4.6 The change in (A) VCD (mm), (B) AXL (mm), (C) SER (D), (D) relative expression of apoA1 protein normalized to GapDH by western blot and (E) quantification of apoA1 protein by LC-MS after 10 days nicotinic acid treated and LIM 4 days. Mean ±SD, *p<0.05, **p<0.01, ***p<0.001.

After the treatment, the relative expression of apoA1 protein was detected by western blot. The relative expression of apoA1 protein was normalized to GapDH. There was no significantly difference between these two groups (Table 5.4.11, Figure 5.4.6)

Table 5.4.11 Relative expression of apoA1 protein normalized to GapDH after 10 days nicotinic acid treated and LIM 4 days

Treatment		N	Mean	Std. Deviation	Sig. (2-tailed)	
ApoA1/GapDH	NA LIM	8	0.406	0.189	0.116	*
	LIM	8	0.257	0.165		

*P value for Independent T-test

#P value for Mann-Whitney test

After the treatment, the retinal apoA1 protein was quantified by LC-MS (SWATH). The expression of apoA1 protein was significantly higher in NA LIM group than LIM group (Table 5.4.12, Figure 5.4.6).

Table 5.4.12 Quantification of apoA1 protein after 10 days of nicotinic acid treatment and LIM for 4 days by LC-MS (SWATH)

Treatment	N	Mean	Std. Deviation	Sig. (2-tailed)	
NA LIM	8	5.5E+05	1.3E+05	0.041	*
LIM	8	4.3E+05	8.1E+04		

*P value for Independent T-test

#P value for Mann-Whitney test

After SWATH analysis, there were 1306 proteins identified with at least 2 peptides per protein; 30 proteins were found to be changed by $|\log_2$ (fold change)$| \geq 0.379$ and P-value < 0.05 (Figure 5.4.7).

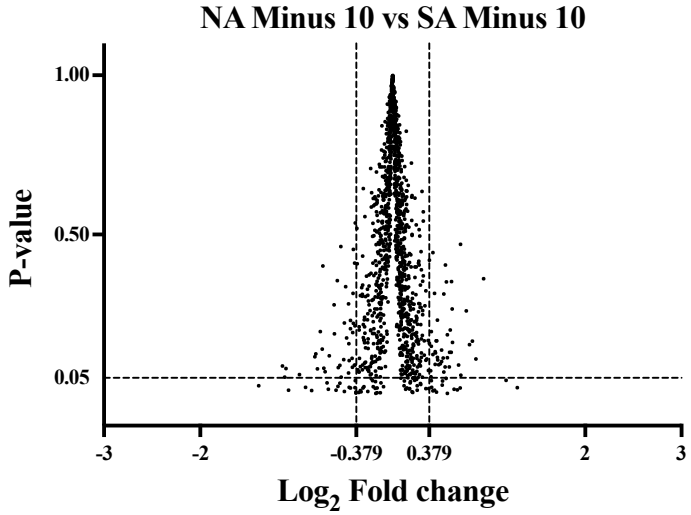

Figure 5.4.7 Volcano plot: All 1306 identified proteins (with at least 2 peptides per protein) are represented in terms of their Log2 fold changes (X-axis) and p-values of their change (Y-axis).

Among these 30 proteins, 16 proteins were found to be down-regulated while 14 proteins were up-regulated after 10 days of nicotinic acid treatment (appendix 2). These 30 proteins were categorized by Gene Ontology database (PANTHER classification system) classifications based on their

molecular function, biological process, cellular component and protein class (below pie charts).

NA LIM vs. LIM

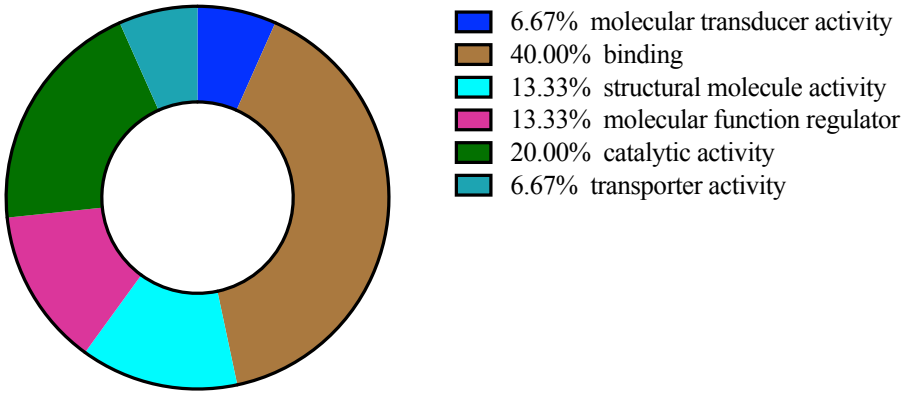

Molecular function

NA LIM vs. LIM

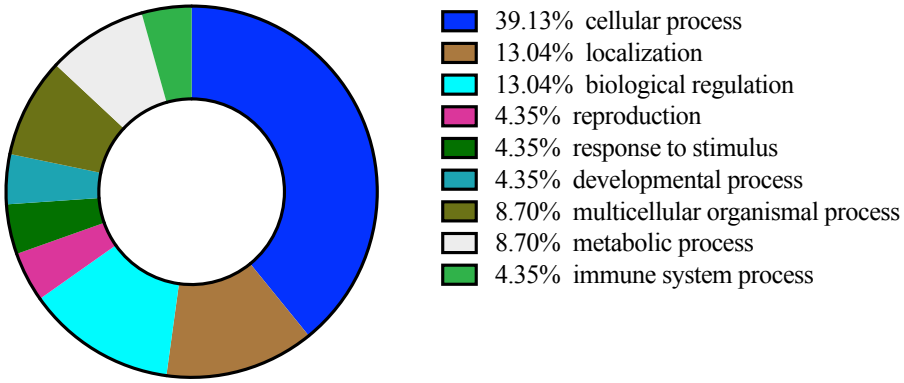

Biological process

NA LIM vs. LIM

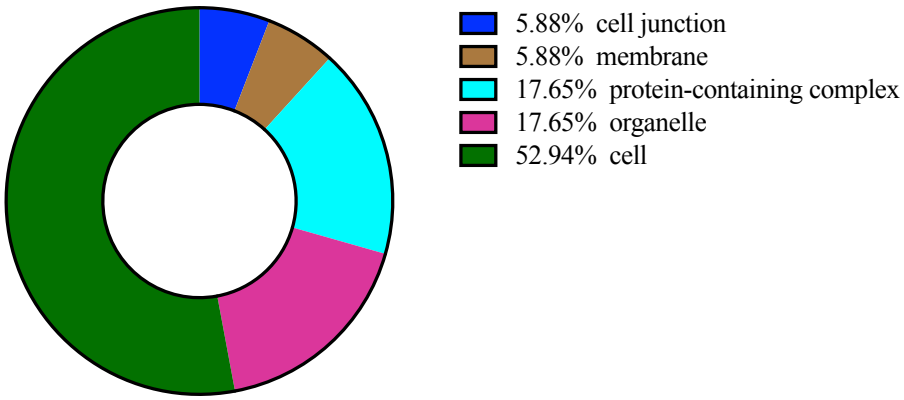

Cellular component

NA LIM vs. LIM

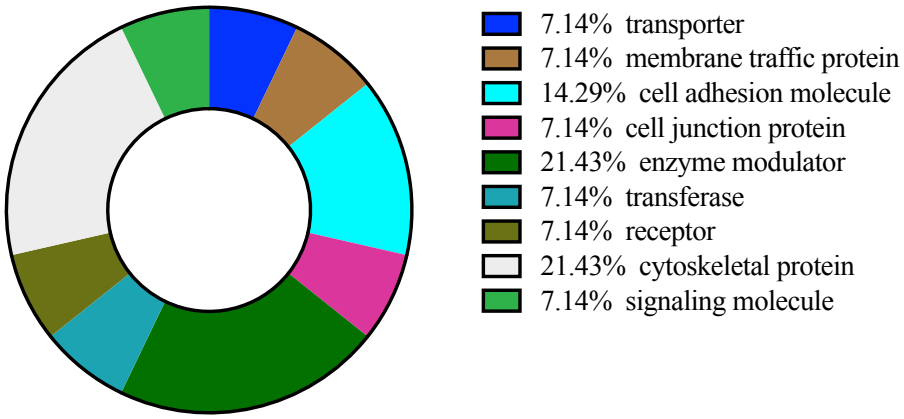

Protein class

Pathway analysis was performed via iPathwayGuide database (Advaita Corporation).

Table 5.4.13 The list of identified pathway and up/down regulation genes

Pathway	Protein	
	Up regulation	Down regulation
Insulin signaling pathway	PKA	GYS
Regulation of actin cytoskeleton	HRAS	ARP2/3
Endocytosis	AP2, Sh3gl2	ARP2/3

5.4.5 Summary

The effects of nicotinic acid on ocular parameters, refractive error, and apao1 protein expression were summarized as below.

Summary the effects of nicotinic acid (NA plano vs plano)		
Protein	before lens wear	Not significantly different (Ocular parameters & Refractive error)
	4 days lens wear	Not significantly different (Ocular parameters & Refractive error)
	Protein by Western blot at day 14	Not significantly different
	Protein by LC-MS (SWATH) at day 14	Up regulation in NA plano group

The effects of nicotinic acid on ocular parameters, refractive error, and apao1 protein expression were summarized as below.

Summary the effects of nicotinic acid (NA Plus vs SA Plus)		
	4 days lens wear	Significantly more hyperopic (Ocular parameters & Refractive error)
	Protein by Western blot at day 14	Not significantly different
	Protein by LC-MS (SWATH) at day 14	Not significantly different

The effects of nicotinic acid on ocular parameters, refractive error, and apao1 protein expression were summarized as below.

Summary the effects of nicotinic acid (NA Minus vs SA Minus)		
	4 days lens wear	Significantly more moypic (Ocular parameters & Refractive error)
	Protein by Western blot at day 14	Not significantly different
	Protein by LC-MS (SWATH) at day 14	Up regulation in NA LIM group

5.5 Discussion

In term of the changes in ocular parameters and refractive error between NA plano and plano groups before lenses attachment, there was no significant difference between these two groups. Therefore, nicotinic acid apparently did not slow down or alter normal eye growth in chicks. After 4 days of +10D lens wear, the eyes became significantly more hyperopic in NA LIH group than LIH group. It showed that nicotinic acid slowed the eyes growth and the eye became more hyperopic. Similarly, after 4 days of LIM, the eyes became significantly less myopic in NA LIM group than LIM group. The results suggested the nicotinic acid can effectively slow eye growth even when it was subjected to LIM. It indicated that nicotinic acid can retard eye growth in both LIH and LIM, but not in normal eye growth.

In terms of the retinal apoA1 protein expression, no difference was detected by western blot, but a significantly increase in the NA plano eyes was found by LC-MS (SWATH) (up-regulation 1.312-fold in NA plano than plano, P=0.037). This discrepancy was likely due to the superior sensitivity of LC-MS (SWATH) over the western blotting method, which could pick up smaller differences between the two samples. However, the increase in apoA1 in the NA plano eyes did not translate into the slowing of eye growth. In the LIH experiment, the retinal apoA1 expression was not significantly different by both methods. It is known that LIH induced up regulation of retinal apoA1 by itself (up-regulation 4.954-fold in LIH than

plano, P=0.067, western blot; up-regulation 2.174-fold in LIH than plano, P=0.026, LC-MS SWATH). The effect of nicotinic acid in further increasing the apoA1 expression may be too small to be differentiated from the LIH effect alone and rendered it insignificantly changed. In the LIM experiment, the apoA1 protein expression was not significantly differential expressed by western blotting, but significantly increased in NA LIM group than LIM group (up-regulation 1.289-fold in NA LIM than SA LIM, P=0.041). Similarly, the difference in observations is likely due to the fact that LC-MS (SWATH) may be a more sensitive and accurate method than western blotting in detecting small protein changes. It showed that oral administration of nicotinic acid can significantly increase the retinal apoA1 protein expression in LIM and normal growth chick retinas as hypothesized. After SWATH and pathway analysis, there were 3 top pathways or activities identified which may be the underlying mechanisms that regulate the eye growth as observed in the above experiments. They are namely the insulin signaling pathway, regulation of actin cytoskeleton and endocytosis pathway (figure 5.5.1, figure 5.5.2, figure 5.5.3).

Insulin signaling pathway

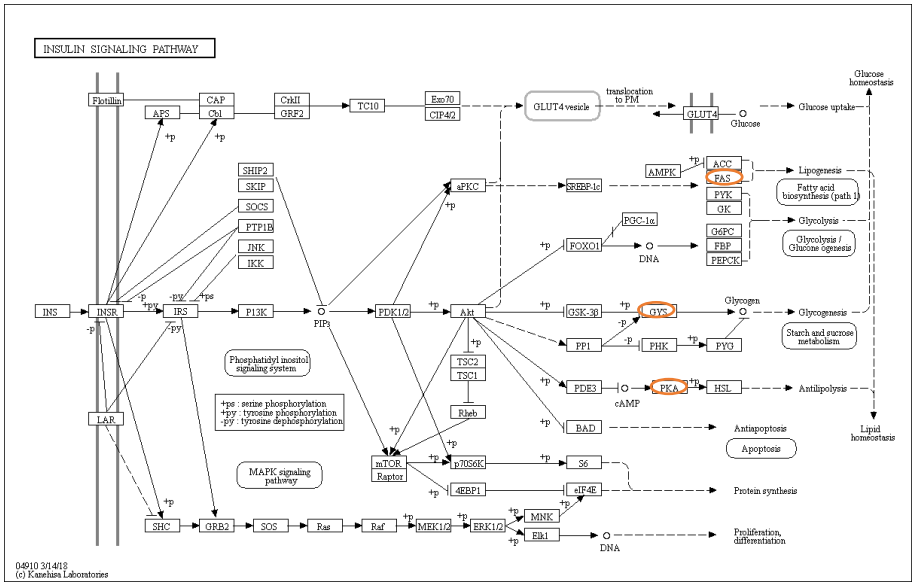

Figure 5.5.1 Insulin signaling pathway map from KEGG website (https://www.kegg.jp/kegg-bin/show_pathway?map04910)

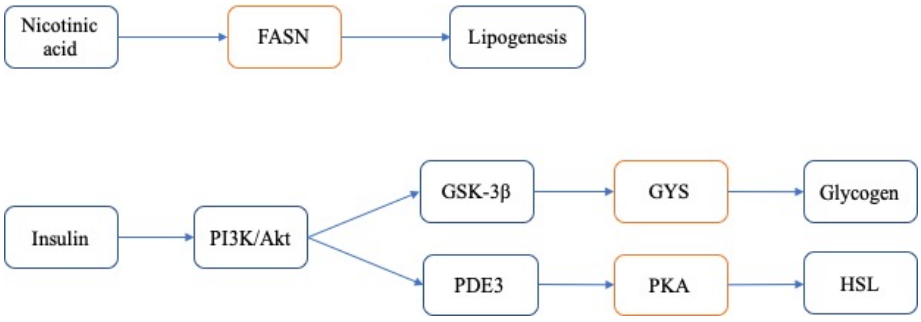

In terms of the nicotinic acid effect on normal eye growth, the FASN (fatty acid synthase) was down-regulated after nicotinic acid treatment. Its main function is to catalyze the synthesis of palmitate from acetyl-CoA and

malonyl-CoA, in the presence of NADPH, into long-chain saturated fatty acids (Jayakumar et al., 1994, Jayakumar et al., 1995, Stoops et al., 1975). Liu et al (2016) has reported that oral intake of nicotinic acid can down-regulate the FASN in rabbit (Liu et al., 2016). In this experiment, nicotinic acid did not affect the PI3K/Akt and MEK/MRK sub-pathways in the insulin signaling (as discussed in chapter 2). If nicotinic acid also decreases FASN in chick's retina, it may be plausible that nicotinic acid only decreased FASN on lipid metabolism but may not affect normal eye growth. In the LIM experiments, PKA (protein kinase A) was up-regulated and GYS were down-regulated after nicotinic acid treatment. PKA is a family of enzymes whose activity is dependent on cellular cyclic AMP (cAMP)(Turnham and Scott, 2016). PKA expression can lead to a decrease in cell proliferation (Liu et al., 2004) and may thereby retard cell growth. GYS is a key enzyme in glycogenesis that converts glucose to glycogen (Seldin et al., 1994, Buschiazzo et al., 2004, Palm et al., 2013). GYS and PKA are downstream targets of PI3K/Akt upon insulin activation. Therefore, nicotinic acid might inhibit PI3K/Akt which in turn down-regulated GYS expression and up-regulated PKA expression to slow cell growth in LIM chick retina.

Regulation of actin cytoskeleton

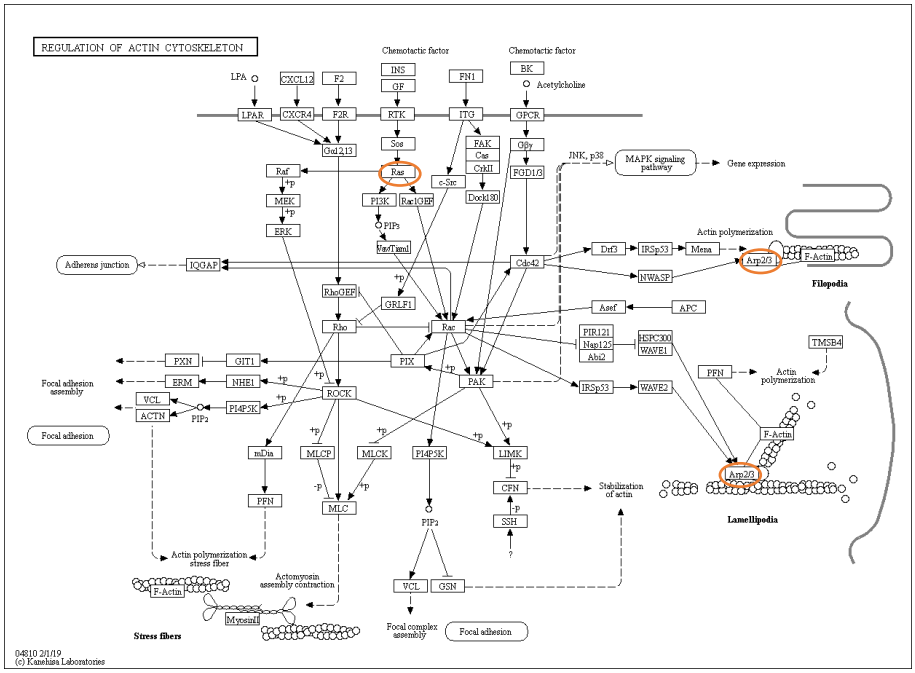

Figure 5.5.2 Regulation of actin cytoskeleton pathway map from KEGG website (https://www.kegg.jp/kegg-bin/show_pathway?map04810)

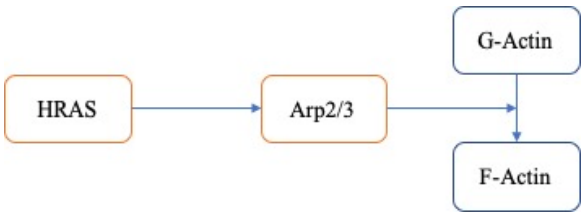

In the LIM experiments, HRAS (GTPase HRas) was up-regulated and ARP2/3 gene was down-regulated in nicotinic acid treated eyes. HRAS can inhibit the ARP2/3 expression which is known to promote G-actin

polymerize to F-actin and enhance cell proliferation (Tran et al., 2015, Hoffman et al., 2018). In this experiment, it is postulated that nicotinic acid may have upregulated HRAS and downregulated ARP2/3, which would lead to the inhibition of G-actin polymerization to F-actin and retardation of eye growth. In chapter 2, in LIH, it was also evident that ARP2/3 was also inhibited which led to the slowing of eye growth.

Endocytosis pathway

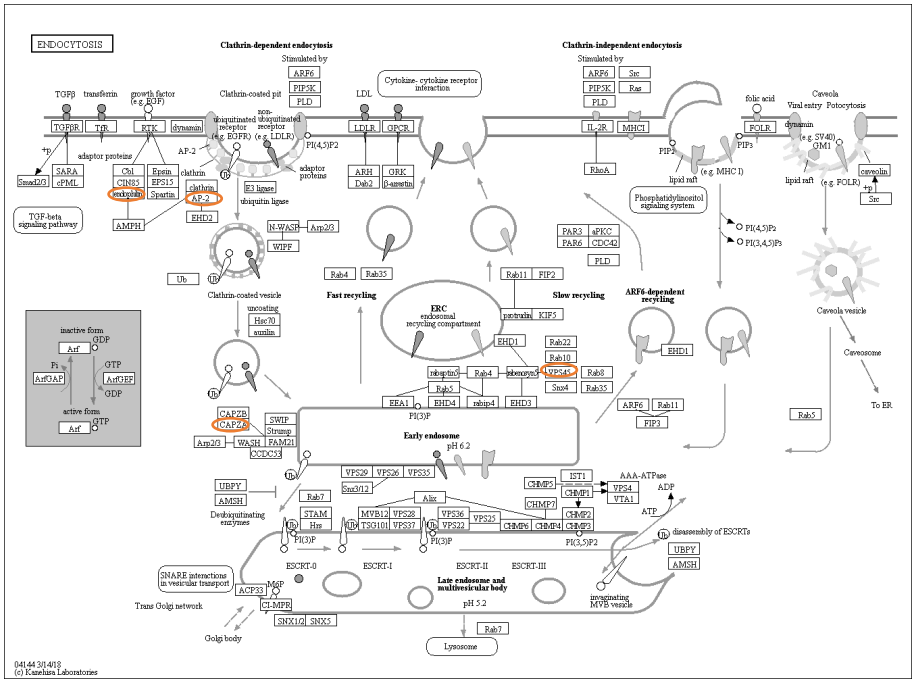

Figure 5.5.3 Endocytosis pathway map from KEGG website (https://www.kegg.jp/kegg-bin/show_pathway?map04144)

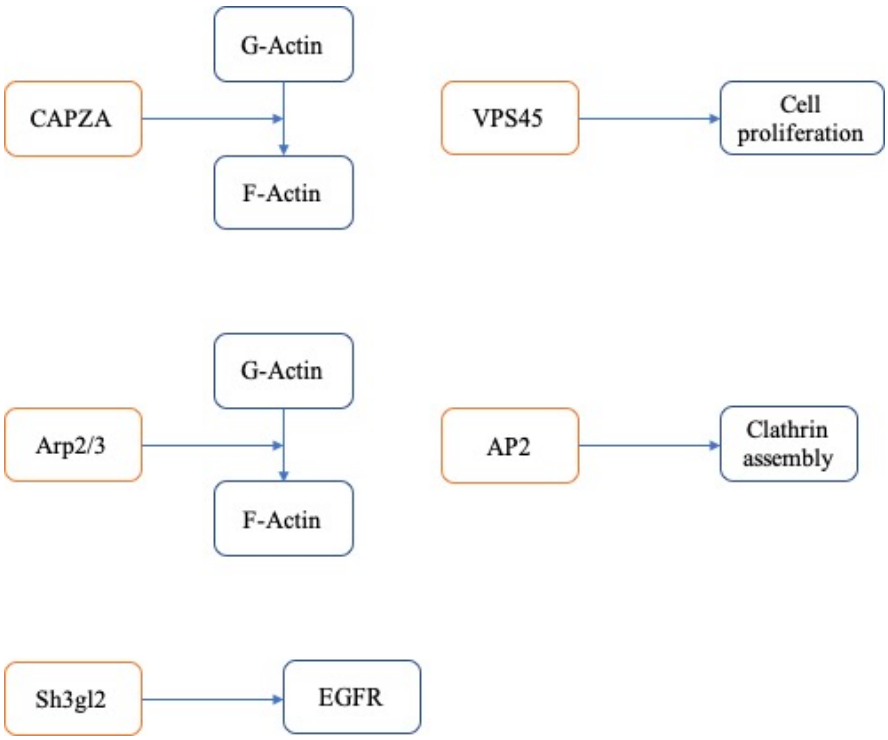

In LIH experiment, CAPZA (F-actin-capping protein subunit alpha) was up-regulated and VPS45 (Vacuolar protein sorting-associated protein 45) was down-regulated in nicotinic acid treated LIH eyes. CAPZA inhibits F-actin synthesis as well as cell proliferation (Kawska et al., 2012). VPS45 plays an important role in the segregation of intracellular molecules into different organelles. Down-regulation of VPS45 may decrease the cell proliferation process and thereby slows cellular growth. In this present case, it may further slow eye growth as a whole.

In LIM experiment, AP2 and Sh3gl2 were upregulated while ARP2/3 was down-regulated in nicotinic acid treated eyes. As described above, ARP2/3 can promote cell endocytic vesicle generation and movement into the

cytoplasm (Galletta et al., 2008), as well as G-actin polymerize to F-actin that can promote cell proliferation (Tran et al., 2015, Hoffman et al., 2018). Therefore, the down-regulation of ARP2/3 may inhibit eye growth. The increased AP2 expression could increase clathrin assembly and activates endocytosis (Conner and Schmid, 2003). Sh3gl2 can inhibit EGFR which promotes cell growth (Dasgupta et al., 2013, Lindsey and Langhans, 2015). It is possible that Sh3g12 inhibits EGFR and in turn inhibits eye growth.

5.6 Conclusions

In the current study, oral intake of nicotinic acid by chicks did not appear to affect normal growth eye. However, nicotinic acid was shown to be able to upregulate the apoA1 protein expression in the retina (5.4.1 and 5.4.2). Oral intake of nicotinic acid can significantly reduce eye growth so much so that it has made those LIH eye even more hyperopic. However, there is no significant increase in apoA1 protein expression in LIH eyes after nicotinic acid treatment (5.4.3). In LIM eyes, nicotinic acid significantly slowed eye growth in the LIM eyes which ended up with less myopia. It was also evident that retinal apoA1 protein was increased after nicotinic acid treatment in these LIM eyes (5.4.4).

Apparently, nicotinic acid may affect lipid metabolism through insulin signaling pathway, but it may not activate the PI3K/Akt and MEK/MRK

sub-pathways to control growth in normal eye. However, in LIM, nicotinic acid was shown to inhibit PI3K/Akt which in turn down-regulated GYS expression and up-regulated PKA expression to slow cell growth in LIM eye. The endocytosis pathway possibly plays a significant role in the nicotinic acid treated LIH and LIM eyes. Nicotinic acid may decrease VPS45 and ARP2/3, while increase CAPZA and Sh3gl2, and then inhibit cell proliferation to slow eye growth in both LIH and LIM eye. The regulation of actin cytoskeleton pathway is possibly related to nicotinic acid treated LIM eyes only. Nicotinic acid may increase HRAS and then inhibit downstream ARP2/3 to slow eye growth.

Chapter 6: Summary and conclusions

One of the aims of this study is to profile the global proteomic protein expressions in normal eye growth, LIM and LIH, and to study the relevant biochemical cascades that may underlie myopia development in chicks. We found that there was an early and significant increase in retinal apoA1 expression in the retina of LIH but not in LIM eyes. According to the proteomic profiling, a number of biological pathways were depicted to play significant roles in myopia development. They include insulin pathway, endocytosis pathway, actin cytoskeleton pathway and hippo pathway.

For insulin signaling pathway, LIH increased the expression of GYS in the retina which acts to convert glucose into glycogen. Down-regulation of GYS would lead to a decrease in the availability of glucose, likely due to a decrease in energy demand during hyperopic eye growth. On the other hand, LIM showed an increase in PYG which acts to release glucose from glycogen. It indicated during LIM that more energy was provided to the retina by making available more glucose so as to support the accelerated eye growth in myopia. In terms of actin cytoskeleton pathway, LIH was shown to up-regulate PIR121 and then down-regulate Arp2/3 (which is downstream of PIR121) that led to the decrease in F-actin expression. The end effect would be the inhibition of cell growth. However, the development of LIM did not elicit differential alteration of the activity of this actin cytoskeleton pathway. For endocytosis pathway, LIH decreased

ARP2/3 and DNM3 expressions which can lead to the inhibition of tissue growth. It could also play an important role in the retention of retinal apoA1 by slowing down its removal. On the contrary, in LIM, the increased expression of RAB11 may imply the up-regulation of endocytosis pathway that may enhance tissue growth. In addition, the increase in endocytosis may in turn promote the removal of retinal apoA1 protein and leads to a diminished retinal apoA1 expression as observed in LIM. For the hippo signaling pathway, the up-regulation of CRB in this pathway in LIM may promote eye growth.

We further examined the source of retinal apoA1 expression as observed in LIM and LIH. The mRNA expression of apoA1 at the retina was measured and all these retinas of normal growing, LIH and LIM chicks expressed apoA1 mRNA. It suggested that chick retina can produce apoA1 protein locally. However, the exactly source of apoA1 protein in chick retinas is still unclear. Whether it was coming from the retina or the blood plasma, or from any other sources remains to be investigated.

Given that apoA1 protein was hypothesized as one of the key stop signals in eye growth, we examined if apoA1 protein may directly interfere with eye growth. ApoA1 was intravitreally injected into normal growing and LIM chick eyes. The results showed that apoA1 can retard eye growth in LIM without influencing normal eye growth. Furthermore, the effects of apoA1 in terms of retardation on eye growth was apparent when it was

administered at the onset of myopia induction, developing and fully developed stages of myopia in LIM eyes. It could even reverse the refraction at the developing and fully developed stages.

From the above proof-of-principle study with intravitreal injection of apoA1, it demonstrated apoA1 can slow down myopia development. We attempted to explore non-invasive ways to increase apoA1 expression of the eye. Nicotinic acid is a clinical drug for raising apoA1 in the blood plasma. In chapter 5, we tested the efficacy of oral intake of nicotinic acid in raising retinal apoA1 expression in chicks. The results showed that indeed it could upregulate the retinal apoA1 protein expression. Nicotinic acid could also significantly slow down growth in LIM eyes with a concomitant increase in the retinal apoA1 expression. Furthermore, it promoted additional hyperopic growth in LIH eyes which became even more hyperopic than LIH alone. Interestingly, there was no significant or detectable increase in apoA1 protein expression in LIH eyes after nicotinic acid treatment. Oral intake of nicotinic acid apparently did not affect normal eye growth.

In terms of the underlying mechanism, nicotinic acid may affect lipid metabolism through insulin signaling pathway, but it may not activate the PI3K/Akt and MEK/MRK sub-pathways in the normal growing eye. However, in LIM, nicotinic acid was shown to inhibit PI3K/Akt which in turn down-regulated GYS expression and up-regulated PKA expression to slow cell growth in LIM eye. Nicotinic acid may also modulate eye growth

through the endocytosis pathway in the LIH and LIM eyes by down-regulation of VPS45 and ARP2/3, and up-regulation of CAPZA and Sh3gl2 to slow eye growth. In addition, nicotinic acid may modulate the actin cytoskeleton pathway by increasing HRAS and then inhibiting downstream ARP2/3 to slowed eye growth in the LIM eyes.

Therefore, the present study supported a prominent role of apoA1 being a stop signal in eye growth. It may be an intriguing new research direction to examine if human myopia may be controlled through the modulation of apoA1 and its related pathways.

Limitations and future work

The present work has four major limitations:

1. In chapter 2, after LC-MS analysis, several pathways were found to be up-regulated or down-regulated, such as insulin pathway, endocytosis pathway, actin cytoskeleton pathway and hippo pathway. Only apoA1 was validated in the present experiment. There are likely other relevant biochemical factors in these pathways that are equally important and relevant to myopia development.
2. In chapter 3, the expression of apoA1 mRNA indicated that chick retinas can produce apoA1 protein locally, but the exact source (or sources) of apoA1 protein in the chick retina is still unclear.
3. In chapter 4, this study strongly suggested that apoA1 protein could directly impact myopic eye growth in chicks. This observation will

need to be replicated in other mammalian myopia models before it can be generalized to human.

4. In chapter 5, the results showed that oral administration of nicotinic acid could retard myopia development in chicks. This effect again will need to be replicated in mammalian myopia models.
5. Moreover, given the complexity of the biochemical cascades behind the apoA1 effect and even with a high throughput proteomic approach, we are only beginning to scratch the surface of the interconnections and interactions among different biological pathways. With more refined time points and bioinformatics analysis on bigger dataset, we may be able to gain better understanding of the temporal and dynamic biological mechanisms of eye growth in the future.
6. In our proteomic study, several biological pathways, such as insulin pathway, endocytosis pathway, actin cytoskeleton pathway and hippo pathway, were found to be important in refractive development of the eye. Insulin signaling, including PI3k/Akt pathway, is known to be related to major players in myopia development such as dopamine, egr-1 and apoA1. Since the insulin signaling pathway is most thoroughly researched, adding to the fact that there are many clinical drugs to regulate this pathway, it may be a profitable direction of future research in terms of unraveling its role in myopia development and control eventually. Given that the Hippo pathway is known to regulate growth

rate and body size, its role in myopia development warrants further research.

7. Apoa1 is an endogenous and physiological plasma protein which is particularly beneficial to cardiovascular health. ApoA1 enhancing agent such as nicotinic acid has been available and routinely administered clinically. Therefore, it will be an intriguing prospect to conduct a clinical myopia control study involving either apoA1 protein directly or apoA1 enhancing drugs in the near future to see if it reproduces an effective myopia control effect in human.

APPENDIX 1

Optimization for intravitreal injection of apolipoprotein A-1 (apoA1) in chicks

1. Volumetric consideration in the intravitreal injection of apoA1

Penha et al injected 12.5 µl insulin, U0126, Ly294002 and saline solution intravitreally to 8 days-old chicks (Penha et al., 2012). The same volume was injected by Gallego et al in 9-12 day-old chicks (Gallego et al., 2012) and by Bertrand et al to 8 day-old chicks (Bertrand et al., 2006). The maximum volume injected was 20 µl in 12-16 day-old chicks (Nickla et al., 2013), while the minimum volume was 5 µl in 5 day-old chicks (Murphy and Crewther, 2013). The youngest chicks which were injected intravitreally were 2 days after hatching with 10 µl MT3 solution (Nickla et al., 2015).

In this study, 10 µl of the solution was injected into 4 days old chick eyes. The 10 µl volume appeared a safe and averaged volume of injection in according to published literature. Considering the developmental stage of the animal, the present study employed 4 days old chicks in lens wear and intravitreal injection.

2. Dose dependency of apoA1 injection and eye growth

- Methods

The method for this optimization experiment was the same as that in Chapter 2.

Thirty-two white leghorn chicks at 4 days after hatching (PN4) were randomly distributed into four groups (Group 1, 2, 3 and 4, each group has 8 chicks). All chicks were orally fed with daily saline (1ml) and wore -10D lenses on both eyes at PN4. The apoA1 protein concentration in original stock is 1μg/μl. In original stock, there is 0.5% sodium lauroyl sarcosine (SLS) in 1×Phosphate buffered saline (PBS). ApoA1 protein (10μl) was injected into the treatment eye while the sham solution (10μl, SLS in 1×PBS) was injected to the control eye. The assignment of control and experimental eyes of the chicks was randomized using the random numbers generated by Microsoft Excel. The intravitreal injection was performed daily for 3 days at the beginning of LIM. The different apoA1 concentration to different group was designed as blow (Table 1).

Table 1. ApoA1 and SLS concentration in each group

group	ApoA1 (μg/μl)	SLS (%)
1	1	0.5
2	0.2	0.1
3	0.1	0.05
4	0.05	0.025

The measurement and statistical analysis in these experiments were the same as that in Chapter 4.

- Results

After 3 days of intravitreal injection, all the treatment eyes which were injected with 1μg/μl apoA1 in group 1 had white precipitate in vitreous chamber. There was no precipitate in the control eyes and in groups 2, 3 and 4.

Comparison between apoA1 and sham treated 3 days and LIM lens wear, in group 2 (apoA1 0.2μg/μl), the changes of VCD, AXL and SER were significant between treatment and control eyes (Table 2 and Figure 1). In group 3 (apoA1 0.1μg/μl), the change of AXL was significant between the treatment and control eyes. However, the changes of VCD and SER were not significant (Table 3 and Figure 1). Similar to group 2, in group 4 (apoA1 0.05μg/μl), the changes of VCD, AXL and SER were significant between the treatment and control eyes (Table 4 and Figure 1).

Table 2. The ocular parameters and refractive error in day 4 and 7 in group 2

	N	Mean	Std. Deviation	Sig. (2-tailed)	
ACD (mm)_Control	8	0.045	0.040	0.024	§
ACD (mm)_Treatment	8	0.009	0.036		
LT (mm)_Control	8	0.122	0.072	0.873	§
LT (mm)_Treatment	8	0.115	0.146		
VCD (mm)_Control	8	0.154	0.144	0.013	§
VCD (mm)_Treatment	8	0.008	0.101		
AXL (mm)_Control	8	0.321	0.128	0.002	§
AXL (mm)_Treatment	8	0.115	0.090		
RT (mm)_Control	8	-0.024	0.029	0.963	§
RT (mm)_Treatment	8	-0.023	0.011		
CT (mm)_Control	8	-0.062	0.051	0.483	§
CT (mm)_Treatment	8	-0.056	0.041		
ST (mm)_Control	8	-0.029	0.012	0.277	§
ST (mm)_Treatment	8	0.009	0.018		
SER (D)_Control	8	-2.438	1.116	0.004	§
SER (D)_Treatment	8	-1.282	0.796		

Table 3. The ocular parameters and refractive error in day 4 and 7 in group 3

	N	Mean	Std. Deviation	Sig. (2-tailed)	
ACD (mm)_Control	5	0.071	0.038	0.193	§
ACD (mm)_Treatment	5	0.022	0.054		
LT (mm)_Control	5	0.137	0.088	0.806	§
LT (mm)_Treatment	5	0.123	0.072		
VCD (mm)_Control	5	0.034	0.159	0.189	§
VCD (mm)_Treatment	5	-0.079	0.133		
AXL (mm)_Control	5	0.241	0.118	0.042	§
AXL (mm)_Treatment	5	0.067	0.149		
RT (mm)_Control	5	-0.034	0.014	0.368	§
RT (mm)_Treatment	5	-0.020	0.023		
CT (mm)_Control	5	0.002	0.029	0.634	§
CT (mm)_Treatment	5	0.023	0.107		
ST (mm)_Control	5	-0.013	0.006	0.005	§
ST (mm)_Treatment	5	0.005	0.009		
SER (D)_Control	5	-1.400	0.518	0.290	§
SER (D)_Treatment	5	-0.900	0.518		

Table 4. The ocular parameters and refractive error in day 4 and 7 in group 4

	N	Mean	Std. Deviation	Sig. (2-tailed)	
ACD (mm)_Control	6	0.039	0.068	0.038	§
ACD (mm)_Treatment	6	-0.014	0.040		
LT (mm)_Control	6	0.137	0.071	0.842	§
LT (mm)_Treatment	6	0.141	0.089		
VCD (mm)_Control	6	0.111	0.077	0.003	§
VCD (mm)_Treatment	6	-0.038	0.081		
AXL (mm)_Control	6	0.287	0.092	0.002	§
AXL (mm)_Treatment	6	0.090	0.127		
RT (mm)_Control	6	-0.010	0.012	0.570	§
RT (mm)_Treatment	6	-0.017	0.020		
CT (mm)_Control	6	-0.051	0.035	0.043	§
CT (mm)_Treatment	6	-0.021	0.041		
ST (mm)_Control	6	0.004	0.011	0.048	§
ST (mm)_Treatment	6	0.016	0.020		
SER (D)_Control	6	-1.958	0.401	0.000	§
SER (D)_Treatment	6	-0.833	0.342		

§P value for paired student's t-test

||P value for signed rank test

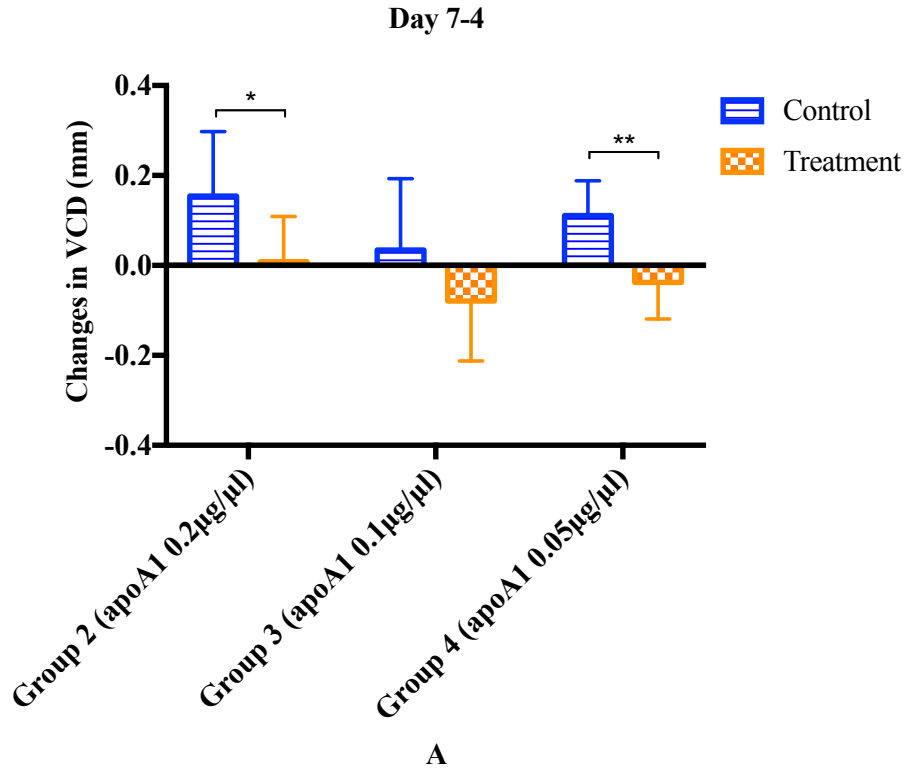
Day 7-4
Changes in VCD (mm)
0.4
0.2
0.0
-0.2
-0.4
*
**
Control
Treatment
Group 2 (apoA1 0.2µg/µl)
Group 3 (apoA1 0.1µg/µl)
Group 4 (apoA1 0.05µg/µl)

A

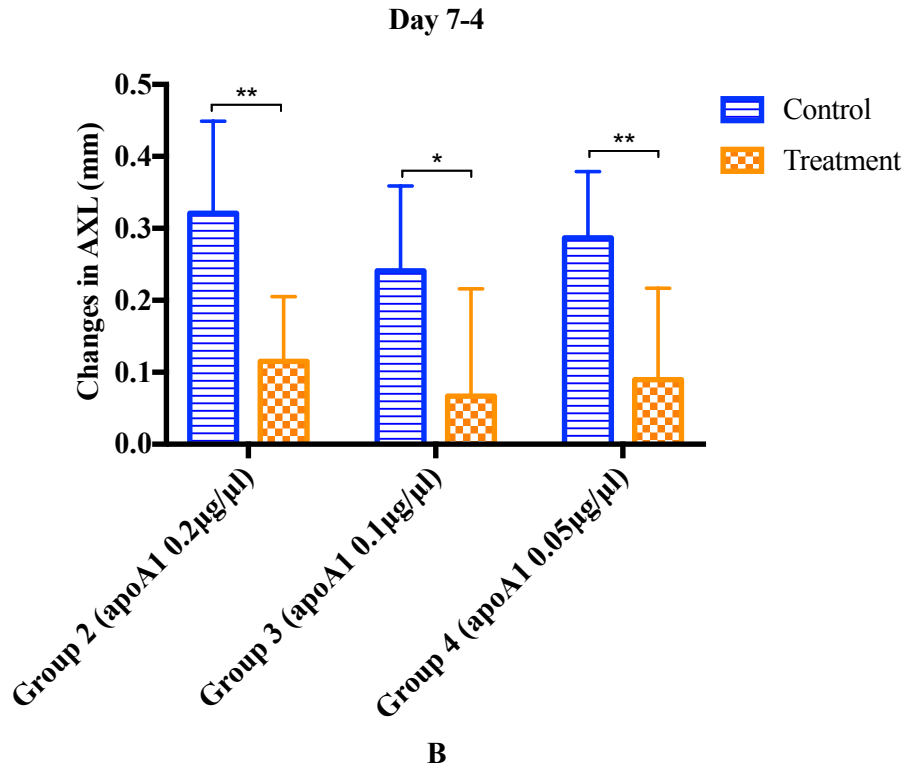
Day 7-4
Changes in AXL (mm)
0.5
0.4
0.3
0.2
0.1
0.0
**
*
**
Control
Treatment
Group 2 (apoA1 0.2µg/µl)
Group 3 (apoA1 0.1µg/µl)
Group 4 (apoA1 0.05µg/µl)

B

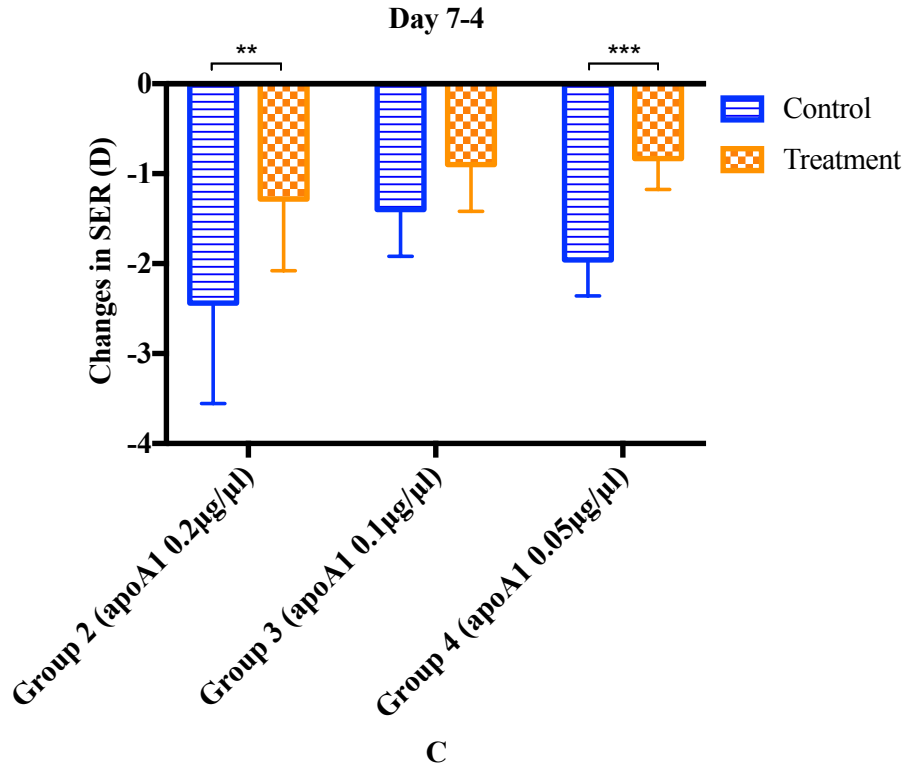

Figure 1. Changes of ocular parameters and refractive error between day 4 and 7 in LIM.

The effects of intravitreal injection of apoA1 on (A) VCD (mm), (B) AXL (mm), (C) SER (D) between day 4 and 7 in LIM. Mean ±SD, *p<0.05, **p<0.01, ***p<0.001

- Discussion and summary

In this pilot study, a number of apoA1 dosages were intravitreal injected into the chick eyes to study the dosage response of apoA1 in controlling eye growth. In group 1 (apoA1 1µg/µl), all the apoA1 treated eyes had precipitate in vitreous chamber. The precipitate in vitreous chamber was undesirable as it might contribute to form deprivation myopia (FDM) and

promote axial elongation and myopic development (Hodos, 1990, McBrien and Norton, 1992, Norton, 1990, Raviola and Wiesel, 1990). The precipitate was observed only in the treatment eyes in group 1. It suggested that the concentration of 1 μg/μl apoA1 with the solvent was too high and induced precipitation in the vitreous chamber.

In term of group 2, 3 and 4, the apoA1 concentration at 0.2, 0.1 and 0.5 μg/μl significantly retarded axial elongation. In group 2, the effect of inhibition eye growth was maximal in these three groups without precipitation.

To further explore apoA1's effect on the retardation of eye growth, the concentration of 0.2 μg/μl apoA1 was used in subsequent experiments in chapter 4.

3. The effects of intravitreal injection of apoA1 at different developmental time points of chicks

The experimental details and statistical analysis in these experiments were the same as that of the Chapter 2.

Twelve white leghorn chicks at 4 days after hatching (PN4) were randomly distributed into two groups. All chicks were orally fed with daily saline (1ml) and wore lenses on both eyes beginning at PN4. The -10D lenses was attached to both eyes in LIM group, as well as plano to control group.

Continual measurements of ocular parameters and reflective errors were conducted for 16 days.

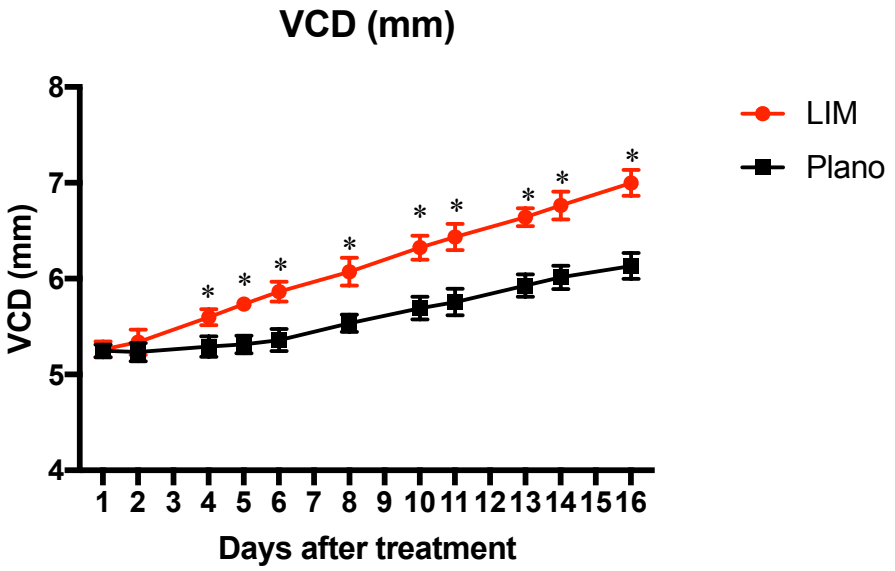

A

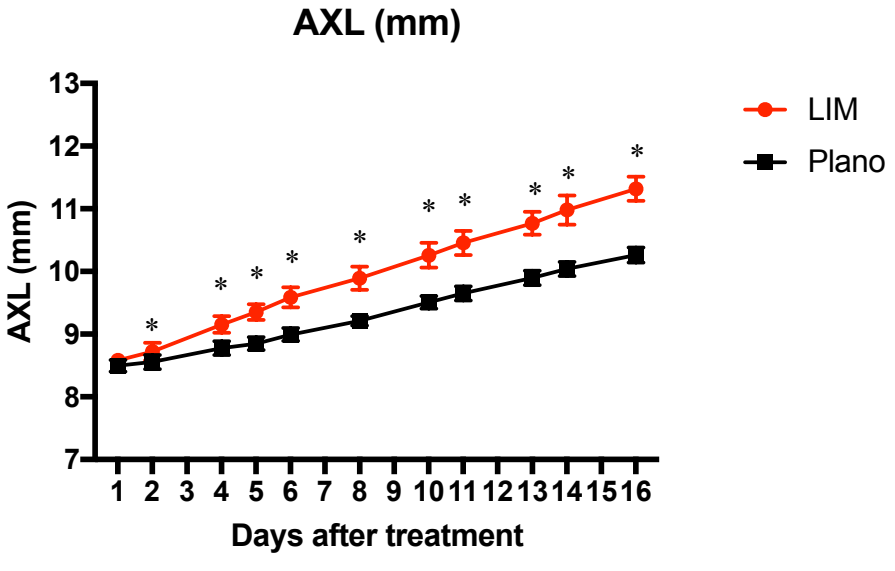

B

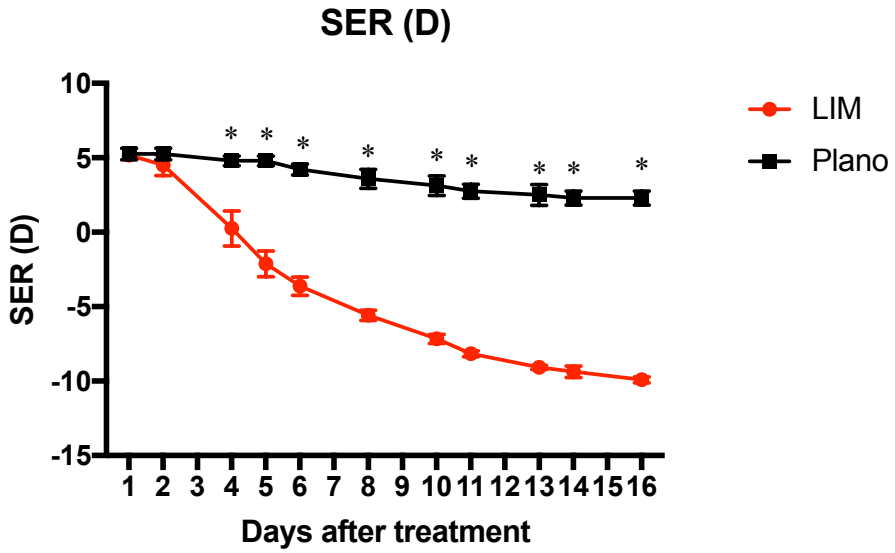

C

Figure 2. Ocular parameters and refractive error measured daily from 1 to 16 days after treatment.

The effects of LIM and plano on (A) VCD (mm), (B) AXL (mm), (C) SER (D) daily from 1 to 16 days after treatment. Mean ±SD, *p<0.05, **p<0.01, ***p<0.001

At 4 days after treatment, the VCD, AXL were elongated significantly, and the reflective error was significantly more myopic in the LIM group. The eye continuously grew towards myopia. At 14 days after LIM, the refractive error was around -10D. From 14 to 16 days after LIM, the eyeballs continuously grew further but the refractive error became myopic matching nearly fully to the attached lens power. After negative lens treatment for 4 days, the eyes were significantly more myopic with accelerated eye growth. This period is analogous to young children in human where their eyes

begins to emmetropise and/or develops myopia. From 14 to 16, the reflective error of the chick eye decreased slowly and nearly fully matched the attachment lenses. The period is analogous to human young adulthood where the refraction has been fully developed. From 4 to 14 days, it might be thought as rapid developing phase as in teenagers.

Therefore, we devised three groups in chapter 4 to study the effects of apoA1 on eye growth at different developmental stages.

APPENDIX 2

LIH vs plano experiment in chapter 2

The list of identified proteins (at least 2 peptides per protein, $|\log_2$ (fold change)$| \geq 0.379$ and P-value < 0.05)

Protein ID	Uniprot Protein accession number	Protein Name	P-value	Log_2 Fold change (LIH/ plano)
1	A2NR64	Defender against death protein 1	0.003	-1.281
2	E1C6D1	Microtubule-associated protein	0.000	-1.196
3	E1C0F1	Dolichyl-diphosphooligosaccharide--protein glycosyltransferase subunit 1	0.010	-0.847
4	F1P4I9	Proteasomal ubiquitin receptor ADRM1	0.031	-0.791
5	F1NG89	Ubiquitin carboxyl-terminal hydrolase	0.007	-0.714

6	Q90732	26S protease regulatory subunit 4	0.010	-0.691
7	F1NHD8	Uncharacterized protein	0.031	-0.646
8	P28683	Green-sensitive opsin	0.026	-0.632
9	F1NQH8	Uncharacterized protein	0.035	-0.606
10	F1N861	Uncharacterized protein	0.016	-0.582
11	R4GKF5	Uncharacterized protein	0.038	-0.455
12	F1NTP3	Uncharacterized protein	0.011	-0.448
13	Q5F3I2	Putative uncharacterized protein	0.022	-0.435
14	R4GFJ7	Uncharacterized protein	0.006	-0.404
15	E1C7W7	Uncharacterized protein	0.009	-0.402
16	F1NIQ4	Uncharacterized protein	0.001	-0.383
17	F1NU40	Nucleolin	0.024	-0.379
18	F1NU79	Uncharacterized protein	0.016	0.392
19	E1BQV4	Uncharacterized protein	0.014	0.399
20	Q5ZLF7	Importin subunit alpha	0.013	0.405
21	E1C1U1	Uncharacterized protein	0.048	0.418
22	F1N9D8	Cathepsin B	0.039	0.420
23	G8H1M4	Synaptic vesicle glycoprotein 2A	0.046	0.431
24	Q5ZLP5	Uncharacterized protein	0.024	0.435

25	Q5ZMV3	Protein Dr1	0.013	0.438
26	F1NE09	Uncharacterized protein	0.017	0.442
27	Q5ZKX2	Uncharacterized protein	0.035	0.444
28	Q5ZMH1	Septin-2	0.010	0.461
29	Q8JIR8	Interphotoreceptormatrix proteoglycan 1	0.040	0.467
30	E1C5R3	Uncharacterized protein	0.010	0.485
31	E1BUR1	Uncharacterized protein	0.041	0.498
32	F1NCP5	MOB-like protein phocein	0.028	0.514
33	E1BXK3	Uncharacterized protein	0.049	0.535
34	E1C6A2	Uncharacterized protein	0.036	0.548
35	F1NUT7	Neurofilament medium polypeptide	0.002	0.549
36	Q5ZL80	Uncharacterized protein	0.003	0.568
37	F1NCI5	Uncharacterized protein	0.040	0.585
38	R4GKR7	Uncharacterized protein	0.033	0.585
39	E1C9I7	Uncharacterized protein	0.025	0.595
40	Q9I9H1	Alpha-synuclein	0.020	0.604
41	F1NV37	Uncharacterized protein	0.022	0.606
42	F1NQB4	Uncharacterized protein	0.024	0.624
43	F1NFP6	Uncharacterized protein	0.000	0.706

44	E1C045	CUGBP Elav-like family member 2	0.047	0.715
45	E1C0U3	Uncharacterized protein	0.013	0.723
46	F1NPA2	Uncharacterized protein	0.004	0.765
47	F6UZR6	Lamin-B receptor	0.011	0.838
48	F1N8N1	Uncharacterized protein	0.034	0.861
49	Q98906	Microtubule-associated protein	0.003	0.971
50	E1C603	Uncharacterized protein	0.035	0.983
51	Q5F406	Uncharacterized protein	0.005	1.030
52	F1NZM1	Eukaryotic translation initiation factor 3 subunit E	0.015	1.034
53	P15720	Myelin basic protein	0.029	1.043
54	E1C6P4	Uncharacterized protein	0.003	1.050
55	P08250	Apolipoprotein A-1	0.043	1.068
56	F1P566	Uncharacterized protein	0.011	1.111
57	F1NLB3	Neural cell adhesion molecule 1	0.003	1.190
58	F1N9D3	Uncharacterized protein	0.001	1.219
59	E1C4Q2	Microtubule-associated protein 6 homolog	0.003	1.273

60	Q9I9G9	Beta-synuclein	0.001	1.289
61	P02112	Hemoglobin subunit beta	0.048	1.732
62	P01994	Hemoglobin subunit alpha-A	0.034	1.940
63	F2Z4L6	Serum albumin	0.005	2.413

LIM vs plano experiment in chapter 2

The list of identified proteins (at least 2 peptides per protein, $|\log_2$ (fold change)$| \geq 0.379$ and P-value < 0.05)

Protein ID	Uniprot Protein accession number	Protein Name	P-value	Log2 Fold change (LIM/ plano)
1	E1C0Q5	Uncharacterized protein	0.026	-0.541
2	F1NIR8	Uncharacterized protein	0.009	-0.517
3	Q5ZHU6	Uncharacterized protein	0.032	-0.481
4	E1C3R4	Uncharacterized protein	0.004	-0.459

5	E1C584	Uncharacterized protein	0.037	-0.448
6	R4GFJ7	Uncharacterized protein	0.013	-0.435
7	E1BT40	Uncharacterized protein	0.007	0.390
8	F1N8H6	Heterochromatin protein 1-binding protein 3	0.037	0.429
9	F1NUT7	Neurofilament medium polypeptide	0.042	0.432
10	P09244	Tubulin beta-7 chain	0.031	0.435
11	E1C5R3	Uncharacterized protein	0.020	0.468
12	F1NE09	Uncharacterized protein	0.016	0.486
13	Q67BJ3	Nicastrin	0.019	0.896

LIM vs LIH experiment in chapter 2

The list of identified proteins (at least 2 peptides per protein, |log2 (fold change)| ≥ 0.379 and P-value < 0.05)

Protein ID	Uniprot Protein accession number	Protein Name	P-value	Log2 Fold change (LIM/ LIH)
1	F2Z4L6	Serum albumin	0.001	-2.372
2	P01994	Hemoglobin subunit alpha-A	0.030	-1.384
3	P08250	Apolipoprotein A-I	0.014	-1.159
4	Q9I9G9	Beta-synuclein	0.005	-1.158
5	F1N9D3	Uncharacterized protein (Fragment)	0.002	-1.134
6	E1C6A2	Uncharacterized protein	0.005	-1.080
7	E1C4Q2	Microtubule-associated protein 6 homolog	0.031	-0.982
8	E1BT93	Uncharacterized protein (Fragment)	0.000	-0.949
9	Q98906	Microtubule-associated protein (Fragment)	0.033	-0.895
10	E1C6P4	Uncharacterized protein	0.001	-0.882

11	F1NPA2	Uncharacterized protein (Fragment)	0.042	-0.845
12	E1C3F8	Uncharacterized protein	0.034	-0.840
13	F1NLB3	Neural cell adhesion molecule 1	0.029	-0.816
14	F1NZM1	Eukaryotic translation initiation factor 3 subunit E	0.016	-0.790
15	E1C586	Uncharacterized protein	0.021	-0.683
16	E1BZY9	Uncharacterized protein	0.025	-0.656
17	F1NZA7	Uncharacterized protein (Fragment)	0.038	-0.630
18	F1NB26	Uncharacterized protein	0.027	-0.629
19	F1NCP5	MOB-like protein phocein	0.004	-0.602
20	E1BYD4	Uncharacterized protein	0.011	-0.579
21	Q8JIR8	Interphotoreceptor matrix proteoglycan 1	0.048	-0.578
22	F1NQB4	Uncharacterized protein (Fragment)	0.040	-0.578

23	Q5ZIF1	Adipocyte plasma membrane-associated protein	0.033	-0.576
24	Q5ZL72	60 kDa heat shock protein, mitochondrial	0.005	-0.541
25	E1C584	Uncharacterized protein	0.025	-0.536
26	E1BRI3	Uncharacterized protein	0.032	-0.525
27	E1BSF5	Branched-chain-amino-acid aminotransferase	0.043	-0.516
28	F1NU79	Uncharacterized protein (Fragment)	0.003	-0.509
29	Q9I9H1	Alpha-synuclein	0.027	-0.490
30	O93468	GTP-binding protein	0.008	-0.489
31	P79781	Ubiquitin-40S ribosomal protein S27a	0.000	-0.483
32	R4GLE6	Eukaryotic translation initiation factor 1	0.004	-0.475
33	E1BT38	Uncharacterized protein	0.012	-0.472
34	P28684	Violet-sensitive opsin	0.032	-0.467
35	Q6XK22	Regulator of G-protein signaling 9-binding protein	0.029	-0.465

36	Q5ZJE6	Uncharacterized protein	0.035	-0.463
37	F1NFP6	Uncharacterized protein	0.039	-0.457
38	O42281	Peripherin-2	0.046	-0.428
39	Q5ZLF7	Importin subunit alpha	0.010	-0.422
40	E1C303	Uncharacterized protein	0.011	-0.419
41	F1N9D8	Cathepsin B	0.046	-0.414
42	Q5ZJ81	Endophilin-B2	0.033	-0.414
43	Q5F3L2	Uncharacterized protein	0.049	-0.413
44	F1NQC3	Glutamine synthetase	0.007	-0.411
45	Q8AXV1	Endophilin-A1	0.028	-0.409
46	E1C0U3	Uncharacterized protein	0.011	-0.384
47	E1C8Y3	Uncharacterized protein (Fragment)	0.016	0.385
48	E1C6T8	Eukaryotic translation initiation factor 3 subunit I	0.021	0.391
49	F1NNF7	Succinate dehydrogenase [ubiquinone] iron-sulfur subunit, mitochondrial	0.035	0.396
50	E1C6R4	Uncharacterized protein	0.015	0.397
51	E1C4U4	Uncharacterized protein	0.034	0.401

52	Q5ZMN9	DNA-directed RNA polymerase	0.022	0.407
53	E1C7W7	Uncharacterized protein	0.003	0.424
54	F1NFU4	Uncharacterized protein (Fragment)	0.044	0.425
55	F1NU40	Nucleolin	0.005	0.428
56	F1P4H4	Uncharacterized protein	0.036	0.454
57	F1NCF1	Uncharacterized protein	0.043	0.467
58	F1N8H6	Heterochromatin protein 1-binding protein 3	0.032	0.471
59	F1NFC6	Uncharacterized protein (Fragment)	0.003	0.477
60	E1BV47	Uncharacterized protein	0.038	0.483
61	E1C8P2	Uncharacterized protein	0.007	0.525
62	F1NG89	Ubiquitin carboxyl-terminal hydrolase (Fragment)	0.037	0.526
63	Q5ZLY6	Uncharacterized protein	0.045	0.564
64	F1P4I9	Proteasomal ubiquitin receptor ADRM1	0.002	0.569
65	Q5ZJZ9	Uncharacterized protein	0.021	0.592

66	F1NPD3	60S ribosomal protein L18a (Fragment)	0.021	0.625
67	F1N861	Uncharacterized protein	0.005	0.626
68	F1NUQ3	Heart fatty acid binding protein	0.011	0.631
69	Q5F3C6	Uncharacterized protein	0.019	0.662
70	E1C0F1	Dolichyl-diphosphooligosaccharide --protein glycosyltransferase subunit 1 (Fragment)	0.038	0.683
71	F1NKC9	Cadherin-related family member 1	0.040	0.794
72	E1C2S3	Uncharacterized protein	0.013	0.799
73	Q90732	26S protease regulatory subunit 4	0.012	0.889
74	F1P0Q6	Uncharacterized protein (Fragment)	0.049	0.934
75	Q7SX63	Heat shock protein 70	0.040	0.958
76	E1C3B2	Cytochrome c oxidase subunit 6A, mitochondrial	0.036	1.072

77	A2NR64	Defender against death protein 1	0.019	1.085
78	Q5F402	Coatomer subunit gamma	0.001	1.337
79	Q5F3W6	14-3-3 protein gamma	0.019	2.258

NA plano vs plano experiment in chapter 5

The list of identified proteins (at least 2 peptides per protein, $|\log_2$ (fold change)$| \geq 0.379$ and P-value < 0.05)

Protein ID	Uniprot Protein accession number	Protein Name	P-value	Log2 Fold change (NA plano/ plano)
1	F1NTL8	Uncharacterized protein	0.002	-1.220
2	E1C6D1	Microtubule-associated protein	0.000	-1.081
3	Q5ZM67	Uncharacterized protein	0.007	-1.027
4	Q802E3	Phosphodiesterase 6 gamma subunit cone form	0.024	-0.950

5	E1BUS4	Uncharacterized protein	0.017	-0.785
6	R4GMC8	Cysteine and glycine-rich protein 2	0.035	-0.757
7	P02552	Tubulin alpha-1 chain	0.042	-0.636
8	E1C584	Uncharacterized protein	0.005	-0.617
9	E1BUW6	Microtubule-associated protein	0.007	-0.607
10	F1P2A1	Uncharacterized protein	0.036	-0.589
11	Q5ZMF7	Uncharacterized protein	0.023	-0.563
12	Q5ZL72	60 kDa heat shock protein, mitochondrial	0.029	-0.539
13	F1NHG6	Uncharacterized protein	0.015	-0.524
14	F1P0A1	Uncharacterized protein	0.014	-0.496
15	F1NPL2	Uncharacterized protein	0.022	-0.496

16	Q5ZMV3	Protein Dr1	0.033	-0.489
17	A2NR64	Defender against death protein 1	0.041	-0.475
18	Q5ZJW4	Vesicle-trafficking protein SEC22b	0.001	-0.475
19	H9L022	Uncharacterized protein	0.035	-0.451
20	Q5ZLJ7	Uncharacterized protein	0.016	-0.447
21	E1C0Q5	Uncharacterized protein	0.047	-0.442
22	Q5F3I2	Putative uncharacterized protein	0.027	-0.436
23	H9KZA6	Uncharacterized protein	0.002	-0.431
24	H9L0B9	Uncharacterized protein	0.011	-0.425
25	Q5ZMC0	Endothelial differentiation-related factor 1 homolog	0.034	-0.412

26	Q5ZJE6	Uncharacterized protein	0.045	-0.382
27	F1NLZ7	Uncharacterized protein	0.028	-0.380
28	F1NYB5	Uncharacterized protein	0.039	0.400
29	E1BV34	Uncharacterized protein	0.023	0.407
30	E1BSP1	Proactivator polypeptide	0.010	0.430
31	E1C4H8	Uncharacterized protein	0.006	0.619
32	R4GH86	Glutathione peroxidase	0.049	0.666

NA LIH vs LIH experiment in chapter 5

The list of identified proteins (at least 2 peptides per protein were sequenced, $|\log_2 \text{(fold change)}| \geq 0.379$ and P-value < 0.05)

Protein ID	Uniprot Protein accession number	Protein Name	P-value	Log2 Fold change (NA LIH/ LIH)
1	O93468	GTP-binding protein	0.010	-0.641
2	F1P3B8	Sister chromatid cohesion protein PDS5 homolog B	0.009	-0.396
3	E1C3A3	Uncharacterized protein	0.026	-0.394
4	Q25QX5	BASH/BLNK N-terminal associated protein 1	0.007	0.379
5	F1NNF7	Succinate dehydrogenase [ubiquinone] iron-sulfur subunit, mitochondrial	0.026	0.419

6	A0M8U0	Capping protein (Actin filament) muscle Z-line, alpha 2	0.004	0.471
7	F1NWE5	Uncharacterized protein	0.030	0.713
8	E1C0F1	Dolichyl-diphosphooligosaccharide--protein glycosyltransferase subunit 1	0.001	0.789
9	H9L0A9	Uncharacterized protein	0.011	0.924
10	F1P0Q8	H/ACA ribonucleoprotein complex subunit 4	0.028	1.672

NA LIM vs LIM experiment in chapter 5

The list of identified proteins (at least 2 peptides per protein, $|\log_2$ (fold change)$| \geq 0.379$ and P-value < 0.05)

Protein ID	Uniprot Protein accession number	Protein Name	P-value	Log2 Fold change (NA LIM/ LIM)
1	F1N8N1	Uncharacterized protein	0.026	-1.393
2	R4GKR7	Uncharacterized protein	0.011	-1.081
3	F1N8J8	Uncharacterized protein	0.021	-0.904
4	E1BW84	Uncharacterized protein	0.010	-0.843
5	F1NQB4	Uncharacterized protein	0.035	-0.682
6	Q5F425	Protein lin-7 homolog C	0.014	-0.668
7	F1NDA0	Glycylpeptide N-tetradecanoyltransferase	0.012	-0.587

8	Q5ZJI7	Uncharacterized protein	0.024	-0.569
9	Q5ZM59	Phosphohippolin-like protein	0.033	-0.548
10	F1NJ60	Protein Hook homolog 1	0.008	-0.503
11	F1N8H6	Heterochromatin protein 1-binding protein 3	0.021	-0.451
12	E1BXK3	Uncharacterized protein	0.019	-0.437
13	Q5ZLK3	Uncharacterized protein	0.019	-0.390
14	F1N9J7	Uncharacterized protein	0.042	-0.389
15	R4GKQ7	Uncharacterized protein	0.002	-0.380
16	P23668	16 kDa beta-galactoside-binding lectin	0.005	-0.380

17	Q5ZJ64	Eukaryotic translation initiation factor 3 subunit M	0.041	0.400
18	R4GFJ7	Uncharacterized protein	0.021	0.405
19	E1C9H8	Uncharacterized protein	0.010	0.420
20	O73685	G-protein coupled receptor kinase 1	0.011	0.436
21	F1NLL2	Beta-galactosidase	0.005	0.453
22	U5LXR4	Glucosamine-6-phosphate deaminase 2 isoform 4	0.027	0.514
23	E1C6R4	Uncharacterized protein	0.040	0.518
24	E1C4P5	Uncharacterized protein	0.049	0.556
25	P28683	Green-sensitive opsin	0.002	0.570
26	F1P0A1	Uncharacterized protein	0.014	0.640

27	Q52P71	Interphotoreceptor retinoid binding protein	0.013	0.670
28	E1C3X0	Uncharacterized protein	0.019	0.701
29	E1BR04	Uncharacterized protein	0.042	1.177
30	F1NJB4	Uncharacterized protein	0.020	1.295

Reference:

ABBOTT, M. L., SCHMID, K. L. & STRANG, N. C. 1998. Differences in the accommodation stimulus response curves of adult myopes and emmetropes. *Ophthalmic Physiol Opt,* 18**,** 13-20.

ALEMANY, S., PELECH, S., BRIERLEY, C. H. & COHEN, P. 1986. The protein phosphatases involved in cellular regulation. Evidence that dephosphorylation of glycogen phosphorylase and glycogen synthase in the glycogen and microsomal fractions of rat liver are catalysed by the same enzyme: protein phosphatase-1. *Eur J Biochem,* 156**,** 101-10.

ALI, R. R. & SOWDEN, J. C. 2011. Regenerative medicine: DIY eye. *Nature,* 472**,** 42-3.

ANDISON, M. E., SIVAK, J. G. & BIRD, D. M. 1992. The refractive development of the eye of the American kestrel (Falco sparverius): a new avian model. *J Comp Physiol A,* 170**,** 565-74.

ANERA, R. G., SOLER, M., DE LA CRUZ CARDONA, J., SALAS, C. & ORTIZ, C. 2009. Prevalence of refractive errors in school-age children in Morocco. *Clin Exp Ophthalmol,* 37**,** 191-6.

ANSON, M. L. 1940. The Reactions of Iodine and Iodoacetamide with Native Egg Albumin. *J Gen Physiol,* 23**,** 321-31.

ASAKUMA, T., YASUDA, M., NINOMIYA, T., NODA, Y., ARAKAWA, S., HASHIMOTO, S., OHNO-MATSUI, K., KIYOHARA, Y. & ISHIBASHI, T. 2012. Prevalence and risk factors for myopic retinopathy in a Japanese population: the Hisayama Study. *Ophthalmology,* 119**,** 1760-5.

ASHBY, R., KOZULIN, P., MEGAW, P. L. & MORGAN, I. G. 2010a. Alterations in ZENK and glucagon RNA transcript expression during increased ocular growth in chickens. *Molecular Vision,* 16**,** 639-49.

ASHBY, R., KOZULIN, P., MEGAW, P. L. & MORGAN, I. G. 2010b. Alterations in ZENK and glucagon RNA transcript expression during increased ocular growth in chickens. *Mol Vis,* 16**,** 639-49.

ASHBY, R., MCCARTHY, C. S., MALESZKA, R., MEGAW, P. & MORGAN, I. G. 2007a. A muscarinic cholinergic antagonist and a dopamine agonist rapidly increase ZENK mRNA expression in the form-deprived chicken retina. *Experimental Eye Research,* 85**,** 15-22.

ASHBY, R., MCCARTHY, C. S., MALESZKA, R., MEGAW, P. & MORGAN, I. G. 2007b. A muscarinic cholinergic antagonist and a dopamine agonist rapidly increase ZENK mRNA expression in the form-deprived chicken retina. *Exp Eye Res,* 85**,** 15-22.

ASHBY, R., OHLENDORF, A. & SCHAEFFEL, F. 2009. The effect of ambient illuminance on the development of deprivation myopia in chicks. *Invest Ophthalmol Vis Sci,* 50**,** 5348-54.

ASHBY, R. S. & SCHAEFFEL, F. 2010. The effect of bright light on lens compensation in chicks. *Invest Ophthalmol Vis Sci,* 51**,** 5247-53.

BABEL, J. & HOUBER, J. P. 1970. [Anatomy and histology of the retina]. *Arch Ophtalmol Rev Gen Ophtalmol,* 30**,** 257-75.

BACKHOUSE, S., COLLINS, A. V. & PHILLIPS, J. R. 2013. Influence of periodic vs continuous daily bright light exposure on development of experimental myopia in the chick. *Ophthalmic Physiol Opt,* 33**,** 563-72.

BAIRD, P. N., SCHACHE, M. & DIRANI, M. 2010. The GEnes in Myopia (GEM) study in understanding the aetiology of refractive errors. *Prog Retin Eye Res,* 29**,** 520-42.

BARATHI, V. A., BOOPATHI, V. G., YAP, E. P. & BEUERMAN, R. W. 2008. Two models of experimental myopia in the mouse. *Vision Res,* 48**,** 904-16.

BATEMAN, R., CARRUTHERS, R., HOYES, J., JONES, C., LANGRIDGE, J., MILLAR, A. & VISSERS, J. 2002. A novel precursor ion discovery method on a hybrid quadrupole orthogonal acceleration time-of-flight (Q-TOF) mass spectrometer for studying

protein phosphorylation. *Journal of the American Society for Mass Spectrometry,* 13**,** 792-803.

BEAULIEU, J. M., GAINETDINOV, R. R. & CARON, M. G. 2007. The Akt-GSK-3 signaling cascade in the actions of dopamine. *Trends Pharmacol Sci,* 28**,** 166-72.

BERESFORD, J. A., CREWTHER, S. G., KIELY, P. M. & CREWTHER, D. P. 2001. Comparison of refractive state and circumferential morphology of retina, choroid, and sclera in chick models of experimentally induced ametropia. *Optometry and Vision Science,* 78**,** 40-49.

BERRIDGE, K. C., ROBINSON, T. E. & ALDRIDGE, J. W. 2009. Dissecting components of reward: 'liking', 'wanting', and learning. *Curr Opin Pharmacol,* 9**,** 65-73.

BERTRAND, E., FRITSCH, C., DIETHER, S., LAMBROU, G., MULLER, D., SCHAEFFEL, F., SCHINDLER, P., SCHMID, K. L., VAN OOSTRUM, J. & VOSHOL, H. 2006. Identification of apolipoprotein A-I as a "STOP" signal for myopia. *Mol Cell Proteomics,* 5**,** 2158-66.

BESHARSE, J. C. & MCMAHON, D. G. 2016. The Retina and Other Light-sensitive Ocular Clocks. *J Biol Rhythms,* 31**,** 223-43.

BIRJMOHUN, R. S., HUTTEN, B. A., KASTELEIN, J. J. & STROES, E. S. 2004. Increasing HDL cholesterol with extended-release nicotinic acid: from promise to practice. *Neth J Med,* 62**,** 229-34.

BITZER, M. & SCHAEFFEL, F. 2002. Defocus-induced changes in ZENK expression in the chicken retina. *Invest Ophthalmol Vis Sci,* 43**,** 246-52.

BURGERING, B. M. & COFFER, P. J. 1995. Protein kinase B (c-Akt) in phosphatidylinositol-3-OH kinase signal transduction. *Nature,* 376**,** 599-602.

BUSCHIAZZO, A., UGALDE, J. E., GUERIN, M. E., SHEPARD, W., UGALDE, R. A. & ALZARI, P. M. 2004. Crystal structure of glycogen synthase: homologous enzymes catalyze glycogen synthesis and degradation. *EMBO J,* 23**,** 3196-205.

CALOGERO, A., LOMBARI, V., DE GREGORIO, G., PORCELLINI, A., UCCI, S., ARCELLA, A., CARUSO, R., GAGLIARDI, F. M., GULINO, A., LANZETTA, G., FRATI, L., MERCOLA, D. & RAGONA, G. 2004. Inhibition of cell growth by EGR-1 in human primary cultures from malignant glioma. *Cancer Cell Int,* 4**,** 1.

CAPPIELLO, A., FAMIGLINI, G., MANGANI, F. & PALMA, P. 2002. A simple approach for coupling liquid chromatography and electron ionization mass spectrometry. *J Am Soc Mass Spectrom,* 13**,** 265-73.

CARRE, A. L., JAMES, A. W., MACLEOD, L., KONG, W., KAWAI, K., LONGAKER, M. T. & LORENZ, H. P. 2010. Interaction of wingless protein (Wnt), transforming growth factor-beta1, and hyaluronan production in fetal and postnatal fibroblasts. *Plast Reconstr Surg,* 125**,** 74-88.

CHARMAN, W. N. 1999. Near vision, lags of accommodation and myopia. *Ophthalmic Physiol Opt,* 19**,** 126-33.

CHEN, C., CHEUNG, S. W. & CHO, P. 2013. Myopia control using toric orthokeratology (TO-SEE study). *Invest Ophthalmol Vis Sci,* 54**,** 6510-7.

CHEN, S., ZHI, Z., RUAN, Q., LIU, Q., LI, F., WAN, F., REINACH, P. S., CHEN, J., QU, J. & ZHOU, X. 2017. Bright Light Suppresses Form-Deprivation Myopia Development With Activation of Dopamine D1 Receptor Signaling in the ON Pathway in Retina. *Invest Ophthalmol Vis Sci,* 58**,** 2306-2316.

CHEN, S. J., LU, P., ZHANG, W. F. & LU, J. H. 2012. High myopia as a risk factor in primary open angle glaucoma. *Int J Ophthalmol,* 5**,** 750-3.

CHEN, W., FENG, Y., CHEN, D. & WANDINGER-NESS, A. 1998. Rab11 is required for trans-golgi network-to-plasma membrane transport and a preferential target for GDP dissociation inhibitor. *Mol Biol Cell,* 9**,** 3241-57.

CHENG, D., SCHMID, K. L., WOO, G. C. & DROBE, B. 2010. Randomized trial of effect of bifocal and prismatic bifocal spectacles on myopic progression: two-year results. *Arch Ophthalmol,* 128**,** 12-9.

CHIA, A., CHUA, W. H., CHEUNG, Y. B., WONG, W. L., LINGHAM, A., FONG, A. & TAN, D. 2012. Atropine for the treatment of childhood myopia: safety and efficacy of 0.5%, 0.1%, and 0.01% doses (Atropine for the Treatment of Myopia 2). *Ophthalmology,* 119**,** 347-54.

CHIA, A., CHUA, W. H., WEN, L., FONG, A., GOON, Y. Y. & TAN, D. 2014. Atropine for the treatment of childhood myopia: changes after stopping atropine 0.01%, 0.1% and 0.5%. *Am J Ophthalmol,* 157**,** 451-457 e1.

CHIANG, M. F., KOUZIS, A., POINTER, R. W. & REPKA, M. X. 2001. Treatment of childhood myopia with atropine eyedrops and bifocal spectacles. *Binocul Vis Strabismus Q,* 16**,** 209-15.

CHO, P. & CHEUNG, S. W. 2012. Retardation of myopia in Orthokeratology (ROMIO) study: a 2-year randomized clinical trial. *Invest Ophthalmol Vis Sci,* 53**,** 7077-85.

CHO, P. & CHEUNG, S. W. 2017. Discontinuation of orthokeratology on eyeball elongation (DOEE). *Cont Lens Anterior Eye,* 40**,** 82-87.

CHO, P., CHEUNG, S. W. & EDWARDS, M. 2005. The longitudinal orthokeratology research in children (LORIC) in Hong Kong: a pilot study on refractive changes and myopic control. *Curr Eye Res,* 30**,** 71-80.

CHO, P. & TAN, Q. 2018. Myopia and orthokeratology for myopia control. *Clin Exp Optom*.

CHUN, R. K., SHAN, S. W., LAM, T. C., WONG, C. L., LI, K. K., DO, C. W. & TO, C. H. 2015. Cyclic Adenosine Monophosphate Activates Retinal Apolipoprotein A1 Expression and Inhibits Myopic Eye Growth. *Invest Ophthalmol Vis Sci,* 56**,** 8151-7.

CLELAND, W. W. 1964. Dithiothreitol, a New Protective Reagent for Sh Groups. *Biochemistry,* 3**,** 480-2.

COHEN, J., HADJICONSTANTINOU, M. & NEFF, N. H. 1983. Activation of dopamine-containing amacrine cells of retina: light-induced increase of acidic dopamine metabolites. *Brain Res,* 260**,** 125-7.

COLE, A. J., SAFFEN, D. W., BARABAN, J. M. & WORLEY, P. F. 1989. Rapid increase of an immediate early gene messenger RNA in hippocampal neurons by synaptic NMDA receptor activation. *Nature,* 340**,** 474-6.

COLLINS, B. C., GILLET, L. C., ROSENBERGER, G., ROST, H. L., VICHALKOVSKI, A., GSTAIGER, M. & AEBERSOLD, R. 2013.

Quantifying protein interaction dynamics by SWATH mass spectrometry: application to the 14-3-3 system. *Nat Methods,* 10**,** 1246-53.

CONNER, S. D. & SCHMID, S. L. 2003. Differential requirements for AP-2 in clathrin-mediated endocytosis. *J Cell Biol,* 162**,** 773-9.

COOK, R. C. & GLASSCOCK, R. E. 1951. Refractive and ocular findings in the newborn. *Am J Ophthalmol,* 34**,** 1407-13.

COOPER, J. & TKATCHENKO, A. V. 2018. A Review of Current Concepts of the Etiology and Treatment of Myopia. *Eye Contact Lens,* 44**,** 231-247.

COX, D., LEE, D. J., DALE, B. M., CALAFAT, J. & GREENBERG, S. 2000. A Rab11-containing rapidly recycling compartment in macrophages that promotes phagocytosis. *Proc Natl Acad Sci U S A,* 97**,** 680-5.

CUMBERLAND, P. M., BAO, Y., HYSI, P. G., FOSTER, P. J., HAMMOND, C. J., RAHI, J. S., EYES, U. K. B. & VISION, C. 2015. Frequency and Distribution of Refractive Error in Adult Life: Methodology and Findings of the UK Biobank Study. *PLoS One,* 10**,** e0139780.

DASGUPTA, S., JANG, J. S., SHAO, C., MUKHOPADHYAY, N. D., SOKHI, U. K., DAS, S. K., BRAIT, M., TALBOT, C., YUNG, R. C., BEGUM, S., WESTRA, W. H., HOQUE, M. O., YANG, P., YI,

J. E., LAM, S., GAZDAR, A. F., FISHER, P. B., JEN, J. & SIDRANSKY, D. 2013. SH3GL2 is frequently deleted in non-small cell lung cancer and downregulates tumor growth by modulating EGFR signaling. *J Mol Med (Berl),* 91**,** 381-93.

DE SOUSA ABREU, R., PENALVA, L. O., MARCOTTE, E. M. & VOGEL, C. 2009. Global signatures of protein and mRNA expression levels. *Mol Biosyst,* 5**,** 1512-26.

DERBY, H. 1874. On the Atropine Treatment of Acquired and Progressive Myopia. *Trans Am Ophthalmol Soc,* 2**,** 139-54.

DOHERTY, G. J. & MCMAHON, H. T. 2008. Mediation, modulation, and consequences of membrane-cytoskeleton interactions. *Annu Rev Biophys,* 37**,** 65-95.

DOLGIN, E. 2015. The myopia boom. *Nature,* 519**,** 276-8.

DOMON, B. 2012. Considerations on selected reaction monitoring experiments: implications for the selectivity and accuracy of measurements. *Proteomics Clin Appl,* 6**,** 609-14.

DONG, J., FELDMANN, G., HUANG, J., WU, S., ZHANG, N., COMERFORD, S. A., GAYYED, M. F., ANDERS, R. A., MAITRA, A. & PAN, D. 2007. Elucidation of a universal size-control mechanism in Drosophila and mammals. *Cell,* 130**,** 1120-33.

DUESTER, G. 2008. Retinoic acid synthesis and signaling during early organogenesis. *Cell,* 134**,** 921-31.

EDWARDS, M. H., LI, R. W., LAM, C. S., LEW, J. K. & YU, B. S. 2002. The Hong Kong progressive lens myopia control study: study design and main findings. *Invest Ophthalmol Vis Sci,* 43**,** 2852-8.

FELDKAEMPER, M. & SCHAEFFEL, F. 2013. An updated view on the role of dopamine in myopia. *Exp Eye Res,* 114**,** 106-19.

FERGUSON, S. M. & DE CAMILLI, P. 2012. Dynamin, a membrane-remodelling GTPase. *Nat Rev Mol Cell Biol,* 13**,** 75-88.

FISCHER, A. J., MCGUIRE, J. J., SCHAEFFEL, F. & STELL, W. K. 1999. Light- and focus-dependent expression of the transcription factor ZENK in the chick retina. *Nat Neurosci,* 2**,** 706-12.

GALLEGO, P., MARTINEZ-GARCIA, C., PEREZ-MERINO, P., IBARES-FRIAS, L., MAYO-ISCAR, A. & MERAYO-LLOVES, J. 2012. Scleral changes induced by atropine in chicks as an experimental model of myopia. *Ophthalmic Physiol Opt,* 32**,** 478-84.

GALLETTA, B. J., CHUANG, D. Y. & COOPER, J. A. 2008. Distinct roles for Arp2/3 regulators in actin assembly and endocytosis. *PLoS Biol,* 6**,** e1.

GALVIS, V., TELLO, A., PARRA, M. M., MERAYO-LLOVES, J., LARREA, J., JULIAN RODRIGUEZ, C. & CAMACHO, P. A. 2016. Topical Atropine in the Control of Myopia. *Med Hypothesis Discov Innov Ophthalmol,* 5**,** 78-88.

GASS, J. D. M. 1973. Nicotinic-Acid Maculopathy. *American Journal of Ophthalmology,* 76**,** 500-510.

GENTLE, A., LIU, Y., MARTIN, J. E., CONTI, G. L. & MCBRIEN, N. A. 2003. Collagen gene expression and the altered accumulation of scleral collagen during the development of high myopia. *J Biol Chem,* 278**,** 16587-94.

GIMBEL, H. V. 1973. The control of myopia with atropine. *Can J Ophthalmol,* 8**,** 527-32.

GOLDBERG, A. F., MORITZ, O. L. & WILLIAMS, D. S. 2016. Molecular basis for photoreceptor outer segment architecture. *Prog Retin Eye Res,* 55**,** 52-81.

GOLEY, E. D. & WELCH, M. D. 2006. The ARP2/3 complex: an actin nucleator comes of age. *Nat Rev Mol Cell Biol,* 7**,** 713-26.

GORDON, E. M., FIGUEROA, D. M., BAROCHIA, A. V., YAO, X. & LEVINE, S. J. 2016. High-density Lipoproteins and Apolipoprotein A-I: Potential New Players in the Prevention and Treatment of Lung Disease. *Front Pharmacol,* 7**,** 323.

GORDON, R. A. & DONZIS, P. B. 1985. Refractive development of the human eye. *Arch Ophthalmol,* 103**,** 785-9.

GORSHKOVA, I. N., LIU, T., ZANNIS, V. I. & ATKINSON, D. 2002. Lipid-free structure and stability of apolipoprotein A-I: probing the central region by mutation. *Biochemistry,* 41**,** 10529-39.

GOSS, D. A. 1990. Variables related to the rate of childhood myopia progression. *Optom Vis Sci,* 67**,** 631-6.

GOSS, D. A. 2000. Nearwork and myopia. *Lancet,* 356**,** 1456-7.

GRAHAM, B. & JUDGE, S. J. 1999a. The effects of spectacle wear in infancy on eye growth and refractive error in the marmoset (Callithrix jacchus). *Vision Res,* 39**,** 189-206.

GRAHAM, B. & JUDGE, S. J. 1999b. Normal development of refractive state and ocular component dimensions in the marmoset (Callithrix jacchus). *Vision Res,* 39**,** 177-87.

GREENE, P. R. & MEDINA, A. 2016. The Progression of Nearwork Myopia. *Optom Open Access,* 1.

GRZESCHIK, N. A. & KNUST, E. 2005. IrreC/rst-mediated cell sorting during Drosophila pupal eye development depends on proper localisation of DE-cadherin. *Development,* 132**,** 2035-45.

GRZESCHIK, N. A., PARSONS, L. M., ALLOTT, M. L., HARVEY, K. F. & RICHARDSON, H. E. 2010. Lgl, aPKC, and Crumbs regulate the Salvador/Warts/Hippo pathway through two distinct mechanisms. *Curr Biol,* 20**,** 573-81.

GUO, S. S., SIVAK, J. G., CALLENDER, M. G. & DIEHL-JONES, B. 1995. Retinal dopamine and lens-induced refractive errors in chicks. *Curr Eye Res,* 14**,** 385-9.

GUO, X. & CHEN, S. Y. 2012. Transforming growth factor-beta and smooth muscle differentiation. *World J Biol Chem,* 3**,** 41-52.

GWIAZDA, J., THORN, F., BAUER, J. & HELD, R. 1993. Myopic children show insufficient accommodative response to blur. *Invest Ophthalmol Vis Sci,* 34**,** 690-4.

GWIAZDA, J., THORN, F. & HELD, R. 2005. Accommodation, accommodative convergence, and response AC/A ratios before and at the onset of myopia in children. *Optom Vis Sci,* 82**,** 273-8.

GWIAZDA, J. E., HYMAN, L., NORTON, T. T., HUSSEIN, M. E., MARSH-TOOTLE, W., MANNY, R., WANG, Y., EVERETT, D. & GROUUP, C. 2004. Accommodation and related risk factors associated with myopia progression and their interaction with treatment in COMET children. *Invest Ophthalmol Vis Sci,* 45**,** 2143-51.

HASAN, R. N., PHUKAN, S. & HARADA, S. 2003. Differential regulation of early growth response gene-1 expression by insulin and glucose in vascular endothelial cells. *Arterioscler Thromb Vasc Biol,* 23**,** 988-93.

HE, M., ZENG, J., LIU, Y., XU, J., POKHAREL, G. P. & ELLWEIN, L. B. 2004. Refractive error and visual impairment in urban children in southern china. *Invest Ophthalmol Vis Sci,* 45**,** 793-9.

HEIDENREICH, K. A. & TOLEDO, S. P. 1989. Insulin receptors mediate growth effects in cultured fetal neurons. II. Activation of a protein kinase that phosphorylates ribosomal protein S6. *Endocrinology,* 125**,** 1458-63.

HELLER, M., MATTOU, H., MENZEL, C. & YAO, X. 2003. Trypsin catalyzed 16 O-to-18 O exchange for comparative proteomics: tandem mass spectrometry comparison using MALDI-TOF, ESI-QTOF, and ESI-ion trap mass spectrometers. *Journal of the American Society for Mass Spectrometry,* 14**,** 704-718.

HEPSEN, I. F., EVEREKLIOGLU, C. & BAYRAMLAR, H. 2001. The effect of reading and near-work on the development of myopia in emmetropic boys: a prospective, controlled, three-year follow-up study. *Vision Res,* 41**,** 2511-20.

HIRANO, S. 2012. Western blot analysis. *Methods Mol Biol,* 926**,** 87-97.

HIRAOKA, T., KAKITA, T., OKAMOTO, F., TAKAHASHI, H. & OSHIKA, T. 2012. Long-term effect of overnight orthokeratology on axial length elongation in childhood myopia: a 5-year follow-up study. *Invest Ophthalmol Vis Sci,* 53**,** 3913-9.

HNASKO, T. S. & HNASKO, R. M. 2015. The Western Blot. *Methods Mol Biol,* 1318**,** 87-96.

HODOS, W. 1990. Avian models of experimental myopia: environmental factors in the regulation of eye growth. *Ciba Found Symp,* 155**,** 149-56; discussion 156-9.

HOFFMAN, R. M., MII, S., DUONG, J. & AMOH, Y. 2018. Nerve Growth and Interaction in Gelfoam((R)) Histoculture: A Nervous System Organoid. *Methods Mol Biol,* 1760**,** 163-186.

HOLDEN, B. A., FRICKE, T. R., WILSON, D. A., JONG, M., NAIDOO, K. S., SANKARIDURG, P., WONG, T. Y., NADUVILATH, T. J. & RESNIKOFF, S. 2016. Global Prevalence of Myopia and High Myopia and Temporal Trends from 2000 through 2050. *Ophthalmology,* 123**,** 1036-42.

HONDA, S., FUJII, S., SEKIYA, Y. & YAMAMOTO, M. 1996. Retinal control on the axial length mediated by transforming growth factor-beta in chick eye. *Invest Ophthalmol Vis Sci,* 37**,** 2519-26.

HOSSEINI, H. S., BEEBE, D. C. & TABER, L. A. 2014. Mechanical effects of the surface ectoderm on optic vesicle morphogenesis in the chick embryo. *J Biomech,* 47**,** 3837-46.

HOSSEINI, H. S. & TABER, L. A. 2018. How mechanical forces shape the developing eye. *Prog Biophys Mol Biol,* 137**,** 25-36.

HOWLETT, M. H. & MCFADDEN, S. A. 2006. Form-deprivation myopia in the guinea pig (Cavia porcellus). *Vision Res,* 46**,** 267-83.

HOWLETT, M. H. & MCFADDEN, S. A. 2009. Spectacle lens compensation in the pigmented guinea pig. *Vision Res,* 49**,** 219-27.

HUA, W. J., JIN, J. X., WU, X. Y., YANG, J. W., JIANG, X., GAO, G. P. & TAO, F. B. 2015. Elevated light levels in schools have a protective effect on myopia. *Ophthalmic Physiol Opt,* 35**,** 252-62.

HUANG, F. & CHEN, Y. G. 2012. Regulation of TGF-beta receptor activity. *Cell Biosci,* 2**,** 9.

HUANG, Y., KEE, C. S., HOCKING, P. M., WILLIAMS, C., YIP, S. P., GUGGENHEIM, J. A., EYE, U. K. B., VISION, C. & THE, C. C. 2019. A Genome-Wide Association Study for Susceptibility to Visual Experience-Induced Myopia. *Invest Ophthalmol Vis Sci,* 60**,** 559-569.

HUMBERT, P. O., GRZESCHIK, N. A., BRUMBY, A. M., GALEA, R., ELSUM, I. & RICHARDSON, H. E. 2008. Control of tumourigenesis by the Scribble/Dlg/Lgl polarity module. *Oncogene,* 27**,** 6888-907.

HUNG, L. F., ARUMUGAM, B., OSTRIN, L., PATEL, N., TRIER, K., JONG, M. & SMITH, E. L., III 2018. The Adenosine Receptor Antagonist, 7-Methylxanthine, Alters Emmetropizing Responses in Infant Macaques. *Invest Ophthalmol Vis Sci,* 59**,** 472-486.

HUNG, L. F., CRAWFORD, M. L. & SMITH, E. L. 1995. Spectacle lenses alter eye growth and the refractive status of young monkeys. *Nat Med,* 1**,** 761-5.

HUO, L., CUI, D., YANG, X., GAO, Z., TRIER, K. & ZENG, J. 2013. All-trans retinoic acid modulates mitogen-activated protein kinase pathway activation in human scleral fibroblasts through retinoic acid receptor beta. *Mol Vis,* 19**,** 1795-803.

IP, J. M., HUYNH, S. C., ROBAEI, D., ROSE, K. A., MORGAN, I. G., SMITH, W., KIFLEY, A. & MITCHELL, P. 2007. Ethnic differences in the impact of parental myopia: findings from a population-based study of 12-year-old Australian children. *Invest Ophthalmol Vis Sci,* 48**,** 2520-8.

IP, J. M., ROSE, K. A., MORGAN, I. G., BURLUTSKY, G. & MITCHELL, P. 2008a. Myopia and the urban environment: findings in a sample of 12-year-old Australian school children. *Invest Ophthalmol Vis Sci,* 49**,** 3858-63.

IP, J. M., SAW, S. M., ROSE, K. A., MORGAN, I. G., KIFLEY, A., WANG, J. J. & MITCHELL, P. 2008b. Role of near work in myopia: findings in a sample of Australian school children. *Invest Ophthalmol Vis Sci,* 49**,** 2903-10.

IRVING, E. L., SIVAK, J. G. & CALLENDER, M. G. 1992. Refractive Plasticity of the Developing Chick Eye. *Ophthalmic and Physiological Optics,* 12**,** 448-456.

IUVONE, P. M., TIGGES, M., STONE, R. A., LAMBERT, S. & LATIES, A. M. 1991. Effects of apomorphine, a dopamine receptor agonist, on ocular refraction and axial elongation in a primate model of myopia. *Invest Ophthalmol Vis Sci,* 32**,** 1674-7.

JAYAKUMAR, A., CHIRALA, S. S., CHINAULT, A. C., BALDINI, A., ABU-ELHEIGA, L. & WAKIL, S. J. 1994. Isolation and chromosomal mapping of genomic clones encoding the human fatty acid synthase gene. *Genomics,* 23**,** 420-4.

JAYAKUMAR, A., TAI, M. H., HUANG, W. Y., AL-FEEL, W., HSU, M., ABU-ELHEIGA, L., CHIRALA, S. S. & WAKIL, S. J. 1995. Human fatty acid synthase: properties and molecular cloning. *Proc Natl Acad Sci U S A,* 92**,** 8695-9.

JIANG, L., ZHANG, S., SCHAEFFEL, F., XIONG, S., ZHENG, Y., ZHOU, X., LU, F. & QU, J. 2014. Interactions of chromatic and lens-induced defocus during visual control of eye growth in guinea pigs (Cavia porcellus). *Vision Res,* 94**,** 24-32.

JIN, F. Y., KAMANNA, V. S. & KASHYAP, M. L. 1997. Niacin decreases removal of high-density lipoprotein apolipoprotein A-I but not

cholesterol ester by Hep G2 cells. Implication for reverse cholesterol transport. *Arterioscler Thromb Vasc Biol,* 17**,** 2020-8.

JOBLING, A. I., WAN, R., GENTLE, A., BUI, B. V. & MCBRIEN, N. A. 2009. Retinal and choroidal TGF-beta in the tree shrew model of myopia: isoform expression, activation and effects on function. *Exp Eye Res,* 88**,** 458-66.

JONES, D. & LUENSMANN, D. 2012. The prevalence and impact of high myopia. *Eye Contact Lens,* 38**,** 188-96.

JONES, L. A., MITCHELL, G. L., MUTTI, D. O., HAYES, J. R., MOESCHBERGER, M. L. & ZADNIK, K. 2005. Comparison of ocular component growth curves among refractive error groups in children. *Invest Ophthalmol Vis Sci,* 46**,** 2317-27.

JONES, L. A., SINNOTT, L. T., MUTTI, D. O., MITCHELL, G. L., MOESCHBERGER, M. L. & ZADNIK, K. 2007. Parental history of myopia, sports and outdoor activities, and future myopia. *Invest Ophthalmol Vis Sci,* 48**,** 3524-32.

KAKITA, T., HIRAOKA, T. & OSHIKA, T. 2011. Influence of overnight orthokeratology on axial elongation in childhood myopia. *Invest Ophthalmol Vis Sci,* 52**,** 2170-4.

KANG, P. & SWARBRICK, H. 2011. Peripheral refraction in myopic children wearing orthokeratology and gas-permeable lenses. *Optom Vis Sci,* 88**,** 476-82.

KAWSKA, A., CARVALHO, K., MANZI, J., BOUJEMAA-PATERSKI, R., BLANCHOIN, L., MARTIEL, J. L. & SYKES, C. 2012. How actin network dynamics control the onset of actin-based motility. *Proc Natl Acad Sci U S A,* 109**,** 14440-5.

KILBOURNE, E. J., WIDOM, R., HARNISH, D. C., MALIK, S. & KARATHANASIS, S. K. 1995. Involvement of early growth response factor Egr-1 in apolipoprotein AI gene transcription. *J Biol Chem,* 270**,** 7004-10.

KIM, B. 2017. Western Blot Techniques. *Methods Mol Biol,* 1606**,** 133-139.

KINOSHITA, N., KONNO, Y., HAMADA, N., KANDA, Y., SHIMMURA-TOMITA, M. & KAKEHASHI, A. 2018. Additive effects of orthokeratology and atropine 0.01% ophthalmic solution in slowing axial elongation in children with myopia: first year results. *Jpn J Ophthalmol,* 62**,** 544-553.

KNAPSKA, E. & KACZMAREK, L. 2004. A gene for neuronal plasticity in the mammalian brain: Zif268/Egr-1/NGFI-A/Krox-24/TIS8/ZENK? *Prog Neurobiol,* 74**,** 183-211.

KNIP, M., DOUEK, I. F., MOORE, W. P. T., GILLMOR, H. A., MCLEAN, A. E. M., BINGLEY, P. J., GALE, E. A. M. & GRP, E. 2000. Safety of high dose nicotinamide: a review. *Diabetologia,* 43**,** 1337-1345.

KOUSSOUNADIS, A., LANGDON, S. P., UM, I. H., HARRISON, D. J. & SMITH, V. A. 2015. Relationship between differentially expressed mRNA and mRNA-protein correlations in a xenograft model system. *Sci Rep,* 5**,** 10775.

LAM, C. S., TANG, W. C., TSE, D. Y., TANG, Y. Y. & TO, C. H. 2014. Defocus Incorporated Soft Contact (DISC) lens slows myopia progression in Hong Kong Chinese schoolchildren: a 2-year randomised clinical trial. *Br J Ophthalmol,* 98**,** 40-5.

LAM, C. S. & TO, C. H. 2017. a new spectacle lens for myopia control. *16th International Myopia Conference.* Blagoevgrad, Bulgaria.

LAM, T. C., LI, K. K., LO, S. C., GUGGENHEIM, J. A. & TO, C. H. 2006. A chick retinal proteome database and differential retinal protein expressions during early ocular development. *J Proteome Res,* 5**,** 771-84.

LAM, T. T., LANMAN, J. K., EMMETT, M. R., HENDRICKSON, C. L., MARSHALL, A. G. & PREVELIGE, P. E. 2002. Mapping of protein:protein contact surfaces by hydrogen/deuterium exchange, followed by on-line high-performance liquid chromatography-electrospray ionization Fourier-transform ion-cyclotron-resonance mass analysis. *J Chromatogr A,* 982**,** 85-95.

LEE, Y., KIM, D., RYU, J. R., ZHANG, Y., KIM, S., KIM, Y., LEE, B., SUN, W. & HAN, K. 2017. Phosphorylation of CYFIP2, a

component of the WAVE-regulatory complex, regulates dendritic spine density and neurite outgrowth in cultured hippocampal neurons potentially by affecting the complex assembly. *Neuroreport,* 28**,** 749-754.

LESKE, M. C., CHYLACK, L. T., JR. & WU, S. Y. 1991. The Lens Opacities Case-Control Study. Risk factors for cataract. *Arch Ophthalmol,* 109**,** 244-51.

LEUNG, J. T. & BROWN, B. 1999. Progression of myopia in Hong Kong Chinese schoolchildren is slowed by wearing progressive lenses. *Optom Vis Sci,* 76**,** 346-54.

LI, M., YUAN, Y., CHEN, Q., ME, R., GU, Q., YU, Y., SHENG, M. & KE, B. 2016. Expression of Wnt/beta-Catenin Signaling Pathway and Its Regulatory Role in Type I Collagen with TGF-beta1 in Scleral Fibroblasts from an Experimentally Induced Myopia Guinea Pig Model. *J Ophthalmol,* 2016**,** 5126560.

LI, S. M., JI, Y. Z., WU, S. S., ZHAN, S. Y., WANG, B., LIU, L. R., LI, S. Y., WANG, N. L. & WANG, J. J. 2011. Multifocal versus single vision lenses intervention to slow progression of myopia in school-age children: a meta-analysis. *Surv Ophthalmol,* 56**,** 451-60.

LI, X. X., SCHAEFFEL, F., KOHLER, K. & ZRENNER, E. 1992. Dose-dependent effects of 6-hydroxy dopamine on deprivation myopia,

electroretinograms, and dopaminergic amacrine cells in chickens. *Vis Neurosci,* 9**,** 483-92.

LINDSEY, S. & LANGHANS, S. A. 2015. Epidermal growth factor signaling in transformed cells. *Int Rev Cell Mol Biol,* 314**,** 1-41.

LIPSON, M. J., BROOKS, M. M. & KOFFLER, B. H. 2018. The Role of Orthokeratology in Myopia Control: A Review. *Eye Contact Lens,* 44**,** 224-230.

LIU, H. H., XU, L., WANG, Y. X., WANG, S., YOU, Q. S. & JONAS, J. B. 2010. Prevalence and progression of myopic retinopathy in Chinese adults: the Beijing Eye Study. *Ophthalmology,* 117**,** 1763-8.

LIU, J., LI, X. D., ORA, A., HEIKKILA, P., VAHERI, A. & VOUTILAINEN, R. 2004. cAMP-dependent protein kinase activation inhibits proliferation and enhances apoptotic effect of tumor necrosis factor-alpha in NCI-H295R adrenocortical cells. *J Mol Endocrinol,* 33**,** 511-22.

LIU, L., LI, C., FU, C. & LI, F. 2016. Dietary Niacin Supplementation Suppressed Hepatic Lipid Accumulation in Rabbits. *Asian-Australas J Anim Sci,* 29**,** 1748-1755.

LIU, R., QIAN, Y. F., HE, J. C., HU, M., ZHOU, X. T., DAI, J. H., QU, X. M. & CHU, R. Y. 2011. Effects of different monochromatic lights on refractive development and eye growth in guinea pigs. *Exp Eye Res,* 92**,** 447-53.

LIU, Y. & WILDSOET, C. 2011. The effect of two-zone concentric bifocal spectacle lenses on refractive error development and eye growth in young chicks. *Invest Ophthalmol Vis Sci,* 52**,** 1078-86.

LIU, Z. Q., MAHMOOD, T. & YANG, P. C. 2014. Western blot: technique, theory and trouble shooting. *N Am J Med Sci,* 6**,** 160.

LIVANOVA, N. B., CHEBOTAREVA, N. A., ERONINA, T. B. & KURGANOV, B. I. 2002. Pyridoxal 5'-phosphate as a catalytic and conformational cofactor of muscle glycogen phosphorylase B. *Biochemistry (Mosc),* 67**,** 1089-98.

LU, H. & BILDER, D. 2005. Endocytic control of epithelial polarity and proliferation in Drosophila. *Nat Cell Biol,* 7**,** 1232-9.

MA, M., ZHANG, Z., DU, E., ZHENG, W., GU, Q., XU, X. & KE, B. 2014. Wnt signaling in form deprivation myopia of the mice retina. *PLoS One,* 9**,** e91086.

MAHMOOD, T. & YANG, P. C. 2012. Western blot: technique, theory, and trouble shooting. *N Am J Med Sci,* 4**,** 429-34.

MAIER, T., GUELL, M. & SERRANO, L. 2009. Correlation of mRNA and protein in complex biological samples. *FEBS Lett,* 583**,** 3966-73.

MAIMONE, P. E. 2008. Green light in the development of myopia. *Med Hypotheses,* 71**,** 149.

MANGARAJ, M., NANDA, R. & PANDA, S. 2016. Apolipoprotein A-I: A Molecule of Diverse Function. *Indian J Clin Biochem,* 31**,** 253-9.

MAO, J., LIU, S., QIN, W., LI, F., WU, X. & TAN, Q. 2010a. Levodopa inhibits the development of form-deprivation myopia in guinea pigs. *Optom Vis Sci,* 87**,** 53-60.

MAO, J. F., LIU, S. Z., QIN, W. J., LI, F. Y., WU, X. Y. & TAN, Q. 2010b. Levodopa Inhibits the Development of Form-Deprivation Myopia in Guinea Pigs. *Optometry and Vision Science,* 87**,** 53-60.

MATESIC, D. F. & LUTHIN, G. R. 1991. Atropine dissociates complexes of muscarinic acetylcholine receptor and guanine nucleotide-binding protein in heart membranes. *FEBS Lett,* 284**,** 184-6.

MATHIS, U. & SCHAEFFEL, F. 2007. Glucagon-related peptides in the mouse retina and the effects of deprivation of form vision. *Graefes Arch Clin Exp Ophthalmol,* 245**,** 267-75.

MAYER, D. L., HANSEN, R. M., MOORE, B. D., KIM, S. & FULTON, A. B. 2001. Cycloplegic refractions in healthy children aged 1 through 48 months. *Arch Ophthalmol,* 119**,** 1625-8.

MCBRIEN, N. A., MOGHADDAM, H. O. & REEDER, A. P. 1993. Atropine reduces experimental myopia and eye enlargement via a nonaccommodative mechanism. *Invest Ophthalmol Vis Sci,* 34**,** 205-15.

MCBRIEN, N. A. & NORTON, T. T. 1992. The development of experimental myopia and ocular component dimensions in

monocularly lid-sutured tree shrews (Tupaia belangeri). *Vision Res,* 32**,** 843-52.

MCFADDEN, S. & WALLMAN, J. 1995a. Guinea-Pig Eye Growth Compensates for Spectacle Lenses. *Investigative Ophthalmology & Visual Science,* 36**,** S758-S758.

MCFADDEN, S. & WALLMAN, J. Guinea-pig eye growth compensates for spectacle lenses. Investigative Ophthalmology & Visual Science, 1995b. LIPPINCOTT-RAVEN PUBL 227 EAST WASHINGTON SQUARE, PHILADELPHIA, PA 19106, S758-S758.

MCFADDEN, S. A., HOWLETT, M. H. & MERTZ, J. R. 2004a. Retinoic acid signals the direction of ocular elongation in the guinea pig eye. *Vision Research,* 44**,** 643-53.

MCFADDEN, S. A., HOWLETT, M. H. & MERTZ, J. R. 2004b. Retinoic acid signals the direction of ocular elongation in the guinea pig eye. *Vision Res,* 44**,** 643-53.

MEGAW, P. L., BOELEN, M. G., MORGAN, I. G. & BOELEN, M. K. 2006. Diurnal patterns of dopamine release in chicken retina. *Neurochem Int,* 48**,** 17-23.

MENEZO, J. L., SALINAS, E., AVINO, J. A., NAVEA, A. & CISNEROS, A. 1999. Posterior chamber silicone intraocular lens for the

correction of myopia: an experimental study in rabbits. *Eur J Ophthalmol,* 9**,** 276-83.

MENG, W., BUTTERWORTH, J., MALECAZE, F. & CALVAS, P. 2011. Axial length of myopia: a review of current research. *Ophthalmologica,* 225**,** 127-34.

MERTZ, J. R. & WALLMAN, J. 2000. Choroidal retinoic acid synthesis: a possible mediator between refractive error and compensatory eye growth. *Exp Eye Res,* 70**,** 519-27.

MILL, J. F., CHAO, M. V. & ISHII, D. N. 1985. Insulin, insulin-like growth factor II, and nerve growth factor effects on tubulin mRNA levels and neurite formation. *Proc Natl Acad Sci U S A,* 82**,** 7126-30.

MORGAN, I. G. 2003. The biological basis of myopic refractive error. *Clinical and Experimental Optometry,* 86**,** 276-88.

MORGAN, I. G., ASHBY, R. S. & NICKLA, D. L. 2013. Form deprivation and lens-induced myopia: are they different? *Ophthalmic Physiol Opt,* 33**,** 355-61.

MORGAN, I. G., FRENCH, A. N., ASHBY, R. S., GUO, X., DING, X., HE, M. & ROSE, K. A. 2018. The epidemics of myopia: Aetiology and prevention. *Prog Retin Eye Res,* 62**,** 134-149.

MORGAN, I. G., HE, M. & ROSE, K. A. 2017. EPIDEMIC OF PATHOLOGIC MYOPIA: What Can Laboratory Studies and Epidemiology Tell Us? *Retina,* 37**,** 989-997.

MORGAN, I. G., OHNO-MATSUI, K. & SAW, S. M. 2012. Myopia. *Lancet,* 379**,** 1739-48.

MORRIS, V. B., WYLIE, C. C. & MILES, V. J. 1976. The growth of the chick retina after hatching. *Anat Rec,* 184**,** 111-3.

MURPHY, M. J. & CREWTHER, S. G. 2013. Ouabain inhibition of Na/K-ATPase across the retina prevents signed refractive compensation to lens-induced defocus, but not default ocular growth in young chicks. *F1000Res,* 2**,** 97.

MUTTI, D. O. 2014. Vitamin D may reduce the prevalence of myopia in Korean adolescents. *Invest Ophthalmol Vis Sci,* 55**,** 2048.

MUTTI, D. O., MITCHELL, G. L., MOESCHBERGER, M. L., JONES, L. A. & ZADNIK, K. 2002. Parental myopia, near work, school achievement, and children's refractive error. *Invest Ophthalmol Vis Sci,* 43**,** 3633-40.

NAGAI, T., TOMIZAWA, T., NAKAJIMA, K. & MORI, M. 2000. Effect of bezafibrate or pravastatin on serum lipid levels and albuminuria in NIDDM patients. *J Atheroscler Thromb,* 7**,** 91-6.

NICKLA, D. L., YUSUPOVA, Y. & TOTONELLY, K. 2015. The Muscarinic Antagonist MT3 Distinguishes Between Form Deprivation- and Negative Lens-Induced Myopia in Chicks. *Curr Eye Res,* 40**,** 962-7.

NICKLA, D. L., ZHU, X. & WALLMAN, J. 2013. Effects of muscarinic agents on chick choroids in intact eyes and eyecups: evidence for a muscarinic mechanism in choroidal thinning. *Ophthalmic Physiol Opt,* 33**,** 245-56.

NIESSEN, W. M. 2006. *Liquid chromatography-mass spectrometry*, CRC press.

NITTA, K., SUGIYAMA, K., WAJIMA, R. & TACHIBANA, G. 2017. Is high myopia a risk factor for visual field progression or disk hemorrhage in primary open-angle glaucoma? *Clin Ophthalmol,* 11**,** 599-604.

NORTH, R. V. & KELLY, M. E. 1987. A review of the uses and adverse effects of topical administration of atropine. *Ophthalmic Physiol Opt,* 7**,** 109-14.

NORTON, T. T. 1990. Experimental myopia in tree shrews. *Ciba Found Symp,* 155**,** 178-94; discussion 194-9.

NORTON, T. T. 1999. Animal Models of Myopia: Learning How Vision Controls the Size of the Eye. *ILAR J,* 40**,** 59-77.

OPHTHALMOLOGY, A. A. O. 2016-2017. *Fundamentals and Principles of Ophthalmology*, American Academy of Ophthalmology.

OSORIO, D., VOROBYEV, M. & JONES, C. D. 1999. Colour vision of domestic chicks. *Journal of Experimental Biology,* 202**,** 2951-2959.

OSTLUND, G. & SONNHAMMER, E. L. 2012. Quality criteria for finding genes with high mRNA-protein expression correlation and coexpression correlation. *Gene,* 497**,** 228-36.

OTTERBEIN, L. R., GRACEFFA, P. & DOMINGUEZ, R. 2001. The crystal structure of uncomplexed actin in the ADP state. *Science,* 293**,** 708-11.

OVER, R. & MOORE, D. 1981. Spatial Acuity of the Chicken. *Brain Research,* 211**,** 424-426.

PALM, D. C., ROHWER, J. M. & HOFMEYR, J. H. 2013. Regulation of glycogen synthase from mammalian skeletal muscle--a unifying view of allosteric and covalent regulation. *FEBS J,* 280**,** 2-27.

PAPASTERGIOU, G. I., SCHMID, G. F., LATIES, A. M., PENDRAK, K., LIN, T. & STONE, R. A. 1998. Induction of axial eye elongation and myopic refractive shift in one-year-old chickens. *Vision Res,* 38**,** 1883-8.

PARITSIS, N., SARAFIDOU, E., KOLIOPOULOS, J. & TRICHOPOULOS, D. 1983. Epidemiologic research on the role of studying and urban environment in the development of myopia during school-age years. *Ann Ophthalmol,* 15**,** 1061-5.

PARSONS, W. B., JR. & FLINN, J. H. 1959. Reduction of serum cholesterol levels and beta-lipoprotein cholesterol levels by nicotinic acid. *AMA Arch Intern Med,* 103**,** 783-90.

PARSSINEN, O., KAUPPINEN, M., HALEKOH, U., KAPRIO, J. & RANTANEN, T. 2019. Heredity of interocular similarities in components of refraction: a population-based twin study among 66- to 79-year-old female twins. *Acta Ophthalmol*.

PENDRAK, K., NGUYEN, T., LIN, T., CAPEHART, C., ZHU, X. & STONE, R. A. 1997. Retinal dopamine in the recovery from experimental myopia. *Curr Eye Res,* 16**,** 152-7.

PENHA, A. M., BURKHARDT, E., SCHAEFFEL, F. & FELDKAEMPER, M. P. 2012. Effects of intravitreal insulin and insulin signaling cascade inhibitors on emmetropization in the chick. *Mol Vis,* 18**,** 2608-22.

PITT, J. J. 2009. Principles and applications of liquid chromatography-mass spectrometry in clinical biochemistry. *Clin Biochem Rev,* 30**,** 19-34.

PURO, D. G. & AGARDH, E. 1984. Insulin-mediated regulation of neuronal maturation. *Science,* 225**,** 1170-2.

QUEIROS, A., GONZALEZ-MEIJOME, J. M., JORGE, J., VILLA-COLLAR, C. & GUTIERREZ, A. R. 2010. Peripheral refraction in myopic patients after orthokeratology. *Optom Vis Sci,* 87**,** 323-9.

RADA, J. A. & BRENZA, H. L. 1995. Increased latent gelatinase activity in the sclera of visually deprived chicks. *Invest Ophthalmol Vis Sci,* 36**,** 1555-65.

RAVIOLA, E. & WIESEL, T. N. 1978. Effect of dark-rearing on experimental myopia in monkeys. *Invest Ophthalmol Vis Sci,* 17**,** 485-8.

RAVIOLA, E. & WIESEL, T. N. 1990. Neural control of eye growth and experimental myopia in primates. *Ciba Found Symp,* 155**,** 22-38; discussion 39-44.

ROBINSON, B. S., HUANG, J., HONG, Y. & MOBERG, K. H. 2010. Crumbs regulates Salvador/Warts/Hippo signaling in Drosophila via the FERM-domain protein Expanded. *Curr Biol,* 20**,** 582-90.

RODRIGUEZ, J., GUPTA, N., SMITH, R. D. & PEVZNER, P. A. 2008. Does trypsin cut before proline? *J Proteome Res,* 7**,** 300-5.

ROGERS, D. P., ROBERTS, L. M., LEBOWITZ, J., DATTA, G., ANANTHARAMAIAH, G. M., ENGLER, J. A. & BROUILLETTE, C. G. 1998. The lipid-free structure of apolipoprotein A-I: effects of amino-terminal deletions. *Biochemistry,* 37**,** 11714-25.

ROHRER, B. & STELL, W. K. 1994. Basic fibroblast growth factor (bFGF) and transforming growth factor beta (TGF-beta) act as stop and go signals to modulate postnatal ocular growth in the chick. *Experimental Eye Research,* 58**,** 553-61.

ROSE, K. A., MORGAN, I. G., IP, J., KIFLEY, A., HUYNH, S., SMITH, W. & MITCHELL, P. 2008. Outdoor activity reduces the prevalence of myopia in children. *Ophthalmology,* 115**,** 1279-85.

RUCKER, F. J. & WALLMAN, J. 2009. Chick eyes compensate for chromatic simulations of hyperopic and myopic defocus: evidence that the eye uses longitudinal chromatic aberration to guide eye-growth. *Vision Res,* 49**,** 1775-83.

RUDNICKA, A. R., OWEN, C. G., RICHARDS, M., WADSWORTH, M. E. & STRACHAN, D. P. 2008. Effect of breastfeeding and sociodemographic factors on visual outcome in childhood and adolescence. *Am J Clin Nutr,* 87**,** 1392-9.

SANKARIDURG, P., CONRAD, F., TRAN, H. & ZHU, J. 2018. Controlling Progression of Myopia: Optical and Pharmaceutical Strategies. *Asia Pac J Ophthalmol (Phila),* 7**,** 405-414.

SANKARIDURG, P., DONOVAN, L., VARNAS, S., HO, A., CHEN, X., MARTINEZ, A., FISHER, S., LIN, Z., SMITH, E. L., 3RD, GE, J. & HOLDEN, B. 2010. Spectacle lenses designed to reduce progression of myopia: 12-month results. *Optom Vis Sci,* 87**,** 631-41.

SAW, S. M. 2006. How blinding is pathological myopia? *Br J Ophthalmol,* 90**,** 525-6.

SAW, S. M., CHUA, W. H., HONG, C. Y., WU, H. M., CHAN, W. Y., CHIA, K. S., STONE, R. A. & TAN, D. 2002. Nearwork in early-onset myopia. *Invest Ophthalmol Vis Sci,* 43**,** 332-9.

SCHAEFFEL, F., BARTMANN, M., HAGEL, G. & ZRENNER, E. 1995. Studies on the role of the retinal dopamine/melatonin system in experimental refractive errors in chickens. *Vision Res,* 35**,** 1247-64.

SCHAEFFEL, F., BURKHARDT, E., HOWLAND, H. C. & WILLIAMS, R. W. 2004. Measurement of refractive state and deprivation myopia in two strains of mice. *Optom Vis Sci,* 81**,** 99-110.

SCHAEFFEL, F. & FELDKAEMPER, M. 2015. Animal models in myopia research. *Clin Exp Optom,* 98**,** 507-17.

SCHAEFFEL, F., GLASSER, A. & HOWLAND, H. C. 1988. Accommodation, refractive error and eye growth in chickens. *Vision Res,* 28**,** 639-57.

SCHAEFFEL, F., TROILO, D., WALLMAN, J. & HOWLAND, H. C. 1990. Developing eyes that lack accommodation grow to compensate for imposed defocus. *Vis Neurosci,* 4**,** 177-83.

SCHIPPERT, R., BURKHARDT, E., FELDKAEMPER, M. & SCHAEFFEL, F. 2007. Relative axial myopia in Egr-1 (ZENK) knockout mice. *Invest Ophthalmol Vis Sci,* 48**,** 11-7.

SCHLIERF, B., FEY, G. H., HAUBER, J., HOCKE, G. M. & ROSORIUS, O. 2000. Rab11b is essential for recycling of transferrin to the plasma membrane. *Exp Cell Res,* 259**,** 257-65.

SCHMID, K. L. & WILDSOET, C. F. 1997. The sensitivity of the chick eye to refractive defocus. *Ophthalmic and Physiological Optics,* 17**,** 61-67.

SCHMUCKER, C. & SCHAEFFEL, F. 2004. In vivo biometry in the mouse eye with low coherence interferometry. *Vision Res,* 44**,** 2445-56.

SEIDEMANN, A. & SCHAEFFEL, F. 2002. Effects of longitudinal chromatic aberration on accommodation and emmetropization. *Vision Res,* 42**,** 2409-17.

SEIDEMANN, A. & SCHAEFFEL, F. 2003. An evaluation of the lag of accommodation using photorefraction. *Vision Res,* 43**,** 419-30.

SELDIN, M. F., MOTT, D., BHAT, D., PETRO, A., KUHN, C. M., KINGSMORE, S. F., BOGARDUS, C., OPARA, E., FEINGLOS, M. N. & SURWIT, R. S. 1994. Glycogen synthase: a putative locus for diet-induced hyperglycemia. *J Clin Invest,* 94**,** 269-76.

SHACKELFORD, J. E. & LEBHERZ, H. G. 1983. Synthesis and secretion of apolipoprotein A1 by chick breast muscle. *J Biol Chem,* 258**,** 7175-80.

SHAFARENKO, M., LIEBERMANN, D. A. & HOFFMAN, B. 2005. Egr-1 abrogates the block imparted by c-Myc on terminal M1 myeloid differentiation. *Blood,* 106**,** 871-8.

SHAIKH, A. W., SIEGWART, J. T., JR. & NORTON, T. T. 1999. Effect of interrupted lens wear on compensation for a minus lens in tree shrews. *Optom Vis Sci,* 76**,** 308-15.

SHAM, W. K., DIRANI, M., CHONG, Y. S., HORNBEAK, D. M., GAZZARD, G., LI, J. & SAW, S. M. 2010. Breastfeeding and association with refractive error in young Singapore Chinese children. *Eye (Lond),* 24**,** 875-80.

SHAN, S. W., TSE, D. Y., ZUO, B., TO, C. H., LIU, Q., MCFADDEN, S. A., CHUN, R. K., BIAN, J., LI, K. K. & LAM, T. C. 2018a. Data on differentially expressed proteins in retinal emmetropization process in guinea pig using integrated SWATH-based and targeted-based proteomics. *Data Brief,* 21**,** 1750-1755.

SHAN, S. W., TSE, D. Y., ZUO, B., TO, C. H., LIU, Q., MCFADDEN, S. A., CHUN, R. K., BIAN, J., LI, K. K. & LAM, T. C. 2018b. Integrated SWATH-based and targeted-based proteomics provide insights into the retinal emmetropization process in guinea pig. *J Proteomics,* 181**,** 1-15.

SHARMA, R., MAHAJAN, M., SINGH, B., BAL, B. S. & KANT, R. 2006. Apolipoprotein modifying effects of statins and fibrate in various

age groups of coronary artery disease patients. *J Indian Med Assoc,* 104**,** 492-4, 496, 498.

SHEN, W. & SIVAK, J. G. 2007. Eyes of a lower vertebrate are susceptible to the visual environment. *Invest Ophthalmol Vis Sci,* 48**,** 4829-37.

SHEN, W., VIJAYAN, M. & SIVAK, J. G. 2005. Inducing form-deprivation myopia in fish. *Invest Ophthalmol Vis Sci,* 46**,** 1797-803.

SHERMAN, S. M., NORTON, T. T. & CASAGRANDE, V. A. 1977. Myopia in the lid-sutured tree shrew (Tupaia glis). *Brain Res,* 124**,** 154-7.

SHIH, Y. F., CHEN, C. H., CHOU, A. C., HO, T. C., LIN, L. L. & HUNG, P. T. 1999. Effects of different concentrations of atropine on controlling myopia in myopic children. *J Ocul Pharmacol Ther,* 15**,** 85-90.

SIEGWART, J. T., JR. & NORTON, T. T. 2002. The time course of changes in mRNA levels in tree shrew sclera during induced myopia and recovery. *Invest Ophthalmol Vis Sci,* 43**,** 2067-75.

SIEGWART, J. T., JR. & NORTON, T. T. 2011. Perspective: how might emmetropization and genetic factors produce myopia in normal eyes? *Optom Vis Sci,* 88**,** E365-72.

SIMO, R., GARCIA-RAMIREZ, M., HIGUERA, M. & HERNANDEZ, C. 2009. Apolipoprotein A1 is overexpressed in the retina of diabetic patients. *Am J Ophthalmol,* 147**,** 319-325 e1.

SMITH, E. L., 3RD 2011. Prentice Award Lecture 2010: A case for peripheral optical treatment strategies for myopia. *Optom Vis Sci,* 88**,** 1029-44.

SMITH, E. L., 3RD, BRADLEY, D. V., FERNANDES, A. & BOOTHE, R. G. 1999. Form deprivation myopia in adolescent monkeys. *Optom Vis Sci,* 76**,** 428-32.

SMITH, E. L., 3RD, HUNG, L. F. & ARUMUGAM, B. 2014. Visual regulation of refractive development: insights from animal studies. *Eye (Lond),* 28**,** 180-8.

SMITH, E. L., 3RD, HUNG, L. F., ARUMUGAM, B. & HUANG, J. 2013. Negative lens-induced myopia in infant monkeys: effects of high ambient lighting. *Invest Ophthalmol Vis Sci,* 54**,** 2959-69.

SMITH, E. L., 3RD, HUNG, L. F. & HUANG, J. 2009. Relative peripheral hyperopic defocus alters central refractive development in infant monkeys. *Vision Res,* 49**,** 2386-92.

SMITH, E. L., 3RD, HUNG, L. F. & HUANG, J. 2012. Protective effects of high ambient lighting on the development of form-deprivation myopia in rhesus monkeys. *Invest Ophthalmol Vis Sci,* 53**,** 421-8.

SMITH, E. L., 3RD, KEE, C. S., RAMAMIRTHAM, R., QIAO-GRIDER, Y. & HUNG, L. F. 2005. Peripheral vision can influence eye growth and refractive development in infant monkeys. *Invest Ophthalmol Vis Sci,* 46**,** 3965-72.

SMITH, E. L., 3RD, RAMAMIRTHAM, R., QIAO-GRIDER, Y., HUNG, L. F., HUANG, J., KEE, C. S., COATS, D. & PAYSSE, E. 2007. Effects of foveal ablation on emmetropization and form-deprivation myopia. *Invest Ophthalmol Vis Sci,* 48**,** 3914-22.

SNYDER, L. R., KIRKLAND, J. J. & DOLAN, J. W. 2011. *Introduction to modern liquid chromatography*, John Wiley & Sons.

SOLER, M., ANERA, R. G., CASTRO, J. J., JIMENEZ, R. & JIMENEZ, J. R. 2015. Prevalence of refractive errors in children in Equatorial Guinea. *Optom Vis Sci,* 92**,** 53-8.

SORSBY, A. & FRASER, G. R. 1964. Statistical Note on the Components of Ocular Refraction in Twins. *J Med Genet,* 1**,** 47-9.

STONE, R. A., LIN, T., LATIES, A. M. & IUVONE, P. M. 1989. Retinal dopamine and form-deprivation myopia. *Proc Natl Acad Sci U S A,* 86**,** 704-6.

STOOPS, J. K., ARSLANIAN, M. J., OH, Y. H., AUNE, K. C., VANAMAN, T. C. & WAKIL, S. J. 1975. Presence of two polypeptide chains comprising fatty acid synthetase. *Proc Natl Acad Sci U S A,* 72**,** 1940-4.

SUKHATME, V. P., KARTHA, S., TOBACK, F. G., TAUB, R., HOOVER, R. G. & TSAI-MORRIS, C. H. 1987. A novel early growth response gene rapidly induced by fibroblast, epithelial cell and lymphocyte mitogens. *Oncogene Res,* 1**,** 343-55.

SUMMERS, J. A., HARPER, A. R., FEASLEY, C. L., VAN-DER-WEL, H., BYRUM, J. N., HERMANN, M. & WEST, C. M. 2016. Identification of Apolipoprotein A-I as a Retinoic Acid-binding Protein in the Eye. *J Biol Chem,* 291**,** 18991-9005.

SUN, X. J., ROTHENBERG, P., KAHN, C. R., BACKER, J. M., ARAKI, E., WILDEN, P. A., CAHILL, D. A., GOLDSTEIN, B. J. & WHITE, M. F. 1991. Structure of the insulin receptor substrate IRS-1 defines a unique signal transduction protein. *Nature,* 352**,** 73-7.

SUN, Y., XU, F., ZHANG, T., LIU, M., WANG, D., CHEN, Y. & LIU, Q. 2015. Orthokeratology to control myopia progression: a meta-analysis. *PLoS One,* 10**,** e0124535.

SZCZERKOWSKA, K. I., PETREZSELYOVA, S., LINDOVSKY, J., PALKOVA, M., DVORAK, J., MAKOVICKY, P., FANG, M., JIANG, C., CHEN, L., SHI, M., LIU, X., ZHANG, J., KUBIK-ZAHORODNA, A., SCHUSTER, B., BECK, I. M., NOVOSADOVA, V., PROCHAZKA, J. & SEDLACEK, R. 2019. Myopia disease mouse models: a missense point mutation (S673G) and a protein-truncating mutation of the Zfp644 mimic human disease phenotype. *Cell Biosci,* 9**,** 21.

TAMAI, K., SEMENOV, M., KATO, Y., SPOKONY, R., LIU, C., KATSUYAMA, Y., HESS, F., SAINT-JEANNET, J. P. & HE, X.

2000. LDL-receptor-related proteins in Wnt signal transduction. *Nature,* 407**,** 530-5.

TAN, Q., NG, A. L., CHENG, G. P., WOO, V. C. & CHO, P. 2019. Combined Atropine with Orthokeratology for Myopia Control: Study Design and Preliminary Results. *Curr Eye Res***,** 1-8.

TICAK, A. & WALLINE, J. J. 2013. Peripheral optics with bifocal soft and corneal reshaping contact lenses. *Optom Vis Sci,* 90**,** 3-8.

TING, P. W., LAM, C. S., EDWARDS, M. H. & SCHMID, K. L. 2004. Prevalence of myopia in a group of Hong Kong microscopists. *Optom Vis Sci,* 81**,** 88-93.

TKATCHENKO, T. V., SHEN, Y. & TKATCHENKO, A. V. 2010a. Analysis of postnatal eye development in the mouse with high-resolution small animal magnetic resonance imaging. *Invest Ophthalmol Vis Sci,* 51**,** 21-7.

TKATCHENKO, T. V., SHEN, Y. & TKATCHENKO, A. V. 2010b. Mouse experimental myopia has features of primate myopia. *Invest Ophthalmol Vis Sci,* 51**,** 1297-303.

TOKORO, T. 1970. Experimental myopia in rabbits. *Invest Ophthalmol,* 9**,** 926-34.

TONG, L., HUANG, X. L., KOH, A. L., ZHANG, X., TAN, D. T. & CHUA, W. H. 2009. Atropine for the treatment of childhood

myopia: effect on myopia progression after cessation of atropine. *Ophthalmology,* 116**,** 572-9.

TORII, H., KURIHARA, T., SEKO, Y., NEGISHI, K., OHNUMA, K., INABA, T., KAWASHIMA, M., JIANG, X., KONDO, S., MIYAUCHI, M., MIWA, Y., KATADA, Y., MORI, K., KATO, K., TSUBOTA, K., GOTO, H., ODA, M., HATORI, M. & TSUBOTA, K. 2017a. Violet Light Exposure Can Be a Preventive Strategy Against Myopia Progression. *EBioMedicine,* 15**,** 210-219.

TORII, H., OHNUMA, K., KURIHARA, T., TSUBOTA, K. & NEGISHI, K. 2017b. Violet Light Transmission is Related to Myopia Progression in Adult High Myopia. *Sci Rep,* 7**,** 14523.

TRAN, D. T., MASEDUNSKAS, A., WEIGERT, R. & TEN HAGEN, K. G. 2015. Arp2/3-mediated F-actin formation controls regulated exocytosis in vivo. *Nat Commun,* 6**,** 10098.

TRAN, H. D. M., TRAN, Y. H., TRAN, T. D., JONG, M., CORONEO, M. & SANKARIDURG, P. 2018. A Review of Myopia Control with Atropine. *J Ocul Pharmacol Ther,* 34**,** 374-379.

TRIER, K., MUNK RIBEL-MADSEN, S., CUI, D. & BROGGER CHRISTENSEN, S. 2008. Systemic 7-methylxanthine in retarding axial eye growth and myopia progression: a 36-month pilot study. *J Ocul Biol Dis Infor,* 1**,** 85-93.

TROILO, D. 1990. Experimental studies of emmetropization in the chick. *Ciba Found Symp,* 155**,** 89-102; discussion 102-14.

TROILO, D., GOTTLIEB, M. D. & WALLMAN, J. 1987a. Visual deprivation causes myopia in chicks with optic nerve section. *Curr Eye Res,* 6**,** 993-9.

TROILO, D., GOTTLIEB, M. D. & WALLMAN, J. 1987b. Visual deprivation causes myopia in chicks with optic nerve section. *Current Eye Research,* 6**,** 993-9.

TROILO, D., NICKLA, D. L., MERTZ, J. R. & SUMMERS RADA, J. A. 2006. Change in the synthesis rates of ocular retinoic acid and scleral glycosaminoglycan during experimentally altered eye growth in marmosets. *Invest Ophthalmol Vis Sci,* 47**,** 1768-77.

TSE, D. Y. & TO, C. H. 2011. Graded competing regional myopic and hyperopic defocus produce summated emmetropization set points in chick. *Invest Ophthalmol Vis Sci,* 52**,** 8056-62.

TURNHAM, R. E. & SCOTT, J. D. 2016. Protein kinase A catalytic subunit isoform PRKACA; History, function and physiology. *Gene,* 577**,** 101-8.

ULLRICH, O., REINSCH, S., URBE, S., ZERIAL, M. & PARTON, R. G. 1996. Rab11 regulates recycling through the pericentriolar recycling endosome. *J Cell Biol,* 135**,** 913-24.

VEROLINO, M., NASTRI, G., SELLITTI, L. & COSTAGLIOLA, C. 1999. Axial length increase in lid-sutured rabbits. *Surv Ophthalmol,* 44 Suppl 1**,** S103-108.

VILLA-COLLAR, C., CARRACEDO, G., CHEN, Z. & GONZALEZ-MEIJOME, J. M. 2019. Overnight Orthokeratology: Technology, Efficiency, Safety, and Myopia Control. *J Ophthalmol,* 2019**,** 2607429.

VOWINCKEL, J., CAPUANO, F., CAMPBELL, K., DEERY, M. J., LILLEY, K. S. & RALSER, M. 2013. The beauty of being (label)-free: sample preparation methods for SWATH-MS and next-generation targeted proteomics. *F1000Res,* 2**,** 272.

WALLINE, J. J. 2016. Myopia Control: A Review. *Eye Contact Lens,* 42**,** 3-8.

WALLINE, J. J., JONES, L. A., MUTTI, D. O. & ZADNIK, K. 2004. A randomized trial of the effects of rigid contact lenses on myopia progression. *Arch Ophthalmol,* 122**,** 1760-6.

WALLINE, J. J., JONES, L. A. & SINNOTT, L. T. 2009. Corneal reshaping and myopia progression. *Br J Ophthalmol,* 93**,** 1181-5.

WALLMAN, J., ADAMS, J. I. & TRACHTMAN, J. N. 1981. The Eyes of Young Chickens Grow toward Emmetropia. *Investigative Ophthalmology & Visual Science,* 20**,** 557-561.

WALLMAN, J., GOTTLIEB, M. D., RAJARAM, V. & FUGATEWENTZEK, L. A. 1987. Local Retinal Regions Control Local Eye Growth and Myopia. *Science,* 237**,** 73-77.

WALLMAN, J., TURKEL, J. & TRACHTMAN, J. 1978. Extreme myopia produced by modest change in early visual experience. *Science,* 201**,** 1249-51.

WALLMAN, J., WILDSOET, C., XU, A., GOTTLIEB, M. D., NICKLA, D. L., MARRAN, L., KREBS, W. & CHRISTENSEN, A. M. 1995. Moving the retina: choroidal modulation of refractive state. *Vision Research,* 35**,** 37-50.

WALLMAN, J. & WINAWER, J. 2004. Homeostasis of eye growth and the question of myopia. *Neuron,* 43**,** 447-68.

WANG, J. C., CHUN, R. K., ZHOU, Y. Y., ZUO, B., LI, K. K., LIU, Q. & TO, C. H. 2015. Both the central and peripheral retina contribute to myopia development in chicks. *Ophthalmic Physiol Opt,* 35**,** 652-62.

WIESEL, T. N. & RAVIOLA, E. 1977. Myopia and eye enlargement after neonatal lid fusion in monkeys. *Nature,* 266**,** 66-8.

WILDSOET, C. 2003. Neural pathways subserving negative lens-induced emmetropization in chicks--insights from selective lesions of the optic nerve and ciliary nerve. *Current Eye Research,* 27**,** 371-85.

WINAWER, J. & WALLMAN, J. 2002. Temporal constraints on lens compensation in chicks. *Vision Research,* 42**,** 2651-68.

WITKOVSKY, P. 2004. Dopamine and retinal function. *Doc Ophthalmol,* 108**,** 17-40.

WOJCIECHOWSKI, R. 2011. Nature and nurture: the complex genetics of myopia and refractive error. *Clin Genet,* 79**,** 301-20.

WONG, Y. L. & SAW, S. M. 2016. Epidemiology of Pathologic Myopia in Asia and Worldwide. *Asia Pac J Ophthalmol (Phila),* 5**,** 394-402.

WU, H., CHEN, W., ZHAO, F., ZHOU, Q., REINACH, P. S., DENG, L., MA, L., LUO, S., SRINIVASALU, N., PAN, M., HU, Y., PEI, X., SUN, J., REN, R., XIONG, Y., ZHOU, Z., ZHANG, S., TIAN, G., FANG, J., ZHANG, L., LANG, J., WU, D., ZENG, C., QU, J. & ZHOU, X. 2018a. Scleral hypoxia is a target for myopia control. *Proc Natl Acad Sci U S A,* 115**,** E7091-E7100.

WU, P. C., HUANG, H. M., YU, H. J., FANG, P. C. & CHEN, C. T. 2016. Epidemiology of Myopia. *Asia Pac J Ophthalmol (Phila),* 5**,** 386-393.

WU, P. C., TSAI, C. L., WU, H. L., YANG, Y. H. & KUO, H. K. 2013. Outdoor activity during class recess reduces myopia onset and progression in school children. *Ophthalmology,* 120**,** 1080-5.

WU, Y., LAM, C. S., TSE, D. Y., TO, C. H., LIU, Q., MCFADDEN, S. A., CHUN, R. K., LI, K. K., BIAN, J. & LAM, C. 2018b. Early quantitative profiling of differential retinal protein expression in

lens-induced myopia in guinea pig using fluorescence difference two-dimensional gel electrophoresis. *Mol Med Rep*.

X, Z., LIU, Y., GARNIEZ, J. & WALLMAN, J. 2004. The temporal dynamics of spectacle-lens-compensation in chicks. *Investigative Ophthalmology & Visual Science,* 45**,** U415-U415.

YAM, J. C., JIANG, Y., TANG, S. M., LAW, A. K. P., CHAN, J. J., WONG, E., KO, S. T., YOUNG, A. L., THAM, C. C., CHEN, L. J. & PANG, C. P. 2019. Low-Concentration Atropine for Myopia Progression (LAMP) Study: A Randomized, Double-Blinded, Placebo-Controlled Trial of 0.05%, 0.025%, and 0.01% Atropine Eye Drops in Myopia Control. *Ophthalmology,* 126**,** 113-124.

YEH, L. K., LIU, C. Y., KAO, W. W., HUANG, C. J., HU, F. R., CHIEN, C. L. & WANG, I. J. 2010. Knockdown of zebrafish lumican gene (zlum) causes scleral thinning and increased size of scleral coats. *J Biol Chem,* 285**,** 28141-55.

YOUNG, T. L. 2009. Molecular genetics of human myopia: an update. *Optom Vis Sci,* 86**,** E8-E22.

ZHANG, Y., RAYCHAUDHURI, S. & WILDSOET, C. F. 2016. Imposed Optical Defocus Induces Isoform-Specific Up-Regulation of TGFbeta Gene Expression in Chick Retinal Pigment Epithelium and Choroid but Not Neural Retina. *PLoS One,* 11**,** e0155356.

ZHANG, Y. & WILDSOET, C. F. 2015. RPE and Choroid Mechanisms Underlying Ocular Growth and Myopia. *Prog Mol Biol Transl Sci,* 134**,** 221-40.

ZHENG, Y. F., PAN, C. W., CHAY, J., WONG, T. Y., FINKELSTEIN, E. & SAW, S. M. 2013. The economic cost of myopia in adults aged over 40 years in Singapore. *Invest Ophthalmol Vis Sci,* 54**,** 7532-7.

ZHOU, X., LU, F., XIE, R., JIANG, L., WEN, J., LI, Y., SHI, J., HE, T. & QU, J. 2007. Recovery from axial myopia induced by a monocularly deprived facemask in adolescent (7-week-old) guinea pigs. *Vision Res,* 47**,** 1103-11.

ZHOU, X., PARDUE, M. T., IUVONE, P. M. & QU, J. 2017. Dopamine signaling and myopia development: What are the key challenges. *Prog Retin Eye Res,* 61**,** 60-71.

ZHU, X., PARK, T. W., WINAWER, J. & WALLMAN, J. 2005. In a matter of minutes, the eye can know which way to grow. *Invest Ophthalmol Vis Sci,* 46**,** 2238-41.

ZYLBERMANN, R., LANDAU, D. & BERSON, D. 1993. The influence of study habits on myopia in Jewish teenagers. *J Pediatr Ophthalmol Strabismus,* 30**,** 319-22.